Loughborough University

THESIS ACCESS FORM

Copy No …………..…………………… **Location** …….……………….........................……

Author   **Dipesh Patel**

Title   **Synthesis of *n*-Hexyl Acetate in Batch and Chromatographic Reactors**

Status of access **OPEN** / ~~RESTRICTED~~ / ~~CONFIDENTIAL~~

Moratorium Period:…………………… years, ending…………../…..............…./.......20......

Conditions of access approved by (CAPITALS):   **DANISH MALIK**

Supervisor (Signature) …………………………………………….........................………

Department of Chemical Engineering

Author's Declaration: *I agree the following conditions:*

Open access work shall be made available (in the University and externally) and reproduced as necessary at the discretion of the University Librarian or Head of Department. It may also be digitised by the British Library and made freely available on the Internet to registered users of the EThOS service subject to the EThOS supply agreements.

*The statement itself shall apply to **ALL** copies including electronic copies:*

This copy has been supplied on the understanding that it is copyright material and that no quotation from the thesis may be published without proper acknowledgement.

Restricted/confidential work: All access and any photocopying shall be strictly subject to written permission from the University Head of Department and any external sponsor, if any.

Author's signature…………………………….………..Date   **22 June 2011**

users declaration: for signature during any Moratorium period (Not Open work): *I undertake to uphold the above conditions:*			
Date	Name (CAPITALS)	Signature	Address

Synthesis of *n*-Hexyl Acetate in Batch and Chromatographic Reactors

By

Dipesh Patel

A Doctoral Thesis submitted in partial fulfilment of the requirements for the award of Doctoral of Philosophy of Loughborough University

Department of Chemical Engineering

June 2011

CERTIFICATE OF ORIGINALITY

This is to certify that I am responsible for the work submitted in this thesis, that the original work is my own except as specified in acknowledgments or in footnotes, and that neither the thesis nor the original work contained therein has been submitted to this or any other institution for a higher degree.

Author's signature

Dipesh Patel
22 June 2011

To my family
(Late) Grandfather (Vithalbhai)
Grandmother (Parvatiben)
Aunties (Sarlaben and Ruxmaniben)
Mother (Manju)
and
Wife (Sushma)

Jai Gayatri Mata

when I required their assistance. A lot of hours were saved thanks to their presence and availability.

I would also like to thank Dr. Abhijeet Kulkarni, Dr. Krzysztof Ambroziak and Mr Jayasheelan Vaithilingam for their valuable suggestions and comments on my research work.

I would like to thank my family as well as my in-laws for their sincere support and prayers throughout my research.

Finally, I thank my wife, Sushma for her support throughout my period of research and I strongly believe it would have not been an easier task to finish my research work without her moral support.

ABSTRACT

Petrochemical and fine chemical industries face a daunting problem in recovering acetic acid from its aqueous solutions. The recovery of acetic acid could be done through esterification reaction. However, esterification is an equilibrium limited reaction. Multi-functional reactors such as chromatographic reactor (CR) and reactive distillation column (RDC) are promising technologies mainly for equilibrium limited reactions wherein reaction and separation of products are carried out in a single equipment that tends to shift the equilibrium towards the desired direction which is not possible in a classical batch reactor.

Physical and chemical characterisation of ion exchange resin catalysts such as scanning electron microscopy, Brunauer-Emmett-Teller (BET) surface area measurement, pore size distribution, elemental analysis, true density and particle size distribution were carried out to access the catalysts performance for *n*-hexyl acetate synthesis.

Esterification of acetic acid with *n*-hexanol was studied with both dilute and concentrated acid in the presence of cation exchange resins (macroporous and gelular) in a jacketed stirred batch reactor to synthesise a value added ester, namely *n*-hexyl acetate and also to study the recovery of acetic acid from the waste aqueous streams. The effect of various parameters such as speed of agitation, catalyst particle size, feed mole ratio of *n*-hexanol to acetic acid, reaction temperature, catalyst loading and reusability of catalysts was studied for the optimisation of the reaction condition in a batch reactor. The non-ideality of each component in the reacting mixture was accounted for by using the activity coefficient via the use of the UNIFAC group contribution method. The kinetic data were correlated with both pseudo-homogeneous (PH) and adsorption based heterogeneous reaction rate models, e.g., Eley-Rideal (ER), Langmuir-Hinshelwood-Hougen-Watson (LHHW), and the modified LHHW (ML). Pseudo-homogeneous (PH) model gave the best representation of the kinetic data found experimentally.

The feasibility of reactive distillation for the recovery of acetic acid using *n*-hexanol was evaluated through residue curve map (RCM) determination experiments. RCM provides information to a design engineer of the existence of separation boundaries imposed by the singular points corresponding to the reactive/non-reactive azeotropes, thus provides an insight into the feasibility of reactive distillation for this purpose.

A laboratory scale batch chromatographic reactor was designed and constructed. Batch chromatographic reactor experiments were carried out using different parameters such as feed flow rate, feed mole ratio of *n*-hexanol to acetic acid, desorbent (*n*-hexanol) flow rate and reaction step to maximise the formation of *n*-hexyl acetate as well to achieve complete conversion of acetic acid.

Continuous chromatographic reactor was designed, constructed and commissioned on the basis of the results obtained from the batch chromatographic reactor experiments. The experiments carried out in continuous chromatographic reactor correlated very well with the results from the batch chromatographic reactor for the optimised condition.

Keywords: Acetic acid, batch reactor, batch kinetic modelling, chromatographic reactor, esterification, heterogeneous catalysis, *n*-hexanol, *n*-hexyl acetate, ion exchange resins, reactive chromatography, residue curve map.

NOMENCLATURE

a_i	activity of the ith component in the liquid phase
A, B, C, D	acetic acid, *n*-hexanol, *n*-hexyl acetate and water respectively
A_f	Arrhenius pre-exponential factor for the forward reaction (m^3 Kmol^{-1} s^{-1})
A_r	Arrhenius pre-exponential factor for the reverse reaction (m^3 Kmol^{-1} s^{-1})
C_{A0}	initial concentration of acetic acid (mol cm^{-3})
c_{i-s}	concentration of component i at the catalyst site
c_s	concentration of vacant site on the catalyst surface
d	diameter of the column (m)
E_f	effluent
E_0	activation energy of the reaction
E	extract line
F	feed line
I	intermittent line
k	reaction rate constant
K_{eq}	equilibrium constant of the reaction
K_i	adsorption equilibrium constant for component i
L	length of the column (m)
N	all samples
N_{AO}	initial moles of the acetic acid in reacting mixture (mol)
r	rate of the reaction (m^3 Kmol^{-1} s^{-1})
$-r_A$	reaction rate of acetic acid (m^3 Kmol^{-1} s^{-1})
R_f	raffinate line
R	universal gas constant (8.314472 J mol^{-1} K^{-1})
S_f	solvent line
S	vacant active catalyst site
S_i	concentration of sites occupied by species i
t	time (min)

T	temperature (K)
V	volume of the reacting mixture (m^3)
x_i	mole fraction of ith component
X	transformed mole composition
X_A	% conversion of acetic acid

Greek Symbols

α	constant in modified LHHW model
ɣ	activity coefficient of component
θ_i	catalytic sites occupied by component i
θ_{total}	total coverage of the catalytic sites

List of Abbreviations

AcH	acetic acid
A, B, C, D	acetic acid, *n*-hexanol, *n*-hexyl acetate, and water respectively
BCR	batch chromatographic reactor
CCR	continuous counter-current chromatographic reactor
CPCR	centrifugal partition chromatographic reactor
CR	chromatographic reactor
CRACR	continuous rotation annulus chromatographic reactor
COSHH	control of substances, hazardous to health
HxOAc	*n*-hexyl acetate
HxOH	*n*-hexanol
ER	Eley-Rideal model
FBCR	fixed bed chromatographic reactor
FMR	feed mole ratio
GC	gas chromatograph
LHHW	Langmuir-Hinshelwood-Houge*n*-Watson model
ML	modified LHHW model
PH	pseudo-homogeneous model

RCM	residue curve map
RDC	reactive distillation column
RFCR	reversed flow chromatographic reactor
SEM	scanning electron microscopy
SDS	safety data sheet
SMBR	simulated moving bed reactor
TCR	true counter-current chromatographic reactor

Subscripts

A, B, C, D	acetic acid, *n*-hexanol, *n*-hexyl acetate and water respectively
calc	calculated values
eq	equilibrium
exp	experimental values
f	forward reaction
i	component
r	reverse reaction

TABLE OF CONTENTS

LIST OF FIGURES

CHAPTER 1
INTRODUCTION

1. INTRODUCTION

1.1. MOTIVATION

In chemical industries, performance of conventional processes can be greatly improved by integrated processes using multi-functional reactors. Multi-functional reactors may be defined as single equipment in which reaction and separation is carried out simultaneously. The objective of the multi-functional reactor is to save capital and operating costs, reduce equipment size and to improve selectivity and productivity. Integration of unit operation with chemical reaction in a reactor, called as multi-functional reactor, has received significant importance in the past two decades (Gyani, 2010).

The multi-functional reactors such as reactive distillation column (RDC) and chromatographic reactors (CR) could be the solutions to several problems experienced in industrial applications such as recovery of acetic acid from waste streams.

1.2. RECOVERY OF ACETIC ACID

Acetic acid is produced in large quantities as a by-product from various industrial processes (Teo and Saha, 2004). Examples of these are listed in Table 1.1.

Table 1.1. Weight% of acetic acid obtained from various process streams.

Process	% of Acetic Acid (w/w)
Wood Distillate	1 – 8
Glyoxal synthesis	5 – 20
Cellulose Acetylation	35
Terephthalic Acid	65

Recovery of acetic acid (see Table 1.1) is therefore of utmost importance. Recovery of acetic acid by esterification of *n*-butanol is reported in the literature (Neumann and Sasson, 1984; Saha *et al.*, 2000; Gangadwala *et al.*, 2003; Gangadwala *et al.*, 2004). Batch kinetic studies

were therefore carried out in the presence of both dilute and concentrated acetic acid to study their effect on the recovery of acetic acid as well as synthesising the desired product i.e. *n*-hexyl acetate synthesis.

1.3. BATCH KINETIC STUDIES

For all reacting systems, the batch kinetic studies are important to understand the equilibrium behaviour of multi-component liquid mixtures over a wide range of operating conditions in presence of suitable catalysts. The batch kinetic studies were perfomed before carrying out experiments in multi-functional reactors.

1.4. CHROMATOGRAPHIC REACTOR

Chromatographic reactor (CR) is a multi-functional reactor in which reaction and separation are carried out in a single vessel. It is based on the adsorptivitiy of the different species involved. Chromatographic reactor is mostly suitable for the equilibrium limited reactions since reaction and separation of the products are carried out simultaneously which results in high purity products. The catalyst/adsorbent used for the chromatographic reactor may be same or a mixture of catalyst and adsorbent. Also, the catalyst itself may act both as a catalyst for the reaction mixture and an adsorbent for the separation. Chromatographic reactor experiments was carried out and reported in the thesis (see Chapter 6) to investigate its feasibility for the synthesis of *n*-hexyl acetate and the experimental conditions where maximum conversion of acetic acid could be obtained.

Chromatographic reactor utilises differences in adsorption affinity of the different components involved rather than volatility as in the case for reactive distillation column (RDC) which is explained in the following section.

1.5. REACTIVE DISTILLATION COLUMN (RDC)

Reactive distillation is also a multi-functional reactor like chromatographic reactor, where chemical reaction and separation are conducted in a single unit. The difference between a chromatographic reactor and reactive distillation is based on the working principles where latter is based on volatility of different species involved whilst the former is based on adsorptivity of the different species involved. It can be used to conduct processes that would be prohibitively complicated if handled in a conventional process consisting of mainly many individual single-operation units (Krishna, 2002).

Although reactive distillation is highly regarded as a potential alternative process in replacing the conventional reaction-separation process, it is not always advantageous. A systematic method is required to analyse the feasibility and applicability of reactive distillation for a given reaction system. A residue curve map (RCM) is a suitable tool for the synthesis and analysis of reactive distillation. Therefore, RCM determination experiments were carried out as part of this research work. However, RDC experiments were not carried out as this was beyond the scope of current research work.

1.6. OUTLINE OF THE RESEARCH WORK

In this research work, the acetate ester of *n*-hexanol, namely *n*-hexyl acetate used in wide range of industrial applications especially in perfumes, was synthesised in a jacketed batch reactor, simple distillation experiments, batch and continuous chromatographic reactors.

The characterisation of ion exchange resin catalysts used in this research was carried out as reported in this thesis (see Chapter 3). The kinetic behaviour of the heterogeneously catalysed esterification of acetic acid with *n*-hexanol was studied in a jacketed batch reactor using Purolite$^®$ CT-124, Purolite$^®$ CT-151, Purolite$^®$ CT-175 and

Purolite$^®$ CT-275 catalysts to produce *n*-hexyl acetate. The effect of various parameters such as reaction temperature, catalyst loading, feed mole ratio (FMR) of reactants, speed of agitation and reusability of the catalyst was studied to optimise the reaction condition in a jacketed batch reactor.

The batch kinetic data obtained from batch kinetic experiments were correlated with pseudo-homogeneous (PH) and heterogeneous kinetic models i.e., Eley-Rideal (ER), Langmuir-Hinshelwood-Houge*n*-Watson (LHHW), and the modified LHHW (ML). The non-ideal mixing behaviour of the bulk liquid phase was taken into consideration by using the activity coefficients, which were calculated using UNIFAC group contribution method.

The residue curve map (RCM) determination experiments were carried out in the presence of the best performed catalyst (Purolite$^®$ CT-124) for *n*-hexyl acetate synthesis from the batch kinetic experiments to check the feasibility of *n*-hexyl acetate synthesis in reactive distillation column (RDC).

Batch chromatographic reactor (BCR) experiments were conducted at different reaction step time, feed flow rate, feed mole ratio (FMR) of the reactants (*n*-hexanol : acetic acid), reaction temperature and desorbent (*n*-hexanol) flow rate for the optimisation of *n*-hexyl acetate synthesis and to maximise the conversion of acetic acid. The continuous chromatographic reactor (CCR) was designed, constructed and commissioned on the basis of the results obtained from the batch chromatographic reactor.

1.7. ORGANISATION OF THE THESIS

The thesis is organised as follows: Chapter 1 provides the broad overview of the research, which includes motivation and objectives of the research

work. Chapter 2 covers detailed literature review of chromatographic reactors and ion exchange resin catalysts. In Chapter 3, characterisation of the resin catalysts used in the research work is given. Chapter 4 describes the batch kinetic studies for *n*-hexyl acetate synthesis conducted in a jacketed batch reactor in the presence of ion exchange resin catalysts to optimise the reaction condition. Residue curve map (RCM) determination experiments were carried out and are explained in detail in Chapter 4. Chapter 5 contains the batch kinetic modelling results. The modelling results were correlated with the results obtained from batch kinetic experiments.

Chapter 6 shows the results of batch chromatographic reactor experiments for *n*-hexyl acetate synthesis. The experiments were carried out to optimise the condition of batch chromatographic reactor for complete conversion of acetic acid. The continuous chromatographic reactor (CCR) was designed, constructed and commissioned as a part of this research work. The CCR experimental results are discussed in Chapter 6. In Chapter 7, the overall concluding remarks from this research work are summarised and recommendations for future prospects in this field of research are outlined.

CHAPTER 2

LITERATURE REVIEW

2. LITERATURE REVIEW

2.1. INTRODUCTION

Multi-functional reactors such as chromatographic reactor and reactive distillation column (RDC) play an important role in various important industrial applications. However, the application of esterification reaction of acetic acid and *n*-hexanol to produce *n*-hexyl acetate in presence of suitable catalyst and to use these multi-functional reactors as both separation and recovery tool has not been investigated.

This chapter summarises the numerous applications of chromatographic reactor and reactive distillation column (RDC). Ion exchange resin catalysts have been used for this research work. This chapter highlights the advantages of using ion exchange resins as catalysts. This chapter also summarises various applications of ion exchange resins that have been employed in chromatographic reactors and reactive distillation column (RDC).

2.2. BATCH KINETIC STUDIES

A careful study of the reaction kinetics is essential as it plays an important role in the performance and also helps in working out a reliable design for a multi-functional reactor. On a laboratory scale, the kinetics is usually studied using a batch reactor. These kinetic studies generally involve reacting components over a range of operating conditions such as catalyst loading, mole ratio, reaction temperature etc. In Chapter 4, materials and methods used, experimental set-up and procedure and results and discussion for batch experiments are explained in detail.

The heterogeneous kinetics of esterification of acetic acid with *iso*-butanol in the presence of Amberlite IR-120 catalyst and without catalyst was studied by Altiokka and Citak (2001). It was reported that the initial reaction rate increased linearly with low alcohol concentration and acid concentration for Amberlite IR-120 catalyst and that it was nearly

independent of alcohol concentration at high levels. The activation energy for the experiments performed without catalyst was reported as 59.3 KJ/mol and for Amberlite IR-120 catalyst it was reported as 49 KJ/mol. Hence, it was concluded that experiments performed with Amberlite IR-120 catalyst reduces the activation energy required for the acceleration of the esterification reaction.

Gangadwala *et al.* (2003) studied the kinetics of heterogeneously catalysed esterification reaction of acetic acid with butanol in the presence of Amberlyst-15. Negligible mass transfer resistance at 1000 rpm was reported. Eley-Rideal (ER), Langmuir-Hinshelwood-Hougen-Watson (LHHW) modified Langmuir-Hinshelwood-Hougen-Watson (ML) and pseudo-homogeneous (PH), rate models were developed. The effect of various parameters such as temperature, mole ratio, catalyst loading and particle size on the kinetics was studied. It was reported that Amberlyst-15 performs well for the esterification of acetic acid and butanol compared to Indion-130, Amberlite IR-120 and Tulsion TX-66MP catalysts.

The kinetics of side-reaction di-butyl ether (DBE) which is an etherification reaction was also studied by Gangadwala *et al.* (2003). It was reported that both LHHW and ML models fit with the experimental data over a wide range of catalyst loading and temperature for both esterification and side etherification reactions.

The heterogeneous kinetics of an esterification reaction of acetic acid and methanol in the presence of Amberlyst-15 at various temperatures and catalyst concentrations was studied by Song *et al.* (1998). The reaction kinetics for methanol dehydration was also discussed to study the importance of side reactions and the effect of pressure on product selectivity. LHHW rate model was developed to represent the reaction kinetics.

Lee *et al.* (2000) studied the kinetic behaviour of heterogeneous catalysed esterification reaction of acetic acid with amyl alcohol using cation exchange resin Dowex 50Wx8-100. ER, LHHW, ML and Quasi-homogeneous (QH) models were developed to correlate the kinetic data. It was reported that the kinetic behaviour of the esterification reaction between acetic acid and amyl alcohol was best represented by ML rate model. The performance of Amberlyst-15 (previously studied) was compared with Dowex 50Wx8-100 for the synthesis of amyl acetate. It was reported that the latter gives better results for the synthesis of amyl acetate.

Kinetics of heterogeneous catalysed esterification reaction with acetic acid and *iso*-amyl alcohol in the presence of cation exchange resin catalyst, Purolite CT-175 was studied (Teo and Saha, 2004). The effect of various parameters such as speed of agitation, catalyst particle size, mole ratio of the reactants, reaction temperature, catalyst loading, reusability of the catalyst and the concentration of acetic acid were studied to optimise the reaction condition. It was reported that there is negligible mass transfer resistance if the speed of the agitator is in the range of 300 – 800 rpm. It was reported that the equilibrium conversion of acetic acid increased with increase in temperature and by using excess of *iso*-amyl alcohol in the reacting mixture. LHHW rate model was developed for the correlation with the kinetic data obtained from the synthesis of *iso*-amyl acetate.

Deshmukh *et al.* (2009) studied heterogeneous catalysed esterification reaction of acetic acid with butyl cellulose and reported that modified LHHW model represents the kinetic data very well over a wide range of operating parameters.

As mentioned above the catalysis with ion exchange resins can be explained by various heterogeneous kinetic models such as Eley–Rideal (ER), Langmuir–Hinshelwood–Hougen–Watson (LHHW) and

modified Langmuir–Hinshelwood–Hougen–Watson (ML) as well as with the pseudo-homogeneous (PH) kinetic model. The derivations of all the different kinetic models are given in Chapter 5. These kinetic models were tested with the experimental data obtained from the heterogeneously catalysed esterification reaction between acetic acid and *n*-hexanol (see Chapter 4) to find out the best kinetic data (see Chapter 5) that represent the experimental data very well. The non-ideal mixing behaviour of the bulk liquid phase was taken into consideration by using the activity coefficients, which were calculated using UNIFAC group contribution method.

2.3. CHROMATOGRAPHIC REACTOR

Simultaneous reaction and separation carried out in a single vessel (also known as multi-functional reactor) are gaining interest for the reasons that they can be highly feasible. Some chemical reactions which are limited by chemical equilibrium are solved by multi-functional reactors since the reaction and separation takes place at the same time. Examples of the multi-functional reactors are the chromatographic reactor, reactive distillation column (RDC), etc. Chromatographic reactor concept lies in the adsorptivity of the different components involved. The concept of chromatographic reactor, different reactions that can be operated in chromatographic reactor is explained in detail in the following sections.

2.3.1. Concept of a Chromatographic Reactor

The basic concept of chromatographic reactor can be easily understood by studying a single chromatographic column, operated in the conventional batch mode. Consider an equilibrium limited reaction in a single chromatographic column given by reaction (2.1):

$$A \Leftrightarrow C + D \tag{2.1}$$

where, D is the most strongly adsorbed on the catalyst while A and C are less adsorbed on the catalyst.

Reaction (2.1) takes place under diluted conditions in an inert solvent. Consider a pulse of A being injected into a fixed bed comprising an adsorbent of high affinity towards D, and lower one towards A and C. As the reaction takes place, both product species migrate through the reactor at different velocities, with D being retained more strongly than A and C, and thus staying behind the reactive front. This continuous separation of the two products leads to a suppression of the backward reaction, thus driving the conversion towards completion and enabling the withdrawal of two high-purity product fractions at the column outlet. It is worth mentioning the following things:

❖ In a chromatographic reactor separation of the two products can only be achieved if complete conversion has been achieved.

❖ It is not necessary to have a reactant of intermediate affinity towards the stationary phase as long as C and D can be separated.

The extension of the above concept to bimolecular reactions is straightforward. However, it must be noted that in a bimolecular reactions one has to avoid the separation of the reactants by choosing a suitable stationary phase and solvent. This can easily be achieved in applications by using one of the reactants as solvent in order to ensure its availability at the reaction locus (Mazzotti *et al*., 1997; Kawase *et al*., 1999). There are several classes of reactions to which reactive chromatography can be applied. Probably, the widest one is given by esterification reactions, catalysed, for example, by acidic ion exchange resins (Kawase *et al*., 1996; Mazzotti *et al*., 1997) as here the obvious polarity difference between the two products (i.e. ester and water) make their

separation easy on different adsorbents, for example ion exchange resins which acts both as a catalyst and an adsorbent.

In general, the packing of a chromatographic reactor column is carried out with two different solid particles one being the catalyst and other is the adsorbent (Ray and Carr, 1995). Recently, Amberlyst-15, a cation exchange resin catalyst which acts both as the catalyst for the reaction and adsorbent for the chromatographic reactor was used to carry out the reactions in chromatographic reactors (Kawase *et al.*, 1996; Mazzzoti *et al.*, 1996; Mazzzoti *et al.*, 1997; Kawase *et al.*, 1999; Zhang *et al.*, 2001; Yu *et al.*, 2003; Yu *et al.*, 2004; Gelosa *et al.*, 2003; Gelosa *et al.*, 2006; Strohlein *et al.*, 2006).

Similarly, Amberlyst-31 (Kawase *et al.*, 1999), DOWEX 50W-X8 (Falk and Seidal-Morgenstern, 1999; Vu and Seidal-Morgenstern, 2005) and TS-1 (Rangsunvigit and Kulprathipanja, 2004) have been used in the chromatographic reactor experiments for their dual characteristics of both catalyst and adsorbent. The industrial application of chromatographic separation is in the field of chiral and bioseparations (Juza *et al.*, 2000). Chromatographic reactors can be operated in both batch and continuous mode.

2.3.2. Types of Chromatographic Reactor

A chromatographic reactor mainly consists of a stationary phase and a mobile phase. It can be operated in either batch (discontinuous) mode or continuous mode i.e., the reactant or the reactant mixture are fed continuously or discontinuously to the chromatographic reactor. The stationary phase acts both as an adsorbent and a catalyst. As a result, the reaction and the separation take place simultaneously inside the chromatographic reactor. The common stationary phases are solids typically in the form of porous media with large specific surface areas. The solid phases can be individual adsorbent for self-catalytic or homogeneous

catalysed reactions, adsorbent activated by metal ions or functional groups or a mixture of catalyst and adsorbent. The stationary phase may be a liquid coated on a solid support or a liquid retained by centrifugal force (Gyani, 2010). Based on the employed phases and the working principles, chromatographic reactor can be classified as explained in the following section.

2.3.2.1. Batch Chromatographic Reactor (BCR)

Batch chromatographic reactor (BCR) consists of a fixed volume packed with catalyst and/or adsorbent. For most of BCR experiments, the catalyst also acts as an adsorbent. In BCR, the adsorption is followed by the catalytic reaction after which the unreacted feed along with the products are eluted from the chromatographic reactor one after the other depending on the affinity towards the adsorbent (Falk and Seidel-Morgenstern, 1999). Figure 2.1 shows the schematic of a batch chromatographic reactor (BCR) experimental set-up. Consider the reactions (2.2 and 2.3):

$$A \Leftrightarrow C + D \tag{2.2}$$

$$A + B \Leftrightarrow C + D \tag{2.3}$$

Two kinds of experiments are carried out in a batch chromatographic reactor for each of the above two reactions mentioned. One is the reaction step and other is the regeneration step. During the reaction step, a known amount of reactant mixture, [A or A+B, depend on the reaction (2.2) or (2.3)] is continuously fed to the column which is initially saturated with a desorbent [B, in case of the reaction (2.3) and inert solvent in case of the reaction (2.2)]. As soon as the reactants enter the column, A or A+B reacts in presence of the catalyst to produce C and D. D, which has a higher affinity towards resin gets readily adsorbed on the resin while C, with lesser affinity soon gets desorbed. As a result, C gets separated with D, moves towards the exit of the column along with A and B. Since C is

separated from the reaction, the reaction proceeds until consumption of the limiting reactant (A).
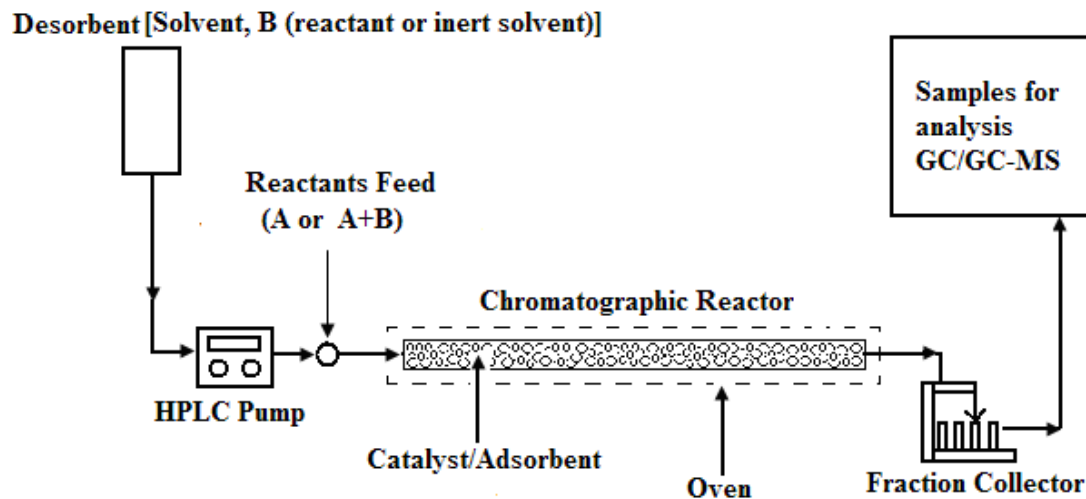
Figure 2.1. Schematic of a batch chromatographic reactor (BCR) experimental set-up.

With any specific location in the column, this process continues until the resin catalyst becomes saturated with A, C and D. When the resin catalyst becomes saturated, chemical equilibrium is achieved and the composition at every point in the column remains the same. At this point, the reaction step is stopped and the regeneration step is started. Pure B or inert solvent [depend on the reaction (2.2) or (2.3)] is continuously fed to the column for the regeneration by removing A, C and D which are present in the column. When the composition of the exit of the column becomes same as the composition of the inlet B, the regeneration step is considered to be complete.

For bimolecular reactions, separation of the reactants should be avoided by choosing a suitable stationary phase and solvent, as well as proper operating conditions (Kawase *et al.*, 1996). This can be easily achieved by using one of the reactants as the solvent in order to ensure its availability at the reaction locus (Kawase *et al.*, 1999).

The major disadvantages of batch chromatographic reactors are low yields due to poor utilisation of stationary phase, high dilution of products due to high desorbent required and discontinuous operation. Comparison of batch chromatographic reactor and plug flow reactor (PFR) was reported by Falk e*t al.* (1999). The comparison of these reactors showed that the conversion of both reactors seems to be similar at the same dilution ratio, but the fixed-bed chromatographic reactor (FBCR) is more attractive for products separation without assistance of a downstream separator. The materials and methods used, experimental set-up and procedure and results and discussion for the batch chromatographic reactor experiments are discussed in detail in Chapter 6.

2.3.2.2. True Counter-Current Chromatographic Reactor (TCR)

Figure 2.2 shows the schematic of a true counter-current chromatographic reactor (TCR). Consider the reaction (2.4):

$$A + B \Leftrightarrow C + D \tag{2.4}$$

where, component D is strongly adsorbed onto the adsorbent/catalyst followed by components A and B, while C is the least adsorbed component.

In TCR, the direction of the fluid flow is opposite to the direction of the true solid flow. The TCR is divided into four different sections. Each section performs specific function so that complete conversion and separation could be achieved.

❖ Section I is located between the desorbent (eluent) and the extract port. The flow rate is higher in this section compared to other sections. The higher flow rate is necessary to remove strongly adsorbed component (D) from the adsorbent/catalyst so that regeneration of the chromatographic reactor column is carried out.

❖ In Section II, between the extract and the feed port, components C and D are formed. For complete conversion of A and separation of products (i.e. C and D), flow rate of this section should be adjusted such that C gets desorbed from the solid phase before reaching the extract port while D remains adsorbed in the solid phase which leads to a higher purity of D at the extract port.
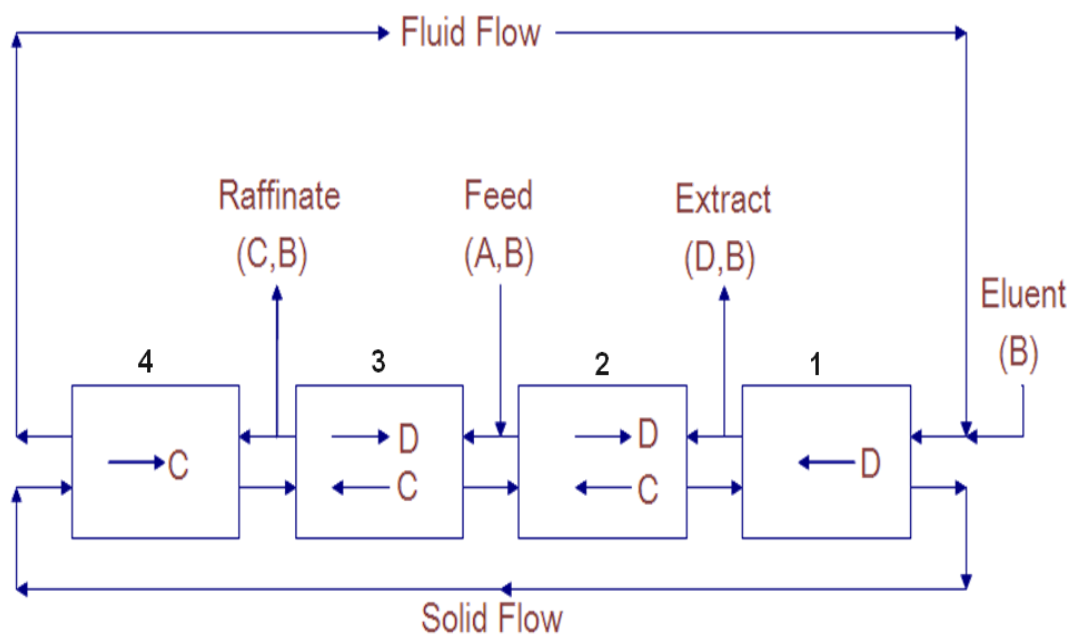
Figure 2.2. Concept of a true counter-current chromatographic reactor (TCR).

❖ Section III is located between the feed and raffinate ports. The reaction takes place in this section and hence, this section is also referred to as the reactive section. Like section II, flow rate in this section is adjusted such that reaction time should be sufficient and the component D could get adsorbed on the solid phase. Thus, the fluid collected at the raffinate port has a very high concentration of the least adsorbed component (C).

❖ Section IV is placed between the raffinate and the desorbed ports. Before the fluid is recycled, it is cleaned in section IV. Component (C) is adsorbed from the fluid phase and transported back to section III along with the solid phase so that desorbent (B) is purified before being recycled to section I.

True counter-current chromatographic reactor (TCR) suffers from practical problems with handling the solid phase as well as its requirement to achieve large rate of solid movement. Also, the abrasion between the solid particles and back mixing are difficult to avoid. Hence, a simplified version of TCR, i.e. continuous chromatographic reactor (CCR) also known as simulated moving bed reactor (SMBR) is more popular and considered to be a better option and is explained in the next section.

2.3.2.3. Continuous Counter-Current Chromatographic Reactor (CCR)
Continuous counter-current chromatographic reactor (CCR) is also referred to as simulated moving bed reactor (SMBR). The CCR was first developed by UOP (Universal Oil Products) in 1960 for the non-reactive separation of mixed xylenes (Broughton and Gerhold, 1961). This process was licensed as the SORBEX process.

Figure 2.3 shows the schematic of a continuous counter-current chromatographic reactor (CCR) experimental set-up. It consists of several batch chromatographic reactor (BCR) columns packed with adsorbent/catalyst connected in series. The inlet and outlet ports of the reactants and products are switched at regular intervals. The time period between the successive switches of ports is called switching time (t_s). Consider the reaction (2.5):

$$A + B \Leftrightarrow C + D \tag{2.5}$$

where, component D is strongly adsorbed onto the adsorbent/catalyst followed by components A and B, while C is the least adsorbed component.
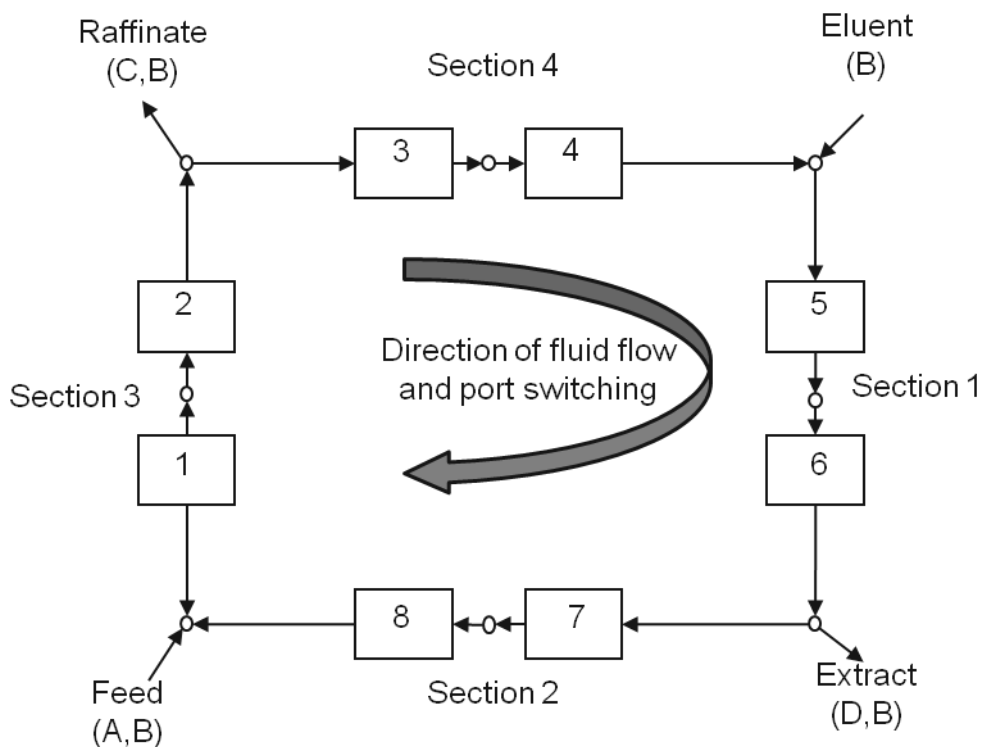
Figure 2.3. Schematic of a continuous counter-current chromatographic reactor (CCR).

There are two inlet fluid streams [feed (A, B) and eluent (B)] and two outlet fluid streams [raffinate (C, B) and extract (D, B)] as shown in Figure 2.3. These two inlet and outlet fluid port divides the unit into four sections (i.e., I, II, III and IV). Each section of CCR is replaced with several subsection packed with catalyst/adsorbent and each section performs specific job so that complete conversion and separation could be achieved. Component B acts both as feed reactants along with A as well as desorbent. For complete separation of products, component C should be least adsorbed and component D should be strongly adsorbed. The outlet ports are switched in the direction of fluid flow by one bed volume

length. The working principle of CCR remains the same as TCR as explained in detail in section 2.3.2.2 except that there is no movement of the solid phase in the CCR.

Depending on the reactive system different CCR configuration set-up can be found in the literature. If the least adsorbed product (component C) does not get adsorbed, the recycling of the pure desorbent is not possible; and section IV can be eliminated (Kawase *et al.*, 1999). Also, if the regeneration of the adsorbent requires a change in the operating conditions i.e. temperature, pressure or change in desorbent then it would be more convenient to remove section I and perform the regeneration of the solid phase separately (Shieh and Barker, 1995). It may be noted that the adsorbent and catalyst materials used for CCR may be same, different or a mixture of the two.

A comparison of CCR and TCR processes which have been discussed in detail by Lode *et al.* (2003) can be summarised as follows:

- ❖ TCR does not really apply to CCR units with finite number of columns per section, i.e. CCR tends to behave like TCR only for infinite columns in each section of infinite lengths.

- ❖ The two reactors (TCR and CCR) exhibit different residence time distributions and lead to different degrees of conversion.

- ❖ TCR reaches true steady state while the CCR only reaches cyclic steady state.

2.3.2.4. Centrifugal Partition Chromatographic Reactor (CPCR)

Centrifugal partition chromatographic reactor (CPCR) is an integration of reaction and centrifugal partition chromatographic separation where counter-current distribution of species takes place in the absence of an

adsorbent or catalyst. In this chromatographic reactor, two immiscible liquid phases with different densities are separated. The stationary phase with higher density is retained in the column by a combination of centrifugal force and geometric channel, while the mobile phase pass through the column as micro-droplets. A schematic of a centrifugal partition chromatographic reactor (CPCR) column is shown in Figure 2.4. A mixture of components A and B is separated due to their different affinities towards the two-liquid phases. The advantage of this chromatographic reactor is the large capacity of stationary phase compared to the conventional technique with liquid on solid support (i.e. liquid-liquid extraction). CPCR has been successfully applied for enzymatic reactions (Den Hollender *et al.*, 1998; Den Hollender *et al.*, 1999).

Figure 2.4. Schematic of a centrifugal partition chromatographic reactor (CPCR) (Den Hollander *et al.*, 1999).

2.3.2.5. Continuous Rotation Annulus Chromatographic Reactor (CRACR)

In a continuous rotation annulus chromatographic reactor (CRACR), the stationary phase is packed into the annulus of two concentric cylinders, rotating continuously about the common axis. The mobile phase (eluent) is fed uniformly over the whole cross-section at the top of the annular space while the reactant is fed to a fixed feed inlet port.
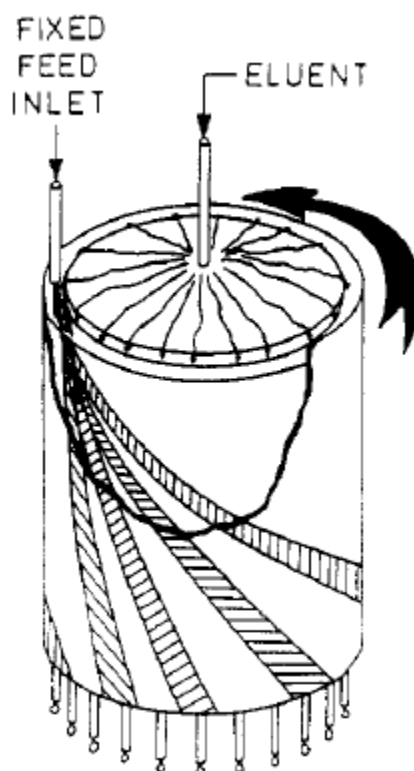
Figure 2.5. Schematic of a continuous rotation annular chromatographic reactor (CRACR) (Howard *et al.*, 1988).

The reacting species are conveyed along the longitudinal axis of the annular space due to mobile phase flow, whereas they have a circumferential displacement by adsorption, desorption and rotational movement of annular. Hence, the components are separated and eluted from the reactor in different angles, compared to the fixed feed port. A

schematic of a continuous rotation annular chromatographic reactor (CRACR) (Howard *et al.*, 1988) is shown in Figure 2.5.

The performance of a continuous rotation annular chromatographic reactor (CRACR) is similar to that of a batch chromatographic reactor (BCR) system except that the operation is carried out in continuous mode in CRACR (Lode *et al.*, 2001). The continuous operation of CRACR results in an inefficient utilisation of the solid phase and high desorbent consumption because complete separation is achieved without recycling of mixed fractions.

2.3.2.6. Reversed Flow Chromatographic Reactor (RFCR)

The concept of a reversed flow chromatographic reactor is similar to that of an adsorptive reactor which is used for heat accumulation for regeneration, but it is related to mass accumulation (Gyani, 2010). The reverse-flow chromatographic reactor (RFCR) is a fixed-bed reactor packed with suitable adsorbent/catalyst. One of the reactant is fed at the middle of the reactor and the flow direction of the carrier is periodically switched. A schematic of a reversed flow chromatographic reactor (RFCR) is shown in Figure 2.6. If the reactants are strongly adsorbed onto the adsorbent/catalyst whilst products are least adsorbed onto the adsorbent/catalyst, the periodic switching of the carrier could lead to trap the strongly adsorbed reactant within the reactor.

Two three way valves are controlled to keep the concentration profile of the reactant propagated in both the directions, but not out of the column. It was first applied by Agar and Ruppel (1988) for the reduction of NOx with NH_3, where only NH_3 is adsorbed and the reactant is fed at the middle of the reactor. Recently, RFCR has been reviewed and it has shown that it can significantly improve conversion and yield for equilibrium or selectivity limited reactions (Jeong and Luss, 2003; Viecco and Caram, 2004;

Viecco and Caram, 2005). Little or no experimental information is available for this case (Gyani, 2010).
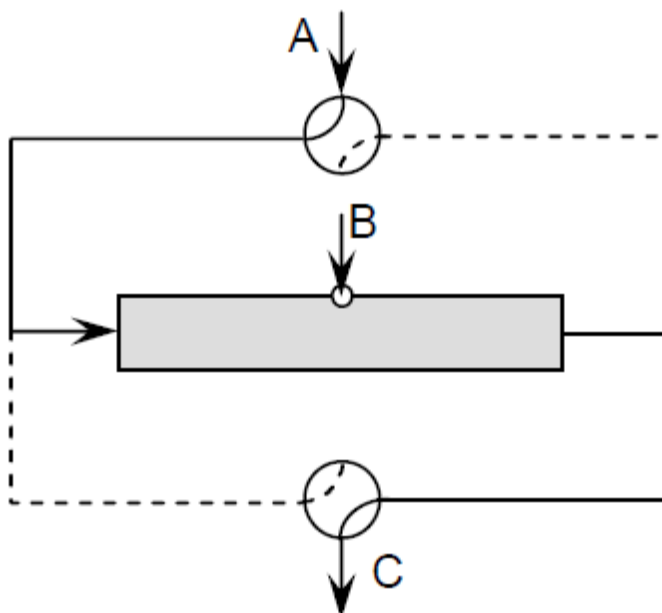
Figure 2.6. Schematic of a reversed flow chromatographic reactor (RFCR) (Vu-Dinh, 2007).

2.3.3. Applications of a Chromatographic Reactor

There are several applications of chromatographic reactor and are explained in detail in the following sections:

2.3.3.1. Esterification Reaction

Triacetence Synthesis (Esterification of acetic acid with glycerol):

Triacetine (glycerol triacetate) is used as plasticisers including filters in cigarettes and hence it is required to be of food grade quality. Gelosa *et al.* (2003) studied the synthesis of triacetine which is a series of three steps esterification of glycerol with acetic acid in the presence of acidic polymeric resins (Amberlyst-15) in a chromatographic reactor. Water molecule formed in each step of esterification along with monoacetine in first step, diacetine in the second step and finally triacetine in the third step of esterification.

The kinetics of esterification was studied in a batch reactor with and without Amberlyst-15. Gelosa *et al.* (2003) reported that the conversion of non-catalysed esterification reaction was lower than 10% in one hour as compared to catalysed esterification which had already attained equilibrium within that time. It was further reported that the effect of interphase mass transport resistances on the kinetics of triacetine synthesis was negligible by carrying out experiments using different stirrer speeds which gave similar results. However, it was also reported that intraphase mass-transport resistances may affect the kinetics of the process by conducting a non-reactive experiment where a small amount of water was added to the batch reactor containing only resin and glycerol at 333 K. They also studied multi-component adsorption equilibria for three binary mixtures (i.e., water-acetic acid, water-glycerol and acetic acid-triacetine) and reported that water has a higher affinity for the resin due to the strong polarity that was made inside the resin by the sulfonic acid groups, followed by glycerol, acetic acid, monoacetine, diacetine and then triacetine. The effect of various parameters such as the reaction temperature, feed molar ratio of the reactants (acetic acid to glycerol) and catalyst to reactant ratio (resin to glycerol) was studied for the modelling of the chromatographic reactor. They concluded that there was a good agreement between the experimental findings and predicted values. The samples from the outlet of the jacketed glass column were analysed typically by titrating acetic acid with NaOH and the concentration of water was measured by Karl Fischer technique and other components (i.e., glycerol, monoacetine, diacetene and triacetin) by gas chromatography.

One important concern was addressed by Gelosa *et al.* (2003) regarding the regeneration of the resin. Since acetic acid was used as a desorbent to remove a high degree of water from the column in the regeneration step, it has to be separated before recycling it back into the column which is an expensive operation. Otherwise, the water left in the resin after the

regeneration step (largely because of recycling dilute acetic acid) may react in the breakthrough experiments with the purified triacetine to produce diacetine which could affect the process efficiency. This will affect the performance of the chromatographic reactor where a good separation between triacetine and diacetine is achieved when a well regenerated column was used. Therefore, the usage of either a dry acetic acid or desulfonated resins (lesser affinity towards water) was purposed by Gelosa *et al.* (2003).

Gelosa *et al.* (2003) carried out esterification of glycerol with acetic acid in the presence of Amberlyst-15 in a chromatographic reactor to address the concern of the column regeneration mentioned above with a possible solution. For these experiments instead of pure acetic acid, a reactive adsorbent (i.e. a mixture of acetic acid and acetic anhydride) were used as desorbent. Acetic anhydride reacts with water to produce acetic acid (the desorbent itself) in the regeneration step which resulted in the enhancement of process efficiency and reduction in the desorbent requirements.

Methyl Acetate Synthesis (Esterification of acetic acid with methanol):
Yu *et al.* (2004) carried out synthesis of methyl acetate in a chromatographic reactor in the presence of Amberlyst-15. Both reactive and non-reactive experiments were performed in a chromatographic reactor. Adsorption parameters were calculated from non-reactive experiments while kinetic parameters were obtained from reactive experiments. Methanol was used as a carrier solvent. A mixture of methyl acetate and water dissolved in methanol were used as a feed for the non-reactive breakthrough experiments, while a binary mixture of acetic acid and water were used as a feed for a reactive breakthrough experiments. Experiments were carried out at different temperatures, feed concentrations and flow rates. The samples were taken from the column outlet at regular intervals and were analysed. Methanol was used for the

regeneration of the resin. Quasi-homogeneous (QH) kinetic model was developed assuming that the reaction in the polymer phase to be homogeneous because of the presence of large volume of methanol in the reaction mixture. It was observed that methyl acetate has less affinity towards the resin than water and that the calculated adsorption constants of water and methyl acetate decreased with an increase in the temperature (since adsorption is an exothermic process). The model predicted the experimentally measured breakthrough curves very well.

However, for a non-reactive breakthrough curves, the model was able to predict the experimental results for methyl acetate very well but not for water. The reason reported was that the tailing effect may be responsible for this and use of non-linear adsorption isotherm was purposed. Similarly, determination of adsorption and kinetic parameters for hydrolysis reaction were evaluated and have been reported in the section 2.3.3.2.

Yu *et al.* (2004) carried out synthesis of methyl acetate in the presence of Amberlyst-15 in a simulated moving-bed reactor (SMBR). Four jacketed steel columns in series were used and each column was connected to four rotary valves actuated by the control system. Methanol was used as a mobile phase. Effect of different switching times, feed and desorbent flow rates were studied in detail and observation respective to various parameters were reported.

Methyl Acrylate Synthesis (Esterification of acrylic acid with methanol):
Acrylic esters are monomers that are widely used for the production of coatings, adhesives, plastics etc. A conventional acrylic ester production involves several distillation columns (a reactor column, a water removal column, an azeotropic column and a column to separate the desired product from the undesired or by-products). In addition, an inhibitor has to be used in the whole process to minimise polymerisation of acrylic acid acrylic ester and to avoid its local depletion Moreover, reduced pressures

are employed in the distillation columns to reduce the boiling temperatures. Besides polymerisation and fouling, one of the major problems of this process is the thermodynamic limitation due to the reaction equilibrium.

Due to the drawbacks of the current production process, an increasing interest can be seen to develop alternative production technologies. The option to employ a heterogeneous catalyst, e.g. an ion exchange resin, makes the use of integrated reactor-separator processes like reactive distillation or reactive chromatography feasible. Since the former process would have similar drawbacks as the conventional one, i.e., fouling and polymerisation due to elevated temperatures, the latter could be a viable option since the separation is accomplished by selective adsorption in the liquid phase.

For the above reason, esterification of acrylic acid with methanol for the production of methyl acrylate in the presence of Amberlyst-15 in a chromatographic reactor was carried out by Strohlein *et al.* (2006). A jacketed batch column was filled with Amberlyst-15 in the hydrogen form immersed in methanol. The composition of the column outlet was analysed by gas chromatography. Methanol was used for the regeneration of the column. The batch column property was characterised by determining the total column porosity using tracer experiments. The effect of various parameters such as feed compositions, flow direction and flow rates have been studied for modelling the chromatographic reactor. A heterogeneous kinetic model, lumped kinetics and a linear driving force transport model have been developed. A more dispersed breakthrough and a sharp desorption profile was seen for the top-down flow and vice-versa for the bottom-up flow as observed by Strohlein *et al.* (2006). Also it was found that water adsorbs more strongly than the other components.

β-Phenethyl Acetate Synthesis (Esterification of acetic acid with β-Phenethyl alcohol):

Synthesis of β-phenethyl acetate by esterification of acetic acid and β-phenethyl alcohol was investigated by Kawase *et al.* (1996) in a simulated moving-bed reactor (SMBR). Amberlyst-15 catalyst was packed in eight stainless steel columns (in series) for this purpose. Each column had five solenoid valves to which desorbent, feed, extract, raffinate and effluent lines were connected. 1,4-Dioxane was used as a desorbent. It was reported that overall conversion in the range of 100% was achieved by the application of simulated moving-bed reactor if the following criteria was satisfied:

- ❖ The products should be separated out chromatographically, and

- ❖ The reaction rate should be large enough so that the reactant does not elute from the column outlet.

2.3.3.2. Hydrolysis Reaction

Hydrolysis of four esters (i.e. methyl formate, methyl acetate, ethyl formate and ethyl acetate) were carried out in a chromatographic reactor with Dowex 50W-X8 catalyst (Mai *et al.*, 2004). HPLC column was used for carrying out the experiments. Water was used as the mobile phase. Various parameters such as temperature, flow rate, feed concentration and injection volume were varied. Following observations were reported by Mai *et al.* (2004):

- ❖ Hydrolysis reaction of methyl formate and ethyl formate was faster as compared to methyl acetate and ethyl acetate.

- ❖ Even at low flow rate, methyl acetate and ethyl acetate eluted from the column again confirming that these were the slowest reaction compared to methyl formate and ethyl formate.

❖ The peaks width was reduced considerably as the temperature was increased and in contrast, there was no major effect of temperature on the retention times in the studied range i.e. 298 – 328 K.

❖ The heterogeneous rate constants decreases in the order of methyl formate, ethyl formate, methyl acetate and ethyl acetate.

Similarly, the heterogeneously catalysed hydrolysis reaction of methyl formate and methyl acetate in the presence of Dowex 50W-X8 was studied by Vu *et al.* (2005). It was reported that for the reaction, $2A \Leftrightarrow B + C$, complete conversion and separation were only possible if reactant A has an intermediate adsorptivity. On the other hand, for the reactions, $A \Leftrightarrow B + C$, complete conversion and separation were possible for any order of adsorptivities.

Falk and Seidel-Morgenstern, (2002) also carried out hydrolysis of methyl formate in the presence of Dowex 50W-X8 in a chromatographic reactor. The effect of temperature, residence time, feed, concentration and cycle time on the performance of the reactor was evaluated. Pseudo-homogeneous (PH) model was able to predict the experimental data over a wide range of parameters.

Yu *et al.* (2004) carried out hydrolysis of methyl acetate in a chromatographic reactor in the presence of Amberlyst-15. Both reactive and non-reactive experiments were performed in a chromatographic reactor. Adsorption parameters were calculated from non-reactive experiments while kinetic parameters were obtained from reactive experiments. Water was used as a carrier solvent. A mixture of methanol (or acetic acid) dissolved in water was used as a feed for the non-reactive breakthrough experiments, while a mixture of acetic acid and methanol dissolved in water or a binary mixture of methyl acetate and water was

used as a feed for a reactive breakthrough experiments. Experiments were carried out at different temperatures, feed concentrations and flow rates. The samples were taken from the column outlet at regular intervals and were analysed. Water was used for the regeneration of the resin.

Quasi-homogeneous (QH) kinetic model was developed assuming the reaction in the polymer phase is homogeneous because of the presence of large volume of water in the reaction mixture. The model predicted the experimentally measured breakthrough curves very well. It was reported that the reaction equilibrium constant of the hydrolysis of methyl acetate increased with an increase in the temperature as the backward reaction is an endothermic reaction.

2.3.3.3. Hydroxylation

Phenol hydroxylation [hydroquinone (HQ) and catechol (CT) production]:
Hydroquinone (HQ) and catechol (CT) are used in photographic processing and polymerisation inhibitors. Both HQ and CT can be produced by hydroxylation of phenol along with benzoquinone (BQ). Rangsunvigit and Kulrathipanja, (2004) studied phenol hydroxylation in the presence of TS-1 catalyst (structure similar to silicalite) in a chromatographic reactor for the production of HQ and CT. Stainless steel columns were used and the samples from column outlet were collected in a fraction collector which was analysed by HPLC. Unreacted H_2O_2 was analysed by H_2O_2 kit (model HYP-1). Aqueous mixture of H_2O_2 or water was used as a desorbent. It was reported that TS-1 could be easily regenerated by using pure water. Rangsunvigit and Kulrathipanja, (2004) also reported that the separation of each product can be achieved with water as desorbent depending upon the amount of phenol in the feed and that the selectivity of CT on TS-1 was found to be concentration dependent.

Table 2.1. Some of the applications of chromatographic reactors.

Systems	Catalyst/Adsorbent	References
Biosynthesis of dextran from sucrose	Dextransucrose	Zafer and Barker (1988)
Esterification of acetic acid and ethanol	Amberlyst-15	Mazzoti *et al.* (1997)
Esterification of acetic acid and glycerol	Amberlyst-15	Gelosa *et al.* (2003)
Esterification of acetic acid and *n*-hexanol	Purolite® CT-124	Patel *et al.* (2010)
Esterification of acetic acid and β-phenethyl alcohol	Proton type ion exchange resins	Kawase *et al.* (1996)
Esterification of acrylic acid and methanol	Amberlyst-15	Strohlein *et al.* (2006)
Hydrogenation of 1,3,5-trimethyl benzene	Platinum supported on alumina	Fish and Carr (1989); Ray *et al.* (1994)
Hydrolysis of methyl formate	Dowex 50W-X8	Falk *et al.* (2002)
Inversion of sucrose	Invertase	Sarmadi and Barker (1993); Meurer *et al.* (1996)
Lactosucrose synthesis	β-fructofuranosidase	Kawase *et al.* (2001)
Methanol synthesis from syngas	Metal catalyst	Kruglov *et al.* (1996)
Oxidative coupling of methane	Oxide type of catalyst	Tonkovich and Carr (1994)
Isomerisation of glucose	Immobilized isomerise	Hoshimoto *et al.* (1983)
Isomerisation of *p*-xylene	ZSM-4	Minceva *et al.* (2008)
Synthesis of bisphenol-A from acetone and excess phenol	Amberlyst-31	Kawase *et al.* (1999)
Synthesis of butyl cellosolve	Amberlyst-15	Deshmukh *et al.* (2009)
Synthesis of diethylacetal from acetaldehyde and ethanol	Amberlyst-15	Silva and Rodrigues (2002; 2005)
Synthesis of diethylacetal from acetaldehyde and methanol	Amberlyst-15	Pereira *et al.* (2008)
Synthesis of methyl acetate	Amberlyst-15	Lode *et al.* (2001; 2003)
Synthesis of MTBE	Amberlyst-15	Zhang *et al.* (2001)

Table 2.1. shows the summary of some of the applications of chromatographic reactors.

2.4. REACTIVE DISTILLATION COLUMN (RDC)

In chemical process industries, chemical reactions and the purification of the desired products by distillation are usually carried out sequentially. In many cases, the performance is greatly improved by the integration of reaction and distillation in a single multi-functional process unit. This integration concept is called "reactive distillation" (RD). Therefore, reactive distillation (RD) is a combination of separation and reaction in a single vessel (Sundmacher and Kienle, 2003). The quote "The versatility of the fractionating column in the dual role of continuous reactor and separator as applied to chemical processing is well established" (Berman *et al.*, 1948a) was appeared in the print in the year 1948, more than six decades ago. Thus the concept of combining the reaction unit and the separation unit is not new to chemical engineering world. The heterogeneous catalysed esterification reaction of acetic acid and *n*-hexanol in the presence of Amberlyst CSP2 catalysed was studied in a reactive distillation column by Schmitt *et al*, (2004).

2.4.1. Applications of Reactive Distillation Column (RDC)

The recovery of ammonia in the classic Solvay process for soda ash in 1860s may be cited as probably the first commercial application of reactive distillation. In recent years there are a large number of papers published on reactive distillation. Taylor and Krishna (2000) and Sharma and Mahajani (2003) reviewed the industrial important reactions that have been studied using the reactive distillation technology.

2.4.2. Advantages and Disadvantages of Reactive Distillation Column (RDC)

The benefits of reactive distillation can be summarised as follows:

❖ Simplification or elimination of a separation system will lead to huge capital savings.

❖ Conversion can be greatly improved. Many process leads to almost 100% conversion. This increased conversion reduces the recycle cost.

❖ If one of the product is continuously removed from the reaction mixture, then the rate of side reactions will be reduced significantly, thus improving the selectivity of the desired products.

❖ The requirement of the catalyst is reduced when compared with the conventional process for the same conversion.

❖ By-product formation is greatly reduced. Hot-spots and runaways are avoided using liquid vapourisation.

❖ Azeotropes are avoided in reactive distillation unit.

❖ Reactive distillation is advantageous when the product is a mixture of species that can form several azeotropes with each other. Reactive distillation conditions can allow the azeotropes to be reacted away in a single unit.

Reactive distillation columns (RDC) also suffer from the following drawbacks:

❖ *Volatility Constraints*:
The reactants and products must have suitable volatility to maintain the high concentrations of reactants and the low concentrations of products in the reaction zone.

❖ *Process conditions mismatch*:

The various process conditions, e.g. temperature and pressure for some processes may not be possible to carry out in a reactive distillation column.

❖ *Residence time requirement*:

If the residence time for the reaction is long, a large sized column may be required. In such cases, it is more appropriate to use conventional reactor separator arrangement.

❖ Scale up to large flows:

It is difficult to design reactive distillation processes for large flows because of liquid distribution problems in reactive distillation unit.

Therefore, it is necessary to study the process parameters before applying the same to reactive distillation.

2.4.3. Residue Curve Map (RCM)

A reactive distillation column (RDC) may not always be advantages because of some of its drawbacks as mentioned in section 2.4.2. As a result, a systematic tool is required to analyse the feasibility and applicability of reactive distillation for a given reaction system. A residue curve map is a suitable tool for the synthesis and analysis of reactive distillation.

The method for synthesis and analysis of both non-reactive and reactive residue curve map (RCM) for methyl acetate system was reported by Song *et al*. (1998). Non-reactive residue curve map for butyl acetate (BuAc) + butanol (BuOH) + water (H_2O) is reported in the literature (Venimadhavan *et al.,* 1999; Gangadwala *et al*., 2004). Non-reactive residue curve map analysis for the methyl acetate (MeAc) +

butanol (BuOH) + butyl acetate (BuAc) + methanol (MeOH) was studied by Jimenez *et al.* (2002).

Saha *et al.* (2005a) studied the feasibility of synthesis of *iso*-amyl acetate in a reactive distillation column (RDC) using residue curve map (RCM) determination experiments and found that the optimal feed mole ratio obtained from experiments carried out in a reactive distillation column (RDC) corresponds well with the findings from the residue curve map (RCM) experiments (Saha *et al.* 2005b).

For the above mentioned reason, one of the objectives of this research work was to carry out only the RCM determination experiments (see Chapter 4). The RDC experiments were not carried out as this was beyond the scope of current research work.

2.5. CATALYSIS

A catalyst is defined as a substance which increases the rate of reaction without itself undergoing a permanent chemical change. Catalysts can be classified as homogeneous (e.g. sulphuric acid), heterogeneous (e.g. porous solid resins) or biological (e.g. enzymes). A catalyst may be classified on the basis of "phase". A phase may be defined as a boundary between two components, even if they exist in the same physical state e.g. a mixture of oil and water consists of two phases. When the catalyst is in the same phase as the reactants and no phase boundary is existent, it is called homogeneous catalysis (Bond, 1987). Homogeneous catalysis can take place either in the liquid phase or in the gas phase. On the other hand, the catalyst is termed heterogeneous if the phase boundary separates the catalyst from the reactants. In heterogeneous catalysis, one or more of the reactants adsorbed onto the catalyst surface.

Heterogeneous catalysis systems have become popular over homogeneous catalysis because of its advantages over the latter. The

advantages of heterogeneous catalysis systems include non-toxic, easy to handle, safe to store, long lifetime, could withstand high temperatures and pressures and safe disposal.

Even though the advantages of heterogeneous catalysis outweigh the homogeneous catalysis systems, they are still employed in some industrial processes because the heterogeneous catalysis system has a significant impact on the mechanical design and operation of the processes. The main advantage of a homogeneous catalysis system is that the catalyst can be added or withdrawn at any time. However, in the case of a heterogeneous catalyst, there is a need for special mechanical design to accommodate for the replenishment of the catalyst or the catalyst would have to possess a long sustainability in order to avoid constant maintenance.

2.5.1. Catalysis by Ion Exchange Resins

The structure of the polymer matrix plays an important role in the catalytic activity of the ion exchange resin. The resins are classified according to the amount of divinylbenzene that is used during the resin preparation. The ion exchange resins can be divided into two groups, namely the gelular and the macrorecticular resins.

The gelular ion exchange resins are rigid, transparent and spherical beads. Gelular resins are characterised by divinylbenzene content below 12%. A typical resin bead is a three dimensional homogeneous structure with no discontinuities in the pore system. The catalytic activity of the gelular resins (on dry basis) is negligible and may increase significantly in a suitable solvent. The swelling of the gelular resins is also dependant on the degree of cross-linking within the matrix structure. Gelular resins possess poor mechanical strength and are prone to attrition losses during the reaction carried out at a higher stirrer speed.

The macroporous resins are characterised by divinylbenzene content in the region of 5 – 60% in the presence of diluents. During the polymerisation process, phase separation occurs and after the extraction of the diluents and drying, permanent pores of various sizes are created. When the amount of divinylbenzene is increased, the nuclei are less fused and the surface area is increased. Hence, the reactant can permeate easily into these pores regardless of whether the matrix is swollen by the reacting medium. Since the macroporous resins have a fixed pores structure, the reactants can enter the matrix through the macropores and interact with the large number of sulfonic acid sites. The macroporous ion exchange resins have greater resistance to attrition as compared to gelular resins. Chakrabarti and Sharma (1993) stated that a significant difference between gelular and macroporous resins is that the gelular resins can only function in a swelling medium whereas macroporous resins can also function in non-swelling solvents.

2.5.2. Applications of Ion Exchange Resins as Catalysts

Alexandratos (2009) has reviewed the developments of ion exchange resins as catalysts over 100 years (1909 – 2009) published in the Industrial and Engineering Chemistry Research and its predecessor's journal. Harmer and Sun (2001) and Gelbard (2005) presented the wide range of applications of the ion exchange resins as catalysts. Some of the important commercial processes catalysed by ion exchange resins are given in Table 2.2 and some of the esterification reactions of acetic acid with different reactants are given in Table 2.3.

Sharma (1995), Harmer and Sun (2001) and Gelbard (2005) reported on different ion exchange resins used as catalysts in a reactive distillation column.

Table 2.2. Some important commercial processes catalysed by ion exchange resins.

Name of the Product	Key Reactants	References
tert-Amyl ethyl ether	*tert*-Amyl alcohol and ethanol	Boonthamtirawuti *et al.* (2009)
tert-Amyl methyl ether (TAME)	*tert*-amyl alcohol and methanol	Yadav and Joshi (2001)
tert-Butanol	*iso*-Butylene and water	Armor (1991)
n-Butyl acetate and methyl alcohol	*n*-Butanol and methyl acetate	Bozek-Winkler and Gmehling (2006)
tert-Butyl alcohol	*iso*-Butene	Zhang *et al.* (2003)
n-Butyl propionate	*n*-Butanol and propionic acid	Lee *et al.* (2002)
iso-Butylene	*tert*-Butanol	Vora *et al.* (1990);
Di-*iso*-butylene, Tetra-*iso*-butylene and Tri-*iso*-butylene	*iso*-Butene	Alcantara *et al.* (2000)
1-Butyl propionate, ethyl propionate and methyl propionate	1-Butanol, ethanol, methanol and propionic acid	Ali (2009)
p-Cresylphenyl acetate	*p*-Cresol and phenylacetic acid	Yadav and Lande (2005)
Ethyl benzoate and water	Benzoic acid and ethanol	Lee *et al.* (2005)
Ethyl *tert*-butyl ether (ETBE)	*tert*-Butyl alcohol and ethanol	Umar *et al.* (2009)
Ethyl lactate and water	Ethanol and lactic acid	Delgado *et al.* (2007)
Ethyl propionate	Ethyl alcohol and propionic acid	Toukoniitty *et al.* (2005)
Ethylene glycol and dimethyl carbonate	Ethylene carbonate and methanol	Dhuri and Mahajan (2006)
Methyl lactate	Lactic acid and methanol	Sanz *et al.* (2002)
Dimethyl adipate	Adipic acid and methanol	Chan *et al.* (2010)
Dimethyl glutarate	Glutaric acid and methanol	Tsai *et al.* (2011)
iso-Propyl *tert*-butyl ether (IPTBE)	*iso*-Butene and 2-propanol	Cunill *et al.* (2000); Pera-Titus *et al.* (2007)
iso-Propyl lactate	Lactic acid and *iso*-propyl alcohol	Yadav and Kulkarni (2000)
Propyl propionate	1-Propanol and propionic acid	Ali *et al.* (2007)

Table 2.3. Esterification of acetic acid over different systems using ion exchange resins.

System	Catalyst	References
Acetic acid + Amyl alcohol	Dowex 50Wx8-100	Lee *et al.* (2000)
Acetic acid + *iso*-Amyl alcohol	Purolite® CT-175	Teo and Saha (2004)
Acetic acid + Benzyl alcohol	Dowex 50Wx8	Ali and Merchant (2009)
Acetic acid + Butanol	Amberlyst 15, Smopex -101	Peters *et al.* (2006)
Acetic acid + *n*-Butanol	Amberlite IR120, Amberlyst 200,	Bianchi *et al.* (2003)
Acetic acid + 2-Ethyl-1-hexanol	Amberlyst 15 and Nafion NR50	
Acetic acid + *iso*-Butanol	Amberlite IR-120	Altıokka and Citak (2003)
Acetic acid + *iso*-Butanol	Amberlite IR-120 and Dowex 50 Wx2	Izci and Bodur (2007)
Acetic acid + Cyclohexene	Amberlyst-15	Chakrabarti and Sharma (1992)
Acetic acid + Epichlorohydrin	Purolite® A-520E	Muresan *et al.* (2008)
Acetic acid + Ethanol	Amberlyst-15	Calvar *et al.* (2007)
Acetic acid + Ethylene glycol	Amberlyst-36	Schmid *et al.* (2008)
Acetic acid + Ethanol	Nafion SAC-13	Suwannakarn *et al.* (2007)
Acetic acid + Methanol		
Acetic acid + *n*-Hexanol	Purolite® CT-124	Patel and Saha (2007); Patel and Saha (2010)
Acetic acid + Methanol	Amberlyst-15	Popken *et al.* (2000)
Acetic acid + Methanol	Nafion/silica nanocomposite catalyst (SAC-13)	Liu *et al.* (2006)
Acetic acid + 2-propanol	Amberlite IR-120, Amberlyst-15 and Dowex 50Wx8-400,	Ali and Merchant (2006)
Acetic acid + *iso*-Propanol	Amberlyst-15	Sanz and Gmehling (2006a,b)
Acetic acid + Styrene	Ostion KS	Cerveny *et al.* (1988)
Acetic acid + Styrene	Amberlyst-15, Amberlyst XN-1010, Monodisperse K2661/K2631 and Nafion NR-50,	Chakrabarti and Sharma (1991/1992)

2.5.3. Advantages and Disadvantages of Ion Exchange Resins as Catalysts

The use of ion exchange resins as catalysts offers several advantages: Helfferich (1962) reported that ion exchange resin catalyst could lead to high selectivity of the desired products in the reactions as compared to catalysis by dissolved electrolytes, and this selectivity could be exploited for the separation of close boiling point mixtures.

Charkrabati and Sharma (1993) stated that the use of ion exchange resins with the equivalent strength of a strong mineral acid allows for safer handling. Furthermore, the ion exchange resins could often be used in hundreds of catalytic cycles without the need for regeneration and hence bringing the cost of a catalyst (through the use of heterogeneous catalysts) far lower than their homogeneous counterparts.

The use of ion exchange resins offer far less non-corrosive conditions so that a less expensive material of construction could be used. This is due to the heterogeneous nature of the ion exchange resin which meant that the number of acid groups at the surface of the resin bead in contact with the equipment constitutes a small percentage of the total number of acid groups present and hence obviating the problem of corrosion (Charkrabati and Sharma, 1993). In addition, there is an advantage of higher product purity and yield with lower by-product formation.

Sharma (1995) reported that the waste disposal problem through the production of bad effluents associated with the use of homogeneous catalysts is eliminated because no washing of the homogeneous acid is required. The resin matrix allows for the reactions to be conducted in aqueous as well as non aqueous and polar or non polar media.

Amberlyst-15 in the form of ion exchange resin catalyst was used for many important applications. They are as follows:

- ❖ Alcantara *et al.* (2000): Oglimerisation of *iso*-butene.

- ❖ Ali (2009): Esterification of propionic acid with methanol, ethanol and 1-butanol.

- ❖ Ali *et al.* (2007): Esterification of propionic acid with 1-propanol

- ❖ Bozek-Winkler and Gmehling (2006): Transesterification of methyl acetate and *n*-butanol.

- ❖ Calvar *et al.* (2007): Esterification of acetic acid with ethanol.

- ❖ Sanz and Gmehling (2006b): Esterification of acetic acid with *iso*-propanol.

- ❖ Toukoniitty *et al.* (2005): Esterification of propionic acid with ethyl alcohol.

Ion exchange resin as catalyst for the forward esterification reaction as well as for the reverse hydrolysis reaction for many reaction schemes were reported in the last decade. They are as follows:

- ❖ Ali and Merchant (2009): Esterification of acetic acid and benzyl alcohol and hydrolysis of benzyl acetate.

- ❖ Delgado *et al.* (2007): Esterification of lactic acid with ethanol and hydrolysis of ethyl lactate.

- ❖ Lee *et al.* (2005): Esterification of benzoic acid and ethanol and hydrolysis of ethyl benzoate.

❖ Popken *et al.* (2000): Esterification of acetic acid and methanol and hydrolysis of methyl acetate.

❖ Sanz and Gmehling (2006a): Esterification of acetic acid with *iso*-propanol and hydrolysis of *iso*-propyl acetate.

❖ Schmid *et al.* (2008): Esterification of acetic acid with ethylene glycol and hydrolysis of ethylene glycol monoacetate.

2.6. SUMMARY

In this Chapter, reported journals related to my research work have been analysed. After reviewing literature, ion exchange resin catalyst was found to be preferred choice for the esterification reaction of acetic acid and *n*-hexanol to produce *n*-hexyl acetate for its numerous advantages. The characterisation of the ion exchange resin catalysts used for this research work is given in Chapter 3. Subsequently, batch kinetic studies carried out with ion exchange resin catalysts for *n*-hexyl acetate synthesis are explained in Chapter 4. Also, in Chapter 4, residue curve map (RCM) determination experiments have been conducted to check the feasibility for its operation in a reactive distillation columns (RDC) for *n*-hexyl acetate synthesis are explained in detail. Batch kinetic modelling has been presented in Chapter 5. The batch kinetic modelling results are also correlated with the batch kinetic experimental results in Chapter 5. The concept and working principle of different chromatographic reactors are explained in detail in this literature review chapter. Based on the literature review, the batch and continuous chromatographic reactors (BCR and CCR) were chosen for the *n*-hexyl acetate synthesis. The design, construction and experimental results of these two chromatographic reactors are discussed in detail in Chapter 6. Finally, concluding statements/remarks from this research work (thesis) and future recommendation are given in Chapter 7.

CHAPTER 3

CATALYST

CHARACTERISATION

3. CATALYST CHARACTERISATION

3.1. INTRODUCTION

The characteristics of ion exchange resin catalysts provide the basis to elucidate the catalytic activity for heterogeneous catalytic processes. The characterisation of the catalysts (Purolite® CT-124, Purolite® CT-151, Purolite® CT-175 and Purolite® CT-275) were performed using scanning electron microscopy (SEM), surface area measurement, pore size distribution using Density Functional Theory (DFT) model based on nitrogen adsorption, elemental analysis, true density determination and particle size distribution.

3.2. MATERIALS AND CATALYSTS

Acetic acid (99.85%), *n*-hexanol (98%) and methanol (99.9+%) were purchased from Acros Organics, UK; *n*-hexyl acetate (99%) was supplied by Aldrich Chemical Company, Inc. and *n*-butanol (99+%) was purchased from Fisher Scientific, UK. The purity of all chemicals was verified by gas chromatography (GC) analysis. These chemicals were used without further purification. Sulfonated cation exchange resins, Purolite® CT-124, Purolite® CT-151, Purolite® CT-175 and Purolite® CT-275 (supplied courtesy of Purolite® International Limited, UK) were used for the present work. Physical and chemical properties of Purolite® CT-124, Purolite® CT-175, Purolite® CT-151 and Purolite® CT-275 catalysts are given in Table 3.1. Purolite® catalysts used were first washed with methanol, dried in a vacuum oven at 373 K for 6 h to remove any water sorbed on the catalyst, before carrying out the experiments. Safety data sheet (SDS) of all the chemicals and the catalysts used are attached in Appendix 9.2.1 and 9.2.2. COSHH (Control of Substances Hazardous to Health) and Risk Assessment (RA) records for all the experiments were carried out before conducting the experiments and are attached in Appendix 9.3 and 9.4, respectively.

Table 3.1. Physical and chemical properties of Purolite[®] CT-124, Purolite[®] CT-175, Purolite[®] CT-151 and Purolite[®] CT-275 catalysts.

Properties	Purolite[®] CT-124	Purolite[®] CT-151	Purolite[®] CT-175	Purolite[®] CT-275
Physical form	Golden coloured spherical beads	Dark spherical beads	Dark spherical beads	Dark spherical beads
Matrix	Gelular	Macroporous	Macroporous	Macroporous
Moisture retention, (H%)*	56 – 61	56 – 58	52 – 57	54 – 57
Total H^+ capacity	1.2	1.7	1.8	1.7
Particle size (µm)	+ 1000 < 5% - 350 < 6%	+ 1200 < 2% - 425 < 1.8%	+ 1200 < 2% - 425 < 2%	+ 1200 < 2% - 425 < 2%
Median pore diameter, d_{50} (nm)*	a	25 – 45	60 –70	60 –75
Specific surface area ($m^2 g^{-1}$)	a	15 – 25	20 – 40	20 – 35
Temperature limit (H^+ form) [K]*	418	418	418	418
Pore Volume, ($cm^3 g^{-1}$)	a	0.17	0.31	0.24
True density ($g cm^{-3}$)	1.45	1.40	1.95	1.65
Measured BET surface, ($m^2 g^{-1}$)	a	25.2	21.3	20.5
BET surface area to pore volume ratio ($m^2 m^{-3}$)	a	14.8×10^7	6.87×10^7	8.54×10^7

*Manufacturers data, [a]Data not available

3.3. SCANNING ELECTRON MICROSCOPY (SEM)

Scanning electron micrographs were taken on a Carl Zeiss 1430 microscope at room temperature to visualise the surface morphology of the ion exchange resin catalysts. The normal secondary electron mode (i.e. not back scattering) was used and the accelerating voltage was set to 5 kV. Prior to analysis, the catalyst sample was dried in a vacuum oven at room temperature and mounted using PVA glue on an aluminium platform and gold coated to make the sample conductive

Figures 3.1 – 3.4 represent the microscopic examination of the surface morphology of Purolite$^®$ ion exchange resin catalysts. Figure 3.1 shows very smooth and gel-like surface of Purolite$^®$ CT-124 that corresponds well with its gelular polymeric matrix structure (as shown in Table 3.1). Figure 3.2 shows hair line cracks on the surface of Purolite$^®$ CT-151 catalyst. Figures 3.3 and 3.4 illustrate the surface morphology of Purolite$^®$ CT-175 and Purolite$^®$ CT-275 ion exchange resin catalysts, respectively. They show agglomerates of microspheres which look like cauliflowers, and smaller nuclei (10 – 30 nm) more or less fused together that are observed within each microsphere. Intermediate pores (20 – 50 nm), known as mesopores, are accountable for the moderate surface areas. Large pores (50 – 1000 nm), otherwise known as macropores, are responsible for the pore volume of the catalyst. These large pores allow the reactants to permeate easily into the catalyst structure, regardless of whether the microspheres are swollen by the reactants. Similar observations were reported for Purolite$^®$ CT-175 and Purolite$^®$ CT-275 catalysts by Teo and Saha (2004).
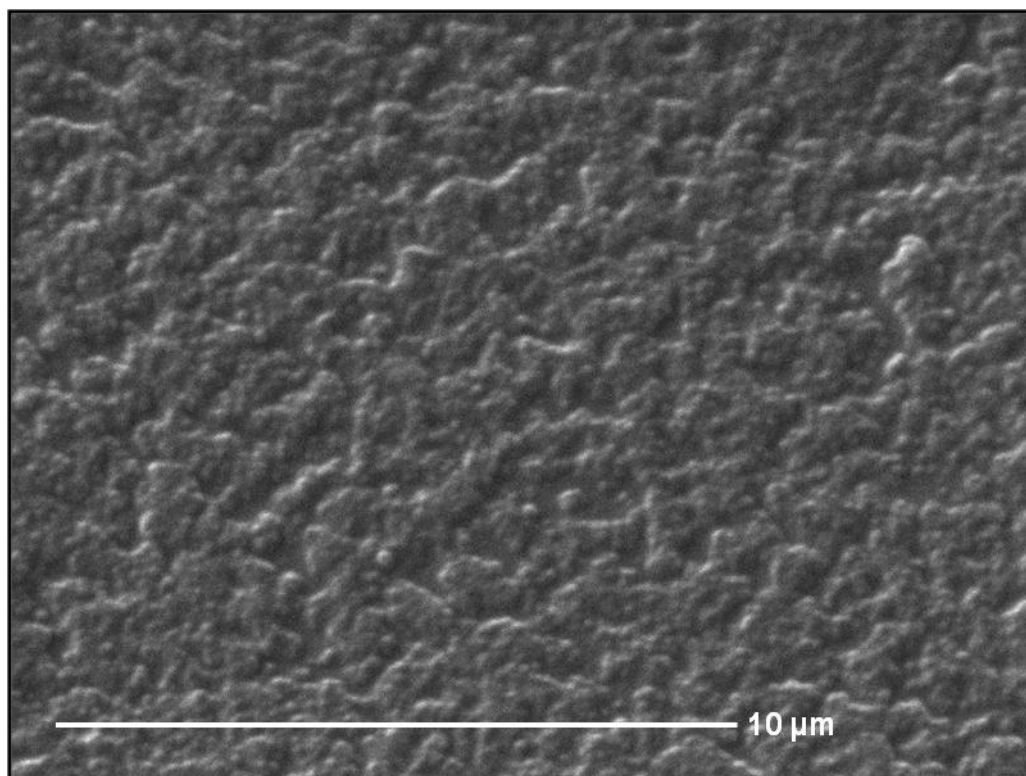
Figure 3.1. Scanning electron micrograph (SEM) of Purolite[®] CT-124 catalyst.
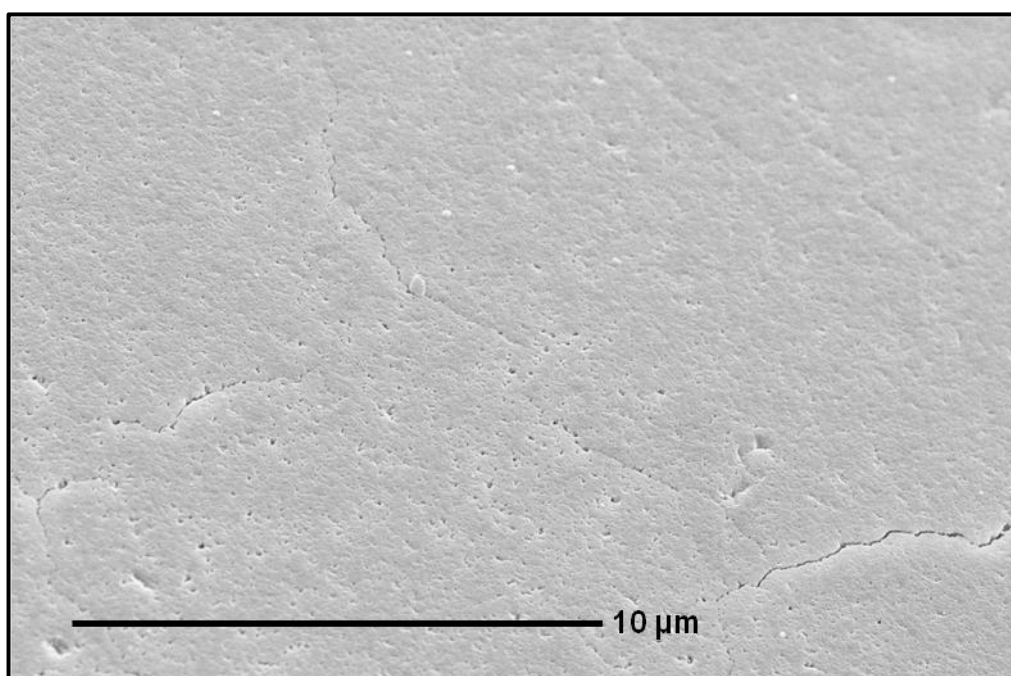
Figure 3.2. Scanning electron micrograph (SEM) of Purolite[®] CT-151 catalyst.
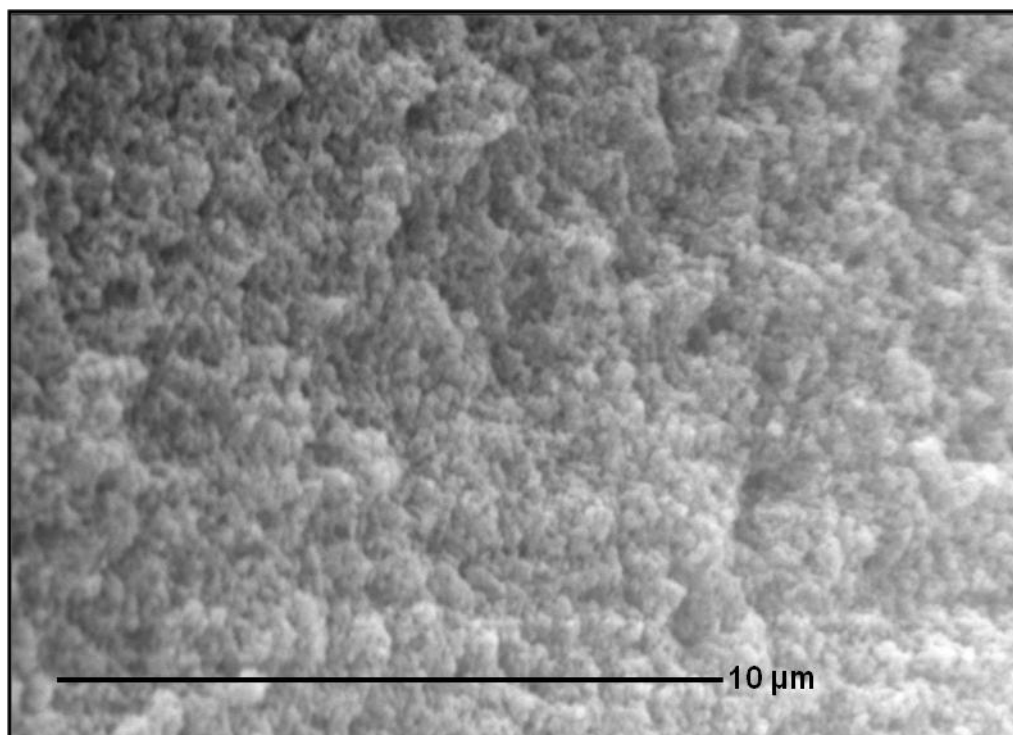
Figure 3.3. Scanning electron micrograph (SEM) of Purolite® CT-175 catalyst.
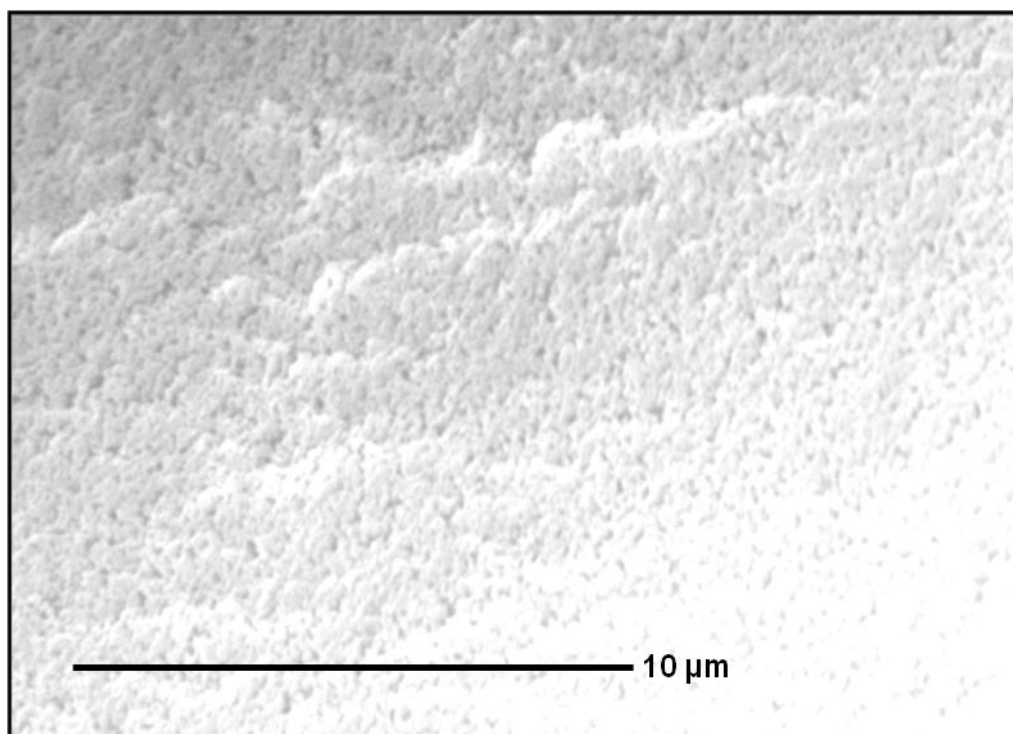
Figure 3.4. Scanning electron micrograph (SEM) of Purolite® CT-275 catalyst.

3.4. SURFACE AREA, PORE VOLUME AND PORE SIZE DISTRIBUTION MEASUREMENTS

Surface area and pore size distribution of the ion exchange resins were measured by nitrogen adsorption and desorption method using a Micromeritics Accelerated Surface Area and Porosimetry (ASAP) 2010 surface analyser. The weighed catalyst was prepared by being out-gassed at 373.15 K for a minimum period of 24 h on the de-gas port of the analyser. Surface area was measured for linear relative pressure range between 0.05 and 0.15. Surface area and pore size distribution analysis for all samples were carried out by N_2 adsorption/desorption method at 77 K. Density Functional Theory (DFT) model was used to analyse the pore size distribution results.

Table 3.1 shows that Purolite$^®$ CT-151 has the largest Brunauer–Emmett–Teller (BET) surface area (25.2 m^2 g^{-1}) among the ion exchange resin catalysts analysed whilst both Purolite$^®$ CT-175 and Purolite$^®$ CT-275 show almost similar surface area values, with Purolite$^®$ CT-175 having a BET surface area of 21.3 m^2 g^{-1} whilst the BET surface area of Purolite$^®$ CT-275 sample is 20.5 m^2 g^{-1}. It can also be seen from Table 3.1 that Purolite$^®$ CT-175 has the biggest pore volume (0.31 cm^3 g^{-1}) among the ion exchange resins analysed. Purolite$^®$ CT-275 exhibited a pore volume of 0.24 cm^3 g^{-1} whilst Purolite$^®$ CT-151 showed a pore volume of 0.17 cm^3 g^{-1}.

Specific surface area to pore volume ratio is inversely proportional to pore diameter. Therefore, smaller the specific surface area to pore volume ratio, bigger is the pore diameter and vice-versa. Table 3.1. shows that Purolite$^®$ CT-151 has highest (14.8 x 10^7 m^2 m^{-3}) BET surface area to pore volume ratio, whereas Purolite$^®$ CT-175 represented the lowest value (6.87 x 10^7 m^2 m^{-3}). Hence, Purolite$^®$ CT-151 has the smallest pore diameter whereas Purolite$^®$ CT-175 has the highest pore diameter. It is to be noted that it was not possible to obtain the surface area and pore size

distribution data for Purolite[®] CT-124 catalyst as the gelular matrix structure of the polymeric resin collapsed during the course of the analysis in the ASAP 2010 analyser.

The pore size distribution of the ion exchange resins were measured through the Density Functional Theory (DFT) model based on nitrogen adsorption assuming slit pore geometry. The DFT model has been recognised as a powerful tool for the study of inhomogeneous fluids (Olivier, 1998; Saha *et al.*, 2000; Teo and Saha, 2004).
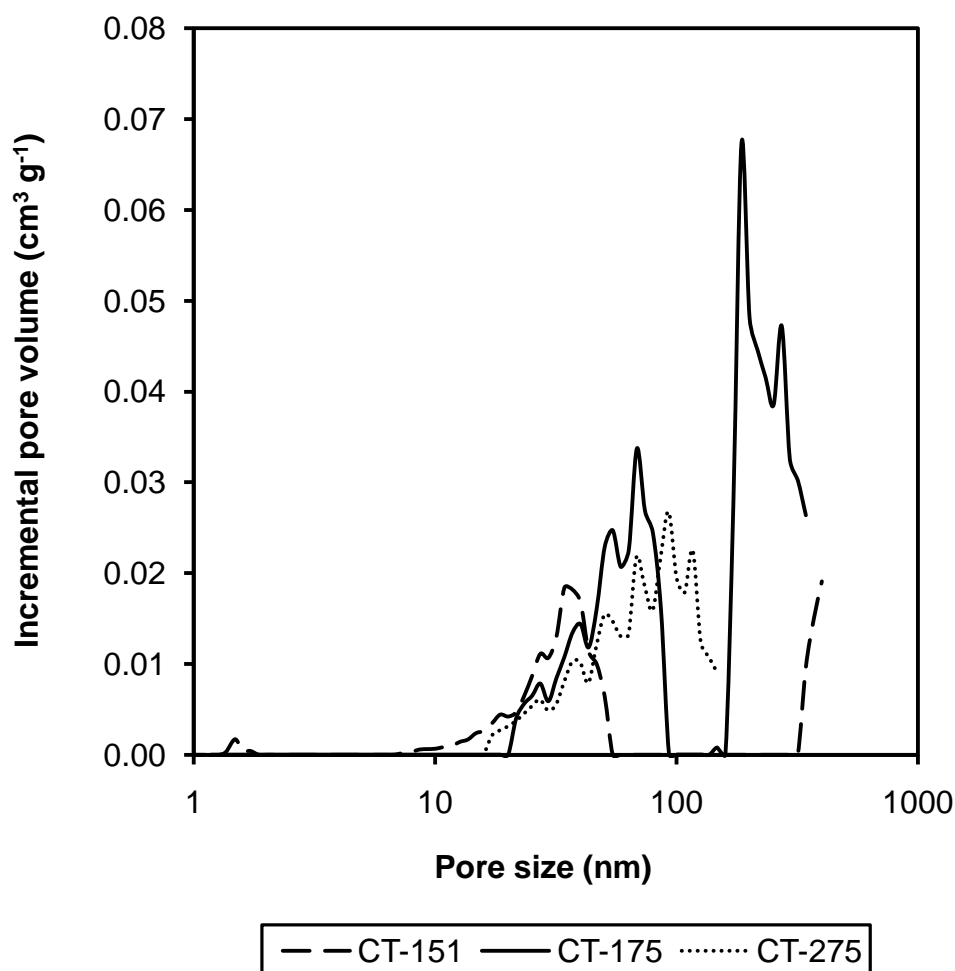
Figure 3.5. Comparison of pore size distribution of various ion exchange resin catalysts.

Figure 3.5 shows a comparison of the pore size distribution results for different ion exchange resin catalysts and it confirms the macroporous nature of all the analysed catalysts. All the polymeric resins exhibited significant pore volume in the macroporous regions. However, more prominent access pores were observed in Purolite® CT-175 as compared to Purolite® CT-151 and Purolite® CT-275 which exhibited much less prominent catalyst access pores.

3.5. ELEMENTAL ANALYSIS

Elemental analysis of ion exchange resin catalysts was performed in the Department of Pure and Applied Chemistry, University of Strathclyde, United Kingdom. The analysis involved weighing the catalyst samples accurately on an aluminium foil and inserting the samples into the Perkin Elmer 2400 Elemental Analyser (Series 2) instrument. Prior to the flash combustion process, the system was purged with helium carrier gas. Flash combustion was performed at 2073 K, and the gaseous combustion

Table 3.2. Elemental analysis results of Purolite® catalysts.

Catalysts used	Weight (%)			
	C	H	S	O
Purolite® CT-124	37.13	6.59	12.46	43.82
Purolite® CT-151	41.04	5.96	13.78	39.22
Purolite® CT-175	44.57	5.64	15.07	34.72
Purolite® CT-275	49.89	4.47	17.50	28.14

products were quantified using a thermal conductivity detector. The results were obtained as weight percentages of carbon, hydrogen and sulphur; the oxygen content was measured by difference. The elemental analysis results are presented in Table 3.2. It is to be noted that nitrogen was not detected in any of the analysed ion exchange resin catalysts. The oxygen content presented in Table 3.2 was not analysed directly from the

elemental analysis. However, it was determined by the difference from the weight percentage compositions of other elements (i.e. C, H and S). It can be seen from Table 3.2 that Purolite® CT-124 catalyst contains the highest proportion of oxygen (43.82%), whereas Purolite® CT-275 catalyst has the highest percentage of sulphur content (17.5%). The elemental analysis also confirms that all the catalysts used are basically sulphonated poly-styrene divinylbenzene polymeric resins.

3.6. TRUE DENSITY DETERMINATION AND PARTICLE SIZE DISTRIBUTION

True density of the catalyst was measured using a density bottle. The density bottle was filled with a known amount of methanol up to the density bottle marker and weighed. A known quantity of catalyst sample was added to the density bottle and reweighed. The volume of methanol displaced by the catalyst was the true density of the catalyst. Density measurements were made for about 4 g of catalyst samples and the measurements were made in duplicate and average values were reported. The measured true density of Purolite® CT-124, Purolite® CT-151, Purolite® CT-175 and Purolite® CT-275 catalysts were 1.45, 1.40, 1.95 and 1.65 g cm^{-3}, respectively.

Particle size distributions of the resin catalysts were determined using standard sized sieves. Prior to sieving the catalyst, every individual sieve was cleaned, weighed and arranged in decreasing sieve diameters. A known amount of the ion exchange resin catalyst was accurately weighed and placed on the top sieve. The catalyst was then sieved down through the tower of sieves with the aid of a mechanical shaker. The weight of each sieve was subsequently measured and the weight of ion exchange resin catalyst collected on each sieve was determined. This procedure was repeated several times to ensure the reproducibility of results. The results of the sieve test were then counter checked using a Malvern Mastersizer. This equipment is used based on the principle of

laser diffraction. A representative amount of catalyst sample was wetted with demineralised water. The sample was agitated with a built-in stirrer and recirculated around a sample loop. The measured values were noted.

The particle size distribution results of different ion exchange resin catalysts are presented in Figures 3.6 – 3.9, respectively. Figure 3.6 shows that Purolite® CT-124 has a wide range of size distribution, with majority of the catalyst particles [~77% (w/w)] lie within the size range of 300 – 600 µm. Figure 3.7 confirms that approximately 86% (w/w) of Purolite® CT-151 catalyst particles lie within the size range of 500 – 600 µm. Purolite® CT-124 exhibits ~22% (w/w) of catalyst particles in the size range of 850 – 1400 µm.
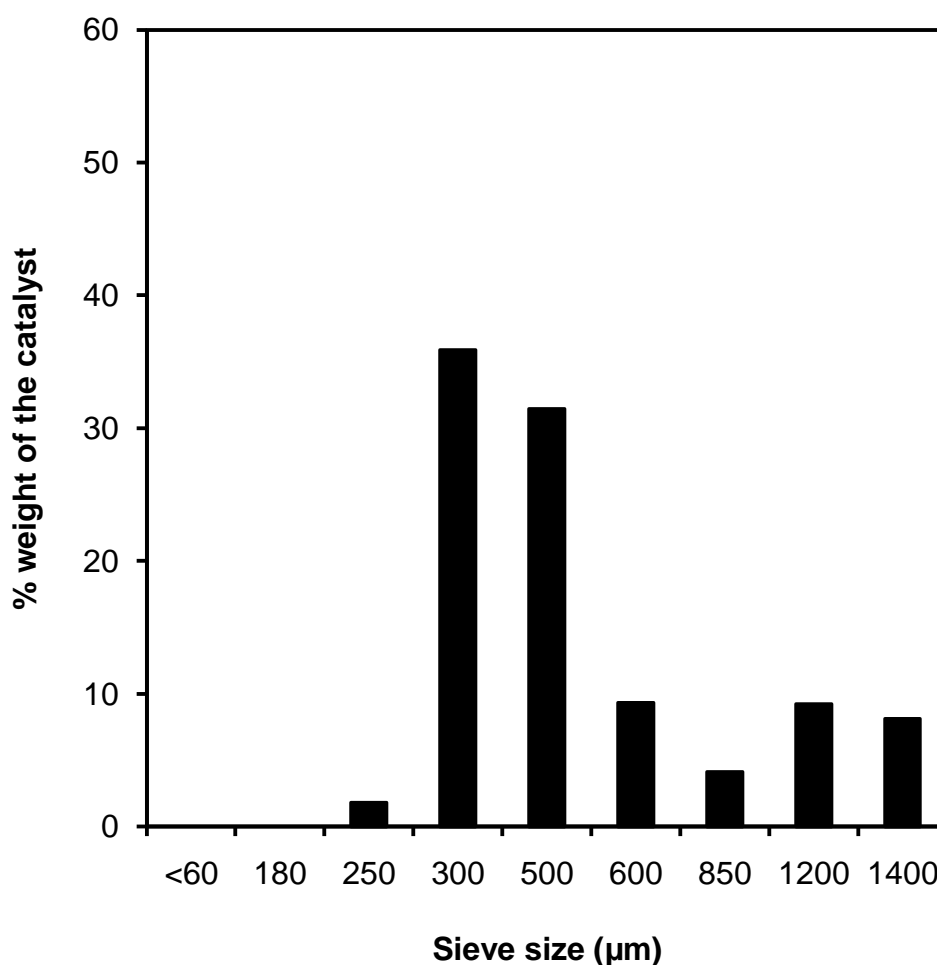
Figure 3.6. Particle size distribution of Purolite® CT-124 catalyst.
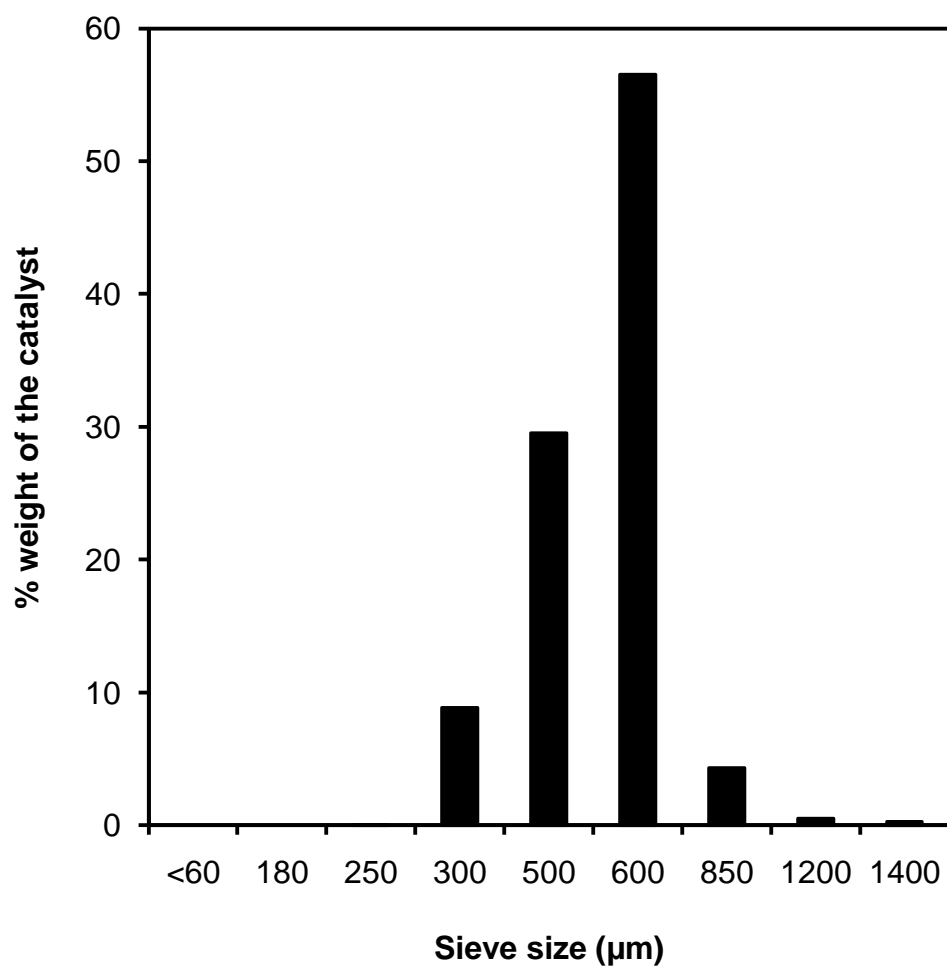
Figure 3.7. Particle size distribution of Purolite[®] CT-151 catalyst.
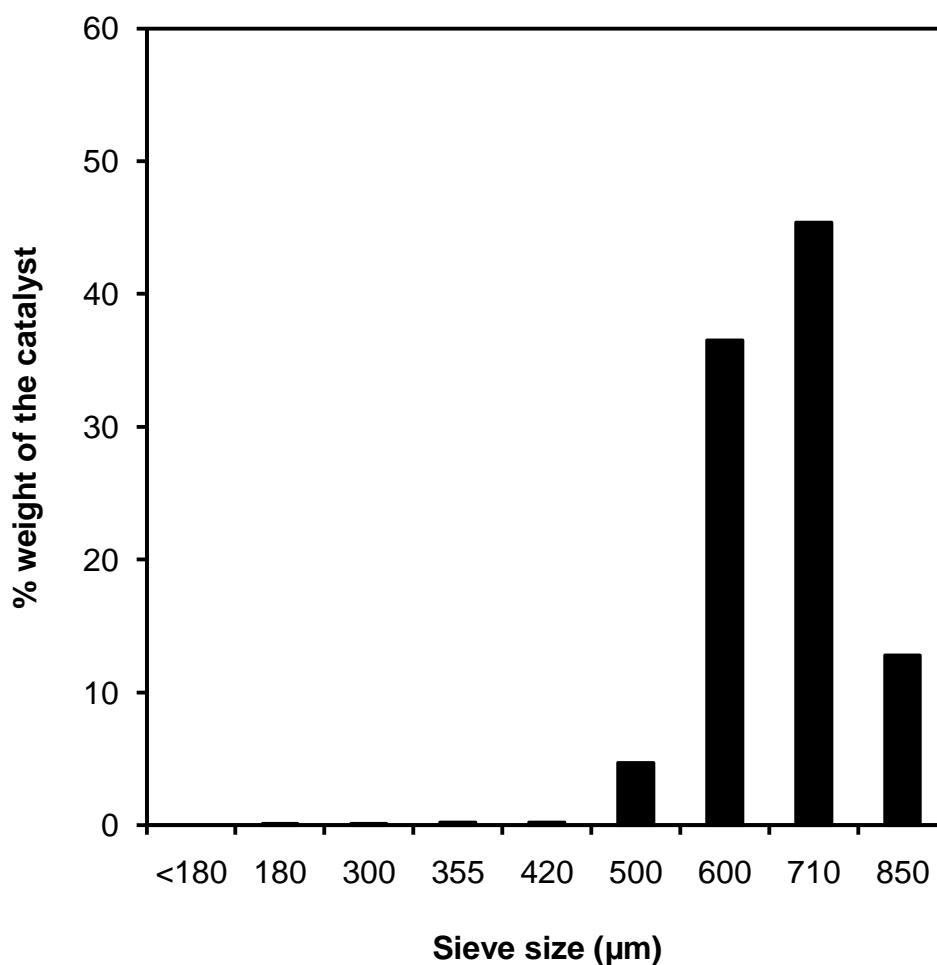
Figure 3.8. Particle size distribution of Purolite® CT-175 catalyst.

Figure 3.8 shows that about 94% (w/w) of Purolite® CT-175 catalyst particles fall within the size range of 600 – 850 µm, while the remaining 6% (w/w) of the catalyst particles are placed within the size range of 355 – 500 µm. Figure 3.9 illustrates that Purolite® CT-275 catalyst has got a wider particle size distribution as compared to Purolite® CT-175 catalyst. It is to be noted that ~89% (w/w) of Purolite® CT-275 catalyst particles lie within the size range of 420 – 710 µm and the remaining 11% (w/w) of the catalyst particles fall within the size range of 180 – 355 µm. Similar results were also reported elsewhere (Teo and Saha, 2004; Teo, 2005).
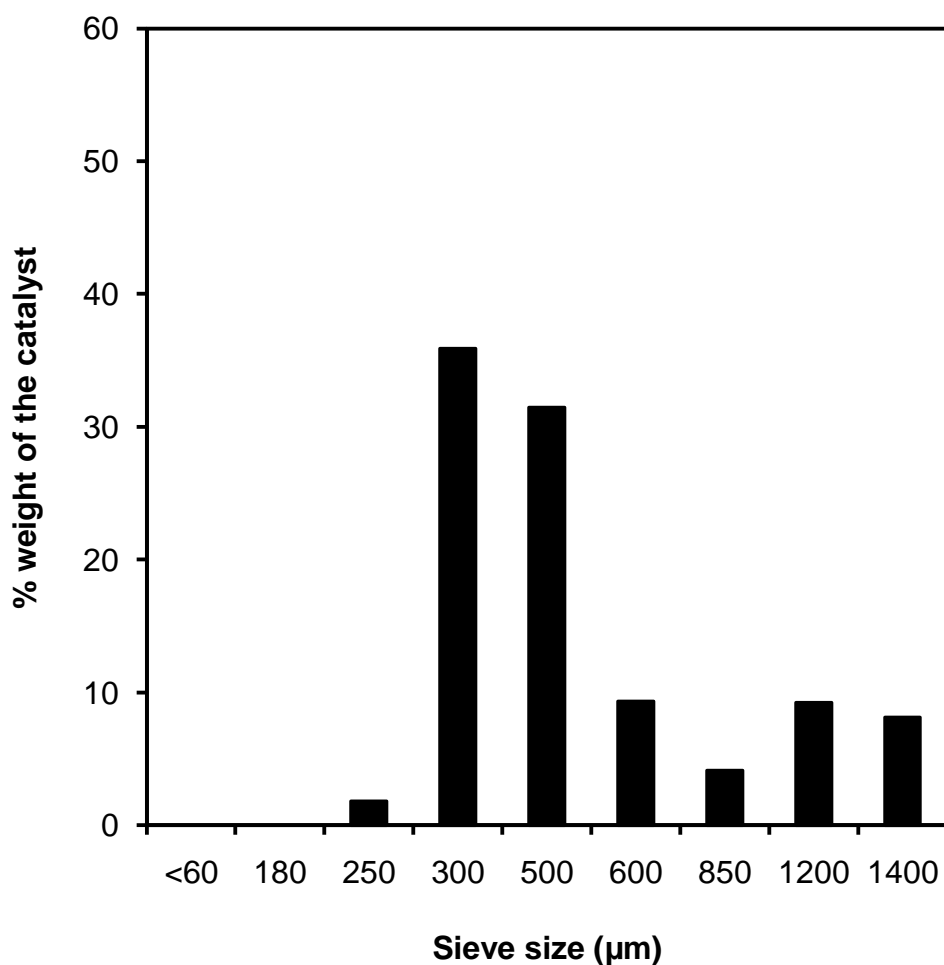
Figure 3.9. Particle size distribution of Purolite$^®$ CT-275 catalyst.

3.7. CONCLUSIONS

The characterisation of various catalysts carried out successfully is explained in this chapter. In the next chapter, batch kinetic studies, residue curve map experiments, method of analysis and mechanism of the reaction are explained in detail. Results from both the batch kinetic studies and residue curve map experiments are also discussed in the next chapter.

CHAPTER 4
BATCH KINETIC STUDIES AND
RESIDUE CURVE MAP (RCM)
DETERMINATION

4. BATCH KINETIC STUDIES AND RESIDUE CURVE MAP (RCM) DETERMINATION

4.1. INTRODUCTION

Batch kinetic studies and residue curve map (RCM) determination experiments carried out over a wide range of experimental conditions using ion exchange resins catalysts are explained in detail. The RCM determination experiments however were carried out for the best catalyst that was found from the batch kinetic experiments. The results obtained from the batch kinetic studies and RCM determination experiments are discussed in detail. A detailed description of the experimental methods and analytical method used are explained in detail for both the batch kinetic experiments and for residue curve map (RCM) experiments.

4.2. BATCH KINETIC STUDIES

4.2.1. Introduction

The batch kinetic experiments were performed by varying various parameters for *n*-hexyl acetate synthesis. In the subsequent sections, materials and catalysts used for the batch kinetic experiments, experimental set-up and procedure, method of analysis and results from the batch kinetic experiments are discussed in detail.

4.2.2. Materials and Catalysts

Acetic acid (99.85%), *n*-hexanol (98%) and methanol (99.9+%) were purchased from Acros Organics, UK; *n*-hexyl acetate (99%) was supplied by Aldrich Chemical Company, Inc. and *n*-butanol (99+%) was purchased from Fisher Scientific, UK. The purity of all chemicals was verified by gas chromatography (GC) analysis. These chemicals were used without further purification. Sulfonated cation exchange resins, Purolite[®] CT-124, Purolite[®] CT-151, Purolite[®] CT-175 and Purolite[®] CT-275 (supplied courtesy of Purolite International Limited, UK) were used for the present work. Purolite[®] catalysts were first washed with methanol, dried in a vacuum oven at 373 K for 6 h to remove any water sorbed on the catalyst,

before carrying out the experiments. Safety data sheet (SDS) of all the chemicals and the catalysts used are attached in Appendix 9.2.1 and 9.2.2. COSHH (Control of Substances Hazardous to Health) and Risk Assessment (RA) records for batch reactor experiments were carried out before conducting the experiments and are attached in Appendix 9.3 and 9.4, respectively.

4.2.3. Batch Kinetic Schematic/Experimental Set-Up and Procedure

The kinetic experiments were conducted in a jacketed stirred (five necked) batch reactor of 0.5×10^{-3} m^3. Figures 4.1 and 4.2 show the schematic and image of the experimental set-up for batch reactor experiments. One of the necks of the reactor was connected to the condenser and the other neck was used for withdrawing samples. The stirring of the reacting mixture was provided by a stirrer motor (IKA–WERKE). A digital thermocouple (Digitron Instrumentation) was inserted through one of the necks of the batch reactor to monitor the temperature of the reacting mixture. Known quantities of acetic acid and *n*-hexanol were charged into the jacketed stirred batch reactor. The temperature of the reacting mixture was allowed to reach the desired value. A known amount of catalyst was added to the jacketed stirred batch reactor when the reacting mixture attained the desired temperature. The time at which the catalyst was added was taken as zero time (t = 0) and sample was withdrawn at t = 0. The samples were withdrawn at regular time intervals and were analysed by a Pye Unicam 104 series gas chromatograph (GC). There may be an experimental error associated with the GC analysis, i.e. maximum about ± 5%, when the samples were analysed manually for the batch kinetic experiments. During the experiment, the temperature of the reacting mixture was maintained in the range of ± 0.5 K. The effect of various parameters such as speed of agitation, catalyst particle size, mole ratio of *n*-hexanol to acetic acid, concentration of acetic acid (w/w), reaction temperature, catalyst loading (w/w) and reusability of the catalysts were studied for the optimisation of the reaction condition.
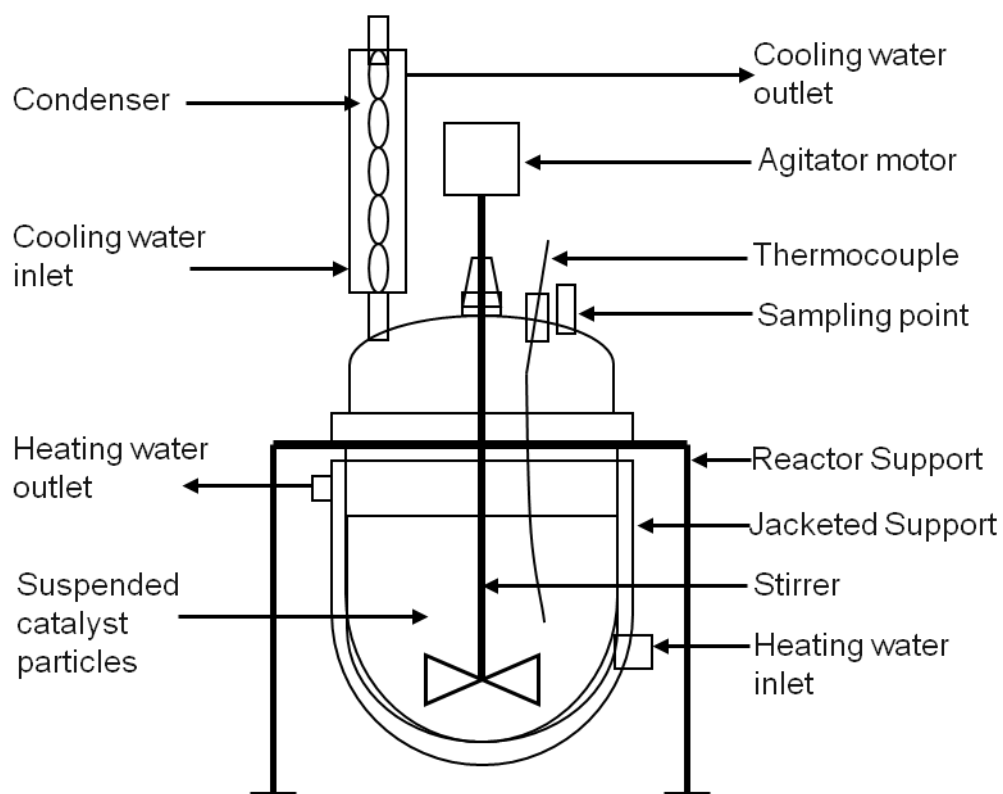
Figure 4.1. Schematic of a batch kinetic experimental set-up.
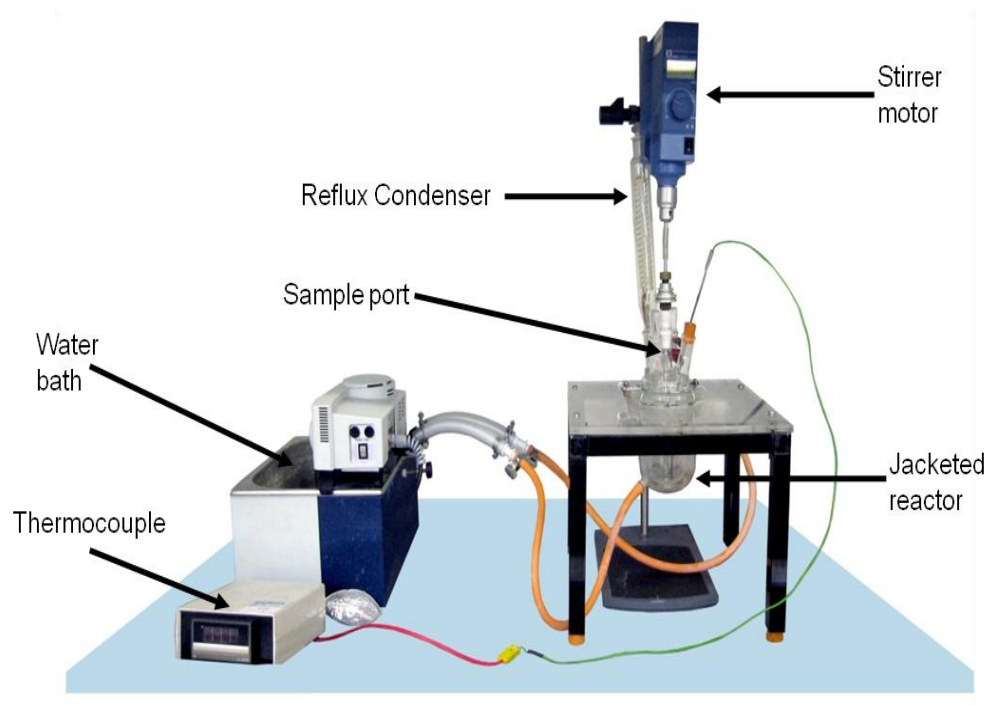
Figure 4.2. Image of a batch kinetic experimental set-up.

4.2.4. Method of Analysis

The samples withdrawn from both the batch kinetic experiments and residue curve map (RCM) experiments were analysed using a Pye Unicam gas chromatograph (GC). The GC was fitted with a thermal conductivity detector (TCD). A packed stainless steel Porapak-Q column (supplied by Supelco) with dimensions (d = 3.175 x 10^{-3} m and L = 1.829 m) was used to separate all the components present in the reaction mixture. High purity (99.9%) helium was used as a carrier gas. The flow rate of the helium gas was maintained at 7.1667 x 10^{-10} m^3 s^{-1}. Both the detector and the injector temperatures were maintained isothermally at 503.15 K.

4.2.4.1. Calibration Curves

Calibration curves were developed to determine the composition of all the components present in the samples collected from batch reactor and residue curve map (RCM) determination experiments. An internal standard method was used to develop the calibration curves and *n*-butanol was used as the internal standard. To develop calibration curves, a number of samples were prepared with known concentration and analysed using Pye Unicam 104 series gas chromatograph. The concentration and area ratio of ith component i.e. CR_i and AR_i, respectively were calculated from Equation (4.1) and (4.2), respectively.

Concentration ratio of ith component (CR_i)

$$= \frac{\text{Concentration of } i^{th} \text{ component } (C_i)}{\text{Concentration of internal standard } (C_{is})} \quad (4.1)$$

$$\text{Area ratio of } i^{th} \text{component } (AR_i) = \frac{\text{Area of } i^{th} \text{ component } (A_i)}{\text{Area of internal standard } (A_{is})} \quad (4.2)$$

Response factor of the ith component (RF_i) is calculated from Equation (4.3).

R.F. of ith component (RF_i)

$$= \frac{\text{Concentration ratio of } i^{th} \text{ component } (CR_i)}{\text{Area ratio of } i^{th} \text{ component } (AR_i)} \qquad (4.3)$$

The above Equation (4.3) can be rearranged in the form of y = m x as shown in Equation (4.4).

$$CR_i = RF_i \times AR_i \qquad (4.4)$$

where,

y = concentration ratio of ith component (CR_i),

x = area of ith component (AR_i), and

slope (m) = response factor of the ith component (RF_i).

A plot of concentration ratio versus area ratio of all the components were plotted for determination of response factor. Once the response factor of individual component was determined, the unknown composition of the samples collected from both batch reactor and residue curve map (RCM) experiments at time t can be determined by Equation (4.4).

4.2.4.2. Internal Standardisation

Internal standard method was used for the analysis of the sample mixture for batch reactor and residue curve map (RCM) experiments. Grob (1995) defined the internal standardisation technique as a method that combines the sample and standard into one injection. A summary of other quantitative analysis is listed in the Appendix 9.5.

The advantages of the internal standardisation technique are given below:
   ❖ The result is expressed as an absolute concentration i.e. if the units of concentration for the internal standard (C_{IS}) for both calibration and analysis are the same; the final answer is expressed in the

concentration units of calibration (C_i). If the units for both C_i and C_{IS} for the calibration are identical, the response factor is dimensionless and it is possible to obtain the final answer in any desired units by simply adjusting the units of C_i for the analysis.

❖ Allowance is made for the response of each component to the detector.

❖ The result of each injection is independent of the injection volume.

The disadvantages associated with using the internal standardisation technique are as follows:

❖ The technique is not readily usable for gaseous samples.

❖ There is a need to select a suitable internal standard.

The pre-requisites for an internal standard are as follows:

❖ The internal standard must be miscible with the samples being analysed.

❖ The internal standard must elute from the column and adequately separated from all samples components i.e. during the GC analysis, the internal standard should give only one peak which must be well resolved from the peaks of the sample components.

❖ The internal standard must elute as near as possible to the desired components and ideally before the last sample peak so that the analysis time is not increased.

❖ The internal standard should preferably be similar in functional group type to the component(s) of interest. If such a compound is

not readily available, an appropriate hydrocarbon should be substituted.

❖ The Internal standard must be stable under the required analytical conditions and must not react with any of the components or solvents present in the sample.

❖ The internal standard must be sufficiently non‑volatile to make allowance for storage of standard solutions for significant periods of time.

❖ In consideration of the prerequisites towards the selection of the internal standard as outlined above, *n*-butanol was chosen as the choice of internal standard for the analysis of the present system.

4.2.4.3. Chromatogram

Figure 4.3 shows a typical chromatogram from Pye Unicam 104 series gas chromatograph. Water peak emerged followed by acetic acid, *n*-butanol, *n*-hexanol and *n*-hexyl acetate. The total time for a single GC run was about 12 min. It is worth noting that the Porapak-Q column separated the sample mixture for this esterification reaction in the order of increasing molecular weight.
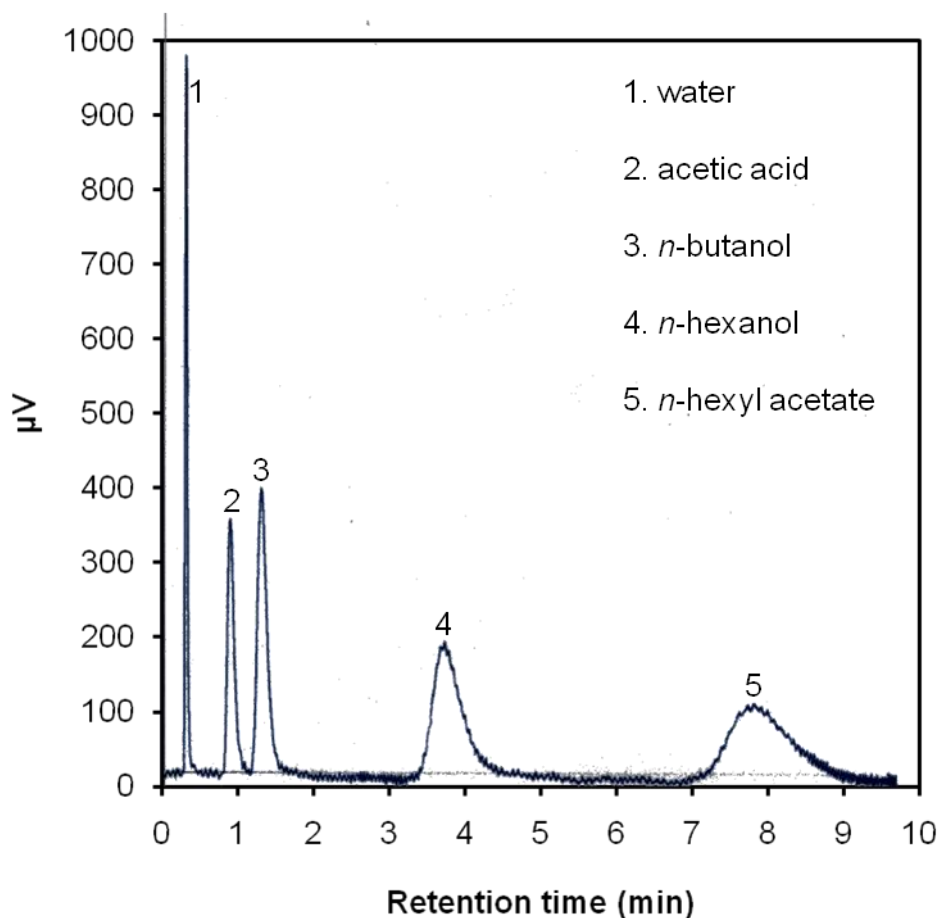
Figure 4.3. A typical chromatogram from Pye Unicam 104 series gas chromatograph (GC).

4.2.5. Mechanism of the Reaction

Acetic acid reacts with *n*-hexanol in the presence of Purolite® CT-124 / Purolite® CT-151 / Purolite® CT-175 or Purolite® CT-275, cation exchange resins to produce a value added ester, *n*-hexyl acetate. It was proposed that the mechanism of this heterogeneous catalysed esterification reaction is similar to homogeneous catalysed esterification reaction (Solomons and Fryle, 2000). The proposed mechanism has been shown in reaction mechanism steps (4.5 – 4.9), respectively.

Reaction mechanism step (4.5):

Acetic acid accepts a proton from strong acid cation exchanger, i.e. Purolite® catalysts as shown in (4.5).

H^+ source: Ion exchange
resin catalyst

(4.5)
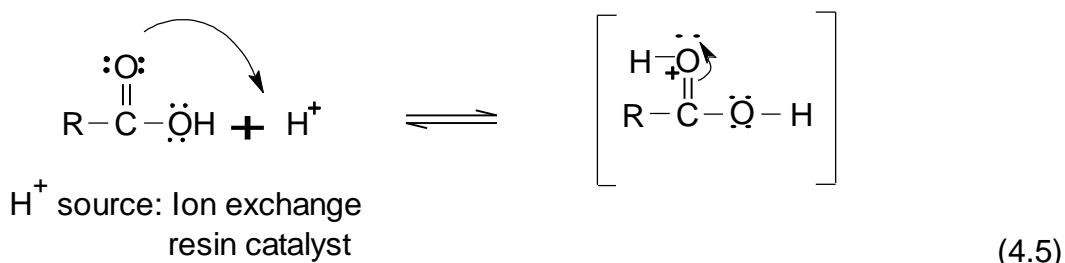
Reaction mechanism step (4.6):

The *n*-hexanol molecule attacks the protonated carbonyl group to form an intermediate as shown in (4.6).

(4.6)
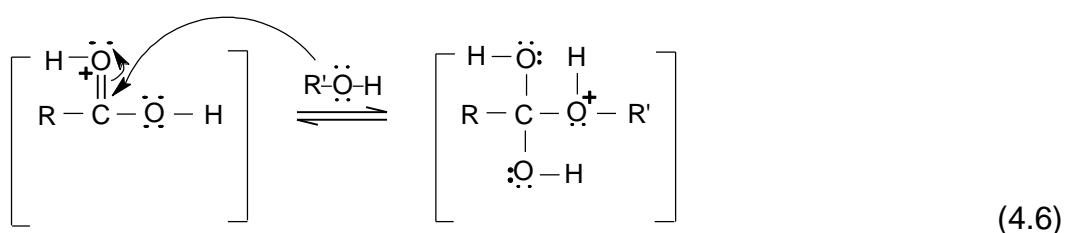
Reaction mechanism step (4.7):

As shown in (4.7) a proton is lost at one oxygen atom and gained at another to form another intermediate.

where, $R = CH_3$ $R' = CH_3(CH_2)_5$

(4.7)
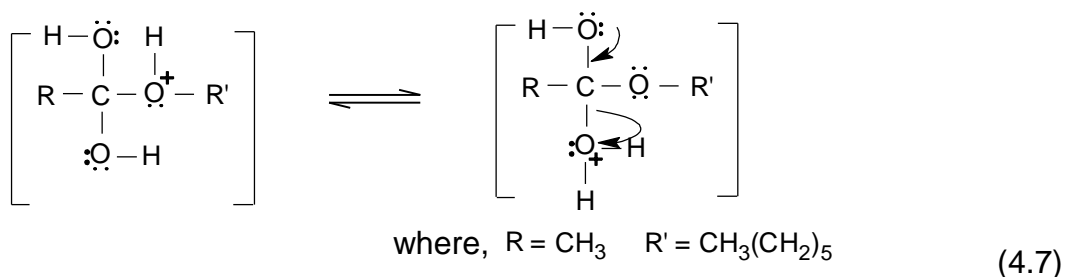
Reaction mechanism step (4.8):

The intermediate formed in the above step then loses a molecule of water to give a protonated ester as shown in (4.8)

where, R = CH$_3$ R' = CH$_3$(CH$_2$)$_5$

(4.8)
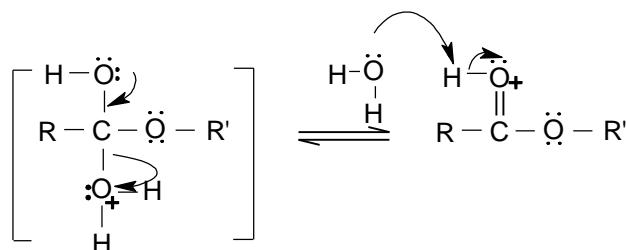
Reaction mechanism step (4.9):

A proton is then transferred to a water molecule to give the desired ester, *n*-hexyl acetate as shown in (4.9).

(4.9)
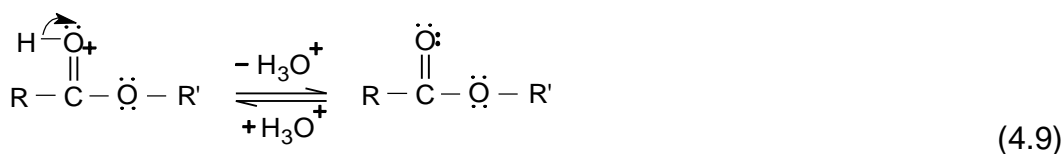
All the above reaction mechanism steps are reversible. It is worth noting that no by-products (such as dihexyl ether or 1-hexene) were formed during the course of the reaction.

4.2.6. Results and Discussion

The effect of agitation speed, catalyst particle size, catalyst types, catalyst loading, acetic acid concentration, feed mole ratio of *n*-hexanol to acetic acid on the rate of reaction and the reusability of the catalysts were investigated for the synthesis of *n*-hexyl acetate in a jacketed stirred batch reactor.

4.2.6.1. Elimination of Mass-Transfer Resistances

The esterification reaction was studied with different stirrer speed using both gelular matrix (Purolite$^®$ CT-124) and macroporous resin (Purolite$^®$ CT-175) catalysts. There are two types of mass transfer resistances associated with this reaction. One across the solid-liquid interface i.e. the influence of external mass transfer resistances and other in the intraparticle space i.e. internal mass transfer resistance which is associated with different catalyst particle size and catalyst internal structure, i.e. porosity, pore size distribution and chemical structure. In order to confirm the influence of external mass transfer resistances, experiments were carried out using different stirrer speed using Purolite$^®$ CT-124 catalyst. The results are shown in Figure 4.4. Figure 4.4 shows that the external mass transfer was absent when experiments were carried out at stirrer speed of 300 rpm and 500 rpm respectively. The conversion of acetic acid at 6 h for a stirrer speed of both 300 rpm and 500 rpm was about 94% respectively. It was therefore confirmed that there was little effect of stirrer speed on the conversion of acetic acid in the range of stirrer speed of 300 rpm and 500 rpm and hence there was no external mass transfer resistances for this esterification reaction. Hence, on the basis of above discussion, it was concluded that there was no influence of mass transfer resistances on the rate of esterification reaction at a stirrer speed of 500 rpm and hence all the further experiments were conducted at 500 rpm with Purolite$^®$ CT-124, Purolite$^®$ CT-151, Purolite$^®$ CT-175 and Purolite$^®$ CT-275 catalysts.

The non-existence of intraparticle resistances was confirmed by using catalyst particles of different size distribution. Also, it was reported in the literature for esterification of acetic acid with *iso*-amyl alcohol (Teo and Saha, 2004) and *n*-butanol (Gangadwala *et al.*, 2003) that no evidence of intraparticle resistances were encountered when the experiments were performed using different catalyst particle sizes. Teo and Saha (2004) used Purolite$^®$ CT-175 catalyst particle sizes of

200 – 400 µm, 500 – 710 µm and 800 – 900 µm, respectively while Gangadwala *et al.* (2003) used Amberlyst 15 catalyst particle sizes of 25 mesh, 72 mesh and 100 mesh, respectively.
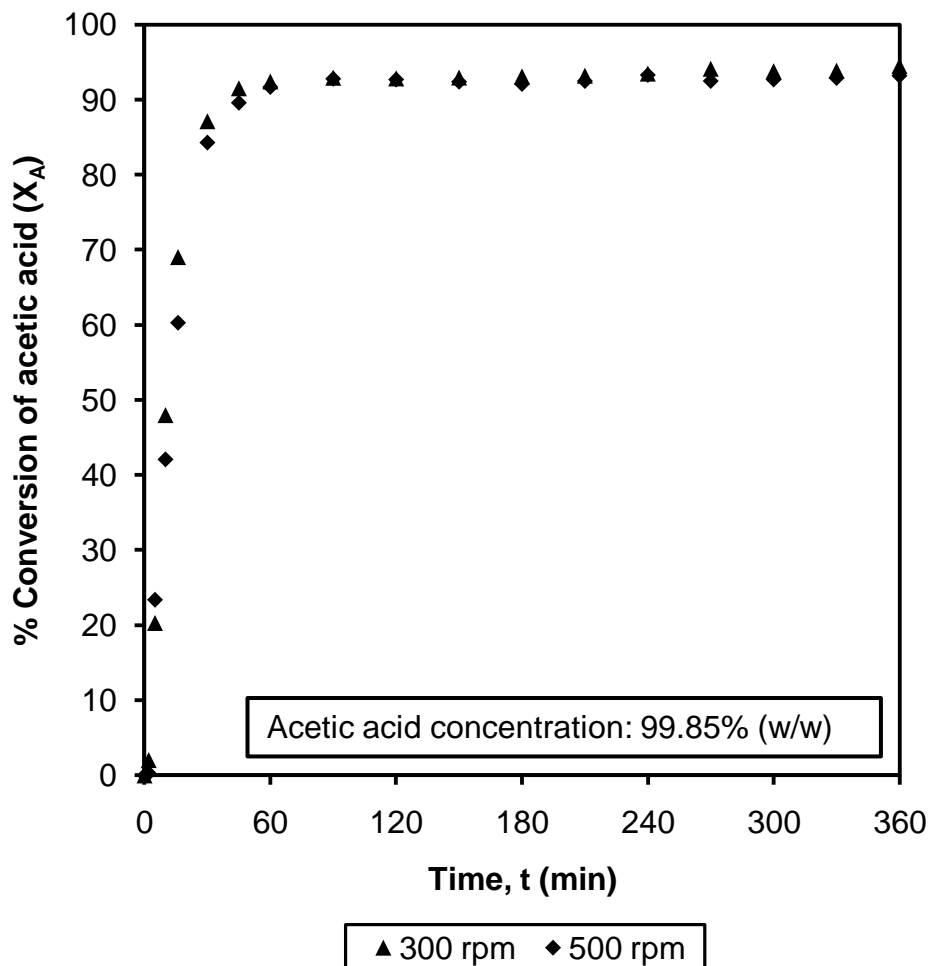
Figure 4.4. Effect of stirrer speed on the conversion of acetic acid at catalyst loading: 5% (w/w); reaction temperature: 368.15 K; feed mole ratio (*n*-hexanol to acetic acid): 4:1; acetic acid concentration: 99.85% (w/w); catalyst: Purolite® CT-124.

4.2.6.2. Effect of Different Catalyst

The synthesis of *n*-hexyl acetate was studied with different types of ion exchange resins, such as Purolite® CT-124, Purolite® CT-151, Purolite® CT-175 and Purolite® CT-275 catalysts. The results are shown in Figures 4.5 and 4.6, respectively. It can be observed from Figure 4.5 that

the performance of Purolite® CT-124 catalyst was the best for this reaction. The conversion of acetic acid after 6 h by using Purolite® CT-124 catalyst was about 78%, whilst that for Purolite® CT-151, Purolite® CT-175 and Purolite® CT-275 (all macroporous) catalysts was about 56%, 60% and 35%, respectively.
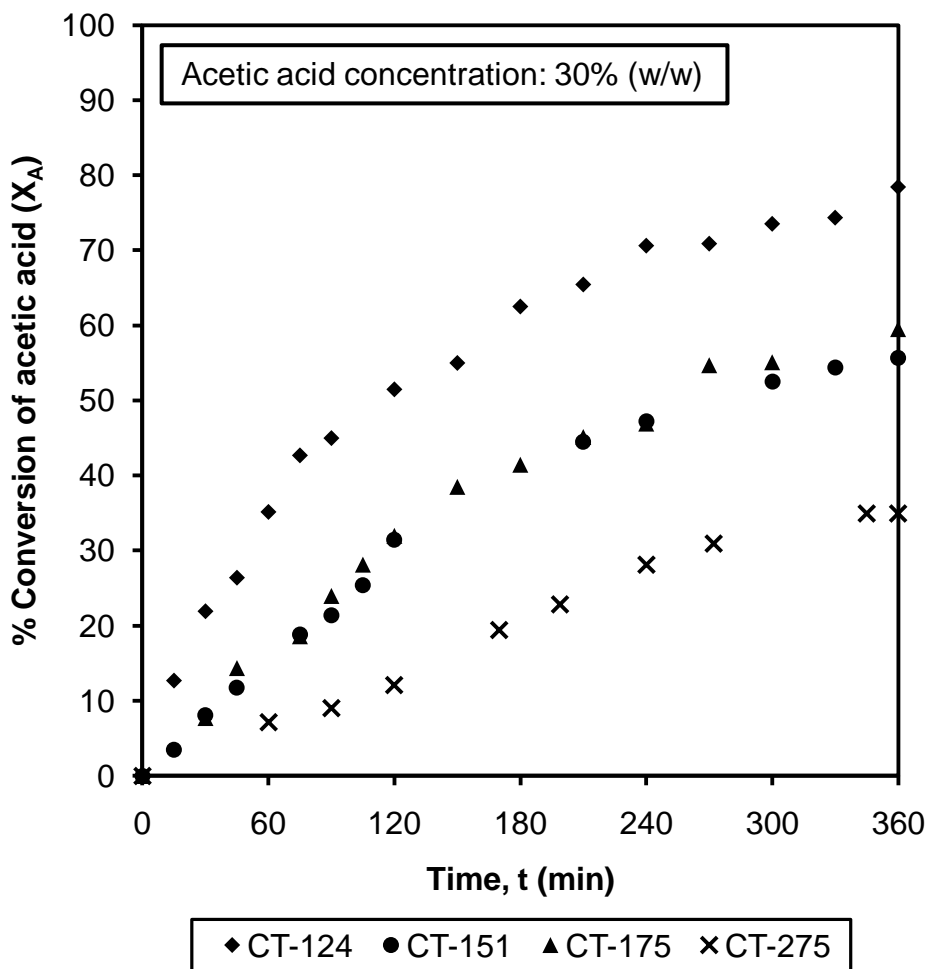
Figure 4.5. Effect of different types of catalyst on the conversion of acetic acid at catalyst loading: 10% (w/w); reaction temperature: 368.15 K; feed mole ratio (*n*-hexanol to acetic acid): 2:1; acetic acid concentration: 30% (w/w); stirrer speed: 500 rpm.

However, Figure 4.6 confirms that all Purolite® ion exchange resin catalysts performed equally for this esterification reaction. The conversion

of acetic acid after 6 h by using Purolite® CT-124, Purolite® CT-151 and Purolite® CT-175 catalysts using concentrated acetic acid was about 94%. It is evident from Figures 4.5 and 4.6, that Purolite® CT-124 was the best performed catalyst irrespective of the concentration of the acetic acid used for the batch reactor experiments.
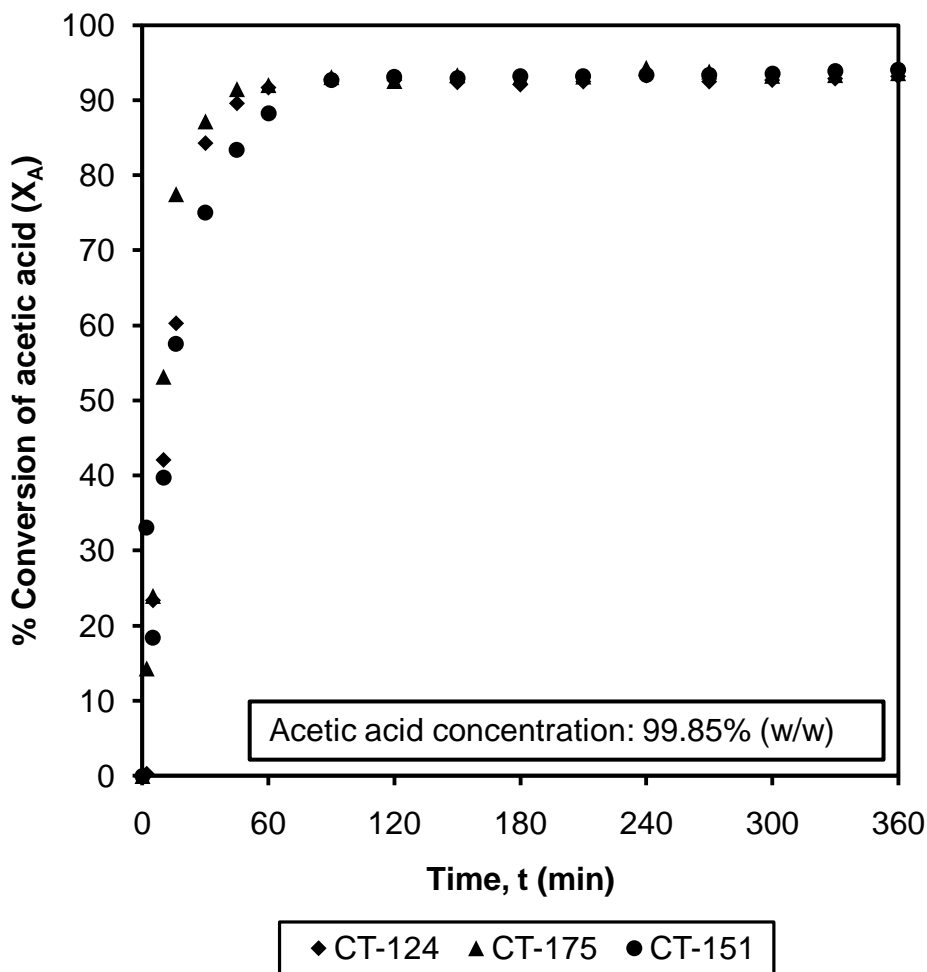
Figure 4.6. Effect of different types of catalyst on the conversion of acetic acid at reaction temperature: 368.15 K; catalyst loading: 5% (w/w); feed mole ratio (*n*-hexanol to acetic acid): 4:1; acetic acid concentration: 99.85% (w/w); stirrer speed: 500 rpm.

It is because the reaction mixture consists of substantial amount of water when using dilute acetic acid as one of the reactants

[containing 30% (w/w) acetic acid and 70% (w/w) water] for experimental results shown in Figure 4.5 and also due to the formation of water during the course of the reaction. It appears that the gelular matrix of Purolite® CT-124 resin catalyst swells in the presence of this reacting mixture for experimental results shown in Figure 4.5 that consists substantial amount of water, which subsequently increases its catalytic activity (Gangadwala *et al.* 2003). On the other hand, four sulphonic groups of the macroporous resins could be attached to one water molecule and since the water is present in abundance, it may hinder the rate of reaction for the macroporous resin catalysts (Zundel, 1969; Saha and Sharma, 1996). Hence all subsequent experiments were conducted with Purolite® CT-124 catalyst for both dilute and concentrated acetic acid.

4.2.6.3. Effect of Catalyst Loading

The esterification reaction was studied at different catalyst loading using Purolite® CT-124 and Purolite® CT-175 catalysts. Catalyst loading is defined as the ratio of mass of catalyst to the mass of reactants fed. The results are shown in Figures 4.7 – 4.9, respectively. Figure 4.7 represents the experiments conducted with dilute acetic acid [30% (w/w)] and Purolite® CT-124 catalysts while Figure 4.8 shows the experiments carried out using dilute acetic acid [30% (w/w)] and Purolite® CT-175 catalyst. It was observed that the increase in catalyst loading increases the rate of reaction and hence improves the conversion of acetic acid. It is because the higher the catalyst loading, the higher is the total number of available active catalytic sites for the esterification reaction. Figure 4.7 illustrates that the conversion of acetic acid after 5 h for a catalyst loading of 5% (w/w) was 37% and that for a 10% (w/w) catalyst loading was 74%. Figure 4.8 shows a similar trend for experiments carried out with dilute acetic acid [30% (w/w)] and Purolite® CT-175 catalyst. From Figure 4.8, it can be seen that the conversion of acetic acid after 6 h for a catalyst loading of 5% (w/w) was 41% and that the conversion of acetic acid after

6 h for a catalyst loading of 10% (w/w) was 60%. For all further experiments involving dilute acetic acid [30% (w/w)], a catalyst loading of 10% (w/w) was chosen.
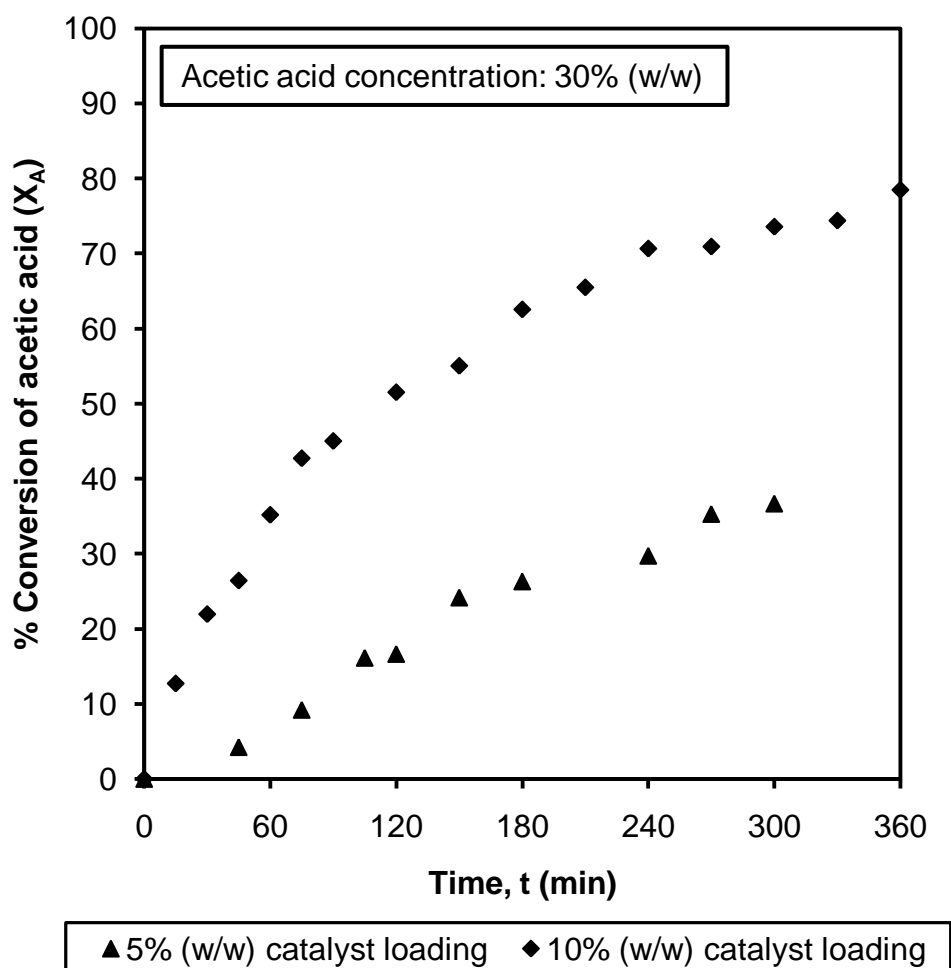
Figure 4.7. Effect of catalyst loading on the conversion of acetic acid at reaction temperature: 368.15 K; feed mole ratio (*n*-hexanol to acetic acid): 2:1; acetic acid concentration: 30% (w/w); catalyst: Purolite® CT-124; stirrer speed: 500 rpm.
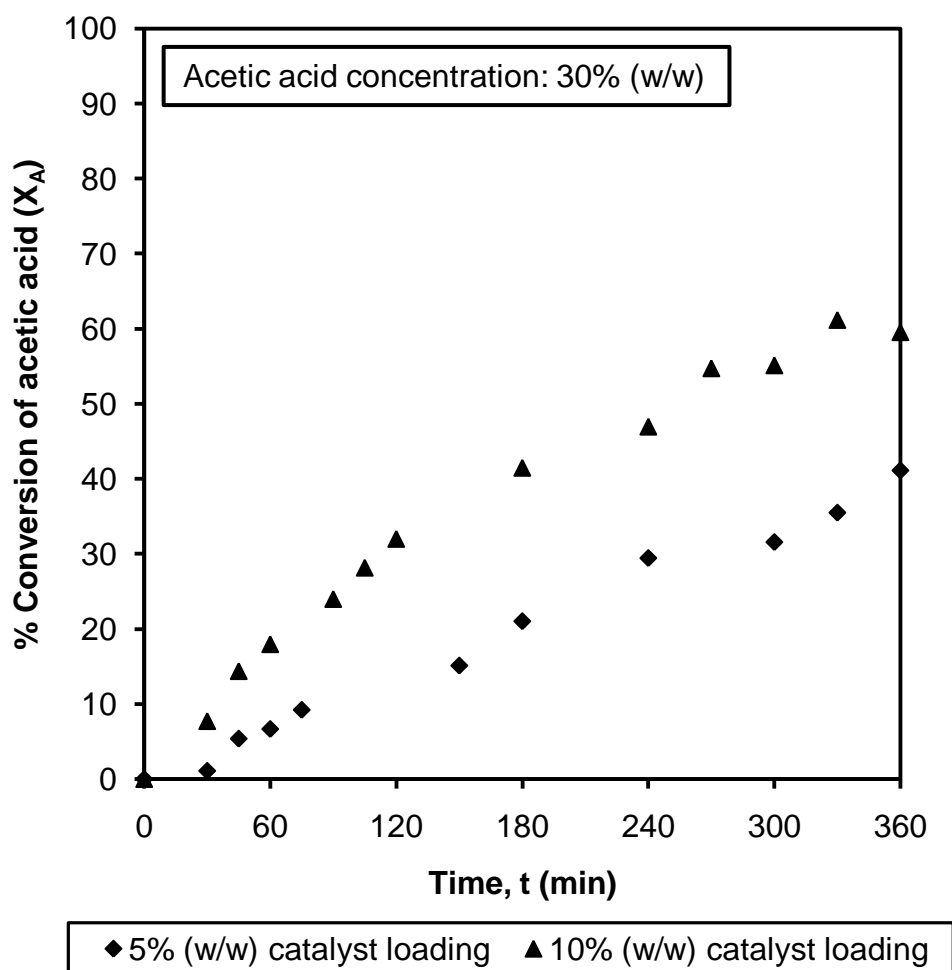
Figure 4.8. Effect of catalyst loading on the conversion of acetic acid at reaction temperature: 368.15 K; feed mole ratio (*n*-hexanol to acetic acid): 2:1; acetic acid concentration: 30% (w/w); catalyst: Purolite® CT-175; stirrer speed: 500 rpm.

The esterification reaction was also studied with concentrated acetic acid at different catalyst loading using Purolite® CT-124 catalyst. The results are shown in Figure 4.9. Figure 4.9 shows that the conversion of acetic acid after 1 h for a catalyst loading of 1.0% (w/w) and 2.5% (w/w) was approximately 60% and 88% while that the conversion of acetic acid after 1 h for a catalyst loading of 5% (w/w) was 92%. For all further experiments involving concentrated acetic acid [99.85% (w/w)], a catalyst loading of 5% (w/w) was chosen. It should be noted in all cases that the equilibrium conversion, however, is independent of the catalyst loading.
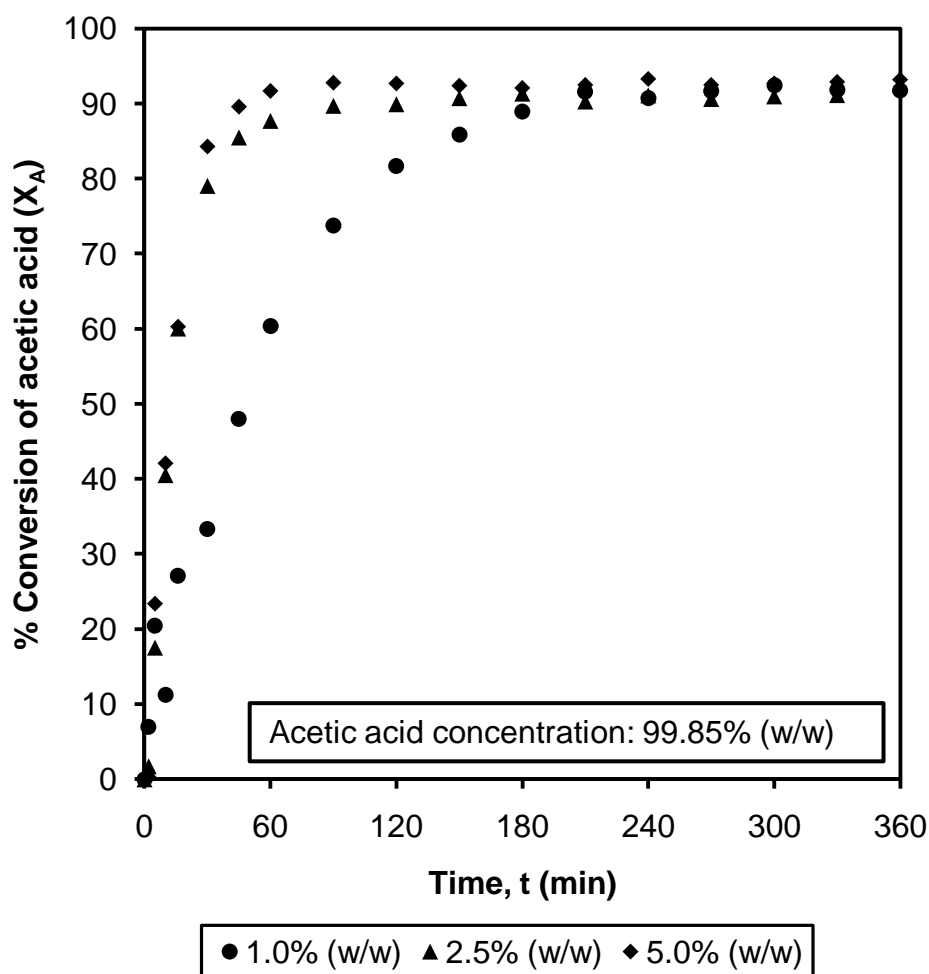
Figure 4.9. Effect of catalyst loading on the conversion of acetic acid at reaction temperature: 368.15 K; feed mole ratio (*n*-hexanol to acetic acid): 4:1; acetic acid concentration: 99.85% (w/w); catalyst: Purolite® CT-124; stirrer speed: 500 rpm.

4.2.6.4. Effect of Feed Mole Ratio (FMR)

Synthesis of *n*-hexyl acetate was studied using different feed mole ratio (FMR) of *n*-hexanol to acetic acid using Purolite® CT-124 catalyst [10% (w/w) catalyst loading] and dilute acetic acid [30% (w/w)]. The results are shown in Figure 4.10. The synthesis of *n*-hexyl acetate is equilibrium limited esterification reaction. The use of an excess *n*-hexanol will therefore increase the rate of reaction and conversion of acetic acid. The results obtained were very similar for the feed mole ratio (*n*-hexanol to acetic acid) of 2:1 and 4:1, respectively. Figure 4.10

demonstrates that the conversion of acetic acid after 4 h for both 2:1 and 4:1 feed mole ratio (*n*-hexanol to acetic acid) was about 71%. All experiments using dilute acetic acid were therefore studied using lower feed mole ratio of *n*-hexanol to acetic acid of 2:1 to minimise the loss of unreacted *n*-hexanol for *n*-hexyl acetate synthesis.
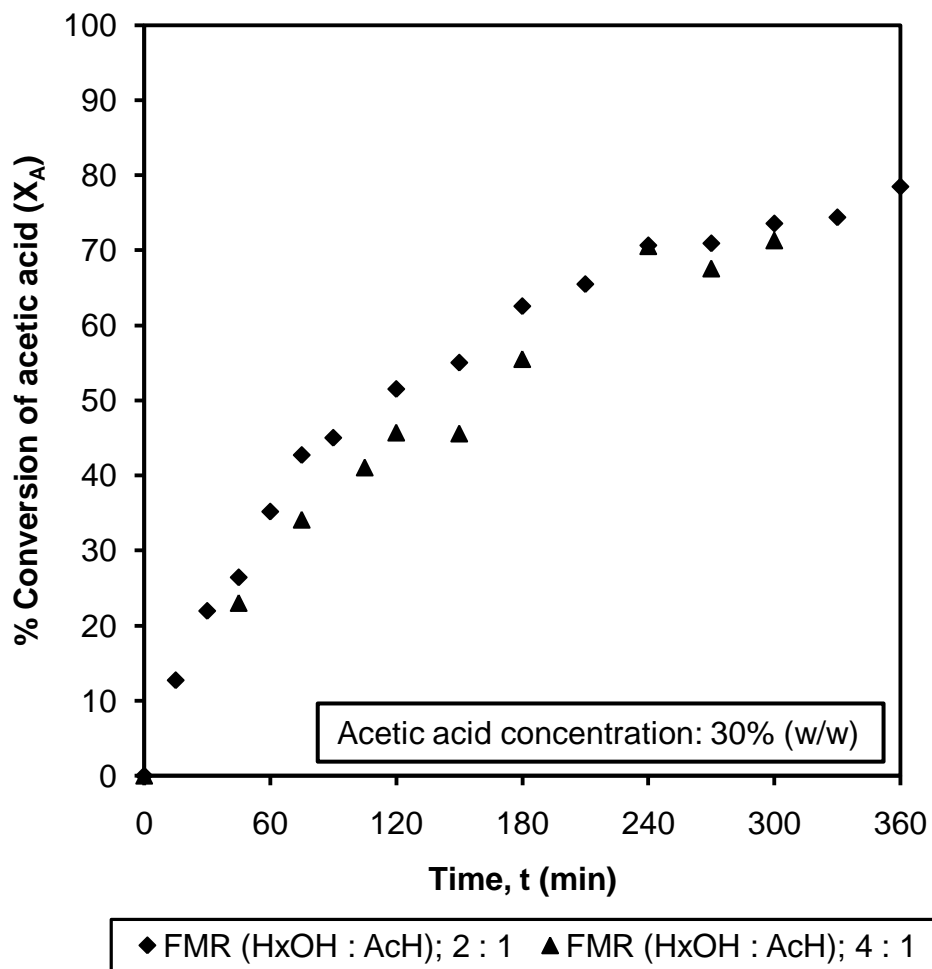
Figure 4.10. Effect of feed mole ratio (FMR) of *n*-hexanol (HxOH) to acetic acid (AcH) on the conversion of acetic acid at reaction temperature: 368.15 K; catalyst loading: 10% (w/w); acetic acid concentration: 30% (w/w); catalyst: Purolite® CT-124; stirrer speed: 500 rpm.

Synthesis of *n*-hexyl acetate was also studied using different feed mole ratio (FMR) of *n*-hexanol to acetic acid using Purolite® CT-124 catalyst [5% (w/w) catalyst loading] and concentrated acetic acid [99.85% (w/w)].

The results are shown in Figure 4.11. Figure 4.11 shows that the conversion of acetic acid after 1 h for 2:1 and 3:1 feed mole ratio (*n*-hexanol to acetic acid) were 74% and 88% respectively, whilst that for 4:1 feed mole ratio (*n*-hexanol to acetic acid) was 92%. All experiments for concentrated acetic acid were therefore studied using a feed mole ratio (*n*-hexanol to acetic acid) of 4:1.
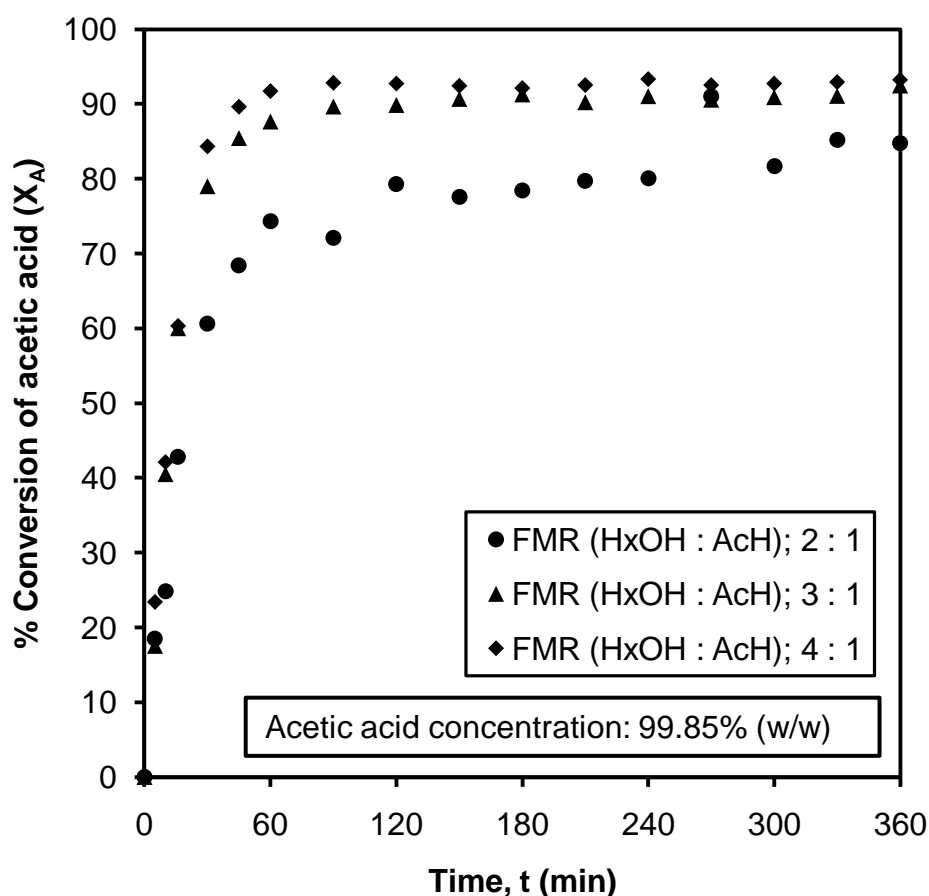
Figure 4.11. Effect of feed mole ratio (FMR) of *n*-hexanol (HxOH) to acetic acid (AcH) on the conversion of acetic acid at reaction temperature: 368.15 K; catalyst loading: 5% (w/w); acetic acid concentration: 99.85% (w/w); catalyst: Purolite® CT-124; stirrer speed: 500 rpm.

4.2.6.5. Effect of Catalyst Reusability

Reusability of Purolite® CT-124 catalyst was studied for the synthesis of *n*-hexyl acetate using dilute acetic acid. The catalyst was reused by washing it with methanol and dried in a vacuum oven at 373 K for about 6 h. The results are shown in Figure 4.12. Figure 4.12 shows that the conversion of acetic acid after 6 h for fresh Purolite® CT-124 catalyst was 63%, while the same for reused (once) catalyst was about 55%.
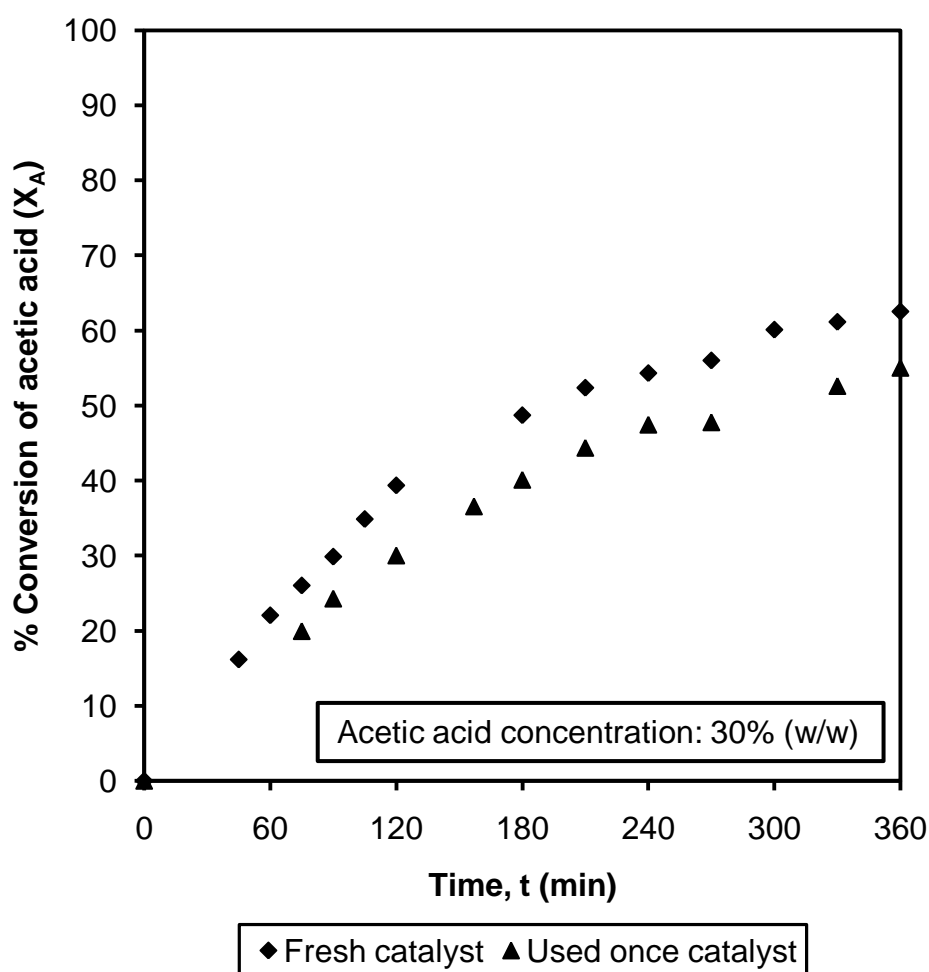
Figure 4.12. Effect of catalyst reusability on the conversion of acetic acid at reaction temperature: 358.15 K; catalyst loading: 10% (w/w); feed mole ratio (*n*-hexanol to acetic acid): 2:1; acetic acid concentration: 30% (w/w); catalyst: Purolite® CT-124; stirrer speed: 500 rpm.

Similarly, the reusability of Purolite® CT-124 catalyst was also studied for the synthesis of *n*-hexyl acetate using concentrated acetic acid. The catalyst was reused washing it with methanol and dried in a vacuum oven at 373 K for about 6 h. The results are shown in Figure 4.13. It can be observed that Purolite® CT-124 catalyst gives very similar conversion of acetic acid after being reused once under otherwise identical condition. It can be seen from Figure 4.13 that the conversion of acetic acid after 1 h for both fresh Purolite® CT-124 catalyst and reused (once) catalyst was
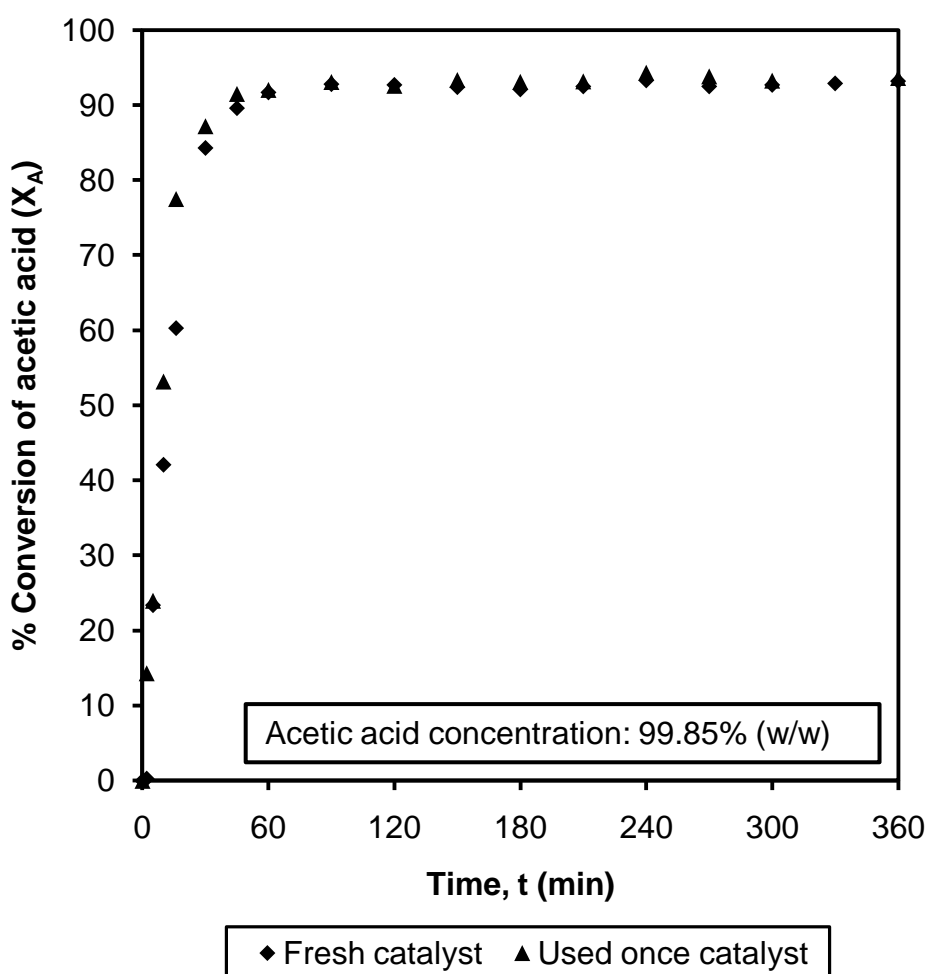
Figure 4.13. Effect of catalyst reusability on the conversion of acetic acid at reaction temperature: 368.15 K; catalyst loading: 5.0% (w/w); feed mole ratio (*n*-hexanol to acetic acid): 4:1; acetic acid concentration: 99.85% (w/w); catalyst: Purolite® CT-124; stirrer speed: 500 rpm.

about 92%. It is therefore concluded that Purolite® CT-124 catalyst can be used for several experimental runs carried out with both dilute and concentrated acetic acid without any appreciable decrease in the conversion of acetic acid. Teo and Saha (2004) also reported that Purolite® CT-175 resin catalyst can be used repeatedly without significant change in conversion of acetic acid for *iso*-amyl acetate synthesis.

4.2.6.6. Effect of Acetic Acid Concentration

Synthesis of *n*-hexyl acetate was studied at different concentration of acetic acid using Purolite® CT-124 catalyst. The experiments were conducted at 10% (w/w) catalyst loading and feed mole ratio (*n*-hexanol to acetic acid) of 2:1. The results are shown in Figure 4.14. Figure 4.14 represents that the conversion of acetic acid after 6 h for 20% (w/w) acetic acid concentration was 73% and that for 30% (w/w) acetic acid concentration was 78%.

All further experiments were carried out with 30% (w/w) acetic acid concentration. Typical values of acetic acid from many chemical and petrochemical processes are in the range of 5 – 65% (w/w) (Teo and Saha, 2004). The study of effect of acetic acid concentration was therefore utmost importance so as to recover the acetic acid from these petrochemical and fine chemical industries.
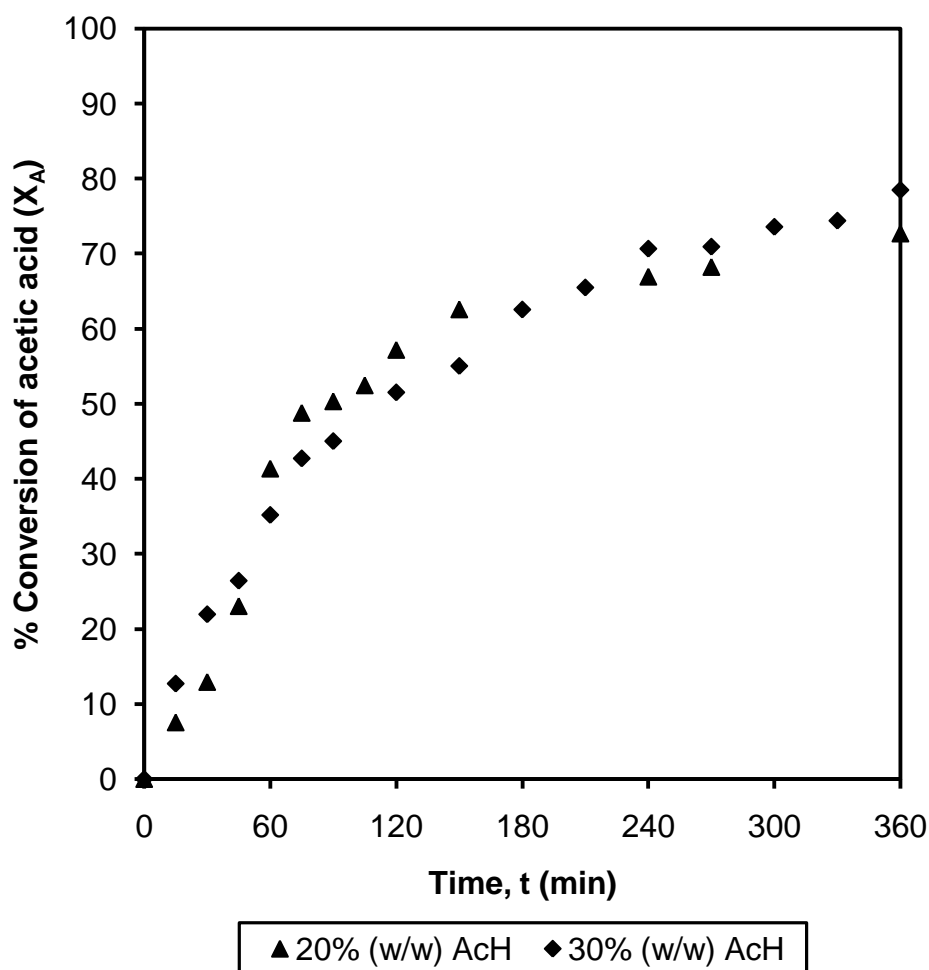
Figure 4.14. Effect of acetic acid concentration on the conversion of acetic acid at reaction temperature: 368.15 K; catalyst loading: 10% (w/w); feed mole ratio (n-hexanol to acetic acid): 2:1; catalyst: Purolite® CT-124; stirrer speed: 500 rpm.

4.3. RESIDUE CURVE MAP DETERMINATION

4.3.1. Introduction

Simple distillation is a process in which a multi-component liquid mixture is slowly boiled in an open pot and the vapours are continuously removed as they form. At any instant of time the vapour is in equilibrium with the liquid remaining in the still. The vapour is always richer in the more volatile components than the liquid; hence the liquid composition changes continuously with time. It therefore becomes more and more concentrated. A simple distillation residue curve is a graph showing how the composition

of the liquid residue curves on the pot changes over time. In other words, the trajectory of liquid compositions starting from some initial point is called simple distillation residue curve or simply a residue curve The collection of all such curves for a given mixture is called a residue curve map (RCM). Residue curve maps contain the same information as phase diagrams, but represent this information in a way that is more useful for understanding how to synthesise a distillation sequence to separate a mixture.

4.3.2. Theory

Residue curve is defined as the locus of the liquid composition remaining from a simple distillation process. Doherty and Perkins (1978) stated that a residue curve is derived from a simple distillation process. Tapp *et al.* (2003) gave an illustration of the simple distillation process. In Figure 4.15, a liquid mixture of known composition is heated in a single batch still at constant pressure without reflux. The components in the liquid will evaporate at different rates due to volatility differences, except at azeotropes. At time t, the liquid is vapourised, and the vapour is removed from the contact with the liquid as it is formed. At this point, the vapour is in equilibrium with the remaining liquid. The vapour is withdrawn from the still as a distillate. As there is no additional feed and reflux of the distillate, the composition of the remaining liquid will be enriched in the less volatile component with respect to time. The vapour formed on the other hand will always be richer in more volatile component than the liquid from which it is formed. The progression of the distillation process will result in the residue becoming more depleted in the more volatile component. Consequently, the distillate withdrawn would be richer in the most volatile component.

Barbosa and Doherty (1998) stated that the residue curves are closely related to the composition profiles in continuous distillation processes, which is one of the main reasons for studying simple distillation. A collection of these residue curves for a given reacting system is called a residue curve map (RCM).
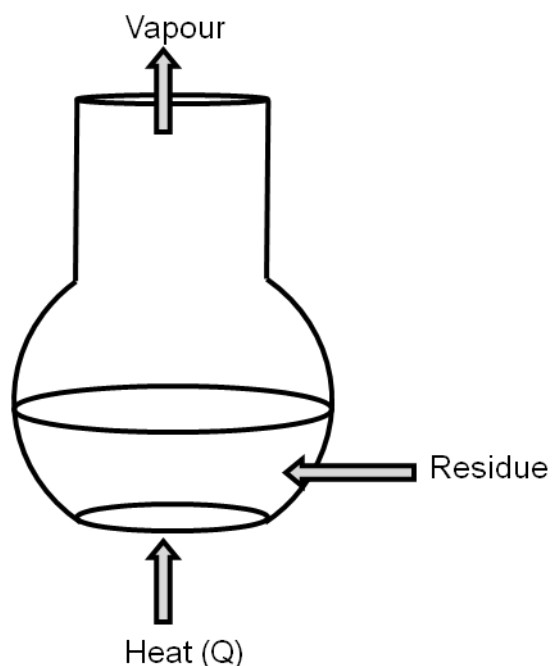
Figure 4.15. A simple batch still.

Definitions of some common terms used for residue curve map (RCM) (Seader and Henley, 1998).

Node

It is the point at which residue curves begins and ends.

Stable Node

It is the point where the component or azeotrope which has the highest boiling point in the region exists. All the residue curves in the region terminates at this point (Figure 4.16a)

Unstable Node

It is the point where the component or azeotrope which has the lowest boiling point in the region exists (Figure 4.16b)

Saddle

It is the point where the residue curves move toward and then move away. Pure components and azeotropes which have a boiling point between the stable and unstable nodes are termed saddles (Figure 4.16c).
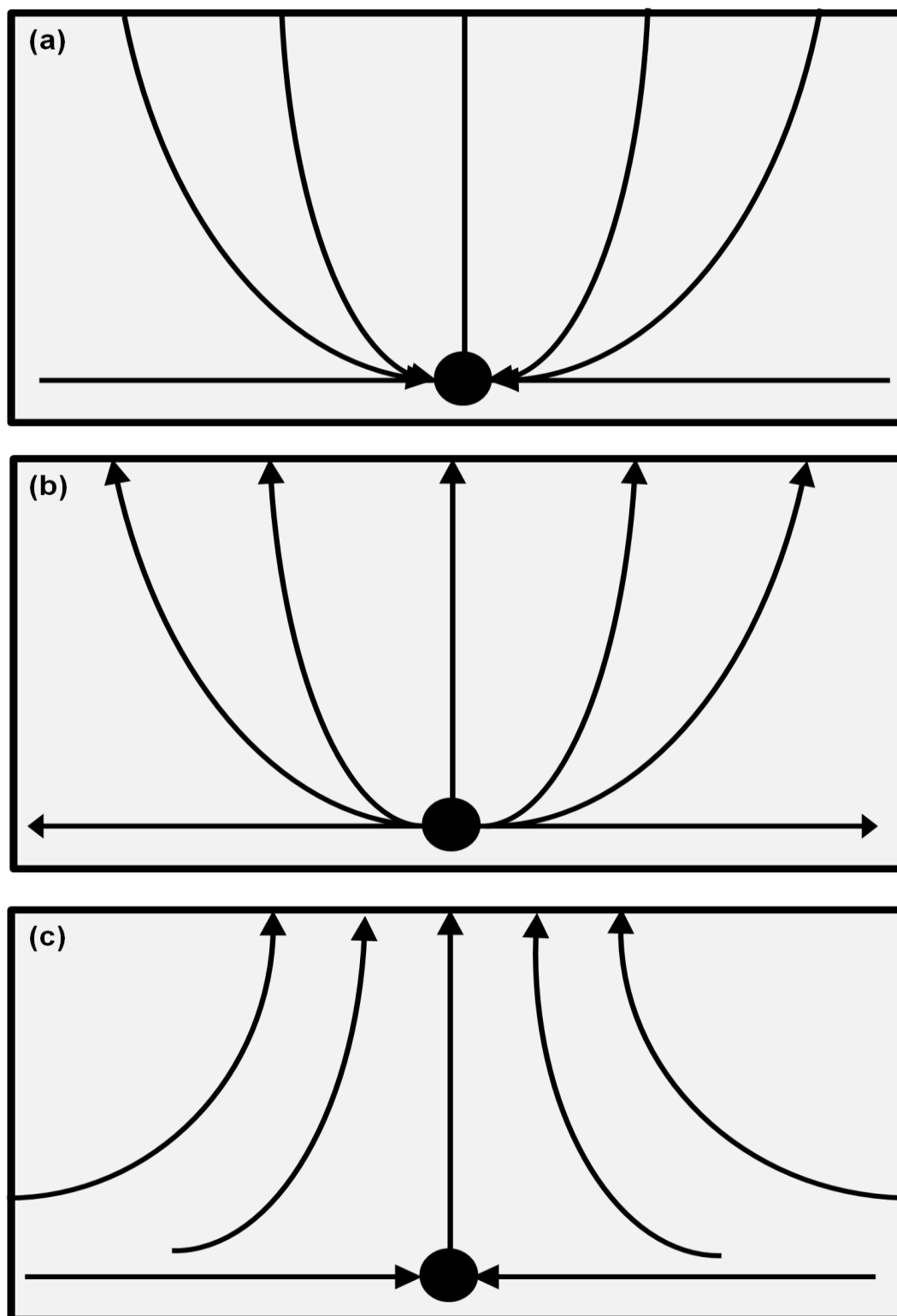
Figure 4.16. Classification of singular points in a residue curve map. (a) a stable node; (b) an unstable node; (c) a saddle point (Fien and Liu, 1994).

All of the residue curves originate at the light (lowest boiling) pure component in a region. It moves towards the intermediate boiling component. In the end it moves at the heavy (highest boiling) pure component in the same region. The lowest temperature nodes are termed as unstable nodes (UN), while the highest temperature points in the region are termed stable nodes (SN). The point that the trajectories approach from one direction and end in a different direction (as always is the point of intermediate boiling component) are termed saddle point (S). Residue curve that divide the composition space into different distillation regions are called distillation boundaries.

A few characteristics of residue curve map (RCM) are given below:

❖ If the direction of the residue curves from the start to end composition is considered, then the arrow on each curve will point from lower to higher boiling component/azeotrope.

❖ Distillation boundaries are created if azeotropes are present. Distillation boundaries cannot be crossed by residue curve.

❖ The distillation boundaries represent the residue curve on which the light or starting residue composition is a lower boiling pure component or azeotrope and the heavy or ending composition residue is a higher pure component or azeotrope.

❖ The distillation boundaries divide the residue curve map into distillation regions. The nature of the regions is such that two pure components which are present in different regions cannot be separated using conventional reactor-separator distillation.

The reactive residue curve map (RCM) for toluene + benzene + *o*-xylene system and for formaldehyde (FA) + methanol (MeOH) + water (H$_2$O) system as well as for non-reactive residue curve map (RCM) for methanol

(MeOH) + methyl acetate (MeAc) + butanol (BuOH) + butyl acetate (BuAc) system and non reactive residue curve map (RCM) for methyl-*tert*-butyl ether (MTBE) + methanol (MeOH) + *iso*-butene (IB) system is reported in the literature (Jimenez *et al.*, 2001).

The method for synthesis and analysis of both non-reactive and reactive residue curve map (RCM) for methyl acetate system was reported by Song *et al.* (1998). Non-reactive residue curve map for butyl acetate (BuAc) + butanol (BuOH) + water (H_2O) is reported in the literature (Venimadhavan *et al.,* 1999; Gangadwala *et al.*, 2004). Non-reactive residue curve map analysis for the methyl acetate (MeAc) + butanol (BuOH) + butyl acetate (BuAc) + methanol (MeOH) was studied by Jimenez *et al.* (2002).

4.3.3. Materials and Catalysts

Acetic acid (99.85%), *n*-hexanol (98%) and methanol (99.9+%) were purchased from Acros Organics, UK; *n*-hexyl acetate (99%) was supplied by Aldrich Chemical Company, Inc. and *n*-butanol (99+%) was purchased from Fisher Scientific, UK. The purity of all chemicals was verified by gas chromatography (GC) analysis. These chemicals were used without further purification. Sulfonated cation exchange resin, Purolite® CT-124, supplied by Purolite® International Limited, UK was used for the residue curve map (RCM) experiments. Purolite® CT-124 catalyst used was first washed with methanol, dried in a vacuum oven at 373 K for 6 h to remove any water sorbed on the catalyst, before carrying out the experiments. Safety data sheet (SDS) of all the chemicals and the catalysts used are attached in Appendix 9.2.1 and 9.2.2. COSHH (Control of Substances Hazardous to Health) and Risk Assessment (RA) records for residue curve map (RCM) determination experiments were carried out before conducting the experiments and are attached in Appendix 9.3 and 9.4, respectively.

4.3.4. Experimental Set-Up and Procedure

Figure 4.17 is a schematic of the experimental set-up used for the residue curve map (RCM) determination. The three neck glass flask of 0.5×10^{-3} m^3 capacity was used for the experiment. Two condensers were
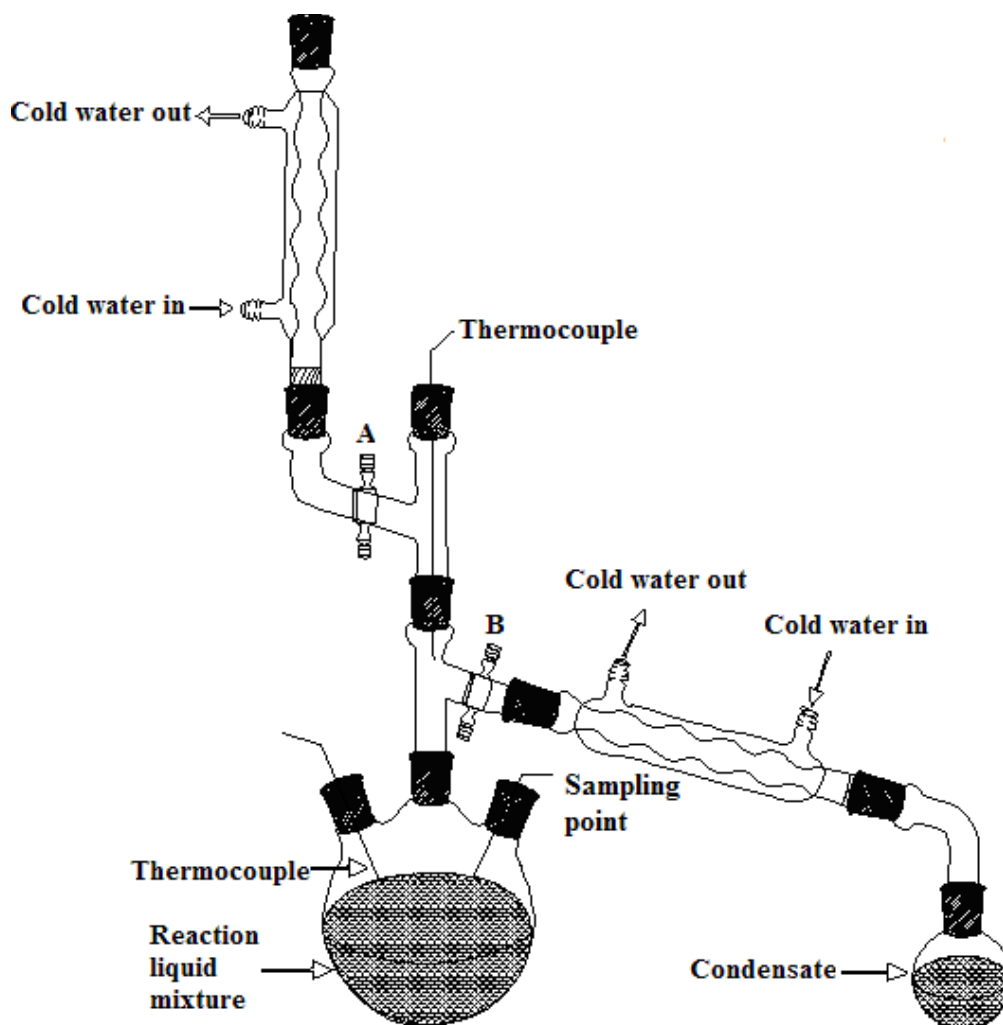
Figure 4.17. Schematic of residue curve map (RCM) determination experimental set-up.

used for the total reflux of the reaction mixture and condensation of the vapour. Two thermocouples were inserted through the glass flask to measure the vapour and liquid temperatures. The reacting mixture in the flask was stirred by a magnetic stirrer. A heating element was used to heat

the reacting mixture in the flask. The reaction flask and distillation head were insulated with glass wool to minimise the heat loss to the surroundings. About 10% (w/w) catalyst loading and about 0.21 – 0.23 L of the liquid mixture of desired initial composition was charged to the reaction flask. Valve A of the distillation head was kept open and valve B was closed. Constant heat input was supplied to the flask and electrical supplies to the magnetic stirrer were switched on so that the liquid was totally refluxed and that the temperatures of both liquid and vapour phases of the mixture reached the steady state. At steady state, valve A was closed and valve B was opened, so that the vapour was condensed continuously into a collection flask. During the distillation process, the liquid samples were taken every 10 min and analysed by a Pye Unicam 104 series gas chromatograph (GC) for their composition. The RCM determination experimental run was stopped when the amount of liquid residue in the reaction flask was small enough to preclude sampling. Subsequent experimental runs were carried out at compositions close to the measured end point of the previous experimental run so as to obtain a significant portion of each residue curve. During the experimental run, the vapour was in equilibrium with the liquid remaining in the still. Since the vapour was always richer in the more volatile components than the liquid, the liquid mixture composition changed continuously with time, becoming more concentrated in the least volatile species. The RCM determination experiment was terminated when the boiling point of the residue reaches the maximum (i.e. the reactant mixture in the still reaches either the maximum boiling azeotrope or the highest boiling pure component composition). Each experimental run takes about 45 to 90 min to reach steady state and about 60 to 180 min depending upon the initial reactant feed composition before the still ran dry for collecting the equilibrium RCM data.

4.3.5. Method of Analysis

The analytical method used for the analysis of the samples for RCM experiments are same as those explained in detail for the batch kinetic experiments (see Chapter 4, section 4.2.4).

4.3.6. Results and Discussion

Residue curve map determination experiments also known as simple distillation experiments were performed to elucidate the feasibility of *n*-hexyl acetate synthesis through the recovery of dilute acetic acid in a reactive distillation column (RDC). All the residue curves originate at the light (lowest boiling) pure component in a region. It then moves towards the intermediate boiling component. At the end it moves towards the heavy (highest boiling) pure component in the same region. The lowest temperature nodes are termed as unstable nodes, while the highest temperature points in the region are termed stable nodes, the point at which the residue curve terminates. The point at which the trajectories approach from one direction and end in a different direction (as always is the point of intermediate boiling component) are termed saddle point. Residue curves that divide the composition space into different distillation regions are called distillation boundaries. The RCM gives a preliminary idea of the feed mole ratio (FMR) of *n*-hexanol to acetic acid which is one of the important parameters for the operation of an RDC. Therefore, for RCM determination, experiments were carried out over a wide range of feed mole ratio (FMR) of *n*-hexanol to acetic acid (FMR = 4:1, FMR = 2:1, FMR = 1:1, FMR = 0.5 : 1 and FMR = 0.3:1) to obtain the maps. Figure 4.18 shows the representation of all the residue curves known as residue curve maps (RCM).
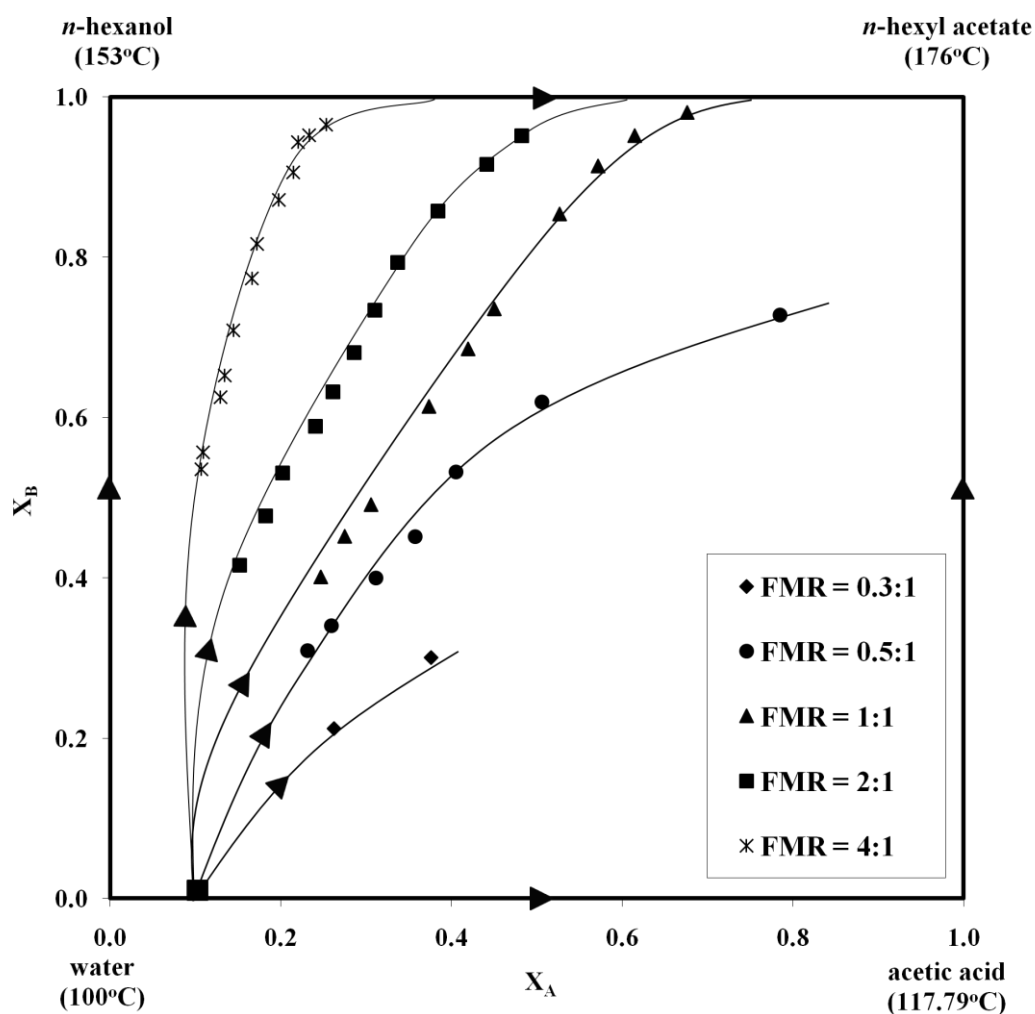
Figure 4.18. Representation of residue curves at different feed mole ratio (FMR) of *n*-hexanol to acetic acid; catalyst loading: 10% (w/w); acetic acid concentration: 30% (w/w); catalyst: Purolite® CT-124; constant stirrer speed; constant heat input.

The residue curve map (RCM) for the esterification of 30% (w/w) dilute acetic acid with *n*-hexanol to produce *n*-hexyl acetate and water was defined by a rectangular diagram as illustrated in Figure 4.18. The four corners of the square represents the four pure components (i.e. acetic acid, *n*-hexyl acetate, *n*-hexanol and water) and the four edges represents the four binary non-reactive mixtures consisting of one reactant and one product (i.e. water – acetic acid; acetic acid – *n*-hexyl acetate;

n-hexyl acetate – *n*-hexanol and *n*-hexanol – water). The interior of the square represents a four component mixture (i.e. water – acetic acid – *n*-hexanol – *n*-hexyl acetate) in phase and reaction equilibrium.

For this esterification reaction the independent transformed composition shown by Equations (4.10), (4.11) and (4.12) are as follows:

$$X_A \quad = \quad X_{acetic\ acid} \quad + \quad X_{n\text{-hexyl acetate}} \tag{4.10}$$

$$X_B \quad = \quad X_{n\text{-hexanol}} \quad + \quad X_{n\text{-hexyl acetate}} \tag{4.11}$$

$$X_C \quad = \quad X_{water} \quad - \quad X_{n\text{-hexyl acetate}} \tag{4.12}$$

where X_A, X_B and X_C are the transformed variables while X_i is the liquid phase molar composition of the component. The azeotropes reacted into a four-component equilibrium mixture in presence of Purolite$^®$ CT-124 gelular resin. The remarkable feature of the RCM was the formation of the four component minimum-boiling reactive azeotrope (see Figure 4.18). The closed big square on the X-axis of Figure 4.18 indicates the position of the reactive azeotrope as closely as it could be determined from the present work of simple distillation experiment. The measured molar composition of the reactive azeotrope was 88.78% water, 10.23% acetic acid, 0.59% *n*-hexanol and 0.4% *n*-hexyl acetate. The corresponding transformed composition of *n*-hexyl acetate system are $X_A = 0.1063$ and $X_B = 0.0099$ at temperature of 375.3 K. From Figure 4.18, it can be seen that if the synthesis of *n*-hexyl acetate is performed in a reactive distillation column using feed mole ratio of *n*-hexanol to acetic acid of 4:1, the top product will be a mixture of mostly *n*-hexanol and the desired product, *n*-hexyl acetate, while the bottom product will consist of mainly water, some unreacted acetic acid and *n*-hexanol. For the recovery of dilute acetic acid in an RDC, it is desirable to have the bottom product that contains mainly water and minute quantity of

acetic acid. Moreover, the presence of huge amount of unreacted *n*-hexanol along with the desired product, *n*-hexyl acetate in the top product stream of RDC is not a viable option. So feed mole ratio (*n*-hexanol to acetic acid) of 4:1 is not recommended for reactive distillation column (RDC) experiments. On the other hand, if very low feed mole ratio of alcohol to acid (0.3 and 0.5) is used, the top product will be a mixture of acetic acid and *n*-hexyl acetate, while the bottom product will be a mixture of mostly water with some quantities of unreacted acetic acid and *n*-hexanol. A low feed mole ratio of *n*-hexanol to acetic acid indicates that the top product in the RDC will contain substantial amount of acetic acid, which is not desirable for the acetic acid recovery point of view. This observation is also supported by the azeotropic data reported by Schmitt *et al.* (2004) and also by the fact that there is a large difference in the boiling point of *n*-hexyl acetate (176°C) and acetic acid (117.79°C). Hence the RCM results suggest that a starting feed mole ratio of *n*-hexanol to acetic acid in the range of 1.2 to 2.0 is the most viable option for the recovery of dilute acetic acid in the continuous RDC operation. The formation of the four component minimum-boiling reactive azeotrope was reported for the esterification of acetic acid with *iso*-amyl alcohol (Gelosa *et al.*, 2003).

4.4. CONCLUSIONS

A residue curve map (RCM) could be used to elucidate the feasibility of reactive distillation for a reacting system. The main conclusions drawn from the residue curve map determination experiments are as follow:

- ❖ The non-reactive azeotropes are eliminated with the addition of Purolite® CT-124 catalyst into the reacting system.

- ❖ A minimum boiling four component reactive azeotrope was formed at 375.3 K. The measured molar composition of the reactive

azeotrope was 10.23% acetic acid, 0.59% *n*-hexanol, 0.4% *n*-hexyl acetate and 88.78% water.

❖ The residue curve map (RCM) suggests the use of starting feed mole ratio (FMR) of *n*-hexanol to acetic acid in the range of 1.2 to 2.0 in the reactive distillation column so that the desired product, *n*-hexyl acetate would only be present in the top product stream. Moreover, a fraction of acetic acid would be present in the bottom product stream.

CHAPTER 5

BATCH KINETIC MODELLING

5. BATCH KINETIC MODELLING

5.1. INTRODUCTION

A batch kinetic model was developed for the esterification reaction of *n*-hexanol with acetic acid in the presence of ion exchange resins. In the subsequent sections, both heterogeneous kinetic models such as Langmuir–Hinshelwood–Hougen–Watson (LHHW), Eley–Rideal (ER) and modified Langmuir–Hinshelwood–Hougen–Watson (ML) and homogeneous kinetic model such as pseudo homogeneous (PH) are derived. These kinetic models were used to correlate the experimental kinetic data under different operating conditions. The kinetic models developed were used to determine the activation energy for this esterification reaction which is explained in detail in the next sections.

5.2. THE KINETIC MODELS

All batch kinetic experiments were carried out in the presence of a solid ion exchange resin catalyst. The heterogeneous kinetic models such as Langmuir–Hinshelwood–Hougen–Watson (LHHW), Eley–Rideal (ER) and modified Langmuir–Hinshelwood–Hougen–Watson (ML) as well as pseudo homogeneous kinetic model (PH) were used for correlating the kinetic data obtained experimentally at different temperatures. Reaction rates were calculated by the differential methods as proposed by Cunill *et al.* (2000). The reaction rates for the heterogeneously catalysed esterification reaction for synthesis of *n*-hexyl acetate can be written as shown in Equation (5.1):

$$-r_A \cdot (V) = N_{A0} \left(\frac{dX_A}{dt} \right) \qquad (5.1)$$

where, $-r_A$ is the reaction rate of decomposition of acetic acid (limiting reactant), V is the volume of the reacting mixture, N_{A0} is the initial number of moles of acetic acid, X_A is the conversion of acetic acid at time (t) and t is the reaction time.

In accounting for the non-ideal mixing behavior of the bulk liquid phase, the activity of the components was taken into account instead of the concentration of the components. Lee *et al.* (2000), Sanz *et al.* (2002) and Zhang *et al.* (2004) adopted the same approach by using the activities whilst taking into account the nonideality of the liquid phase. Fredenslund *et al.* (1975) highlighted that the UNIFAC method for predicting the liquid phase activity coefficients was a useful tool towards the calculation of vapour-liquid equilibrium compositions in situations where no experimental information was available. Reid *et al.* (1987) reported that the UNIFAC group contribution method was used for the estimation of the activity coefficients. Fredenslund *et al.* (1975) and Skjold-Jorgensen *et al.* (1979) stated that the UNIFAC group contribution method for the prediction of activity coefficients in nonelectrolyte liquid mixtures at low to moderate pressures and temperatures between 300 K and 425 K. The method is a combination of the solution of groups concept and a model for activity coefficients based on an extension of the quasi chemical theory of liquid mixtures. The solution of groups concept is based on considering a liquid mixture as a solution of groups instead of a solution of molecules. The groups are individual structural units e.g. CH_3, CH_2, H_2O etc. which when added together form the parent molecules. The activity coefficients of the components are determined by the properties of the groups rather than the properties of the molecules that made up the components. The resulting UNIFAC method provides a simple procedure for calculating activity coefficients (γ_i) on the basis of constants reflecting the difference in sizes and surface area of the individual functional groups (combinatorial part, γ_{ic}) as well as parameters representing the energetic interactions between the functional groups (residual part, γ_{iR}).

The activity coefficient by UNIFAC method is explained elsewhere (Smith *et al.*, 1996). However, the activity coefficients at different temperatures are obtained using the UNIFAC program (Cutlip, 1999). A representative set of activity coefficients are shown in Table 5.1.

Table 5.1. Activity coefficient values at 368.15 K as calculated by UNIFAC group contribution method (A = acetic acid; B = n-hexanol; C = n-hexyl acetate; D = water).

Temperature (K)	Mole Fraction (x_i)				Activity Coefficient (γ_i)			
	x_A	x_B	x_C	x_D	γ_A	γ_B	γ_C	γ_D
368.15	0.081	0.174	0.012	0.733	0.963	3.252	12.908	1.451
	0.072	0.165	0.020	0.742	0.955	3.286	13.021	1.449
	0.068	0.161	0.025	0.746	0.951	3.302	13.074	1.448
	0.060	0.153	0.033	0.754	0.944	3.334	13.180	1.445
	0.053	0.146	0.040	0.761	0.937	3.361	13.270	1.443
	0.051	0.144	0.042	0.763	0.935	3.369	13.299	1.443
	0.045	0.138	0.048	0.769	0.930	3.393	13.376	1.441
	0.042	0.135	0.051	0.773	0.926	3.405	13.417	1.440
	0.035	0.128	0.058	0.780	0.920	3.432	13.507	1.438
	0.032	0.125	0.061	0.782	0.917	3.443	13.541	1.437
	0.027	0.120	0.066	0.787	0.912	3.461	13.602	1.436
	0.027	0.120	0.066	0.787	0.912	3.463	13.606	1.436
	0.025	0.117	0.068	0.790	0.910	3.472	13.637	1.435
	0.024	0.117	0.069	0.791	0.909	3.475	13.647	1.435
	0.020	0.113	0.073	0.794	0.905	3.490	13.695	1.433

5.2.1. Langmuir–Hinshelwood–Hougen–Watson (LHHW) Model

The LHHW kinetic model is applicable whenever the rate determining step is the surface reaction between the adsorbed molecules. In this model, all of the components were assumed in their adsorbed phases. The derivation of the LHHW kinetic model was presented by Carberry (1976). Several assumptions are made for the derivation of the LHHW model. The rate determining step is controlled by the surface reaction, the adsorption sites are uniformly energetic, a monolayer catalytic coverage is assumed and a dual site adsorption mechanism is being used for the reaction. With application to the reacting system between acetic acid and n-hexanol, the LHHW kinetic model is described.

The reversible reaction between acetic acid and *n*-hexanol are as illustrated in Equation (5.2):

Acetic acid + *n*-hexanol $\overset{H^+}{\rightleftharpoons}$ *n*-hexyl acetate + water $\hspace{2cm}$ (5.2)
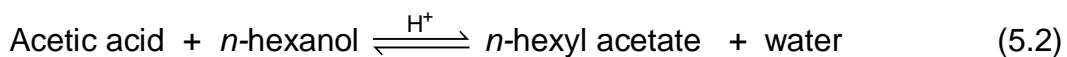
The assumed reaction sequence for the above reaction between acetic acid and *n*-hexanol based on the LHHW mechanism are as follow:

Acetic acid + S $\hspace{3cm}$ ⇌ $\hspace{3cm}$ (Acetic acid – S)

n-hexanol + S $\hspace{3cm}$ ⇌ $\hspace{3cm}$ (*n*-hexanol – S)

Acetic acid – S + *n*-hexanol – S $\hspace{0.5cm}$ ⇌ $\hspace{0.3cm}$ (*n*-hexyl acetate – S) + (water – S)

(*n*-hexyl acetate – S) $\hspace{3cm}$ ⇌ $\hspace{2cm}$ *n*-hexyl acetate + S

(water – S) $\hspace{3.5cm}$ ⇌ $\hspace{3cm}$ water + S
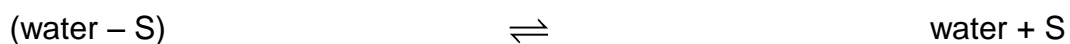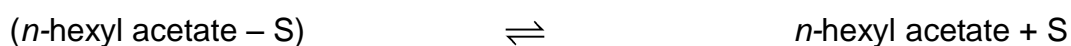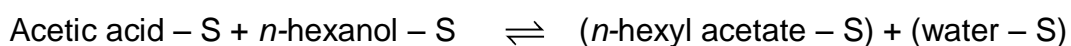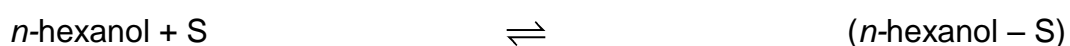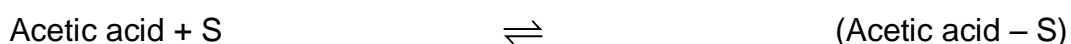
where S denotes a vacant adsorption site.

The assumed reaction sequence for the reaction between acetic acid and *n*-hexanol based on the LHHW mechanism are simplified as follows:

Step 1: A + S $\hspace{2cm}$ ⇌ $\hspace{1.5cm}$ (AS)

Step 2: B + S $\hspace{2cm}$ ⇌ $\hspace{1.5cm}$ (BS)

Step 3: (AS) + (BS) $\hspace{1.5cm}$ ⇌ $\hspace{1.5cm}$ (CS) + (DS)

Step 4: (CS) $\hspace{2.5cm}$ ⇌ $\hspace{1.5cm}$ C + S

Step 5:   (DS) $\rightleftharpoons$ D + S

where A, B, C and D are acetic acid, *n*-hexanol, *n*-hexyl acetate and water, respectively.

Steps 1 and 2 are the adsorption steps of the reactant molecules onto the catalyst surface, Step 3 is the surface reaction between the adsorbed molecules, and Steps 4 and 5 are the desorption steps of the product molecules from the catalyst surface.

With the assumptions that the bimolecular surface reaction (Step 3) is the rate determining step as shown in Equation (5.3).

$$r = k_3 (AS)(BS) - k'_3 (CS)(DS) \tag{5.3}$$

where k_3 is the rate constant for the forward reaction of the rate determining step and k'_3 is the rate constant for the reverse reaction of the rate determining step. Implicit in the concept of a single rate determining step within a sequence of several steps as outlined above is the understanding that all steps except that for the rate controlling exist in equilibrium, or perhaps more accurately, a steady state prevailing. This result in a ratio of reactant and product of constant value for all the steps except the rate controlling step (Step 3). The steady state ratios (K_1, K_2, K_4 and K_5) are expressed in Equations (5.4) to (5.7).

$$\text{Step 1:} \quad \frac{(AS)}{AS} = K_1 \tag{5.4}$$

$$\text{Step 2:} \quad \frac{(BS)}{BS} = K_2 \tag{5.5}$$

Step 4: $\dfrac{(CS)}{CS} = K_4$ $\hspace{3cm}$ (5.6)

Step 5: $\dfrac{(DS)}{DS} = K_5$ $\hspace{3cm}$ (5.7)

Substituting Equations (5.4) to (5.7) into Equation (5.3) and with the overall experimental equilibrium constant K_{eq} being defined as

$K_{eq} = \left(\dfrac{k_3}{k'_3}\right)$ as shown in Equation (5.8).

$$r = k_3(AS)(BS) - k'_3(CS)(DS)$$

$$= k_3(AS)K_1(BS)K_2 - k'_3(CS)K_4(DS)K_5$$

$$= k_3(AB)K_1K_2S^2 - \left\{\dfrac{k_3}{K_{eq}}\right\}(CD)K_4K_5S^2$$

$$\therefore\ r = k_3\,K_1K_2S^2\left[(AB) - \left(\dfrac{K_4K_5}{K_{eq}K_1K_2}\right)(CD)\right]$$
$\hspace{10cm}$ (5.8)

Assuming ideality i.e. no active sites may be created in situ during the catalytic process, the total concentration of active catalytic sites for a given catalyst is designated as S_0. The concentration of unoccupied sites is S, and that occupied by the different adsorbed species are S_A, S_B, S_C, S_D etc. S_0 is defined as shown in Equation (5.9).

$$S_0 = S + S_A + S_B + S_C + S_D$$
$\hspace{10cm}$ (5.9)

$$S_0 = S + (AS) + (BS) + (CS) + (DS) + (IS)$$
$\hspace{10cm}$ (5.10)

where (IS) accounts for the catalytic sites occupied by inert i.e. non-reactive components e.g. nitrogen used as diluents in feed streams.

Substituting Equations (5.4) to (5.7) into Equation (5.10) whilst taking into account adsorption of any inert components as shown in Equation (5.11).

$$S_0 = S + (AS) + (BS) + (CS) + (DS) + (IS)$$

$$= S + SK_1A + SK_2B + SK_4C + SK_5D + SK_6I$$

$$= S(1 + K_1A + K_2B + K_4C + K_5D + K_6I)$$

$$\therefore S = \left[\frac{S_0}{(1 + K_1A + K_2B + K_4C + K_5D + K_6I)} \right] \qquad (5.11)$$

Therefore, the fraction of total catalytic sites that are unoccupied is represented as shown in Equation (5.12).

$$\therefore \frac{S}{S_0} = \left[\frac{1}{(1 + K_1A + K_2B + K_4C + K_5D + K_6I)} \right] \qquad (5.12)$$

The sites occupied by acetic acid (A), *n*-hexanol (B), *n*-hexyl acetate (C), water (D) and inert components (I) are expressed in Equations (5.13) to (5.17).

$$\frac{AS}{S_0} = \frac{SK_1A}{S_0}$$

$$\therefore \frac{(AS)}{S_0} = \left[\frac{K_1A}{(1 + K_1A + K_2B + K_4C + K_5D + K_6I)} \right] \qquad (5.13)$$

$$\frac{BS}{S_0} = \frac{SK_2B}{S_0}$$

$$\therefore \frac{(BS)}{S_0} = \left[\frac{K_2B}{(1+K_1A+K_2B+K_4C+K_5D+K_6I)}\right] \quad (5.14)$$

$$\frac{CS}{S_0} = \frac{SK_4C}{S_0}$$

$$\therefore \frac{(CS)}{S_0} = \left[\frac{K_4C}{(1+K_1A+K_2B+K_4C+K_5D+K_6I)}\right] \quad (5.15)$$

$$\frac{DS}{S_0} = \frac{SK_5C}{S_0}$$

$$\therefore \frac{(DS)}{S_0} = \left[\frac{K_5D}{(1+K_1A+K_2B+K_4C+K_5D+K_6I)}\right] \quad (5.16)$$

$$\frac{IS}{S_0} = \frac{SK_6I}{S_0}$$

$$\therefore \frac{(IS)}{S_0} = \left[\frac{K_6I}{(1+K_1A+K_2B+K_4C+K_5D+K_6I)}\right] \quad (5.17)$$

Alternatively, the fractions of total catalytic sites that are unoccupied could be represented as in Equation (5.18) and (5.19).

$$\frac{S}{S_0} = 1 - \theta_{total} \quad (5.18)$$

where θ_{total} represents the total coverage of the catalytic sites.

$$\theta_A = \frac{(AS)}{S_0}$$

$$\therefore \theta_A = \left[\frac{K_1 A}{(1 + K_1 A + K_2 B + K_4 C + K_5 D + K_6 I)} \right] \tag{5.19}$$

where θ_A is the catalytic sites occupied by acetic acid (A).

Similarly, the catalytic sites occupied by n-hexanol (B), n-hexyl acetate (C), water (D) and inert components (I) are represented in Equations (5.20) to (5.23).

$$\theta_B = \frac{(AS)}{S_0}$$

$$\therefore \theta_B = \left[\frac{K_2 B}{(1 + K_1 A + K_2 B + K_4 C + K_5 D + K_6 I)} \right] \tag{5.20}$$

$$\theta_C = \frac{(CS)}{S_0}$$

$$\therefore \theta_C = \left[\frac{K_4 C}{(1 + K_1 A + K_2 B + K_4 C + K_5 D + K_6 I)} \right] \tag{5.21}$$

$$\theta_D = \frac{(DS)}{S_0}$$

$$\therefore \theta_D = \left[\frac{K_5 D}{(1 + K_1 A + K_2 B + K_4 C + K_5 D + K_6 I)} \right] \tag{5.22}$$

$$\theta_I = \frac{(IS)}{S_0}$$

$$\therefore \theta_I = \left[\frac{K_6 I}{(1 + K_1 A + K_2 B + K_4 C + K_5 D + K_6 I)}\right] \tag{5.23}$$

The total number of catalytic sites that are occupied can be expressed as shown in Equation (5.24).

$$\theta_{total} = \theta_A + \theta_B + \theta_C + \theta_D + \theta_I$$

$$= \left[\frac{K_1 A + K_2 B + K_4 C + K_5 D + K_6 I}{(1 + K_1 A + K_2 B + K_4 C + K_5 D + K_6 I)}\right]$$

$$= \frac{\sum K_i X_i}{1 + \sum K_i X_i} \tag{5.24}$$

In Langmuir–Hinshelwood terms, Equation (5.3) could be written as

$$r = k_3 \theta_A \theta_B - k_3' \theta_C \theta_D \quad \text{where} \quad k_3 \neq k_3' \tag{5.25}$$

Substituting for θ's from Equations (5.19) to (5.22) in Equation (5.25) as shown in Equation (5.26).

$$r = k_3 \left\{ \begin{array}{c} \left[\dfrac{K_1 A}{(1 + K_1 A + K_2 B + K_4 C + K_5 D + K_6 I)}\right] \\ \times \left[\dfrac{K_2 B}{(1 + K_1 A + K_2 B + K_4 C + K_5 D + K_6 I)}\right] \end{array} \right\}$$
$$-k_3' \left\{ \begin{array}{c} \left[\dfrac{K_4 C}{(1 + K_1 A + K_2 B + K_4 C + K_5 D + K_6 I)}\right] \\ \times \left[\dfrac{K_5 D}{(1 + K_1 A + K_2 B + K_4 C + K_5 D + K_6 I)}\right] \end{array} \right\}$$

$$r = k_3 \left\{ \left[\frac{K_1AK_2B}{(1+K_1A+K_2B+K_4C+K_5D+K_6I)^2} \right] \right\}$$

$$- k_3' \left\{ \left[\frac{K_4CK_5D}{(1+K_1A+K_2B+K_4C+K_5D+K_6I)^2} \right] \right\}$$

$$= k_3K_1K_2 \left[\frac{AB - CD\left(\dfrac{K_4K_5}{K_{eq}K_1K_2} \right)}{(1+K_1A+K_2B+K_4C+K_5D+K_6I)^2} \right]$$

$$\therefore r = k_3K_1K_2 \left[\frac{AB - \left(\dfrac{CD}{K_o} \right)}{(1+K_1A+K_2B+K_4C+K_5D+K_6I)^2} \right] \qquad (5.26)$$

A pictorial representation of the LHHW mechanism is illustrated in Figure 5.1. With reference to Figure 5.1, the LHHW mechanism can be described as follows:

Two reactant molecules (acetic acid and *n*-hexanol) adsorb onto the catalyst surface [see Figure 5.1(a)]. The reactant molecules diffuse across the catalyst surface and interact when they are close to each other [see Figure 5.1(b)]. Product molecules i.e. *n*-hexyl acetate and water, are formed which desorbs from the catalyst surface [see Figure 5.1(c)].
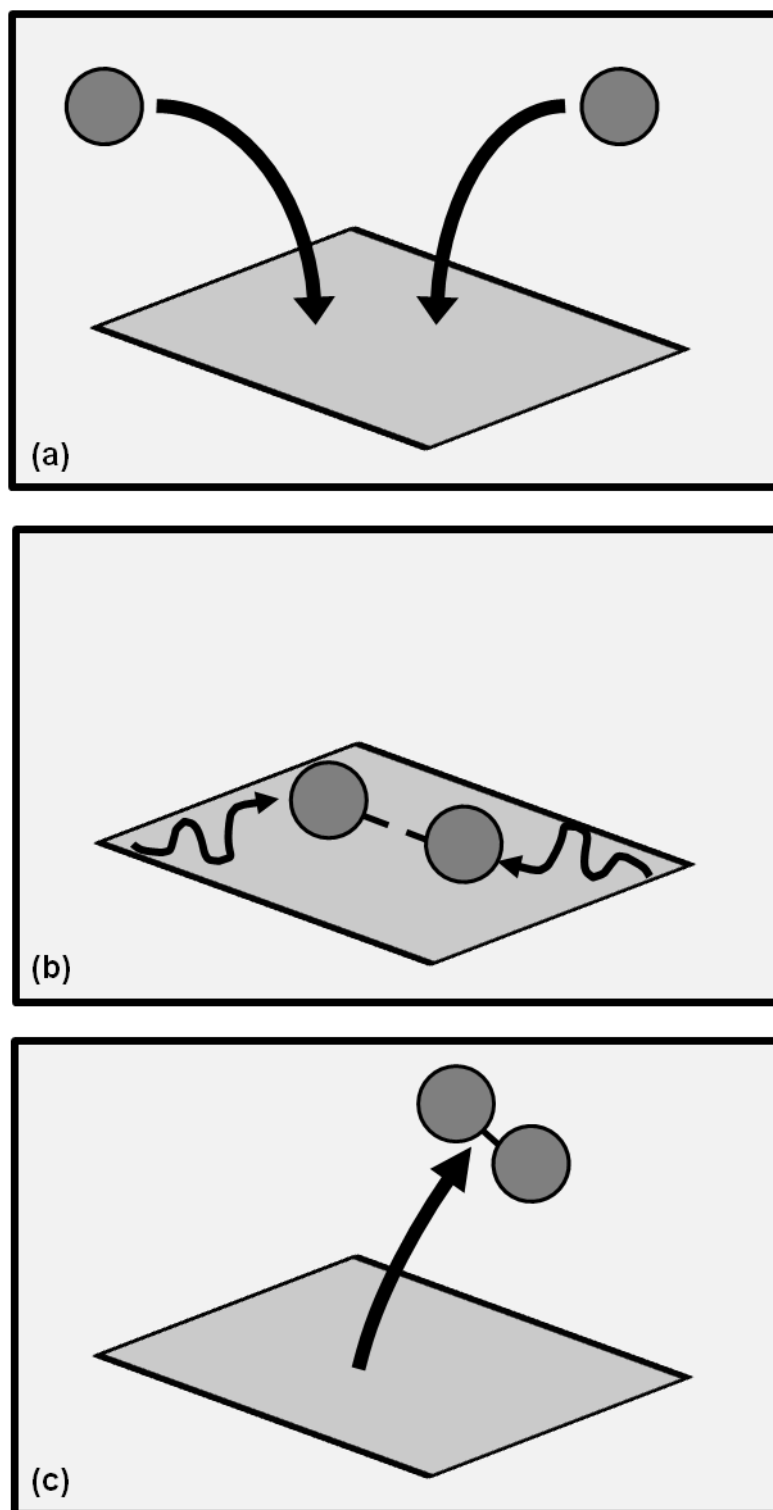
Figure 5.1. Illustration of LHHW mechanism. (a) adsorption of reactant molecules (b) interaction between molecules (c) desorption of product molecules.

The general rate of reaction for the LHHW model can be written as shown in Equation (5.27).

$$-r_A = \frac{A_f\left(-\frac{E_0}{RT}\right)\left(a_A a_B - \left(\frac{A_r}{A_f}\right)a_C a_D\right)}{(1 + K_A a_A + K_B a_B + K_C a_C + K_D a_D)^2}$$

$$-r_A = k\left[\frac{\left(a_A a_B - \frac{a_C a_D}{K_{eq}}\right)}{(1 + K_A a_A + K_B a_B + K_C a_C + K_D a_D)^2}\right] \tag{5.27}$$

where $-r_A$ is the reaction rate of decomposition of acetic acid, A_f and A_r are the pre-exponential factors for the forward and reverse reactions respectively, K represents the reaction rate constant, k_i represents the adsorption coefficient for components i, a_i is the activity of each component and K_{eq} is the reaction equilibrium constant.

The adsorption coefficient (K_i) of the respective component can be defined through the Equation (5.28) (Zhang *et al.*, 2004).

$$k_i = \frac{c_{i-s}}{a_i c_s} \tag{5.28}$$

where c_{i-s} and c_s denotes the concentration of component i at the catalyst surface and concentration of vacant site on the catalyst surface respectively and a_i is the activity for each component.

As the denominator of Equation (5.27) is a multi-component complex, the unknown parameters cannot be regressed correctly on the basis of the experimental results. For this kinetic model, it was assumed that the

adsorption of the molecules was very competitive on the same active site of the catalyst and only those molecules that had the strongest adsorptions were taken into account in the simplified mechanisms. Helfferich (1962) reported that the adsorption of a polar components of the ion exchange resin from a solvent mixture has been found to be considerably stronger then the adsorption of the lesser polar components. Rihko and Krause (1995) and Sanz *et al.* (2002) offered differing opinions regarding which components had the strongest adsorption on the catalyst surface. Mazzotti *et al.* (1997) found that the affinity of Amberlyst 15 for the acetic acid, ethanol, ethyl acetate and water followed the sequential order of water > alcohol > acid > ester.

Gonzalez and Fair (1997) assumed in the LHHW kinetic model that the reaction took place between the water molecule and *iso*-amylene molecule, with both molecules adsorbed on two separate acid sites. Lee *et al.* (2002) suggested that the water affinity of Amberlyst 35 cation exchange resin was the strongest and the adsorption terms of the other components in the investigated reacting system i.e. *n*-butanol, propionic acid as well as *n*-butyl propionate were neglected in the kinetic models as a result. Gangadwala *et al.* (2003) made the assumptions in the LHHW kinetic model that all of the components were in their adsorbed phases for the esterification reaction between acetic acid and *n*-butanol. In this work, two mechanisms were tested to find out which one was more reliable. The first mechanism (mechanism A) assumes that water and *n*-hexanol are adsorbed much more strongly than the other components i.e. acetic acid and *n*-hexyl acetate in the esterification solutions. As a result, the adsorption for both acetic acid and *n*-hexyl acetate were neglected. The equation according to mechanism A could be written as shown in Equation (5.29).

$$-r_A \quad = \quad k\left[\frac{\left(a_A a_B - \dfrac{a_C a_D}{K_{eq}}\right)}{(1 + K_B a_B + K_D a_D)^2}\right] \qquad (5.29)$$

The second mechanism (mechanism B) assumed that water and acetic acid have the strongest adsorption in the esterification solution. As a result, the adsorption for both *n*-hexanol and *n*-hexyl acetate were neglected. The equation according to mechanism B could be written as shown in Equation (5.30).

$$-r_A \quad = \quad k\left[\frac{\left(a_A a_B - \dfrac{a_C a_D}{K_{eq}}\right)}{(1 + K_A a_A + K_D a_D)^2}\right] \qquad (5.30)$$

In mechanisms A and B i.e. Equations (5.29) and (5.30) respectively, there are three parameters to be estimated. In mechanism A [Equation (5.29)], the parameters to be estimated are K, K_B and K_D. In mechanism B [(Equation (5.30)], the parameters to be estimated are K, K_A and K_D.

5.2.2. Eley-Rideal (ER) Model

Eley-Rideal (ER) kinetic model is applicable if the surface reaction taking place between one adsorbed species and one non-adsorbed reactant from the bulk liquid phase is the rate-limiting step. Gangadwala *et al.* (2003) made the assumption that the esterification reaction takes place between adsorbed *n*-butanol and unadsorbed acetic acid on the catalyst surface to give unadsorbed butyl acetate and adsorbed water molecules in the ER kinetic model. In general, the assumptions made for the ER derivation are that the rate determining step is controlled by the surface reaction, the adsorption sites are uniformly

energetic and monolayer coverage as well as a single site adsorption mechanism is being used for the reaction.

The assumed reaction sequence for the reaction between acetic acid and *n*-hexanol based on the ER mechanism are as follows:
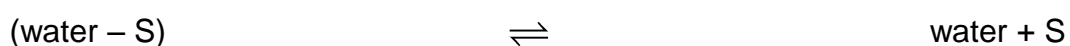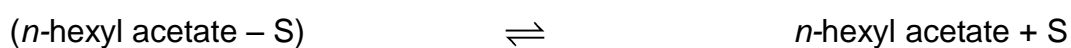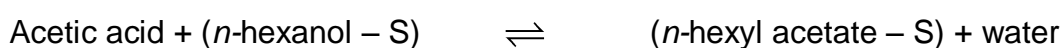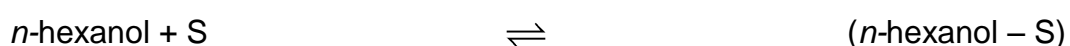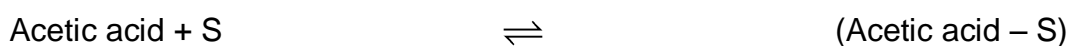
Acetic acid + S	$\rightleftharpoons$	(Acetic acid – S)

n-hexanol + S	$\rightleftharpoons$	(*n*-hexanol – S)

Acetic acid + (*n*-hexanol – S)	$\rightleftharpoons$	(*n*-hexyl acetate – S) + water

(*n*-hexyl acetate – S)	$\rightleftharpoons$	*n*-hexyl acetate + S

(water – S)	$\rightleftharpoons$	water + S

The assumed reaction sequence for the reaction between acetic acid and *n*-hexanol based on the ER mechanism are simplified as follows:

Step 1:   A + S $\rightleftharpoons$ (AS)

Step 2:   B + S $\rightleftharpoons$ (BS)

Step 3:   A + (BS) $\rightleftharpoons$ (CS) + D

Step 4:   (CS) $\rightleftharpoons$ C + S

Step 5:   (DS) $\rightleftharpoons$ D + S
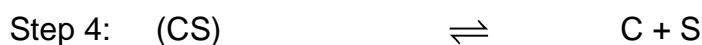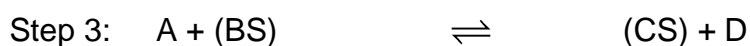
where A, B, C and D are acetic acid, *n*-hexanol, *n*-hexyl acetate and water.

Steps 1 and 2 are the adsorption steps of the molecule onto the catalyst surface, Step 3 is the surface reaction between the one adsorbed molecule and one non-adsorbed molecule and Steps 3 and 4 are the desorption steps from the catalyst surface.

With the assumption that the surface reaction between one adsorbed molecule and one non-adsorbed molecule (Step 3) is the rate determining step, the overall reaction rate is shown in Equation (5.31).

$$r \quad = \quad k_3 A(BS) - k'_3 (CS)D \tag{5.31}$$

where k_3 is the rate constant for the forward reaction and k'_3 is the rate constant for the reverse reaction of the determining step. Similarly to the derivation of the LHHW kinetic model, implicit in the concept of a single rate determining step within a sequence of several steps as outlined above is the understanding that all steps except that for the rate controlling exist in equilibrium, or perhaps more accurately, a steady state prevailing. This results in a ratio of reactant and product of constant value for all the steps except the rate controlling step (Step 3). The steady state ratios (K_1, K_2, K_4 and K_5) are expressed as shown in Equations (5.32) to (5.35).

$$\text{Step 1:} \quad \frac{(AS)}{AS} \quad = \quad K_1 \tag{5.32}$$

$$\text{Step 2:} \quad \frac{(BS)}{BS} \quad = \quad K_2 \tag{5.33}$$

$$\text{Step 4:} \quad \frac{(CS)}{CS} \quad = \quad K_4 \tag{5.34}$$

$$\text{Step 5:} \quad \frac{(DS)}{DS} \quad = \quad K_5 \tag{5.35}$$

Substituting Equations (5.32) to (5.35) into Equation (5.31) and with the overall experimental equilibrium constant K_{eq} defined as $K_{eq} = \left(\dfrac{k_3}{k'_3}\right)$ as shown in Equation (5.36).

$$r = k_3A(BS) - k'_3(CS)D$$

$$= k_3AK_2(BS) - k'_3(CS)K_4D$$

$$= k_3(AB)K_2S - \left(\dfrac{k_3}{K_{eq}}\right)(CD)K_4S$$

$$\therefore r = k_3K_2S\left[(AB) - \left(\dfrac{K_4}{K_{eq}K_2}\right)(CD)\right] \tag{5.36}$$

Assuming ideality i.e. no active sites may be created in situ over the course of the catalytic process, the total concentration of active catalytic sites for a given catalyst is designated as S_0. The concentration of unoccupied sites is S and that occupied by the different adsorbed species are S_A, S_B, S_C, S_D, etc. S_0 is defined as shown in Equation (5.37).

$$S_0 = S + S_A + S_B + S_C + S_D \tag{5.37}$$

$$S_0 = S + (AS) + (BS) + (CS) + (DS) + (IS) \tag{5.38}$$

where (IS) accounts for the catalytic sites occupied by inert i.e. non-reactive components e.g. nitrogen used as diluents in feed streams. Substituting Equations (5.32) to (5.35) into Equation (5.38) whilst taking into account adsorption of any inert components as shown in Equation (5.39).

$$S_0 \;=\; S + (AS) + (BS) + (CS) + (DS) + (IS)$$

$$=\; S + SK_1A + SK_2B + SK_4C + SK_5D + SK_6I$$

$$=\; S(1 + K_1A + K_2B + K_4C + K_5D + K_6I)$$

$$\therefore S \;=\; \left[\frac{S_0}{(1 + K_1A + K_2B + K_4C + K_5D + K_6I)} \right] \tag{5.39}$$

Therefore, the fraction of total catalytic sites that are unoccupied is represented as shown in Equation (5.40).

$$\therefore \frac{S}{S_0} \;=\; \left[\frac{1}{(1 + K_1A + K_2B + K_4C + K_5D + K_6I)} \right] \tag{5.40}$$

The sites occupied by acetic acid (A), n-hexanol (B), n-hexyl acetate (C), water (D) and inert components (I) are expressed in Equations (5.41) to (5.45).

$$\frac{AS}{S_0} \;=\; \frac{SK_1A}{S_0}$$

$$\therefore \frac{(AS)}{S_0} \;=\; \left[\frac{K_1A}{(1 + K_1A + K_2B + K_4C + K_5D + K_6I)} \right] \tag{5.41}$$

$$\frac{BS}{S_0} \;=\; \frac{SK_2B}{S_0}$$

$$\therefore \frac{(BS)}{S_0} \;=\; \left[\frac{K_2B}{(1 + K_1A + K_2B + K_4C + K_5D + K_6I)} \right] \tag{5.42}$$

$$\frac{CS}{S_0} \;=\; \frac{SK_4C}{S_0}$$

$$\therefore \frac{(CS)}{S_0} = \left[\frac{K_4 C}{(1 + K_1 A + K_2 B + K_4 C + K_5 D + K_6 I)} \right] \qquad (5.43)$$

$$\frac{DS}{S_0} = \frac{SK_5 C}{S_0}$$

$$\therefore \frac{(DS)}{S_0} = \left[\frac{K_5 D}{(1 + K_1 A + K_2 B + K_4 C + K_5 D + K_6 I)} \right] \qquad (5.44)$$

$$\frac{IS}{S_0} = \frac{SK_6 I}{S_0}$$

$$\therefore \frac{(IS)}{S_0} = \left[\frac{K_6 I}{(1 + K_1 A + K_2 B + K_4 C + K_5 D + K_6 I)} \right] \qquad (5.45)$$

Alternatively, the fraction of total catalytic sites that are unoccupied could be represented as shown in Equation (5.46).

$$\frac{S}{S_0} = 1 - \theta_{total} \qquad (5.46)$$

where θ_{total} represents the total coverage of the catalytic sites.

$$\theta_A = \frac{(AS)}{S_0}$$

$$\therefore \theta_A = \left[\frac{K_1 A}{(1 + K_1 A + K_2 B + K_4 C + K_5 D + K_6 I)} \right] \qquad (5.47)$$

where θ_A is the catalytic sites occupied by acetic acid (A).

The catalytic sites occupied by n-hexanol (B), n-hexyl acetate (C), water (D) and inert components (I) are similarly represented in Equations (5.48) to (5.51).

$$\theta_B = \frac{(AS)}{S_0}$$

$$\therefore \theta_B = \left[\frac{K_2B}{(1 + K_1A + K_2B + K_4C + K_5D + K_6I)} \right] \tag{5.48}$$

$$\theta_C = \frac{(CS)}{S_0}$$

$$\therefore \theta_C = \left[\frac{K_4C}{(1 + K_1A + K_2B + K_4C + K_5D + K_6I)} \right] \tag{5.49}$$

$$\theta_D = \frac{(DS)}{S_0}$$

$$\therefore \theta_D = \left[\frac{K_5D}{(1 + K_1A + K_2B + K_4C + K_5D + K_6I)} \right] \tag{5.50}$$

$$\theta_I = \frac{(IS)}{S_0}$$

$$\therefore \theta_I = \left[\frac{K_6I}{(1 + K_1A + K_2B + K_4C + K_5D + K_6I)} \right] \tag{5.51}$$

The total number of catalytic sites that are occupied, θ_{total} can be expressed as shown in Equation (5.52).

$$\theta_{total} = \theta_A + \theta_B + \theta_C + \theta_D + \theta_I$$

$$= \left[\frac{K_1A + K_2B + K_4C + K_5D + K_6I}{(1 + K_1A + K_2B + K_4C + K_5D + K_6I)} \right]$$

$$= \frac{\sum K_i X_i}{1 + \sum K_i X_i} \qquad (5.52)$$

In Eley-Rideal (ER) terms, Equation (5.31) could be written as shown in Equation (5.53).

$$r = k_3 A\theta_B - k_3' \theta_C D \quad \text{where } k_3 \neq k_3' \qquad (5.53)$$

Substituting for θ_B [(Equation (5.48)] and θ_C [(Equation (5.49)] in Equation (5.53) as shown in Equation (5.54).

$$r = k_3 \left[\frac{K_2AB}{(1 + K_1A + K_2B + K_4C + K_5D + K_6I)} \right]$$
$$- k_3' \left[\frac{K_4CD}{(1 + K_1A + K_2B + K_4C + K_5D + K_6I)} \right]$$

$$= k_3 K_2 \left[\frac{AB - CD\left(\dfrac{K_4}{K_{eq}K_2}\right)}{(1 + K_1A + K_2B + K_4C + K_5D + K_6I)} \right]$$

$$\therefore r = k_3 K_1 \left[\frac{AB - \left(\dfrac{CD}{K_o}\right)}{(1 + K_1A + K_2B + K_4C + K_5D + K_6I)} \right] \qquad (5.54)$$

A pictorial representation of ER mechanism is illustrated in Figure 5.2. With reference to Figure 5.2, ER mechanism could be described as follows:

A reactant molecule, *n*-hexanol is adsorbed onto the catalyst surface [see Figure 5.2(a)]. An unadsorbed reactant molecule acetic acid in the liquid phase passes by which interacts with the adsorbed *n*-hexanol molecule on the catalyst surface [see Figure 5.2(b)]. Product molecules, *n*-hexyl acetate and water are formed which desorbs from the catalyst surface [see Figure 5.2(c)].
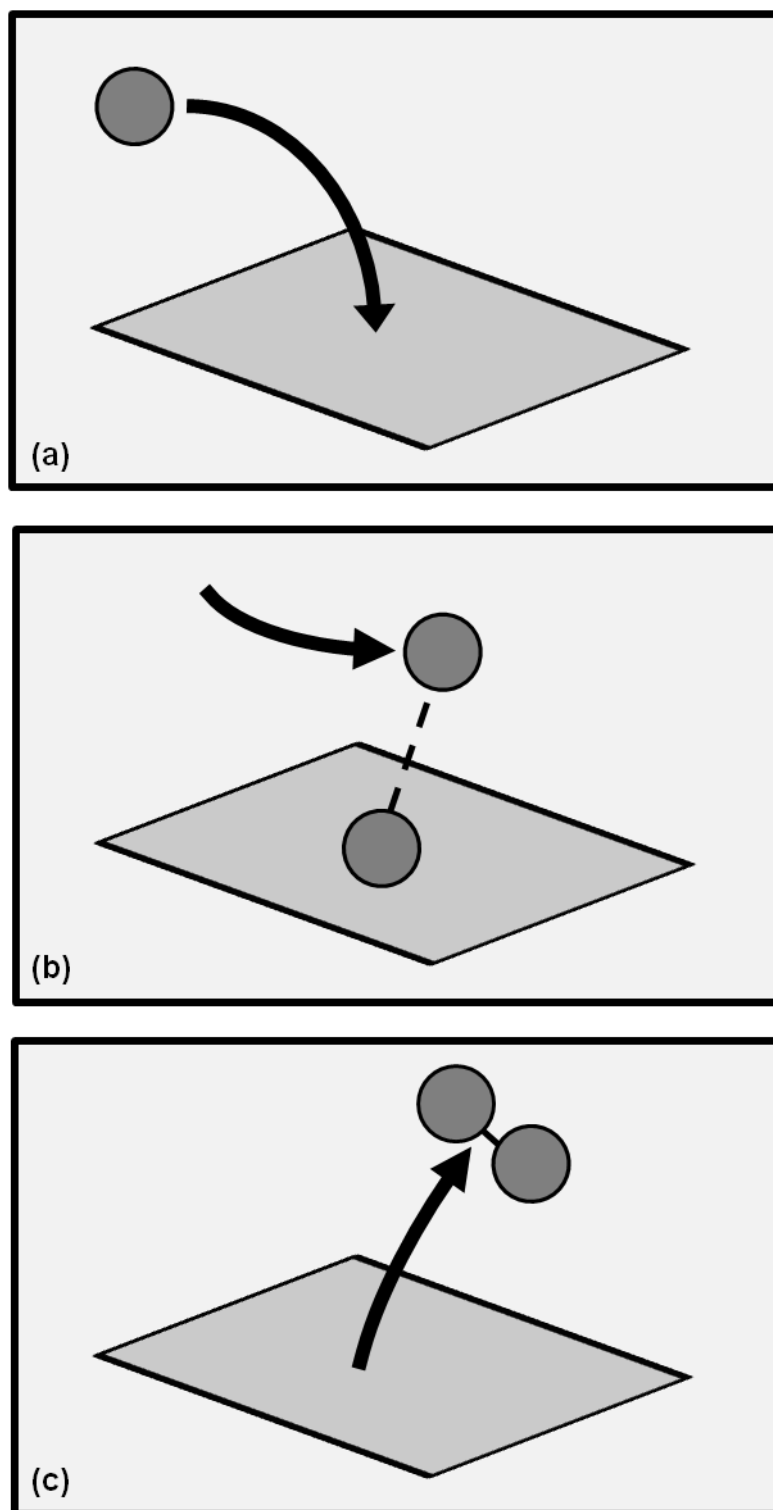
Figure 5.2. Illustration of Eley-Rideal (ER) mechanism (a) adsorption of a reactant molecule (b) interaction between molecules (c) desorption of product molecules.

The general rate of reaction for the ER model can be rewritten as shown in Equation (5.55).

$$-r_A = \frac{A_f\left(-\dfrac{E_0}{RT}\right)\left(a_A a_B - \left(\dfrac{A_r}{A_f}\right)a_C a_D\right)}{(1 + K_A a_A + K_B a_B + K_C a_C + K_D a_D)}$$

$$-r_A = k\left[\frac{\left(a_A a_B - \dfrac{a_C a_D}{K_{eq}}\right)}{(1 + K_A a_A + K_B a_B + K_C a_C + K_D a_D)}\right] \tag{5.55}$$

where $-r_A$ is the reaction rate of decomposition of acetic acid, A_f and A_r are the pre-exponential factors for the forward and reverse reactions respectively, k represents the reaction rate constant, K_i represents the adsorption coefficient for components i, a_i is the activity of each component and K_{eq} is the reaction equilibrium constant.

5.2.3. Modified Langmuir–Hinshelwood–Hougen–Watson (ML) Model

Gonzalez and Fair (1997); Lee *et al.* (2000); Lee *et al.* (2001) and Gangadwala *et al.* (2003) reported that an empirical constant (α) can be introduced in the Langmuir–Hinshelwood–Hougen–Watson (LHHW) model to account for the nonlinear distribution of water concentration in the resin phase. This gives an expression for the Modified Langmuir–Hinshelwood–Hougen–Watson (ML) model as shown in Equation (5.56).

$$-r_A = k\left[\frac{\left(a_A a_B - \dfrac{a_C (a_D)^{\alpha}}{K_{eq}}\right)}{(1 + K_A a_A + K_B a_B + K_C a_C + K_D (a_D)^{\alpha})^2}\right] \tag{5.56}$$

Lee *et al.* (2000) reported that the ML model with α = 3 represented the kinetic behaviour of the catalytic esterification between acetic acid and amyl alcohol over Dowex whilst Lee *et al.* (2001) reported that the ML model with α = 4 represented the kinetic behaviour for the same reacting system over Amberlyst 15. Gangadwala *et al.* (2003) assumed a value of 2 for α in the ML model and gained satisfactory results for the model correlation for the esterification of acetic acid with *n*-butanol.

5.2.4. Pseudo-Homogenous (PH) Model

In contrast to the LHHW and ER mechanisms, the PH model does not allow for any adsorption of the reactant molecules onto the catalyst surface. The solid catalyst is assumed to act like a catalyst which is in the same phase i.e. liquid phase as the reactant. Sanz *et al.* (2002) stated that the PH model assumed complete swelling of the polymeric catalyst in contact with the polar solvents, leading to an easy access of the reacting components to the active catalyst sites. Xu and Chuang (1996) reported that the PH model is derived on the basis of the Langmuir-Hinshelwood formalism with the assumptions that the surface reaction is the controlling step and the adsorption is weak for all components.

With the above assumption that the adsorption is weak for all components in the PH model i.e. values of K_i are negligible, the denominator of Equation (5.55) on the right hand side approaches unity. Therefore, the general rate of reaction for the PH model can be written as expressed in Equation (5.57):

$$-r_A = k \left(a_A a_B - \frac{a_C a_D}{K_{eq}} \right) \tag{5.57}$$

The four kinetic models described were solved using a non linear regression method. A commercially available software package

(Fogler, 1999) was used to carry out the regression and to obtain values of the parameters for each of the kinetic model.

5.2.5. Criteria for Acceptance of Kinetic Models

The estimated rate constant and adsorption coefficient values from each individual kinetic model should be positive values. As the adsorption of the reactant molecules are assumed to have taken place for the different kinetic models (except in the case of the PH kinetic model), a negative value would therefore be meaningless. Gangadwala *et al.* (2003) found that the LHHW model for the esterification of acetic acid with *n*-butanol without modification (i.e. with $\alpha = 1$) gave negative values of the adsorption coefficients, which gave an indication that the LHHW model was not suitable for the reacting system as reported.

5.3. RESULTS AND DISCUSSION

n-Hexyl acetate was synthesised at different temperatures using the best performed Purolite$^{®}$ CT-124 catalyst. The results of all the experiments at different temperatures along with the modeling results are shown in Figure 5.3.

It was observed that with an increase in temperature the rate of reaction and the conversion of acetic acid increases. A number of runs at different temperatures help in modelling the reaction kinetic and hence for the determination of rate constant, activation energy and Arrhenius pre-exponential factor. Both PH model and heterogeneous kinetic rate models, e.g., LHHW, Eley-Rideal (ER) and ML were applied for correlating the kinetic data at different temperatures.

The equilibrium constant for the reaction was calculated from the knowledge of liquid phase mole fraction and activity coefficient of the components at equilibrium through Equation (5.58):

$$K_{eq} = \left(\frac{a_C a_D}{a_A a_B}\right)_{eq} = \left(\frac{x_C x_D}{x_A x_B}\right)_{eq} \times \left(\frac{\gamma_C \gamma_D}{\gamma_A \gamma_B}\right)_{eq} \qquad (5.58)$$
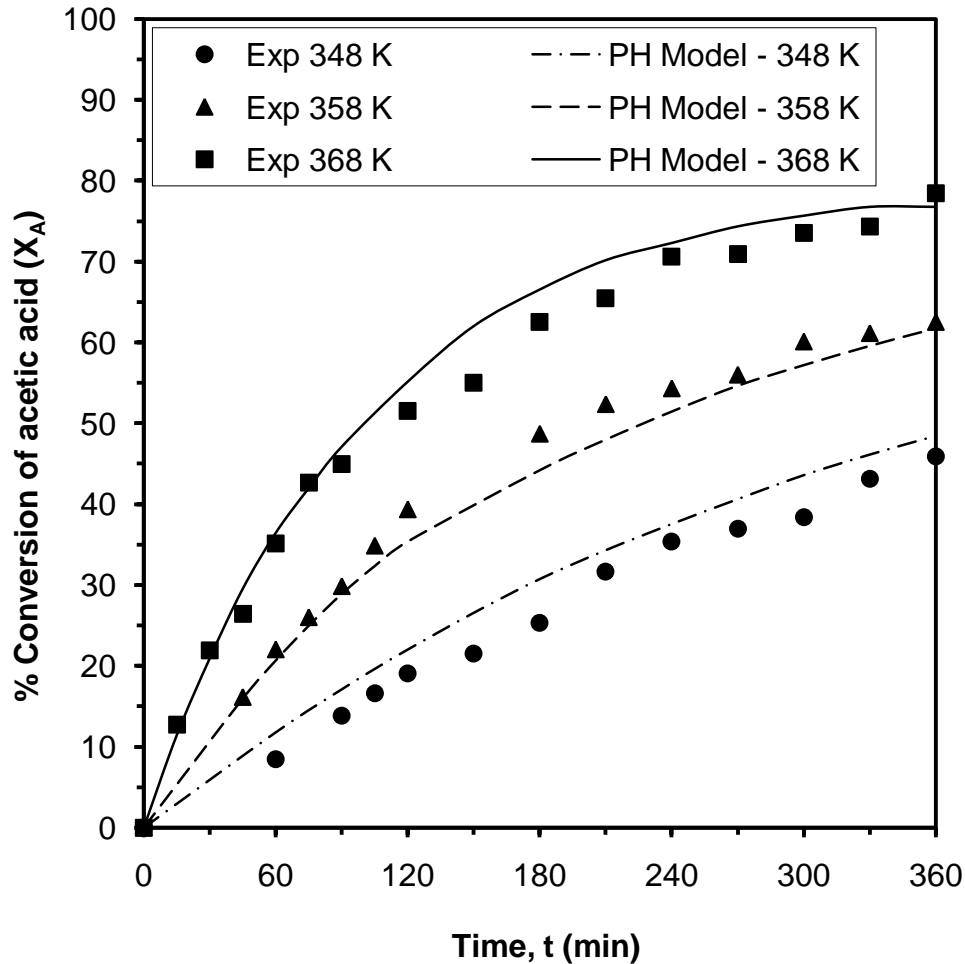
Figure 5.3. Comparison of experimental and calculated values for the effect of reaction temperature on the conversion of acetic acid at catalyst loading: 10% (w/w); feed mole ratio (*n*-hexanol to acetic acid): 2:1; acetic acid concentration: 30% (w/w); catalyst: Purolite® CT-124; stirrer speed: 500 rpm.

where, K_{eq} is the equilibrium constant of the reaction, a_i is the activity of the ith component, x_i is the mole fraction of the ith component and γ_i is the activity coefficient of the ith component. The subscript A, B, C and D represents acetic acid, *n*-hexanol, *n*-hexyl acetate and water, respectively.

PH model is used on the basis of Helfferich (1962) concept which considers that catalysis of liquid phase reactions using ion exchange resins is similar to homogeneous catalysis by dissolved electrolytes. Numerous authors have modeled the heterogeneous kinetic data using PH model (Chopade and Sharma, 1997; Saha, 1999; Jiménez *et al.*, 2002; Gangadwala *et al.*, 2003; Sanz *et al.*, 2004; Steinigeweg and Gmehling, 2004; Schmitt and Hasse, 2006). LHHW and ML model are used whenever the rate determining step is the surface reaction between the adsorbed molecules. On the other hand, ER model is applied if in the rate-limiting step; surface reaction takes place between one adsorbed species and one non-adsorbed reactant from the bulk liquid phase. Moreover, because of the strong affinity of Purolite$^{®}$ CT-124 resin for water, the activity of water in the catalyst gel phase, where the reaction occurs, is distinctly different from that in the liquid phase and was also reported by Lee *et al.* (2000). The rate expressions for each model are as follows:

PH Model:

$$-r_A \quad = \quad A_f\left(\frac{-E_0}{RT}\right)\left(a_A a_B - \frac{A_r}{A_f}a_C a_D\right) \tag{5.59}$$

LHHW Model:

$$-r_A \quad = \quad \frac{A_f\left(\frac{-E_0}{RT}\right)\left(a_A a_B - \frac{A_r}{A_f}a_C a_D\right)}{(1 + K_A a_A + K_B a_B + K_C a_C + K_D a_D)^2} \tag{5.60}$$

ER model:

$$-r_A \quad = \quad \frac{A_f\left(\frac{-E_0}{RT}\right)\left(a_A a_B - \frac{A_r}{A_f}a_C a_D\right)}{(1 + K_A a_A + K_B a_B + K_C a_C + K_D a_D)} \tag{5.61}$$

ML model:

$$-r_A = \frac{A_f\left(\dfrac{-E_0}{RT}\right)\left(a_A a_B - \dfrac{A_r}{A_f} a_C (a_D)^{\alpha}\right)}{(1 + K_A a_A + K_B a_B + K_C a_C + K_D (a_D)^{\alpha})^2} \qquad (5.62)$$

where A_f and A_r are the Arrhenius pre-exponential factors for the forward and the reverse reactions, E_0 is the activation energy of the reaction, R is the gas constant, T is the reaction temperature and K_A, K_B, K_C and K_D are the adsorption equilibrium constants and a_A, a_B, a_C and a_D are the activities for acetic acid, *n*-hexanol, *n*-hexyl acetate and water, respectively; α is the empirical constant that was introduced in the LHHW model to give an expression for the modified LHHW (ML) model.

The activity of the components was taken into account instead of the concentration of the components for kinetic modelling to account for the non-ideal mixing behavior of the bulk liquid phase. The UNIFAC group contribution method was used for the estimation of the activity coefficients (Reid *et al.*, 1987). Activity coefficient values as calculated by UNIFAC group contribution method at 368.15 K are shown in Table 5.1.

The heterogeneous kinetic model parameters were found using POLYMATH software (Fogler, 1999) that gave negative values of adsorption coefficient. Gangadwala *et al.* (2003) also reported the negative values for LHHW model without modification (i.e. α = 1). Schmitt and Hasse (2006) also concluded that the adsorption model for synthesis of *n*-hexyl acetate "fails to correctly describe reaction kinetics".

For PH model equation (5.59) can be written in the form of:

$$-r_A = k\left(a_A a_B - \frac{a_C a_D}{K_{eq}}\right) \qquad (5.63)$$

The above equation can be written in the form of y = m x

where,

$y = -r_A$,

slope, m = k (rate constant), and

$x = a_A a_B - (a_C a_D / K_{eq})$

Equation (5.63) is plotted for experiments conducted at three different temperatures i.e. 348 K, 358 K and 368 K, respectively. The results are shown in Figures 5.4 – 5.6 respectively.

The plot shows data points with the fitted line equation:

$$-r_A = 0.0015254 \times [a_A a_B - (a_C a_D / K_{eq})]$$

The y-axis is labelled $-r_A$ [Kmol m^{-3} s^{-1}] and the x-axis is labelled $[a_A a_B - (a_C a_D / K_{eq})]$.
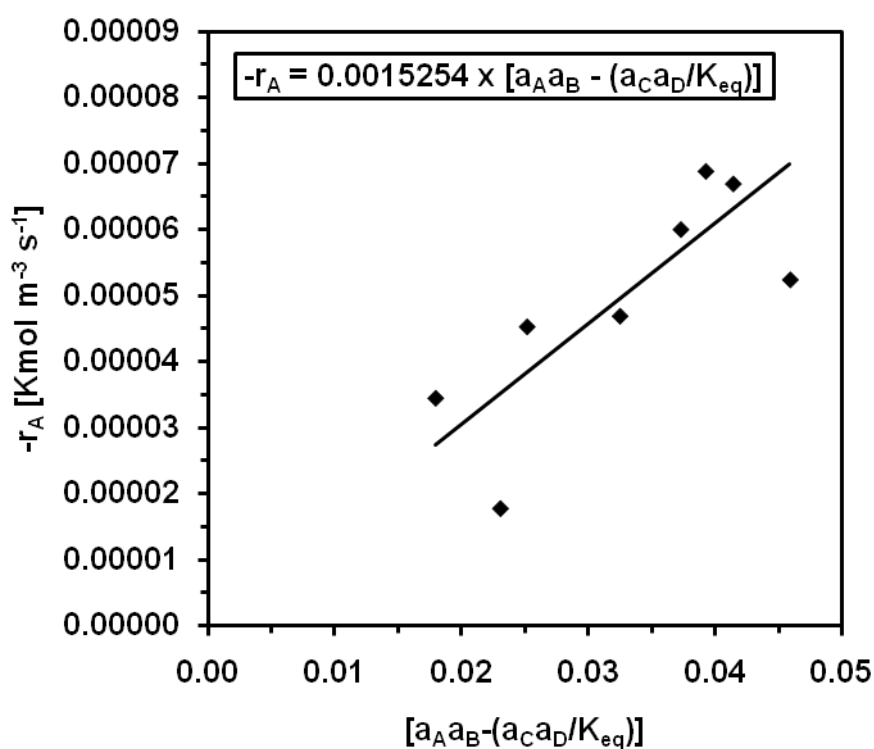
Figure 5.4. Determination of rate constant (k) at temperature 348 K.
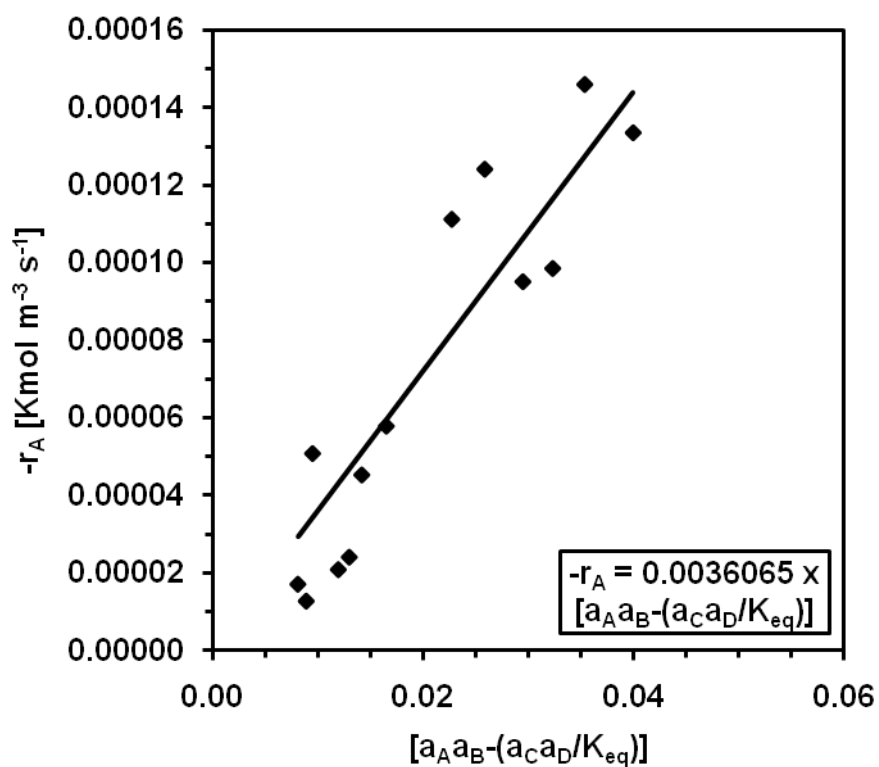
Figure 5.5. Determination of rate constant (k) at temperature 358 K.
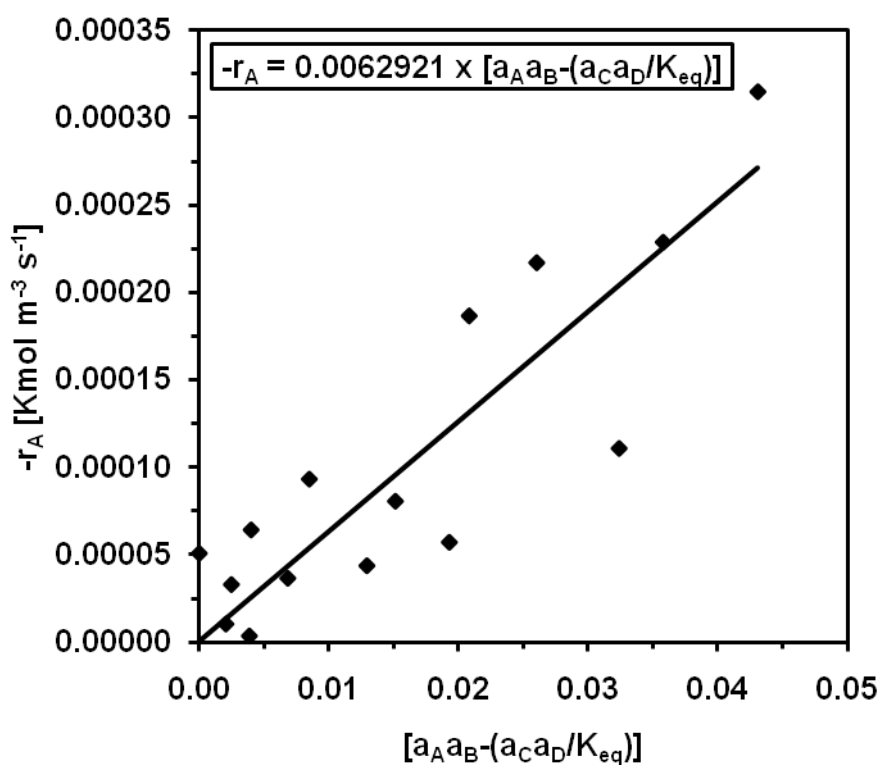
Figure 5.6. Determination of rate constant (k) at temperature 368 K.

The rate constant found for the three different temperatures were used to determine the activation energy (E) and Arrhenius pre-exponential factor (A_0) from the following equation:

$$k = A_0 \, e^{\left(-\frac{E}{RT}\right)} \tag{5.64}$$

Taking log on both the sides, the above equation (5.64) can be written as:

$$\ln(k) = \ln(A_0) - \frac{E}{R}\left(\frac{1}{T}\right) \tag{5.65}$$

where, $y = \ln(k)$, $x = 1/T$

slope, $m = -E/R$

y-intercept $= \ln A_0$
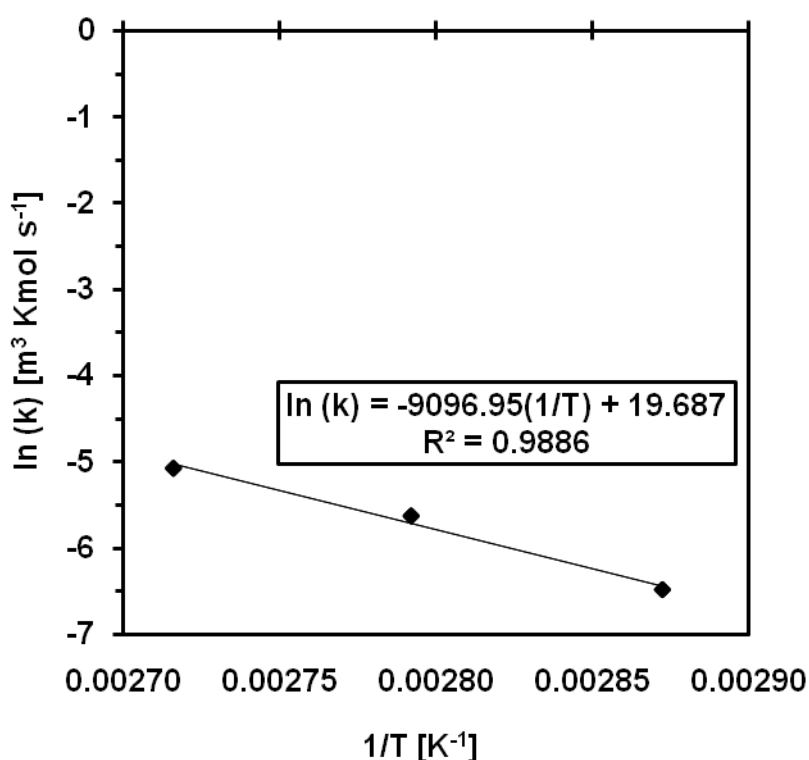
Figure 5.7. Determination of activation energy (E) and pre-exponential factor (A_0) by Arrhenius plot for *n*-hexyl acetate synthesis.

Equation (5.65) was plotted as shown in Figure 5.7. From Figure 5.7, the activation energy and Arrhenius pre-exponential factor were calculated.

Table 5.2. Parameters of the PH model used to fit the experimental data for synthesis of *n*-hexyl acetate.

Temperature, T (K)	Rate Constant, $k \times 10^3$ [m^3 $Kmol^{-1}$ s^{-1}]	Activation Energy, E [KJ/mol]	Pre-Exponential Factor, A_0 [m^3 $Kmol^{-1}$ s^{-1}]
348	1.5254	75.6	3.5×10^8
358	3.6065		
368	6.2921		

Putting the values of rate constant for each temperature in Equation (5.65), modelled rate of reaction and subsequent acetic acid conversion for three temperatures can be calculated which is plotted in Figure 5.3. PH model gave a better correlation between the experimental and model reaction rates as compared to adsorption rate models. The parameters of the PH model used to fit the experimental data are reported in Table 5.2.

5.4. CONCLUSIONS

The following conclusions can be drawn from the batch kinetic modelling:

❖ The pseudo-homogeneous (PH) model yielded the best representation of the experimental data over a wide range of temperatures for the esterification of acetic acid and *n*-hexanol.

❖ The modelling results are in good agreement with the experimental data

The Chapter 5 demonstrated the derivation of kinetic models that can be used to correlate the batch kinetic data. In Chapter 6 chromatographic

reactor (CR) will be used for *n*-hexyl acetate synthesis in presence of Purolite® CT-124 catalyst. Materials and methods, experimental set-up and procedure, analytical method used and results from both the batch and continuous chromatographic reactor are discussed in detail.

CHAPTER 6
CHROMATOGRAPHIC
REACTOR STUDIES

6. CHROMATOGRAPHIC REACTOR STUDIES

6.1. INTRODUCTION

The synthesis of *n*-hexyl acetate in a classical batch reactor produced some interesting result. It was evident from the batch reactor experiments that Purolite$^{®}$ CT-124 was the best catalyst as compared to other catalysts for *n*-hexyl acetate synthesis (Patel and Saha, 2007). Hence, Purolite$^{®}$ CT-124 catalyst has been used to carry out experiments in a batch chromatographic reactor. The main purpose of carrying out experiments in batch chromatographic reactor was to separate the product and carrying out reaction simultaneously in the same equipment which is not possible in classical batch reactor and also to reduce the unreacted limiting reactant (acetic acid).

6.2. BATCH CHROMATOGRAPHIC REACTOR STUDIES

In a batch chromatographic reactor, simultaneous reaction and separation is carried out in a single vessel. Consider an equilibrium limited reaction in a chromatographic column as shown in (6.1):

$$A + B \Leftrightarrow C + D \qquad\qquad (6.1)$$

Two kinds of experiments are carried out in a chromatographic reactor. One is the reaction step and other is the regeneration step. During the reaction step the reactant mixture, (A+B) is continuously fed to the column which is initially saturated with a desorbent (B). As soon as the reactants enter the column, A+B react in the presence of catalyst to produce C and D. The product, D, which has a higher affinity towards resin gets readily adsorbed on the resin while C with lesser affinity soon gets desorbed. As a result, C gets separated with D, moves towards the exit of the column along with A and B. Since C is separated from the reaction, reaction proceeds until consumption of the limiting reactant (A). With any specific location in the column, this process continues until the resin catalyst becomes saturated with A, C and D. When the resin catalyst becomes

saturated, the regeneration step is started. Pure B is continuously fed to the column for the regeneration of catalyst by removing A, C and D which are present in the column. When the composition of the outlet fluid is same as the inlet fluid (i.e. pure B), the regeneration step is said to be completed. In this research work, acetic acid (A) is used as the reactant, *n*-hexanol (B) is used as a solvent (desorbent), *n*-hexyl acetate (C) and water (D) are the products.

The material and catalysts used, swelling experiments method, batch chromatographic experimental set-up and procedure, method of analysis and results and discussion are discussed in detail in the following sections.

6.2.1. Materials and Catalysts

Acetic acid (99.85%), *n*-hexanol (98%) and methanol (99.9+%) were purchased from Acros Organics, UK; *n*-hexyl acetate (99%) was supplied by Aldrich Chemical Company, Inc. and *n*-butanol (99+%) was purchased from Fisher Scientific, UK. The purity of all chemicals was verified by gas chromatography (GC) analysis. These chemicals were used without further purification. Sulfonated cation exchange resin, Purolite® CT-124, which was supplied by Purolite International Limited, UK was used for the experiments in a chromatographic reactor. Purolite® CT-124 catalyst was first washed with methanol, dried in a vacuum oven at 373 K for 6 h to remove any water sorbed on the catalyst, before carrying out the experiments. Safety data sheet (SDS) of all the chemicals and the catalysts used are attached in Appendix 9.2.1 and 9.2.2. COSHH (Control of Substances Hazardous to Health) and Risk Assessment (RA) records for batch chromatographic reactor experiments were carried out before conducting the experiments are attached in Appendix 9.3 and 9.4, respectively.

An empty HPLC column of length 0.25 m and internal diameter of 10 x 10^{-3} m assembly was purchased from Phenomenox, UK for batch chromatographic reactor experiments. The column was packed with Purolite$^®$ CT-124 catalyst using slurry technique. In this method, a known amount of catalyst (~5.5 g) was mixed with *n*-hexanol in a measuring beaker. The catalyst swells in presence of the solvent (*n*-hexanol). The Purolite$^®$ CT-124 catalyst swells faster during the first few minutes and then gradually swells at a very slow rate. The swelling of the catalyst in the measuring cylinder was carried out for 24 h before being packed into the column. It was observed that the volume of Purolite$^®$ CT-124 catalyst increased approximately about 3.5 times than that of the original volume of the catalyst in presence of a solvent (*n*-hexanol). The empty HPLC column was then packed with the swelled Purolite$^®$ CT-124 catalyst as slurry. The packing of the swelled Purolite$^®$ CT-124 catalyst was stopped as soon as the swelled catalyst reached the top of the column. It was found that about 4.5 – 5.0 g (on dry basis) of swelled Purolite$^®$ CT-124 catalyst was packed in the first attempt of column packing. The column was then connected to the solvent (*n*-hexanol) pump and the solvent was pumped through the column at a fixed feed flow rate for approximately half an hour. After half an hour, the solvent pump was stopped and the column was disconnected from the solvent pump. The column was then opened to check if the swelled Purolite$^®$ CT-124 catalyst was packed up to the top of the column or there was still a gap between the packed swelled Purolite$^®$ CT-124 catalyst and the top of the column. Generally, it was found that there was always a gap of about 10 mm to 30 mm between the packed swelled Purolite$^®$ CT-124 catalyst and the top of the column at first trial. The remaining slurry of swelled Purolite$^®$ CT-124 catalyst from the measuring cylinder was again packed into the column until the swelled Purolite$^®$ CT-124 catalyst reached the top of the column. This procedure of packing the swelled Purolite$^®$ CT-124 catalyst and connecting the column to the solvent pump was repeated several times until the column was fully packed with the swelled catalyst. After numerous column packing steps it

was found that the optimum amount of the catalyst packed on dry basis for Purolite® CT-124 was ~5.3 ± 0.1 g.

6.2.2. Swelling Experiments for Purolite® CT-124 Catalyst

It is well known that the swelling of Purolite® CT-124 catalyst is dependent on adsorptive properties. Therefore, the swelling experiments for Purolite® CT-124 catalyst were conducted to find the amount and the rate at which Purolite® CT-124 catalyst swells in presence of various chemicals. The Purolite® CT-124 catalyst is swelled both in the reactants (i.e. acetic acid and *n*-hexanol) and products (i.e. *n*-hexyl acetate and water). A known amount of Purolite® CT-124 catalyst was taken and inserted into a measuring cylinder and the volume of the Purolite® CT-124 catalyst in the cylinder was noted. An excess amount of desired solvent was then poured into the measuring cylinder and the % increase in volume was noted and plotted against time. The above method was repeated for different solvents. The results of these swelling experiments for Purolite® CT-124 catalyst are discussed in detail in section 6.2.5.1.

6.2.3. Batch Chromatographic Reactor Experimental Set-Up and Procedure

Figure 6.1 shows the experimental set-up of a batch chromatographic reactor. It consists of an empty stainless steel column assembly packed with the swelled catalyst as explained in the previous section. The packed column was placed in the oven which can be heated to the desired temperature. The packed column was connected to two HPLC pumps by "Y" connector and two quarter turn plug valves. One HPLC pump is connected to the limiting reactant (acetic acid) and the other pump is connected to the solvent (*n*-hexanol). *n*-Hexanol acts both as the reactant for the reaction step and as a solvent (desorbent) for the regeneration step. A thermocouple was placed just before the packed column inlet for measuring the temperature of the reaction step as well as for the regeneration step. It was found that the oven was required to be heated at

higher temperature to attain the desired temperature for the reaction and regeneration step (as measured by thermocouple). The reactants (acetic acid and *n*-hexanol) were fed to the column at desired flow rates by two HPLC pumps. The reactants then react in the presence of catalyst to produce *n*-hexyl acetate and water. Water, which has a higher affinity towards resin, gets readily adsorbed onto the resin while *n*-hexyl acetate with lesser affinity soon gets desorbed. As a result, *n*-hexyl acetate gets separated with water, moves towards the outlet of the column along with acetic acid and *n*-hexanol. Since *n*-hexyl acetate is separated the reaction proceeds until either the consumption of the limiting reactant (acetic acid) or until the saturation of the column.
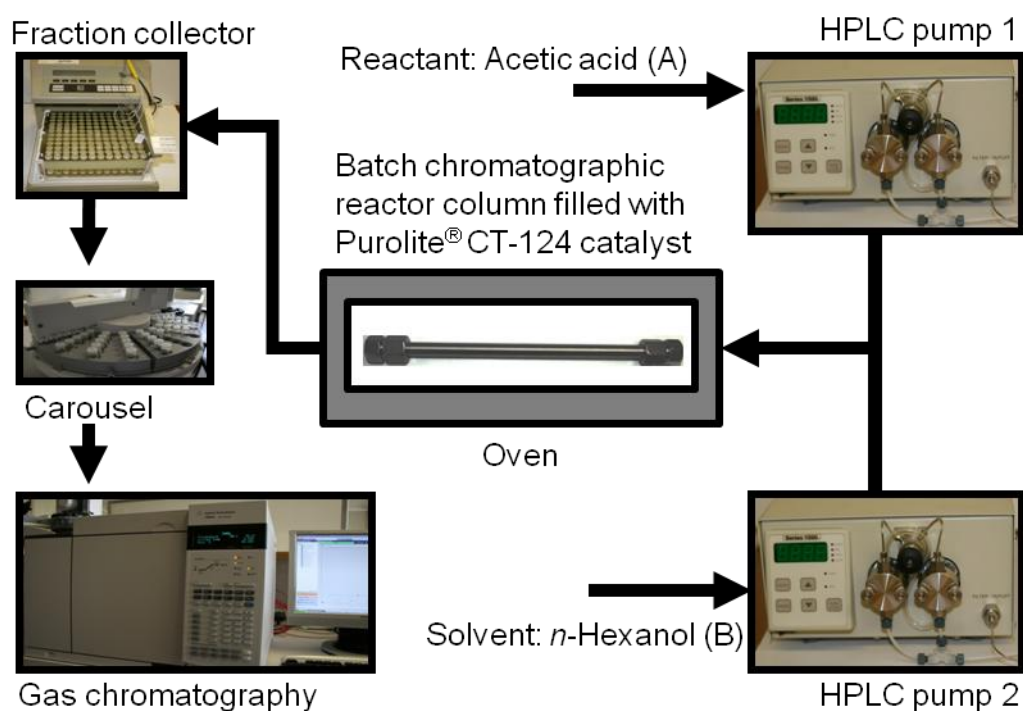
Figure 6.1. Batch chromatographic reactor experimental set-up.

However, in this research work, the chromatographic reactor experiments were carried out for a specific time period i.e. desired reaction step time. The outlet of the packed column was connected to the fraction collector which collects the sample at regular intervals. For experiments that are

carried out at very low flow rates (i.e. less than 0.3 mL/min) the samples were collected manually at regular intervals. Samples collected by fraction collector or by manually from the outlet of the packed column were subjected to GC analysis by internal standard method as explained in the following section.

6.2.4. Method of Analysis

The Pye Unicam 104 series gas chromatograph (GC) was used for most of the batch reactor experiments. However, an Agilent's 7890 series gas chromatograph was used for the analysis of liquid samples from the chromatographic reactor outlet. The main reason was the ready availability of carousel and auto injector present on the Agilent's 7890 series gas chromatograph. The carousel helped to run all the samples continuously in a sequence using an auto injector method without the actual operator present at the time of injection, thus saving significant amount of time for sample analysis. It was also equipped with thermal conductivity detector (TCD) similar to Pye Unicam 104 series gas chromatograph. The column used for Agilent's 7890 series GC was HP-INNOwax (supplied by Agilent), a capillary column with dimensions (30 m x 250 μm x 0.25 μm) instead of packed column (Porapak-Q) as in the case of Pye Unicam 104 series GC. A method was developed for analysis of all the components in the sample mixture. Injector and detector temperatures were maintained at 523 K and 533 K, respectively. A spilt ratio of 50:1 and injection volume of 1 μL were used as part of the GC method. A ramp method was used to separate all the components in the sample mixture. In the ramp method, the initial temperature of the oven was kept at 323 K and the sample was injected by an auto injector. The oven temperature was hold at 323 K for 0.5 min after the sample injection. The oven temperature was then ramped from 323 K to 503 K at the rate of 45 ^{o}C/min. Once the oven temperature reached 503 K, it was hold at this temperature for further 3 min. The total run time for each sample was 8 min. After the sample run was over, the

oven temperature was cooled back to 323 K so that the subsequent run could be started.

6.2.4.1. Calibration Curves

To determine the composition of all the components present in the samples collected from chromatographic experiments, calibration curves were developed. An internal standard method was used to develop the calibration curves and *n*-butanol was used as the internal standard. To develop calibration curves, a number of samples were prepared with known concentration and analysed using Agilent's 7890 series gas chromatograph. The concentration and area ratio of the ith component i.e. CR_i and AR_i, respectively were calculated from Equation (6.2) and (6.3), respectively.

Concentration ratio of ith component (CR_i)

$$= \frac{\text{Concentration of } i^{th} \text{ component } (C_i)}{\text{Concentration of internal standard } (C_{is})} \quad (6.2)$$

$$\text{Area ratio of } i^{th} \text{ component } (AR_i) = \frac{\text{Area of } i^{th} \text{ component } (A_i)}{\text{Area of internal standard } (A_{is})} \quad (6.3)$$

Response factor of the ith component (RF_i) is calculated from Equation (6.4).

R.F. of ith component (RF_i)

$$= \frac{\text{Concentration ratio of } i^{th} \text{ component } (CR_i)}{\text{Area ratio of } i^{th} \text{ component } (AR_i)} \quad (6.4)$$

The above Equation (6.4) can be rearranged in the form of y = m x as shown in Equation (6.5).

$$CR_i = RF_i \times AR_i \qquad\qquad (6.5)$$

where, y = concentration ratio of ith component (CR_i), x = area of ith component (AR_i), and slope (m) = response factor of the ith component (RF_i).

A plot of concentration ratio versus area ratio of all the components were plotted for determination of response factor. Once the response factor of individual component was determined, the unknown composition of the samples collected from chromatographic reactor experiments at time t can be determined by Equation (6.5).

6.2.4.2. Internal Standardisation

Internal standard method was used for the analysis of the sample mixture and *n*-butanol was used as the internal standard. Acetone was used to dilute the sample mixture. This was not required for Pye Unicam 104 series gas chromatograph as it had packed column (Porapak-Q) instead of capillary column (HP-Innowax) in Agilent's 7980 series gas chromatograph. Internal standardisation is explained in detailed in Chapter 4, section 4.2.4.2.

6.2.4.3. Chromatogram

Figure 6.2 shows a typical chromatogram from Agilent's 7890 series gas chromatograph. Acetone as a dilution solvent and *n*-butanol as an internal standard were added to each chromatographic reactor outlet samples. Acetone peak emerges at a retention time (RT) of 1.327 min followed by water at 2.024 min, *n*-butanol at 2.459 min, *n*-hexyl acetate at 3.037 min, *n*-hexanol at 3.362 min and finally acetic acid at a retention time of 3.734 min.
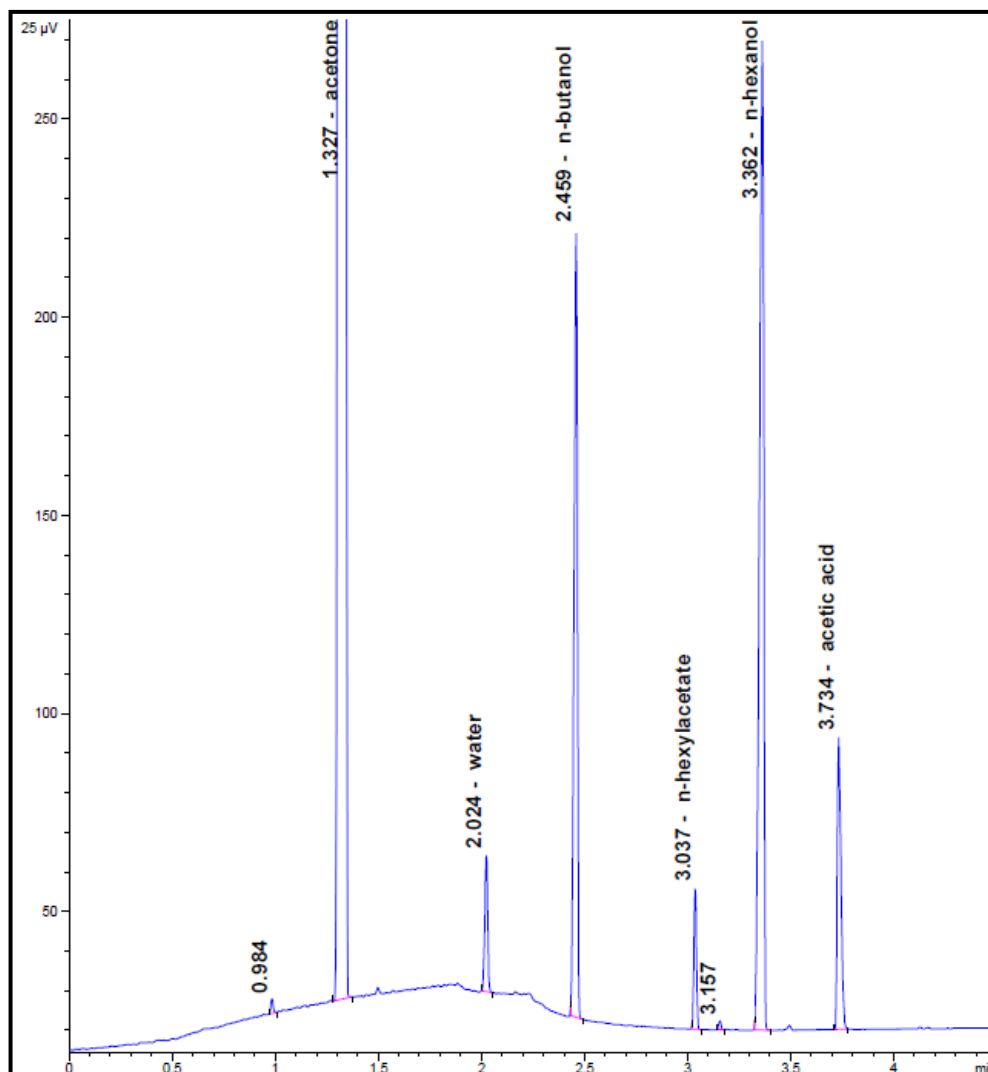
Figure 6.2. A typical chromatogram from Agilent's 7890 series gas chromatograph (GC).

6.2.5. Results and Discussion

Purolite[®] CT-124 swelling results and the batch chromatographic reactor experimental results are discussed in the following section. All the batch chromatographic experiments were carried out with stainless steel column of length 0.25 m and internal diameter of 0.01 m and packed with ~5.3 ± 0.1 g of swelled Purolite[®] CT-124 catalyst while the swelling experiments for Purolite[®] CT-124 catalyst as mentioned earlier were carried out in a measuring cylinder. Batch chromatographic reactor experiments were conducted at different reaction step time, feed flow rate,

feed mole ratio (FMR) of the reactants (*n*-hexanol : acetic acid), temperature and desorbent (*n*-hexanol) flow rate for the optimisation of *n*-hexyl acetate synthesis and maximum conversion of acetic acid.

6.2.5.1. Purolite® CT-124 Catalyst Swelling Experimental Results

Swelling is dependent on adsorptive properties. The Purolite® CT-124 catalyst swelling experimental results for acetic acid, *n*-hexanol, *n*-hexyl acetate and water are shown in Figure 6.3. Figure 6.3 illustrates
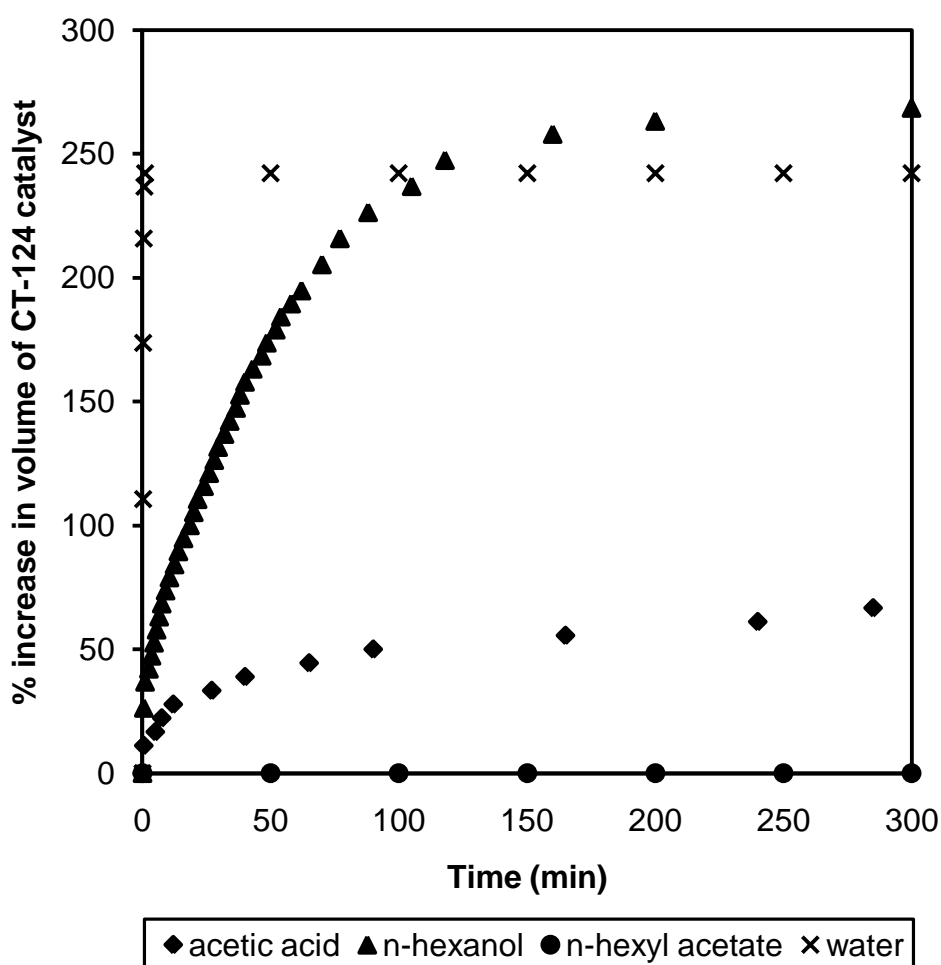
Figure 6.3. Swelling experimental results for Purolite® CT-124 catalyst.

that Purolite® CT-124 catalyst swells instantaneously in presence of water while there is negligible increase in catalyst volume in presence of

n-hexyl acetate. Both acetic acid and *n*-hexanol swells at a steady rate with latter helps the catalyst to swell faster. Negligible swelling of *n*-hexyl acetate on Purolite® CT-124 is preferred so that *n*-hexyl acetate will move through the chromatographic reactor as soon as it is produced and desorbs from the Purolite® CT-124 catalyst. Water on the other hand, being strongly adsorbed will be retained by the catalyst for a longer period. The swelling property of both water and *n*-hexyl acetate for Purolite® CT-124 catalyst favours the reactive chromatography process. Hence, it is evident that water is strongly adsorbed onto the catalyst followed by *n*-hexanol and acetic acid whilst *n*-hexyl acetate is least adsorbed onto Purolite® CT-124 catalyst and the swelling results favours the reactive chromatography operation for *n*-hexyl acetate synthesis.

6.2.5.2. Determination of Reaction Step Time

As previously mentioned that in chromatographic experiments, two steps are involved. The first is the reaction step and other is the regeneration step. In the reaction step, a known amount of reactants are fed to chromatographic reactor for a specific period of time. This time is called as the reaction step time. A number of parameters such as feed flow rate, feed mole ratio (FMR) of the reactants etc. affect the optimum time set for the reaction step. A number of experiments were carried out to find out the various reaction step times that can be used for the chromatographic reactor experiments. All the experimental results discussed in this section are carried out at 353 K. The experiment carried out at 0.5 mL/min of feed flow rate and at a molar ratio of 1:1 (*n*-hexanol : acetic acid) is shown in Figure 6.4 while the experiment conducted at 0.2 mL/min of feed flow rate and at a molar ratio of 3:1 (*n*-hexanol : acetic acid) is shown in Figure 6.5.

It can be observed from Figure 6.4 that the desired product, *n*-hexyl acetate front, first emerges at about 15 min. At about similar time, unreacted acetic acid front also seems to appear at the reactor outlet, which is not desired. The *n*-hexyl acetate front goes to maximum of about

50 mole% at 60 min and then falls to about 30 mole% after 150 min. The reason for this is the result of increase in unreacted acetic acid in the range of 35 mole% after 150 min. The chemical equilibrium composition is achieved at 180 min with acetic acid at 30 mole% and both *n*-hexanol and *n*-hexyl acetate at about 35 mole% each, respectively.
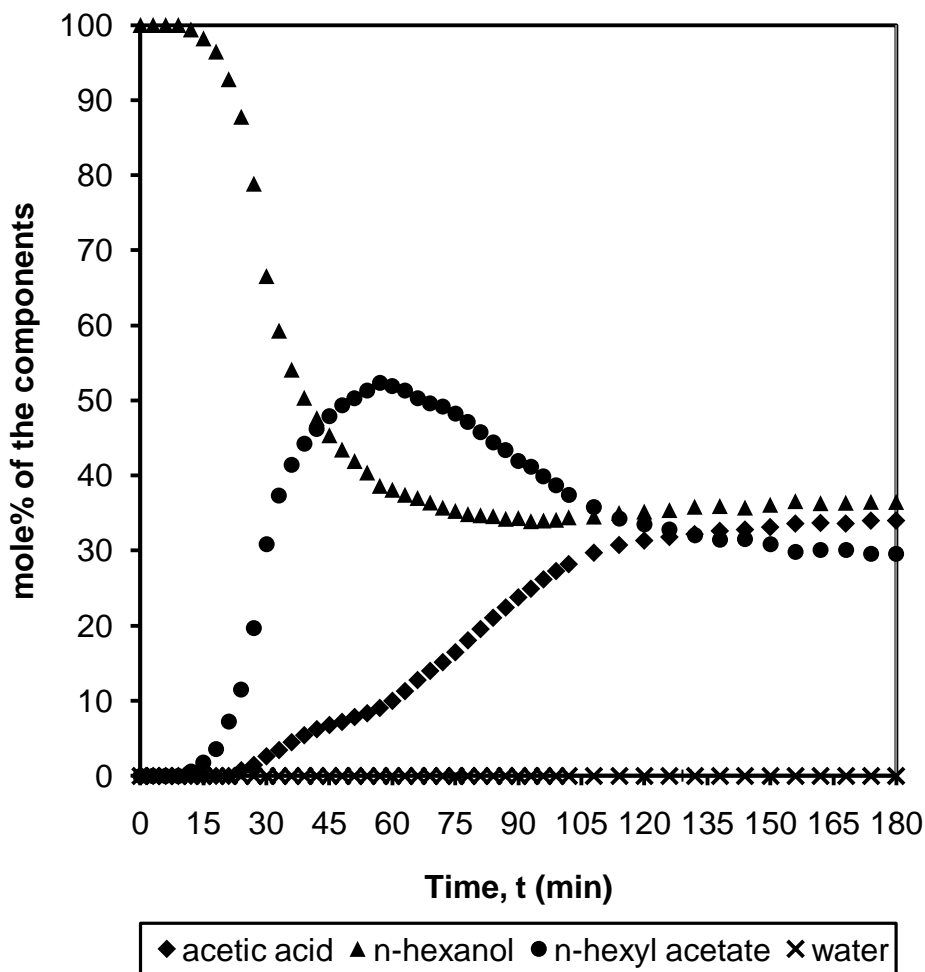
Figure 6.4. Experimental mole% of the samples collected at the chromatographic reactor outlet as a function of time for the reaction step. Operating conditions: Reaction temperature: 353 K; reaction step feed flow rate: 0.5 mL/min; feed mole ratio (*n*-hexanol : acetic acid): 1:1; catalyst: Purolite® CT-124; reaction step time: 180 min; acetic acid flow rate (0 – 180 min): 0.156 mL/min; *n*-hexanol flow rate (0 – 180 min): 0.344 mL/min.
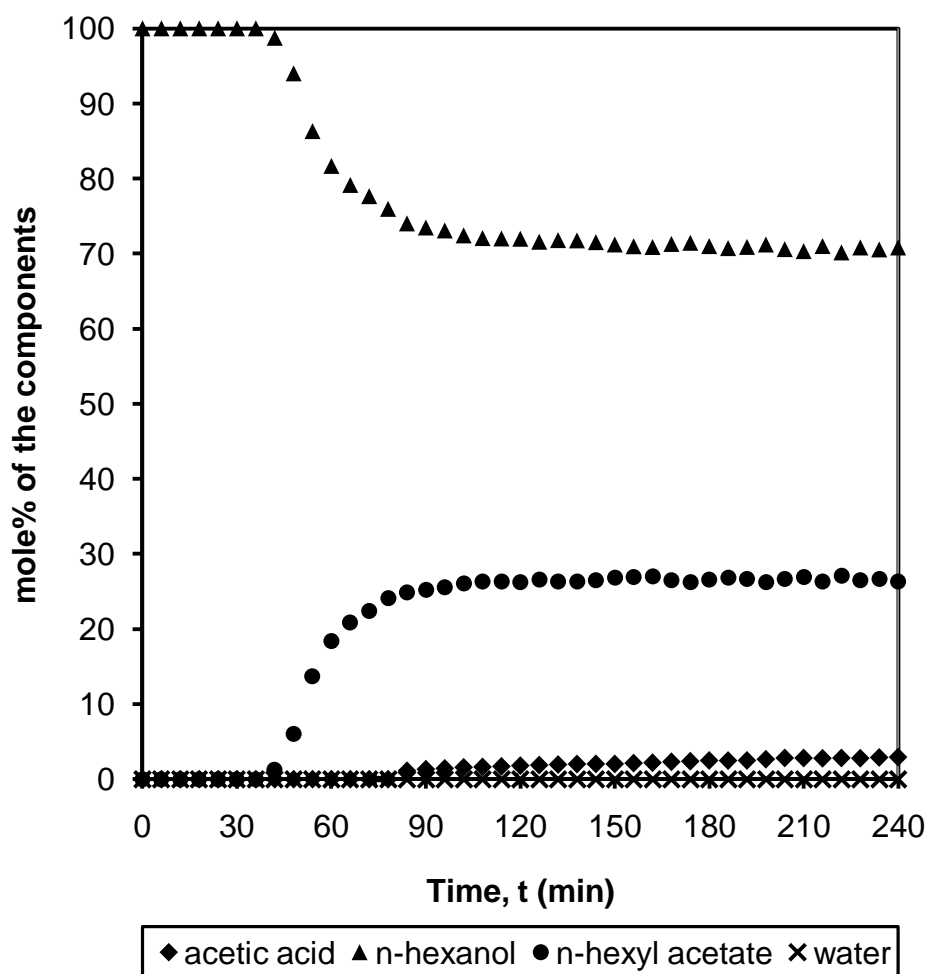
Figure 6.5. Experimental mole% of the samples collected at the chromatographic reactor outlet as a function of time for the reaction step. Operating conditions: Reaction temperature: 353 K; reaction step feed flow rate: 0.2 mL/min; feed mole ratio (n-hexanol : acetic acid): 3:1; catalyst: Purolite® CT-124; reaction step time: 240 min; acetic acid flow rate (0 – 240 min): 0.026 mL/min; n-hexanol flow rate (0 – 240 min): 0.174 mL/min.

Thus it is evident that feed flow rate of 0.5 mL/min decreases the residence time for acetic acid to be converted to product. Also, the stoichiometric feed molar ratio (FMR) of *n*-hexanol to acetic acid could be increased to limit the unreacted acetic acid at the reactor outlet. Also, there is no definite zone where only product comes out of the chromatographic reactor outlet with no acetic acid.

In Figure 6.5, the product, *n*-hexyl acetate front appears at about 40 min and then rises to just under 30 mole% and then remains constant throughout the experiment. Acetic acid front on the other hand, does not emerge until about 80 min and then stays just below 5 mole% over the entire experiment. The equilibrium composition for this experiment seems to be about 3 mole% for acetic acid whilst it is 72 mole% and 25 mole% for *n*-hexanol and *n*-hexyl acetate, respectively. A definite zone where desired product (*n*-hexyl acetate) diluted in solvent (*n*-hexanol) emerged at the reactor outlet without any unreacted acetic acid was found to be between 0 and 80 min. Therefore, it can be concluded that if batch chromatographic reactor experiments are carried out at a reaction step time of 75 min, 3:1 molar ratio of *n*-hexanol to acetic acid and 0.2 mL/min of feed flow rate then only *n*-hexyl acetate diluted in *n*-hexanol will appear at the reactor outlet.

A comparison of last two experimental results is shown in Figure 6.6**.** Water which comes out of the reactor in less than a mole% for both the experiments were not shown in Figure 6.6**.** So for most of the experiments discussed in the next subsequent section a reaction step time of 75 min was mostly used.

Figure 6.6. Comparison of experimental mole% of the samples collected for acetic acid and *n*-hexyl acetate at the chromatographic reactor outlet as a function of time for different reaction feed flow rates (0.2 mL/min and 0.5 mL/min) and at reaction temperature of 353 K.

6.2.5.3. Effect of Feed Flow Rate on *n*-Hexyl Acetate Synthesis

Feed flow rate of the reactants plays an important role in the optimisation of chromatographic reactor operation. A series of experiments were carried out using different feed flow rate at 353 K. The results only with respect to the reaction steps have been discussed in this section. Figure 6.8 shows the experiments carried out at 0.1 mL/min of feed flow rate and 2:1 molar ratio of reactants (*n*-hexanol : acetic acid). Figure 6.8 illustrates that the feed flow rate is very low, since the *n*-hexyl acetate front

emerges at about 90 min. So even though all the acetic acid was converted to *n*-hexyl acetate, the overall cost at this feed flow rate and mole ratio will increase significantly because of the amount of time taken to produce *n*-hexyl acetate and hence this condition was not recommended. Figure 6.9 shows the breakthrough curves for the experiments carried out at feed flow rate of 0.3 mL/min and feed molar ratio (*n*-hexanol : acetic acid) of 2:1 whilst Figure 6.7 shows the experiments conducted at feed flow rate of 0.41 mL/min and feed molar ratio (*n*-hexanol to acetic acid) 1.1:1. The amount of *n*-hexyl acetate produced is more at a feed flow rate of 0.41 mL/min and 1.1:1 molar ratio (*n*-hexanol : acetic acid) as compared to feed flow rate of 0.3 mL/min and feed molar ratio (*n*-hexanol : acetic acid) of 2:1.

However, increase in *n*-hexyl acetate concentration comes at a cost of increase in unreacted acetic acid at the reactor outlet. The amount of unreacted acetic acid at the end of reaction step is in the range of 10 mole% with experiments conducted at feed flow rate of 0.41 mL/min and feed molar ratio (*n*-hexanol : acetic acid) of 1.1:1 as compared to only about 3 mole% with experiments conducted at feed flow rate of 0.3 mL/min and feed molar ratio (*n*-hexanol : acetic acid) of 2:1.
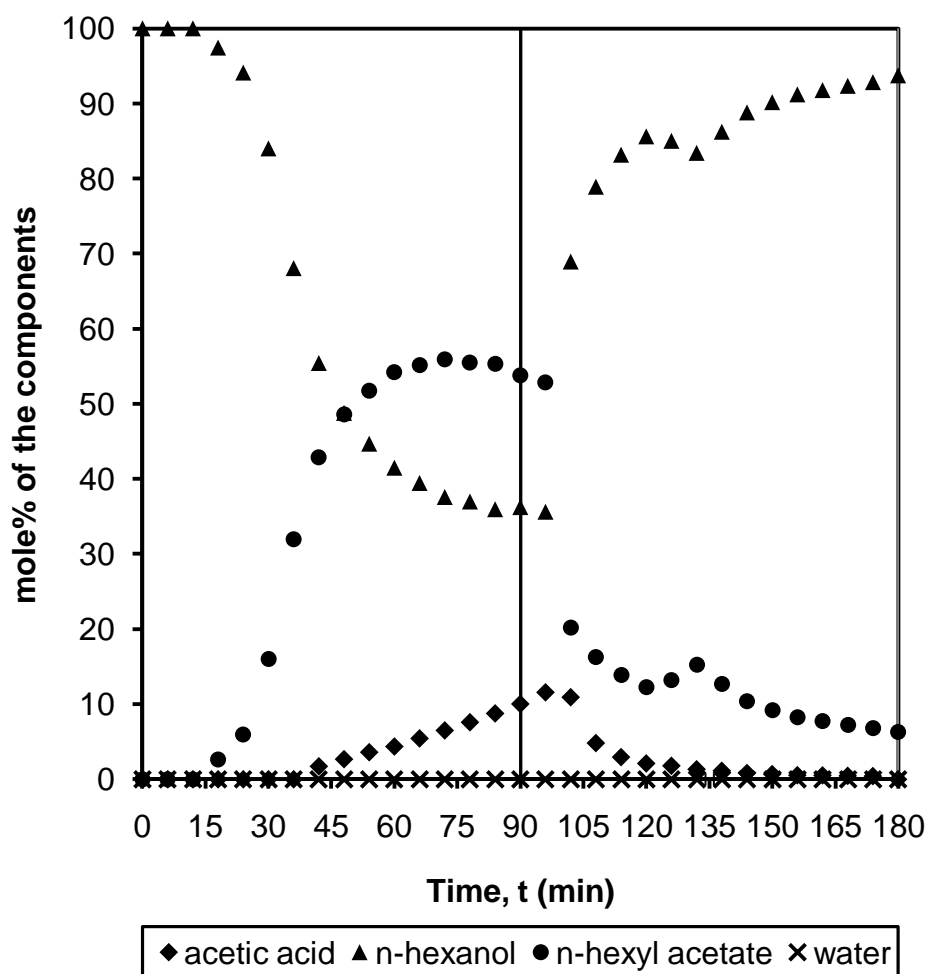
Figure 6.7. Experimental mole% of the samples collected at the chromatographic reactor outlet as a function of time for both the reaction and the column regeneration steps. Operating conditions: Reaction temperature: 353 K; reaction step feed flow rate: 0.41 mL/min; feed mole ratio (*n*-hexanol : acetic acid): 1.1:1; catalyst: Purolite® CT-124; reaction and regeneration steps time: 90 min each; acetic acid flow rate (0 – 90 min): 0.12 mL/min; *n*-hexanol flow rate (0 – 90 min): 0.29 mL/min; *n*-hexanol flow rate (90 – 180 min): 0.41 mL/min.
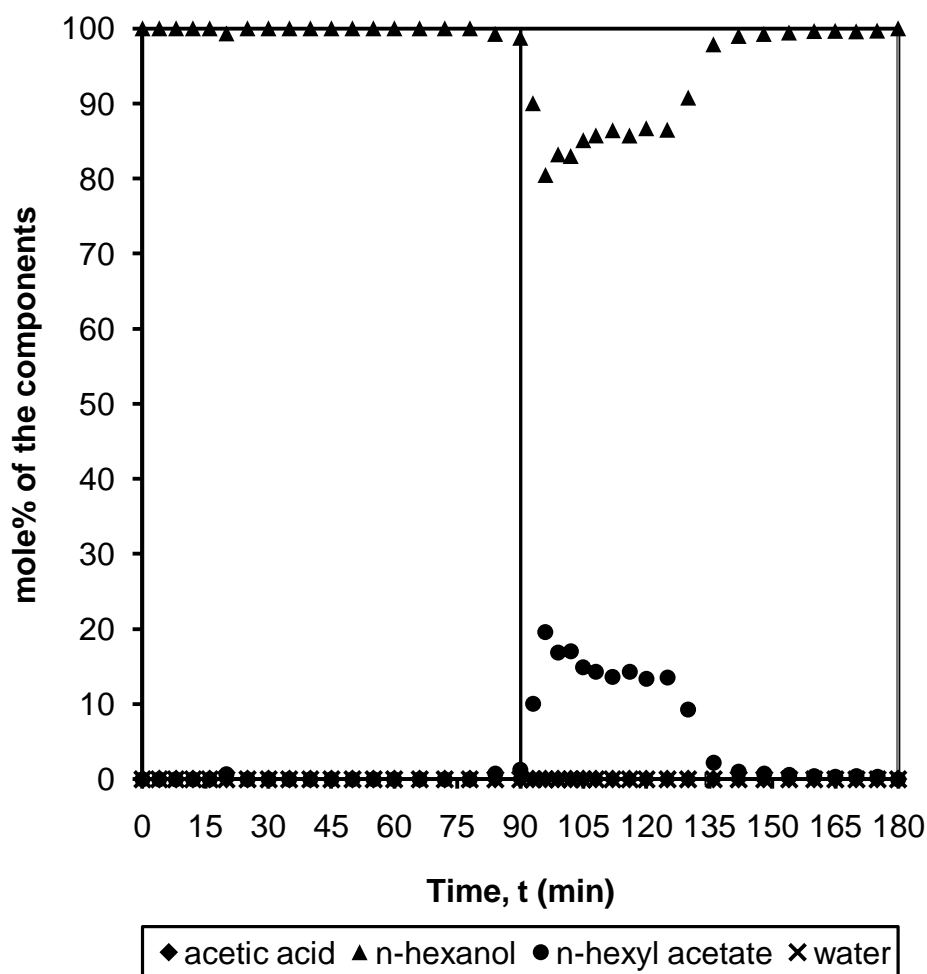
Figure 6.8. Experimental mole% of the samples collected at the chromatographic reactor outlet as a function of time for both the reaction and the column regeneration steps. Operating conditions: Reaction temperature: 353 K; reaction step feed flow rate: 0.1 mL/min; feed mole ratio (*n*-hexanol : acetic acid): 2:1; catalyst: Purolite® CT-124; reaction and regeneration step times: 90 min each; acetic acid flow rate (0 – 90 min): 0.018 mL/min; *n*-hexanol flow rate (0 - 90 min): 0.082 mL/min; *n*-hexanol flow rate (90 – 180 min): 0.5 mL/min.
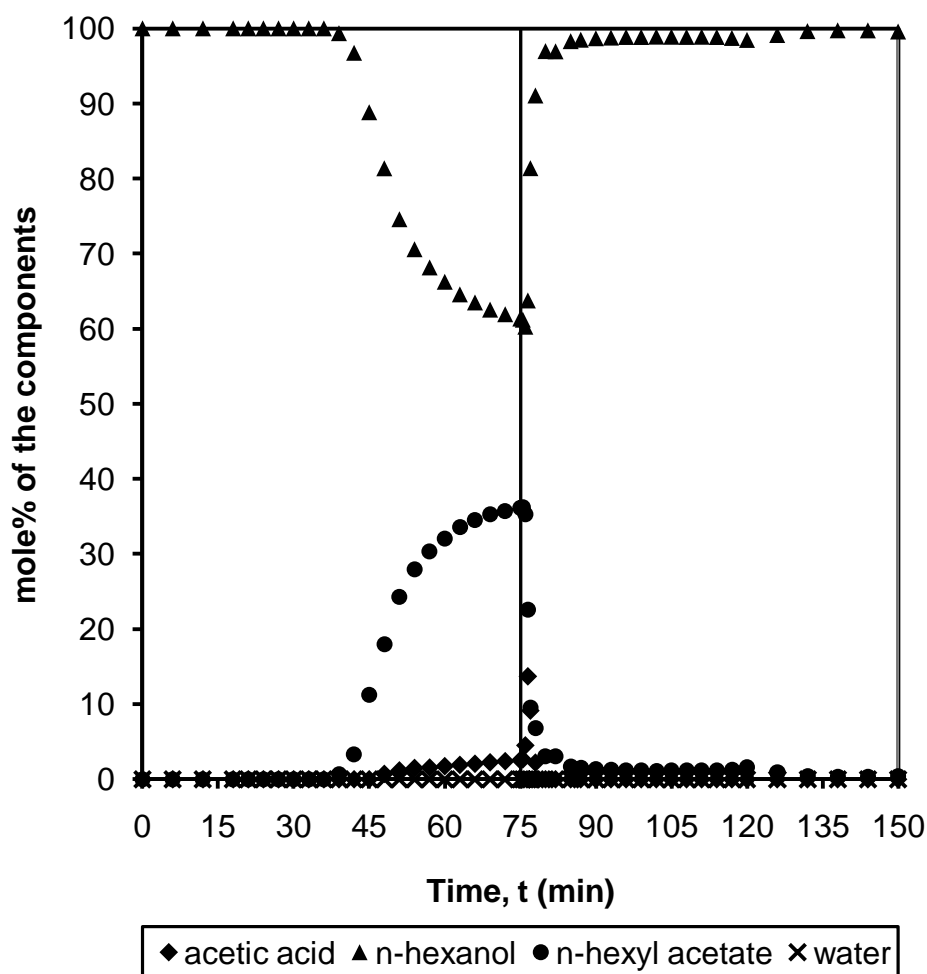
Figure 6.9. Experimental mole% of the samples collected at the chromatographic reactor outlet as a function of time for both the reaction and the column regeneration steps. Operating conditions: Reaction temperature: 353 K; reaction step feed flow rate: 0.3 mL/min; feed mole ratio (*n*-hexanol : acetic acid): 2:1; catalyst: Purolite® CT-124; reaction and regeneration steps time: 75 min each; acetic acid flow rate (0 – 75 min): 0.055 mL/min; *n*-hexanol flow rate (0 – 75 min): 0.245 mL/min; *n*-hexanol flow rate (75 – 150 min): 3.0 mL/min.

Figure 6.10 shows the experiments conducted at feed flow rate of 0.5 mL/min and feed molar ratio (*n*-hexanol to acetic acid) of 1:1 whilst Figure 6.11 shows the experiments carried out at a feed flow rate of 0.5 mL/min and feed molar ratio (*n*-hexanol to acetic acid) of 2:1

Figure 6.10 illustrates the maximum amount of both *n*-hexyl acetate (50 mole%) and unreacted acetic acid (20 mole%) at 75 min compared to *n*-hexyl acetate of about 40 mole% and unreacted acetic acid of 3 mole% at 75 min as shown in Figure 6.11.

Figure 6.10. Experimental mole% of the samples collected at the chromatographic reactor outlet as a function of time for both the reaction and the column regeneration steps. Operating conditions: Reaction temperature: 353 K; reaction step feed flow rate: 0.5 mL/min; feed mole ratio (*n*-hexanol : acetic acid): 1:1; catalyst: Purolite® CT-124; reaction and regeneration steps time: 75 min each; acetic acid flow rate (0 – 75 min): 0.156 mL/min; *n*-hexanol flow rate (0 – 75 min): 0.344 mL/min; *n*-hexanol flow rate (75 – 150 min): 3.0 mL/min.

It can be concluded from Figures 6.10 and 6.11 that increase in feed mole ratio of *n*-hexanol to acetic acid favours the minimisation of unreacted acetic acid without significantly affecting the *n*-hexyl acetate production.
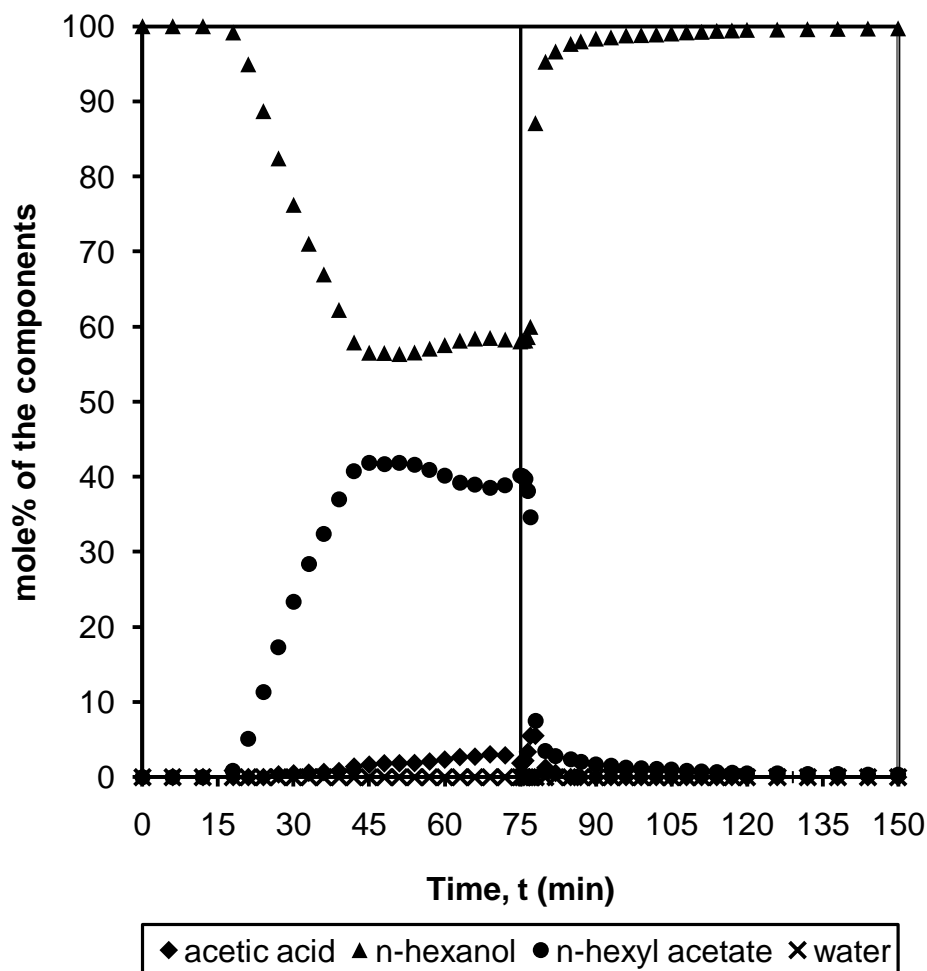
Figure 6.11. Experimental mole% of the samples collected at the chromatographic reactor outlet as a function of time for both the reaction and the column regeneration steps. Operating conditions: Reaction temperature: 353 K; reaction step feed flow rate: 0.5 mL/min; feed mole ratio (*n*-hexanol : acetic acid): 2:1; catalyst: Purolite® CT-124; reaction and regeneration steps time: 75 min each; acetic acid flow rate (0 – 75 min): 0.093 mL/min; *n*-hexanol flow rate (0 – 75 min): 0.407 mL/min; *n*-hexanol flow rate (75 – 150 min): 3.0 mL/min.
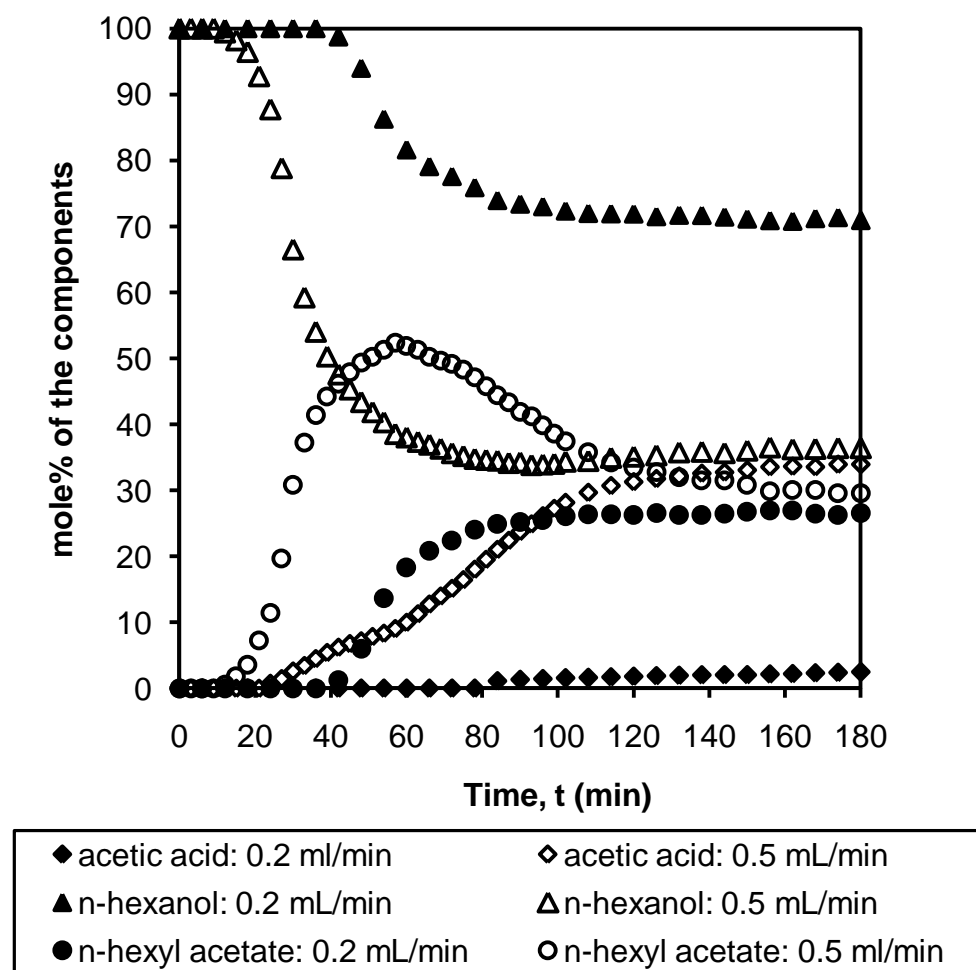
Figure 6.12. Experimental mole% of the samples collected at the chromatographic reactor outlet as a function of time for both the reaction and the column regeneration steps. Operating conditions: Reaction temperature: 353 K; reaction step feed flow rate: 1.0 mL/min; feed mole ratio (*n*-hexanol : acetic acid): 3:1; catalyst: Purolite® CT-124; reaction and regeneration steps time: 75 min each; acetic acid flow rate (0 – 75 min): 0.132 mL/min; *n*-hexanol flow rate (0 – 75 min): 0.868 mL/min; *n*-hexanol flow rate (75 – 150 min): 3.0 mL/min.

Figure 6.12 shows the experiment carried out at a feed flow rate of 1.0 mL/min and feed molar ratio (*n*-hexanol to acetic acid) of 3:1 whilst Figure 6.13 shows the experiment conducted at a feed flow rate of 2.0 mL/min and feed molar ratio (*n*-hexanol to acetic acid) of 3:1. The feed

molar ratio of *n*-hexanol to acetic acid was kept constant to study how the reaction proceeds at 1.0 mL/min and 2.0 mL/min, respectively.

Figure 6.13. Experimental mole% of the samples collected at the chromatographic reactor outlet as a function of time for both the reaction and the column regeneration steps. Operating conditions: Reaction temperature: 353 K; reaction step feed flow rate: 2.0 mL/min; feed mole ratio (*n*-hexanol : acetic acid): 3:1; catalyst: Purolite® CT-124; reaction and regeneration steps time: 75 min each; acetic acid flow rate (0 – 75 min): 0.264 mL/min; *n*-hexanol flow rate (0 – 75 min): 1.736 mL/min; *n*-hexanol flow rate (75 – 150 min): 3.0 mL/min.

From both Figures 6.12 and 6.13, it is evident that the maximum amount of unreacted acetic acid reached the reactor outlet and very little amount of *n*-hexyl acetate was formed. Both these experiments and previous experiments confirm that feed flow rate higher than 0.5 mL/min decreases the residence time for the acetic acid and *n*-hexanol to completely convert to *n*-hexyl acetate and water and hence not recommended.

6.2.5.4. Effect of Feed Molar Ratio on *n*-Hexyl Acetate Synthesis

As seen from the previous section that the increase in feed molar ratio (*n*-hexanol : acetic acid) decreases the amount of unreacted acetic acid at the reactor outlet. From determination of reaction step time, it was found that experiment carried out at 353 K, feed flow rate of 0.2 mL/min, feed molar ratio (*n*-hexanol : acetic acid) of 3:1 and reaction step time of 75 min completely convert all the acetic acid.

A series of experiments were therefore conducted at a flow rate of 0.2 mL/min at different feed mole ratio (*n*-hexanol : acetic acid) to determine the optimum feed mole ratio (*n*-hexanol : acetic acid) ratio required for complete conversion of acetic acid and higher *n*-hexyl acetate formation. The experiments were conducted at feed molar ratio (*n*-hexanol : acetic acid) of 1:1, 2:1 and 2.58:1 and the results are shown in Figures 6.14 – 6.16, respectively.
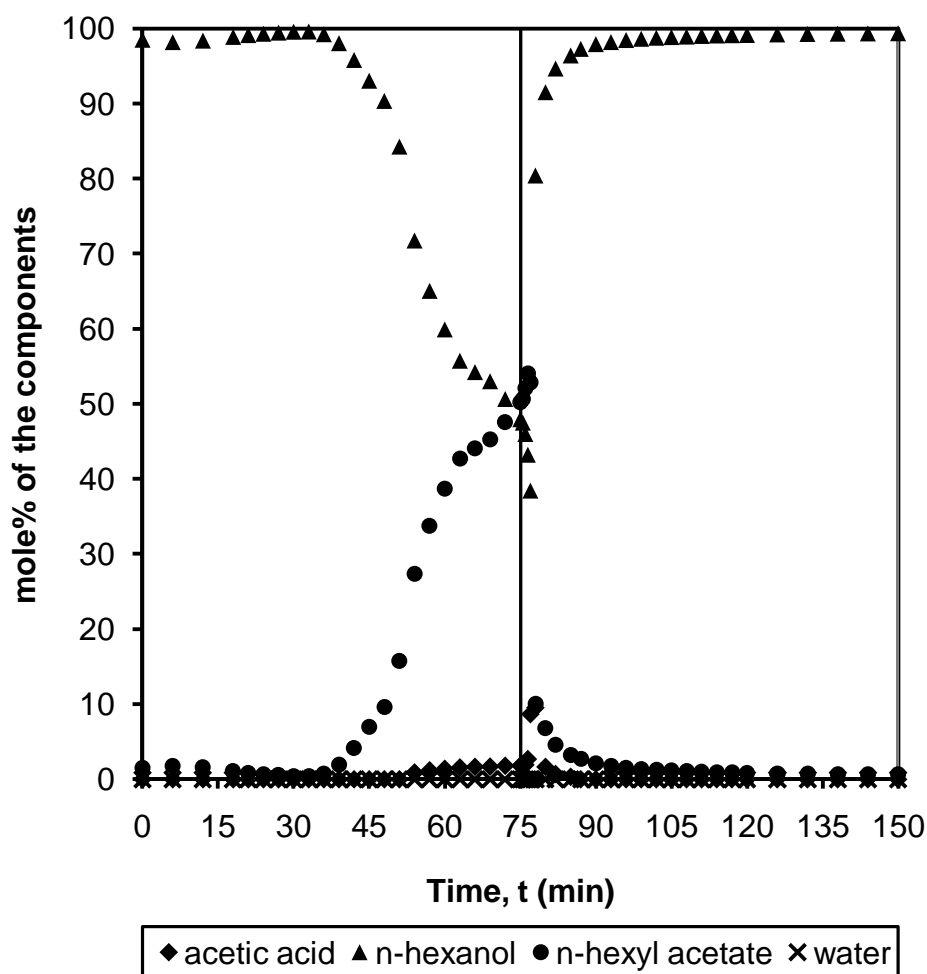
Figure 6.14. Experimental mole% of the samples collected at the chromatographic reactor outlet as a function of time for both the reaction and the column regeneration steps. Operating conditions: Reaction temperature: 353 K; reaction step feed flow rate: 0.2 mL/min; feed mole ratio (*n*-hexanol : acetic acid): 1:1; catalyst: Purolite® CT-124; reaction and regeneration steps time: 75 min each; acetic acid flow rate (0 – 75 min): 0.063 mL/min; *n*-hexanol flow rate (0 – 75 min): 0.137 mL/min; *n*-hexanol flow rate (75 – 150 min): 3.0 mL/min.
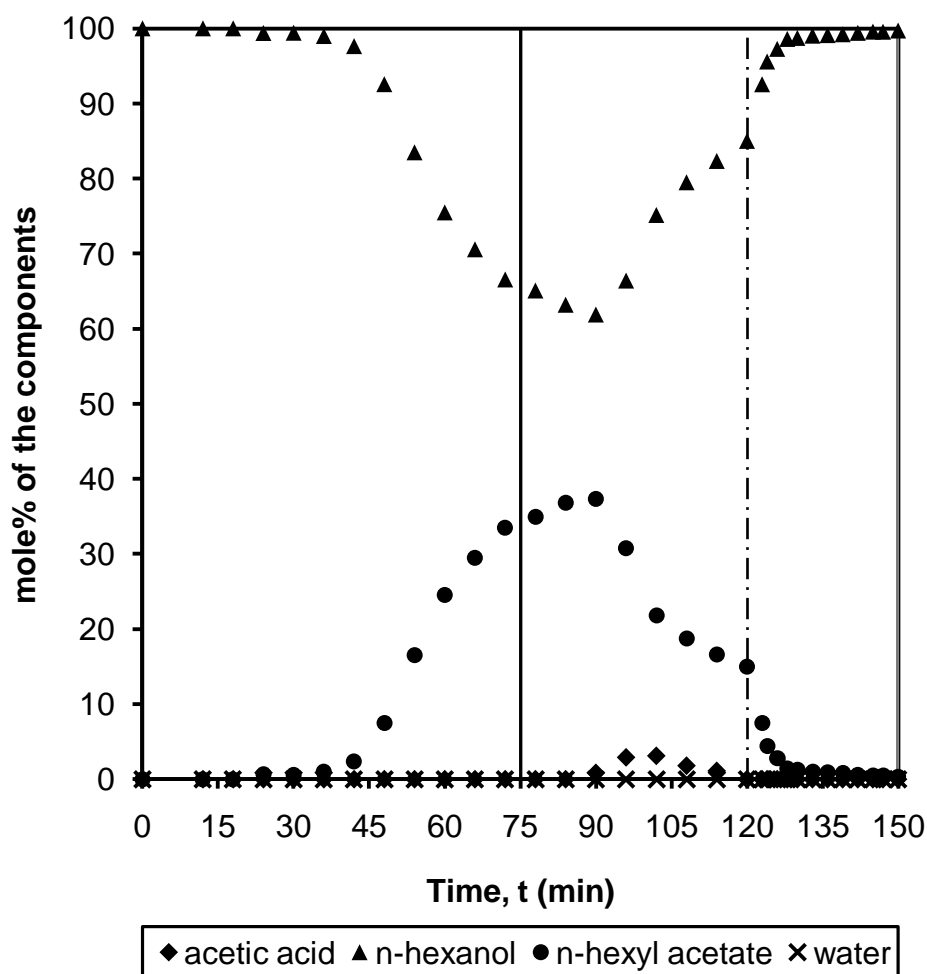
Figure 6.15. Experimental mole% of the samples collected at the chromatographic reactor outlet as a function of time for both the reaction and the column regeneration steps. Operating conditions: Reaction temperature: 353 K; reaction step feed flow rate: 0.2 mL/min; feed mole ratio (*n*-hexanol : acetic acid): 2:1; catalyst: Purolite® CT-124; reaction and regeneration steps time: 75 min each; acetic acid flow rate (0 – 75 min): 0.037 mL/min; *n*-hexanol flow rate (0 - 120 min): 0.163 mL/min; *n*-hexanol flow rate (120 – 150 min): 3.0 mL/min.
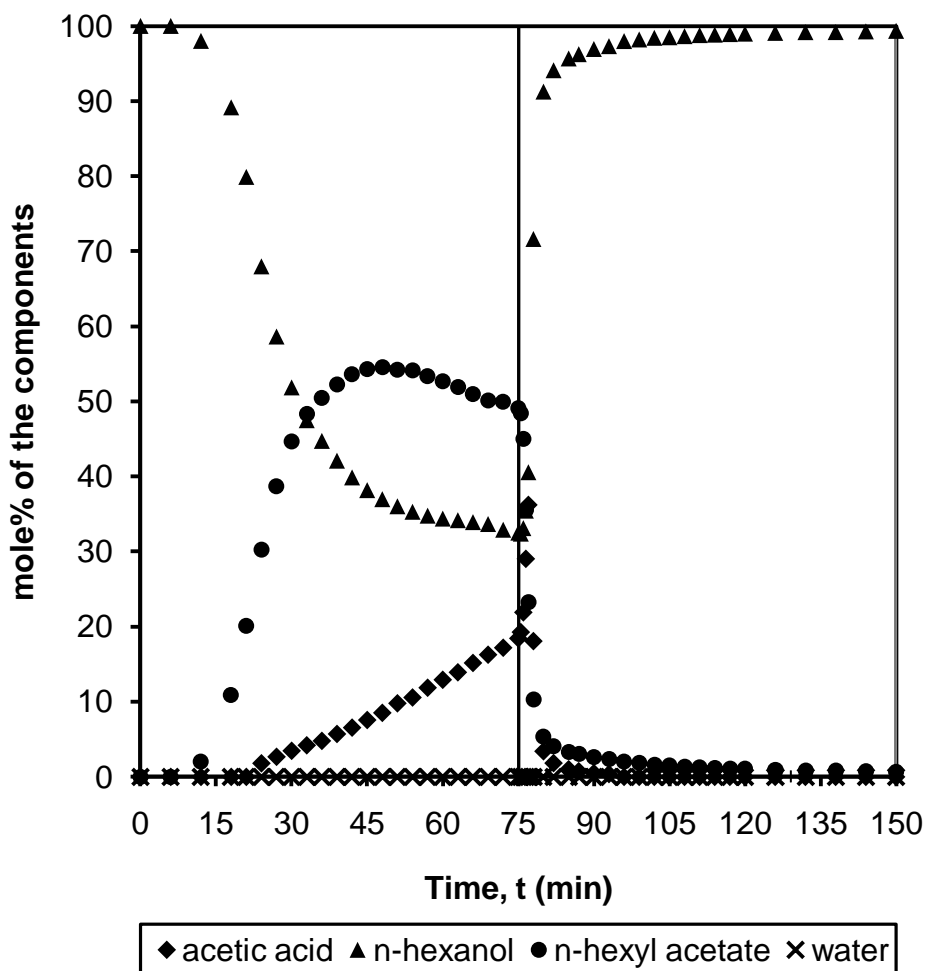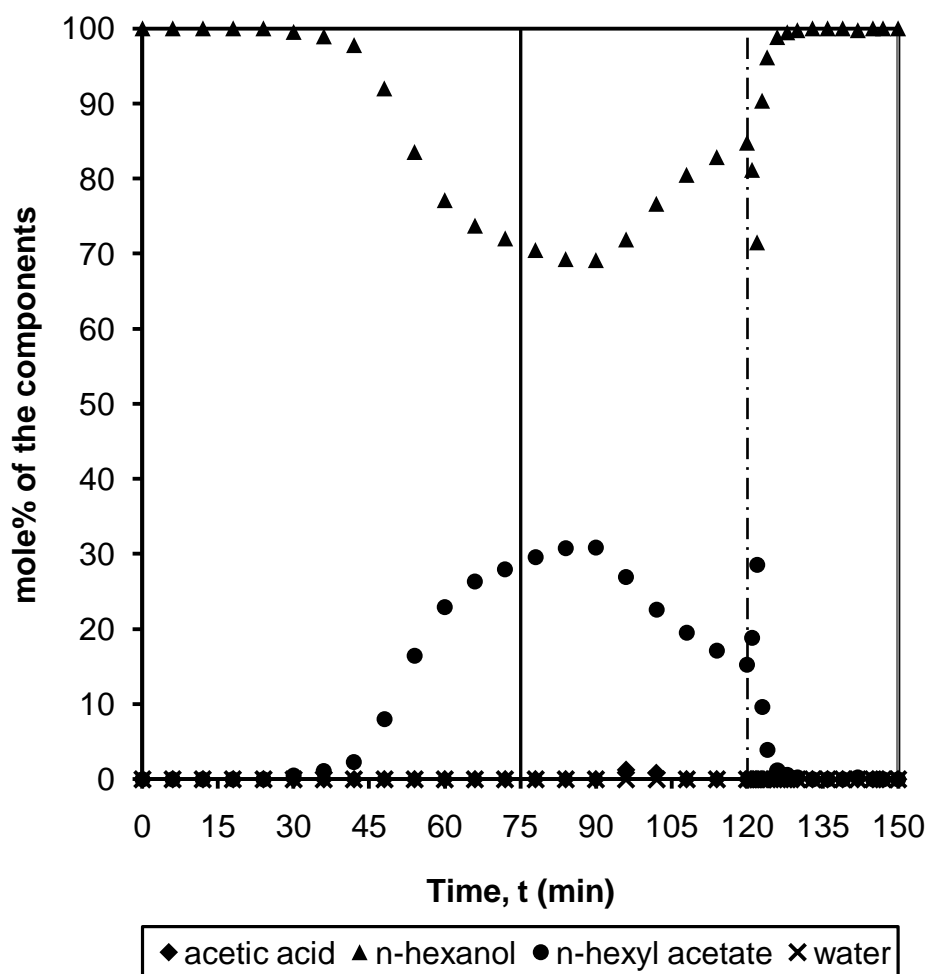
Figure 6.16. Experimental mole% of the samples collected at the chromatographic reactor outlet as a function of time for both the reaction and the column regeneration steps. Operating conditions: Reaction temperature: 353 K; reaction step feed flow rate: 0.2 mL/min; feed mole ratio (*n*-hexanol : acetic acid): 2.58:1; catalyst: Purolite® CT-124; reaction and regeneration steps time: 75 min each; acetic acid flow rate (0 – 75 min): 0.03 mL/min; *n*-hexanol flow rate (0 – 120 min): 0.17 mL/min; *n*-hexanol flow rate (120 – 150 min): 3.0 mL/min.

Figure 6.17 shows the comparison of few of the experiments discussed in this section with the experiment conducted at feed flow rate of 0.2 mL/min, feed molar ratio (*n*-hexanol : acetic acid) of 3:1, other parameters remain unchanged. Figure 6.17 clearly indicates that decrease in feed molar ratio

(FMR) of *n*-hexanol to acetic acid increases the formation of *n*-hexyl acetate, but also increases the unreacted acetic acid at the reactor outlet. The optimum feed molar ratio (*n*-hexanol : acetic acid) was found to be 3:1 for feed flow rate of 0.2 mL/min.
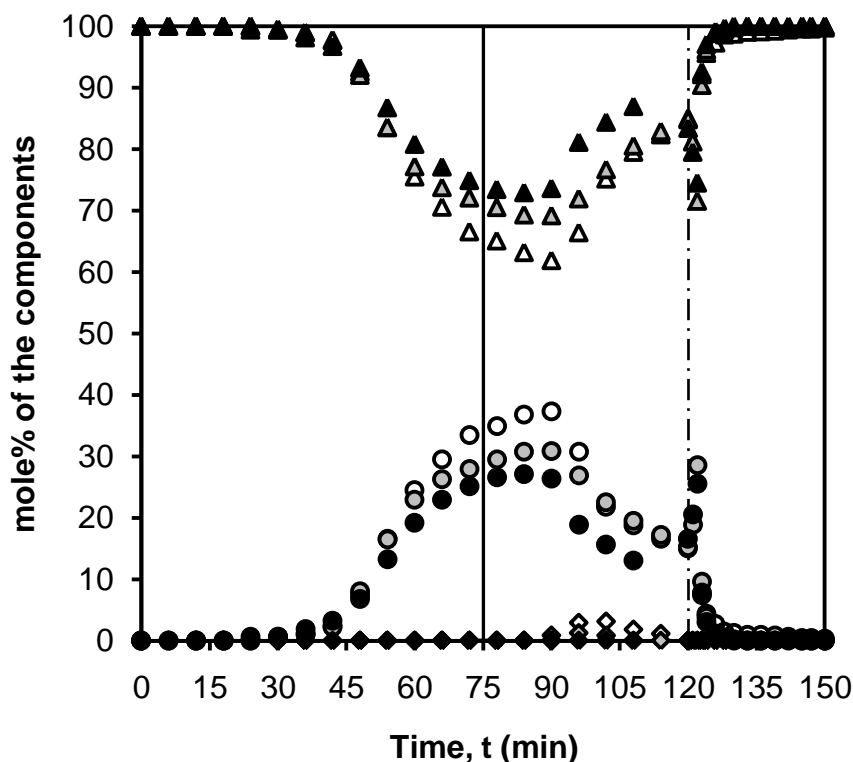
Figure 6.17. Comparison of experimental mole% of the samples collected for acetic acid, *n*-hexanol and *n*-hexyl acetate at the chromatographic reactor outlet as a function of time for different feed mole ratio (*n*-hexanol : acetic acid) at reaction temperature of 353 K.

6.2.5.5. Effect of Temperature

A series of experiments were carried out in a batch chromatographic reactor to find the optimum temperature for chromatographic reactor

operation at a feed flow rate of 0.2 mL/min and feed molar ratio (*n*-hexanol of acetic acid) of 3:1.

Figures 6.18 – 6.20 show the experimental results conducted at 343 K, 348 K and 353 K, respectively. Figure 6.21 compares all the three experiments that are discussed in this section. It is worth noting that the complete conversion of acetic acid was achieved by carrying out batch chromatographic reactor experiments at 343 K, 348 K and 353 K, respectively.

However, the desorption rate of *n*-hexyl acetate is higher at 353 K as compared to 343 K and 348 K. This may affect the regeneration process. A greater amount of solvent (*n*-hexanol) or greater time may be required for complete regeneration of chromatographic reactor. As a result, 353 K was considered to be the optimum temperature for 0.2 mL/min of feed flow rate and feed molar ratio (*n*-hexanol to acetic acid) of 3:1.
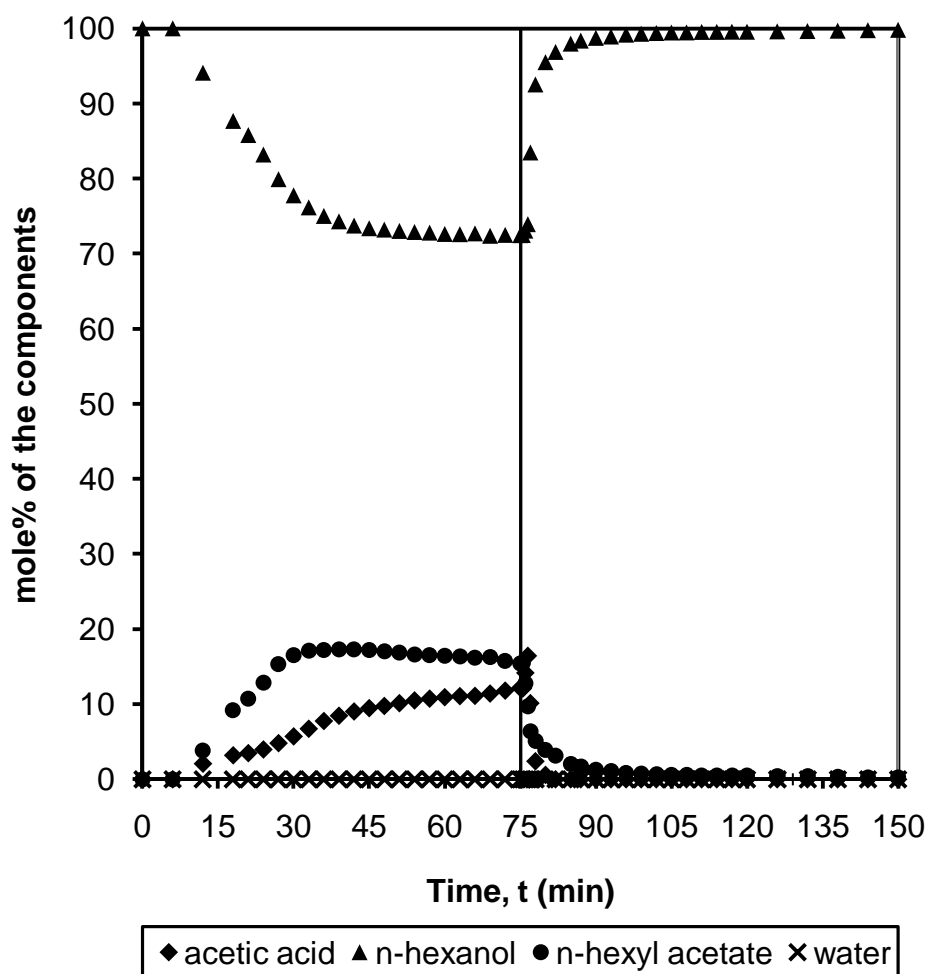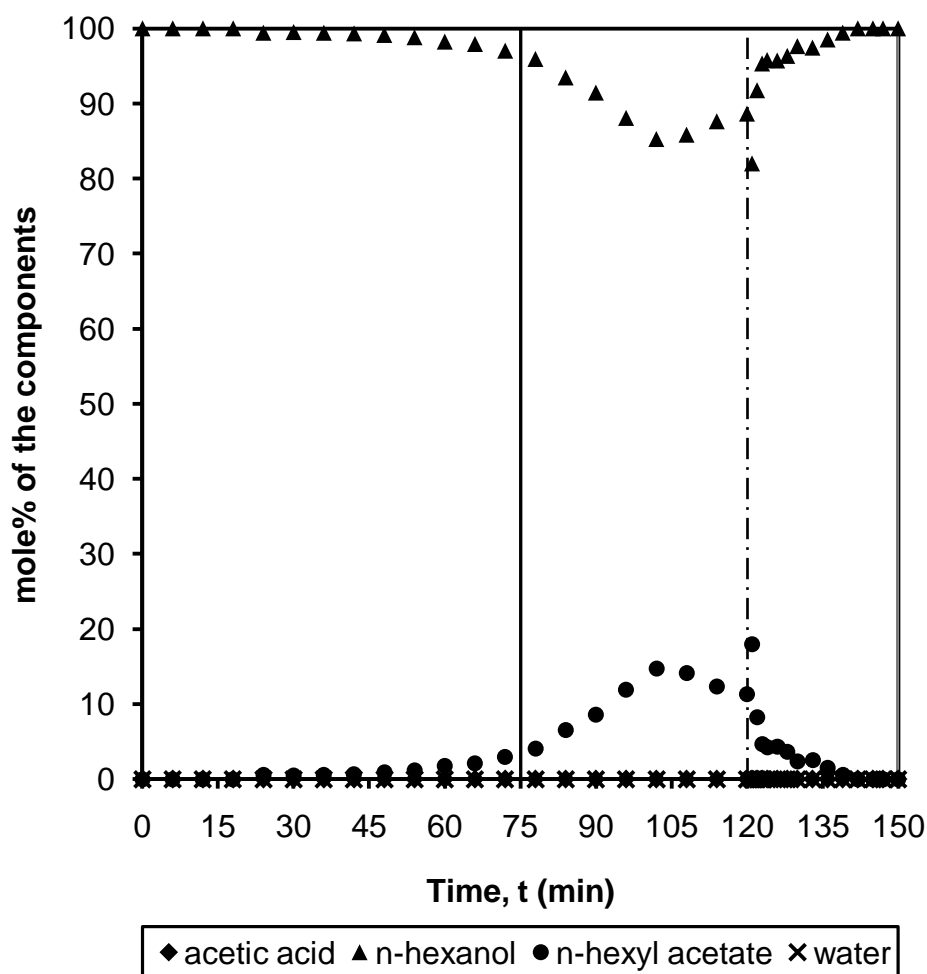
Figure 6.18. Experimental mole% of the samples collected at the chromatographic reactor outlet as a function of time for both the reaction and the column regeneration steps. Operating conditions: Reaction temperature: 343 K; reaction step feed flow rate: 0.2 mL/min; feed mole ratio (*n*-hexanol : acetic acid): 3:1; catalyst: Purolite$^®$ CT-124; reaction and regeneration steps time: 75 min each; acetic acid flow rate (0 – 75 min): 0.026 mL/min; *n*-hexanol flow rate (0 – 120 min): 0.174 mL/min; *n*-hexanol flow rate (120 – 150 min): 3.0 mL/min.
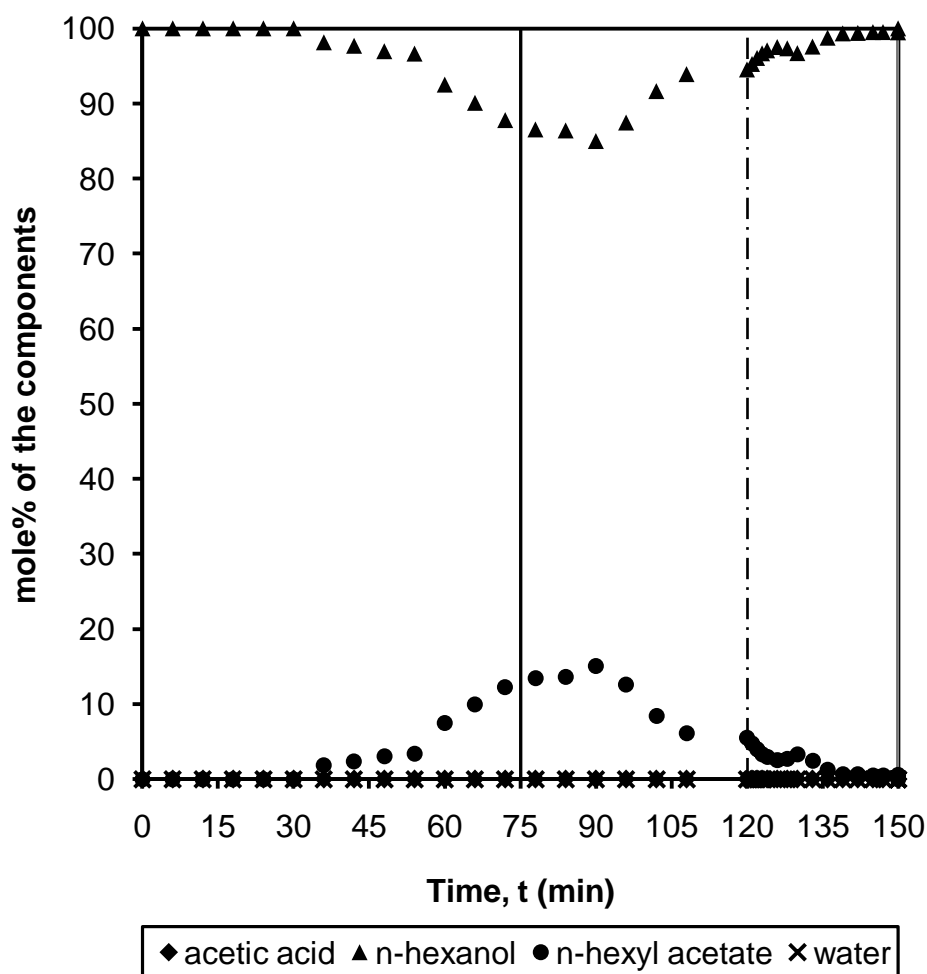
Figure 6.19. Experimental mole% of the samples collected at the chromatographic reactor outlet as a function of time for both the reaction and the column regeneration steps. Operating conditions: Reaction temperature: 348 K; reaction step feed flow rate: 0.2 mL/min; feed mole ratio (*n*-hexanol : acetic acid): 3:1; catalyst: Purolite® CT-124; reaction and regeneration steps time: 75 min each; acetic acid flow rate (0 – 75 min): 0.026 mL/min; *n*-hexanol flow rate (0 – 120 min): 0.174 mL/min; *n*-hexanol flow rate (120 – 150 min): 3.0 mL/min.
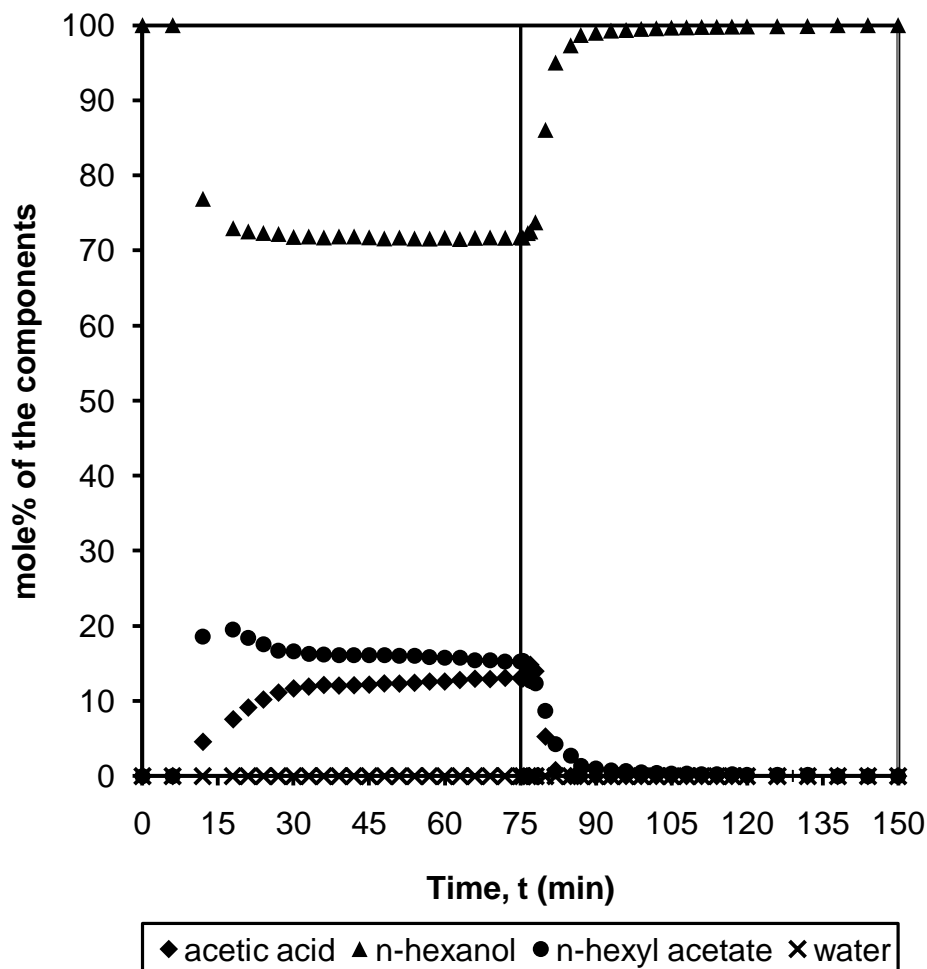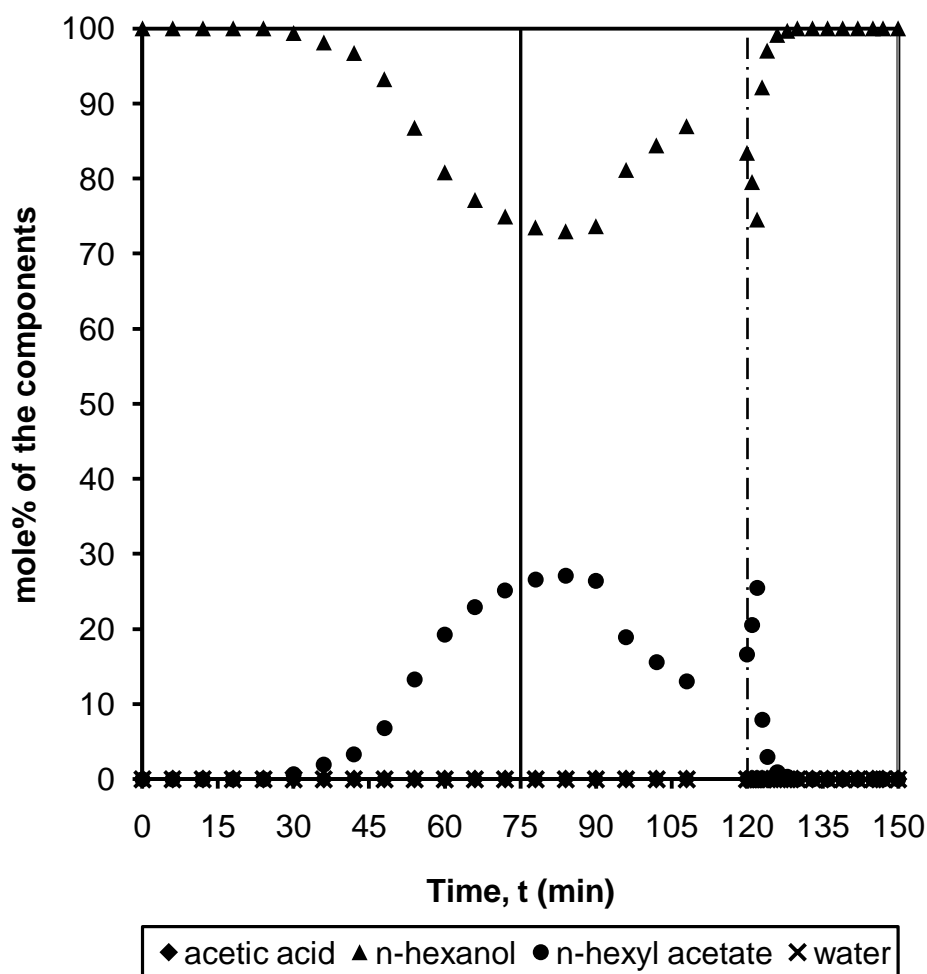
Figure 6.20. Experimental mole% of the samples collected at the chromatographic reactor outlet as a function of time for both the reaction and the column regeneration steps. Operating conditions: Reaction temperature: 353 K; reaction step feed flow rate: 0.2 mL/min; feed mole ratio (*n*-hexanol : acetic acid): 3:1; catalyst: Purolite® CT-124; reaction and regeneration steps time: 75 min each; acetic acid flow rate (0 – 75 min): 0.026 mL/min; *n*-hexanol flow rate (0 – 120 min): 0.174 mL/min; *n*-hexanol flow rate (120 – 150 min): 3.0 mL/min.
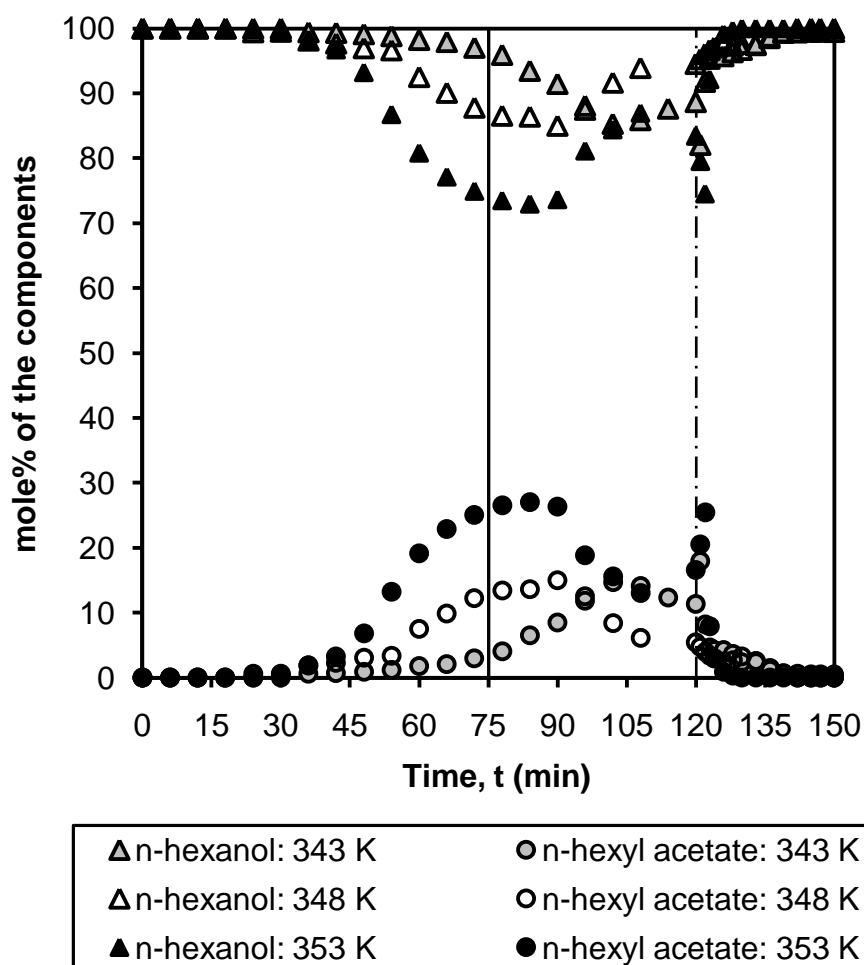
Figure 6.21. Effect of temperature on the mole% of the samples collected for *n*-hexanol and *n*-hexyl acetate at the chromatographic reactor outlet as a function of time. Operating conditions: reaction step feed flow rate: 0.2 mL/min; feed mole ratio (*n*-hexanol : acetic acid): 3:1; catalyst: Purolite® CT-124; reaction and regeneration steps time: 75 min each; acetic acid flow rate (0 – 75 min): 0.026 mL/min; *n*-hexanol flow rate (0 – 120 min): 0.174 mL/min; *n*-hexanol flow rate (120 – 150 min): 3.0 mL/min.

In the next section, materials and methods, experimental set-up and procedure, method of analysis and results and discussion for continuous chromatographic reactor are discussed in detail.

6.3. CONTINUOUS CHROMATOGRAPHIC REACTOR STUDIES

6.3.1. Introduction

In this project, the batch chromatographic reactor experiments were successfully carried out and have been discussed in section 6.2. The major advantages of batch chromatographic reactor over classical batch reactor were to achieve quantitative conversion of the limiting reactant (acetic acid) and separation of products. However, batch chromatographic reactor set-up suffers from one drawback of its limiting batch operation i.e. the process cannot be run continuously. Therefore, a continuous chromatographic reactor set-up was designed on the basis of the results obtained from the batch chromatographic reactor experiments. The materials and the catalyst used for continuous chromatographic reactor, the continuous chromatographic reactor experimental set-up and procedure and the results and discussion are explained in detail in the following sections.

6.3.2. Materials and Catalysts

All chemicals and catalyst used for the continuous chromatographic reactors are the same as those were used for batch chromatographic reactor as explained in detail in section 6.2.1. Safety data sheet (SDS) of all the chemicals and the catalysts used for continuous chromatographic reactor are attached in Appendix 9.2.1 and 9.2.2. COSHH (Control of Substances Hazardous to Health) and Risk Assessment (RA) records for continuous chromatographic reactor experiments were carried out before conducting the experiments and are attached in Appendix 9.3 and 9.4, respectively.

Four empty HPLC column assemblies each of length 0.25 m and internal diameter of 10 x 10^{-3} m were purchased from Phenomenox, UK for continuous chromatographic reactor experiments. Only four columns were used for each continuous chromatographic reactor experiment. These four

columns were packed with the Purolite® CT-124 catalyst using slurry technique as explained in detail in section 6.2.2.

6.3.3. Design, Construction and Commissioning of Continuous Chromatographic Reactor

The concept of designing continuous chromatographic reactor comes largely from the batch chromatographic reactor set-up. Consider only the column inlet and outlet configuration of the batch chromatographic reactor (see Figure 6.1). In a batch chromatographic reactor experiment, the column was fed with the reactants (acetic acid and *n*-hexanol). Samples from the column outlet were collected at regular intervals. For first few minutes, e.g. until time, t = T1 (i.e. part of reaction step), the samples consist of only *n*-hexanol were collected. This is because the reactants or products formed have still not reached the column outlet and the only component that comes out of the chromatographic reactor outlet is the solvent (*n*-hexanol), which was used to pump through the column during the column packing process

Now consider the time between T1 and T2 (i.e., part of reaction step, T2>T1), samples only with *n*-hexyl acetate and *n*-hexanol were collected (extract). This is because *n*-hexyl acetate was produced as a result of reaction between acetic acid and *n*-hexanol in the presence of swelled Purolite® CT-124 catalyst and since *n*-hexyl acetate is less adsorbed onto the Purolite® CT-124 catalyst, it desorbs quickly and moves towards the direction of feed flow i.e. at the reactor outlet. Now consider the time between T2 and T3 (i.e., part of regeneration step, T3>T2), all the components i.e., acetic acid, *n*-hexanol, *n*-hexyl acetate and water were present in the samples collected (raffinate) from the reactor outlet and finally the time between T3 and T4 (i.e., part of regeneration step, T4>T3), the sample consists of only *n*-hexanol (effluent) which indicates that the column regeneration was completed. So there are three definite zones

(i.e. extract, raffinate and effluent) during the reactive chromatography process.

As shown in Figure 6.22, the same batch chromatographic column is now attached with six solenoid valves. Six solenoid valves represent for the two reactants inlet (reaction step), one for extract (rich in *n*-hexyl acetate and *n*-hexanol only), one for the raffinate (all the components), one for effluent (*n*-hexanol only) and one for the intermittent connection to the next column. In essence Figure 6.22 set-up is the same as batch chromatographic reactor experimental set-up but comes with six solenoid valves.

In batch chromatographic reactor only inlet and outlet points are of importance which is carried out in a single column. However, in continuous
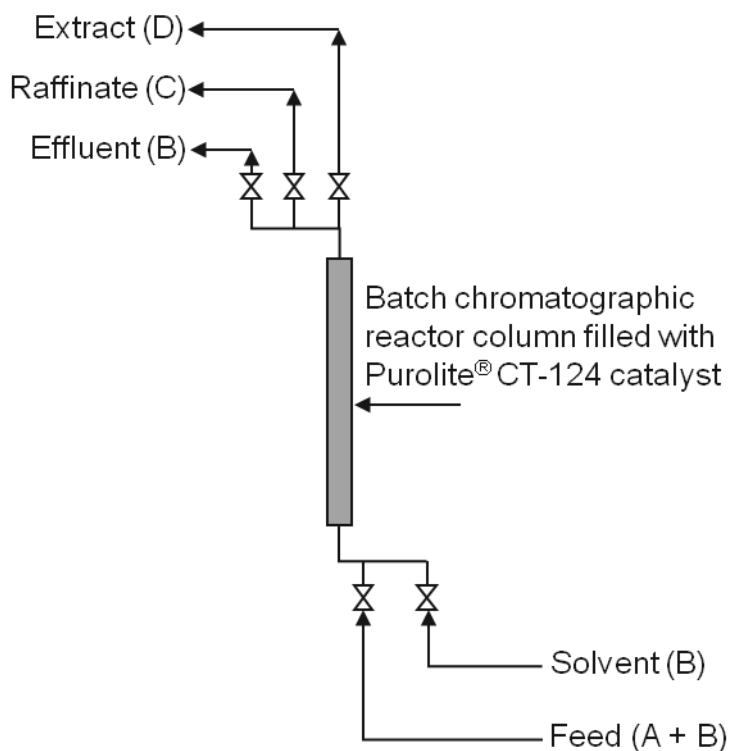
Figure 6.22. Batch chromatographic reactor set-up.

chromatographic reactor one column will represent for feed, others for extract, raffinate and for effluent, respectively. As a result, it was decided that four columns each with six solenoid valves assembly will be used for continuous chromatographic reactor set-up. Figure 6.22 represents one column configuration attached with all the solenoid valves.

Solenoid valves used for continuous chromatographic reactor experiments are normally closed valves. All the solenoid valves were mounted on the thick stainless steel sheet. These valves were connected to the switch box which was designed to open the solenoid valves from closed position using the on/off switch mechanism. Each solenoid valve has an individual switch and hence at any given time, any of the solenoid valves could be opened.

6.3.4. Continuous Chromatographic Reactor Schematic/Experimental Set-Up and Procedure

Figures 6.23 and 6.24 show the schematic and image of the experimental set-up of a continuous chromatographic reactor, respectively. It consists of four empty stainless steel columns packed with the swelled Purolite® CT-124 catalyst (as explained in the section 6.2.1). All the four columns were placed in the oven which could be heated to a desired temperature. The temperature could be monitored by the thermocouple which was placed inside the oven. Each of the four columns was connected to six solenoid valves: two inlets, three outlets and one connecting to the intermittent column. The two inlets are reactant and solvent lines which are connected to two HPLC pumps and the three outlets are the extract, raffinate and the effluent lines as shown in Figure 6.23. Each of the twenty four (24) solenoid valves are normally closed valves (see "Solenoid vales assembly" in Figure 6.24). These twenty four (24) solenoid valves were connected to a switch box (see Figure 6.24). The switch box consists of twenty four (24) switches,

each for one solenoid valve which charged the position of the solenoid valve from closed to open state when switched on.

Extract (C)
Raffinate (D)
Effluent (B)
Solvent (B)
Feed (A + B)
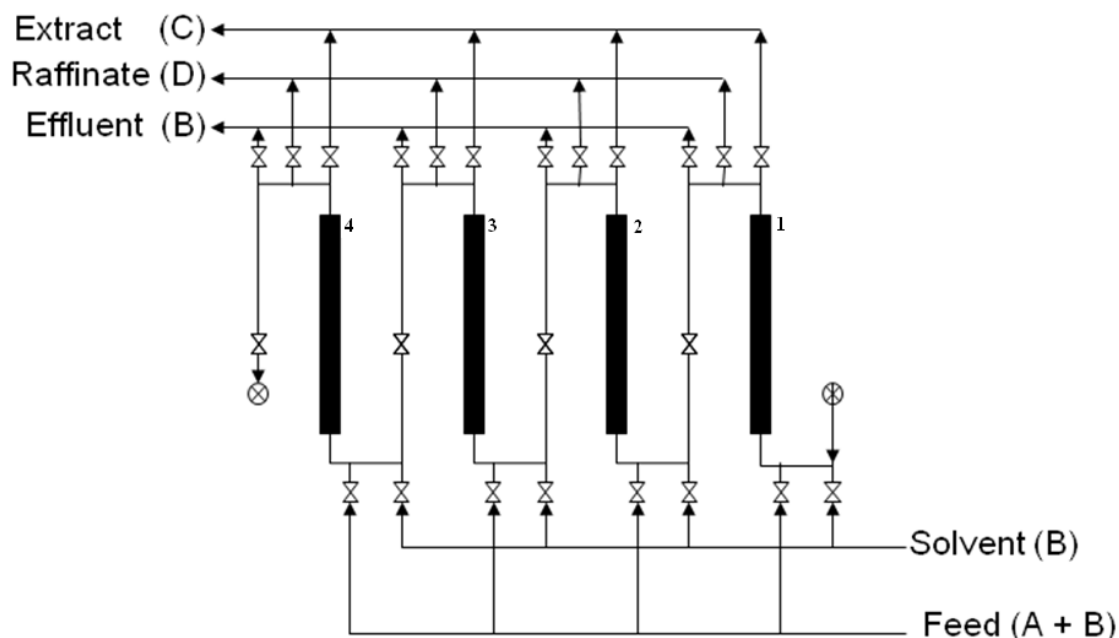
Figure 6.23. Schematic of a continuous chromatographic reactor set-up.

Before starting the continuous chromatographic reactor experiment it was assumed that the first column was already saturated with acetic acid, *n*-hexanol and water. At any given time, three columns were used for the reaction step and one column was used for the regeneration step. The oven was heated to the desired temperature. Once the desired temperature was attained (i.e. t = 0), the reactants (acetic acid and *n*-hexanol) were fed to the first column and the solvent (*n*-hexanol) was fed to the fourth column at desired flow rates. At the same time, the solenoid values connected to the reactants feed line of the first column, intermittent lines of the first and the second column, extract line of the third column were switched on using switch box for reaction step. Similarly, the solenoid valves connected to the solvent line and raffinate line of the fourth column were also switched on using the switch box for regeneration step. The reactants (acetic acid and *n*-hexanol) were fed to the first

column and the outlet fluid was collected from the extract port of the third column while the desorbent, *n*-hexanol is fed to the fourth column (assuming the fourth column was saturated) and the outlet fluid was collected from the raffinate port of the fourth column.
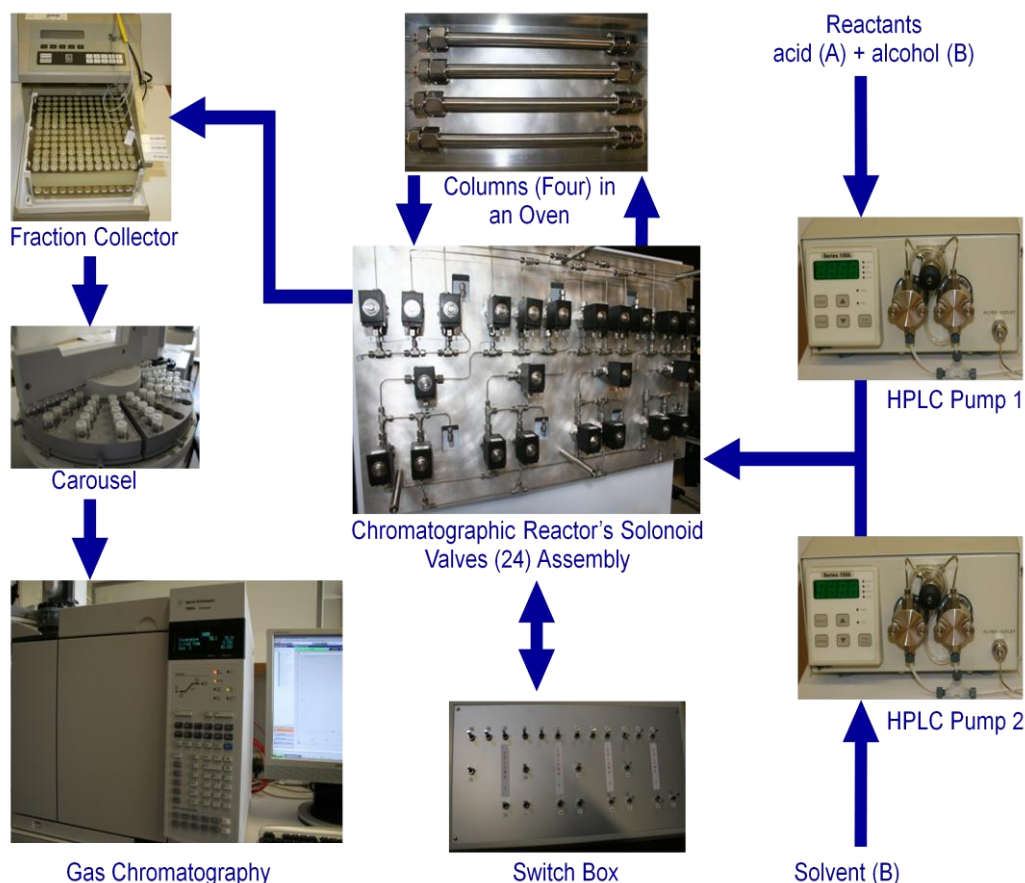
Figure 6.24. Image of a continuous chromatographic reactor experimental set-up assembly.

The samples collected from the extract line of the third column outlet and from the effluent line of the fourth column outlet were collected at regular intervals by fraction collector. The reactants (acetic acid and *n*-hexanol) fed to the first column reacts in the presence of Purolite® CT-124 catalyst to produce *n*-hexyl acetate and water. Water which has higher affinity towards resin is readily adsorbed onto the resin whilst *n*-hexyl acetate with lesser affinity gets desorbed quickly, moves from first column to the

second and to the third column and finally collected from the extract port of the third column diluted in *n*-hexanol. Since *n*-hexyl acetate was separated the reaction proceeds until either the consumption of the limiting reactant (acetic acid) or until the saturation of the column.

At time, t = T1 when the first column would be saturated (on the basis of the results obtained from the batch chromatographic reactor experiments) i.e. unreacted acetic acid would be coming out from the third column outlet, the reactants line was switched from the first column to the fourth column and the solvent line was switched from the fourth column to the first column which would be saturated at time t = T1. Subsequently, extract lines and raffinate lines were also switched to the fourth and first columns, respectively. The flow of switching feed, solvent, extract and raffinate lines were counter-current to the flow direction of reactants and products and hence this process is also called as continuous counter-current chromatographic reactor. Continuous chromatographic reactor experiments can also be operated in co-current mode of operation. The process of switching the columns used for the reaction and the regeneration steps were repeated until at least one complete cycle i.e., feed inlet from the first column to the fourth column and finally back to the first column was carried out.

As mentioned earlier in this section, the outlets from the packed columns were connected to a fraction collector which collects the sample at regular intervals from the three lines i.e. extract, raffinate and effluent. The samples collected by fraction collector from the outlets of the three lines were subjected to GC analysis by internal standard method as explained in Chapter 4, section 4.2.4. The samples were then placed in the carousel and were analysed by Agilent's 7890 series gas chromatograph (GC).

Design, construction and commissioning of continuous chromatographic reactor contributed to a major part of this project. The optimum parameter

at which 100% conversion of acetic acid was achieved using batch chromatographic reactor was therefore be used for testing the working condition of continuous chromatographic reactor. In the batch chromatographic reactor experiments only one column was used compared to three columns that were used for the reaction step of continuous chromatographic reactor. Hence, the optimum feed flow rate was therefore increased to three times i.e. 0.6 mL/min from 0.2 mL/min that was used for the optimum batch chromatographic reactor experiment under otherwise identical conditions. The results are discussed in detail in section 6.3.6.

6.3.5. Method of Analysis

The samples collected from the continuous chromatographic reactor outlets were analysed in the same way as the outlet samples from the batch chromatographic reactor and is already explained in detail (see section 6.2.4).

6.3.6. Results and Discussion

The continuous chromatographic reactor experiments were conducted at 353 K, feed flow rate of 0.6 mL/min i.e. 0.2 mL/min for each column, feed molar ratio (*n*-hexyl acetate to acetic acid) of 3:1 for the reaction step, solvent (*n*-hexanol) flow rate of 3 mL/min for the regeneration step and the switching time for both the reaction and the regeneration experiment of 75 min. Three columns were used for the reaction step and one column was used for the regeneration step. The operating parameters for the continuous operation were the same as the optimised parameters for the batch chromatographic reactor. The only difference between the batch and the continuous chromatographic reactor was the number of columns used for the reaction step.
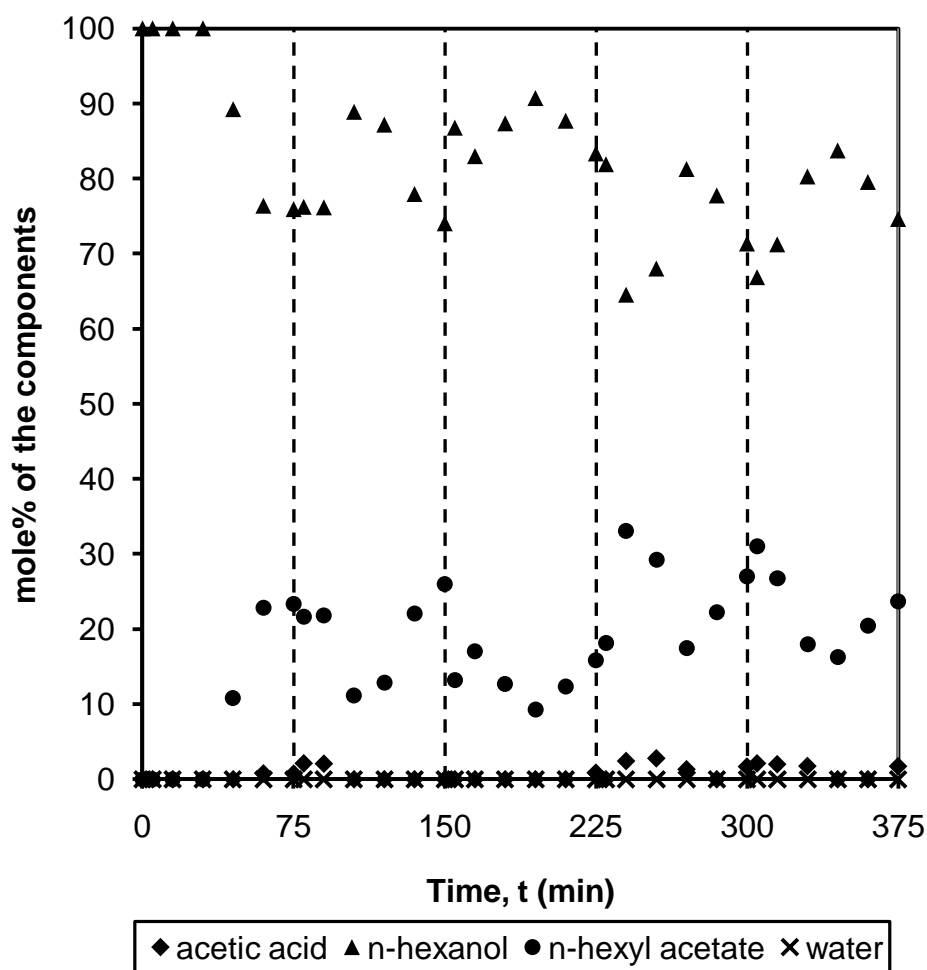
Figure 6.25. Overall experimental mole% of the samples collected at the counter-current continuous chromatographic reactor outlet as a function of time for the reaction step. Operating conditions: Reaction temperature: 353 K; feed flow rate: 0.6 mL/min; feed mole ratio (*n*-hexanol : acetic acid): 3:1; number of columns used for the reaction step: three (3); catalyst: Purolite® CT-124; reaction step time or the column switching time: 75 min; acetic acid flow rate: 0.078 mL/min; *n*-hexanol flow rate: 0.522 mL/min.
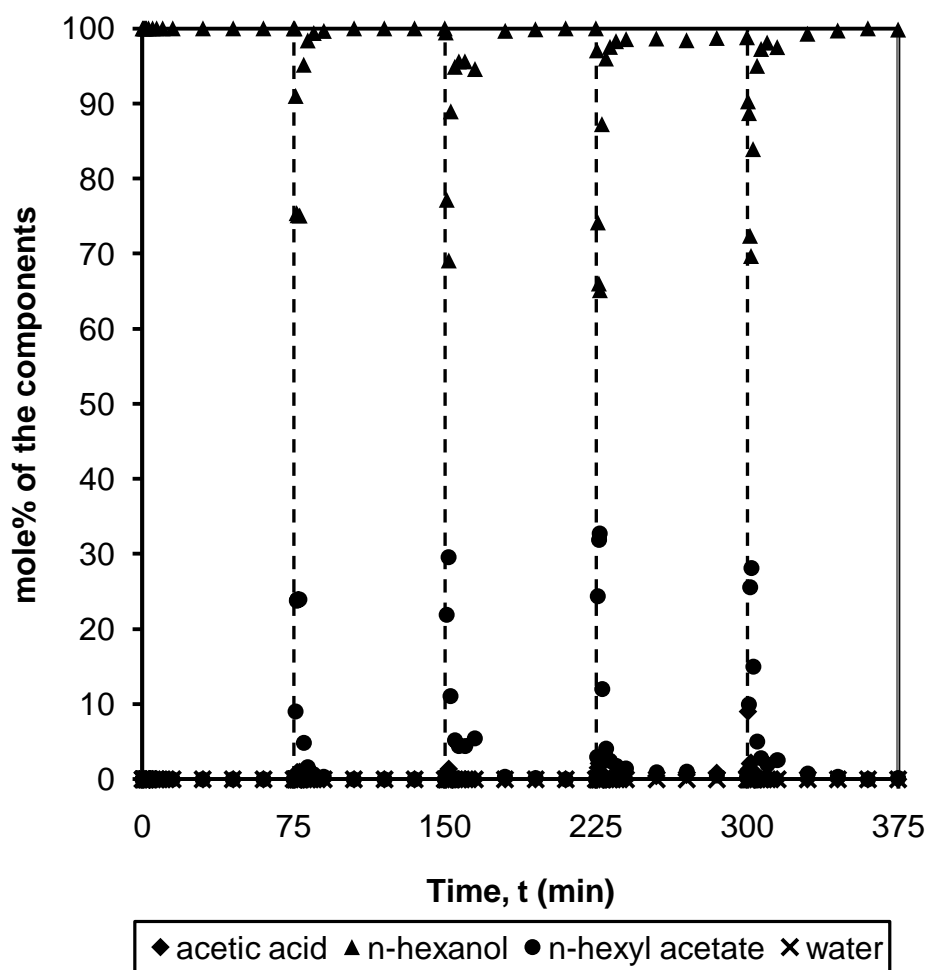
Figure 6.26. Overall experimental mole% of the samples collected at the counter-current continuous chromatographic reactor outlet as a function of time for the column regeneration step. Operating conditions: Reaction temperature: 353 K; number of columns used for the regeneration step: one (1); catalyst: Purolite® CT-124; regeneration step time: 75 min; n-hexanol flow rate: 3.0 mL/min.

The CCR experimental results for five switching periods are shown in Figure 6.25 for the reaction step and Figure 6.26 for the regeneration step, respectively. Also, the switching pattern of the solenoid valves for CCR experiments is shown in Table 6.1.

Table 6.1. Switching pattern and status of all the solenoid valves (X = open state) for continuous chromatographic reactor experiments (F = reactants feed line, S_f = solvent feed line, E = extract line, R_f = raffinate line, E_f = Effluent line and I = intermittent line).

Switching Period (t_s) [min]	Column 1						Column 2						Column 3						Column 4					
	F	S_x	E	R_x	E_f	I	F	S_x	E	R_x	E_f	I	F	S_x	E	R_x	E_f	I	F	S_x	R_x	R	E_f	I
0 – 75 (First)	X					X						X			X					X		X		
75 – 150 (Second)						X		X						X	X				X					X
150 – 225 (Third)			X					X	X				X				X							X
225 – 300 (Fourth)		X	X				X					X					X			X				
300 – 375 (Fifth)	X					X						X			X					X		X		

First switching period (0 – 75 min)

During the first switching period, columns 1, 2 and 3 were used for the reaction step and the column 4 was used for the regeneration step (see Figure 6.23). The reactants were fed to first column and the outlet fluid was collected from the extract port of the third column for the reaction step (see Table 6.1). For regeneration step, the solvent was fed through the solvent line of the fourth column and the outlet fluid was collected from the raffinate port of the fourth column (see Table 6.1). The results of the first switching period for the reaction step and the regeneration step are shown in Figures 6.25 and 6.26, respectively. It can be seen from Figure 6.25 that the n-hexyl acetate front appears at 45 min. This result replicates the result obtained from the batch chromatographic reactor experiment. The small error in the values of the composition of all the species was attributed due to the increased dead volume for the longer pipework involved for the continuous chromatographic reactor compared to the batch chromatographic reactor.

Figure 6.26 shows that since the column was assumed to be saturated with all the species, the solvent (n-hexanol) was fed at 3 mL/min to remove all the species so that the fourth column was regenerated. Since the fourth column was not saturated, only n-hexanol was found at the outlet for the first switching period. The reason for assuming that the fourth column was initially saturated was to carry out both the reaction and the regeneration steps in the continuous chromatographic reactor at time t = 0.

Second switching period (75 – 150 min):

During the second switching period, the columns 1, 2 and 4 were used for the reaction step and the third was used for the regeneration step (see Table 6.1) At time t = 75 min, inlet feed reactants for the reaction step was switched from the first column to the fourth column since the fourth column was used for the regeneration step from 0 – 75 min. The outlet fluid for the reaction step was collected from the extract port of the second

column. The direction of the flow of the reactants started from the fourth column to the first column and finally directed to the second column. The *n*-hexanol (desorbent) feed inlet was also switched at the same time from the fourth column to the first column and the outlet fluid was collected from the raffinate port of the first column.

Figure 6.25 shows the composition profile of all the species for the reaction step during the second switching period (75 – 150 min). The *n*-hexyl acetate composition was about 22 mole% at time t = 75 min, when the inlet and outlet of the columns were switched. After time t = 75 min the *n*-hexyl acetate composition dropped to about 11 mole% at time t = 105 min. This is because at time t = 75 min, the *n*-hexyl acetate composition was maximum in the third column followed by the second column and the least amount of *n*-hexyl acetate was present in the first column.

After time t = 75 min, the outlet for the reaction step was switched to the second column which had less *n*-hexyl acetate than the third column. The inlet feed was also switched to the fourth column from the first column which had no *n*-hexyl acetate. All these factors contributed to the fall in the mole% of the *n*-hexyl acetate. After time t = 105 min, the composition of *n*-hexyl acetate rises similar to reaction step profile for last 30 min from the first switching period.

Figure 6.26 shows the composition profile of all the species for the regeneration step during the second switching period. At time t = 75 min, the inlet for regeneration column was switched from the fourth column to the third column. Since, the third column was used as the last column for the reaction step from time t = 0 to 75 min, it consists of high concentration of *n*-hexyl acetate. At time t = 75 min, the third column is connected to solvent (*n*-hexanol) line and fed at 3 mL/min to remove all the species present in the third column. It can be seen from Figure 6.26 that it takes

about 15 min for complete regeneration of the column. This outcome is similar to most batch chromatographic experimental results where the column was regenerated at 3 mL/min within 10 to 15 minutes.

Third (150 – 225 min), fourth (225 – 300 min) and the fifth (300 – 375 min) switching periods.

The third switching period (150 – 225 min) was similar to the second switching period. Table 6.1 shows which solenoid valves were opened during the third switching period. The result of the third switching period for the reaction step is shown in Figure 6.25 while that for regeneration step is shown in Figure 6.26.

Similarly, the fourth switching period (225 – 300 min) was also similar to the second and third switching periods. The solenoid valves that remained open during the fourth switching period is shown in Table 6.1 The result of the fourth switching period for reaction step is shown in Figure 6.25 while that for regeneration step is shown in Figure 6.26.

The operation of the fifth switching period was same as the first switching period. The result of fifth switching period (300 – 375 min) for the reaction step is shown in Figure 6.25 while that for regeneration step is shown in Figure 6.26 The only difference between the first and the fifth switching periods was the result obtained from the regeneration step. The fourth column which was used for the regeneration step during the first switching period consists of only *n*-hexanol (see Figure 6.25). However, it now consists of species from the fourth switching period during the fifth switching period which needs to be removed from the column (see Figure 6.26). The assumption regarding the status of the fourth column was therefore made in the first switching period so that there were no operational differences in the first and the fifth switching period.

The switching period can be further extended as required as a result of continuous reaction, separation of the species and regeneration of the columns that can be carried out successfully in a continuous chromatographic reactor.

6.4. CONCLUSIONS

The batch chromatographic reactor experiments were carried out successfully in a stainless steel column packed with swelled ion exchange resin catalyst, Purolite® CT-124. Various parameters including the reaction step time, feed flow rate, feed molar ratio of the reactants (*n*-hexanol : acetic acid), temperature and desorbent (*n*-hexanol) flow rate were studied for the optimisation of *n*-hexyl acetate synthesis and maximum conversion of acetic acid in a batch chromatographic reactor. An increase in reaction step time increases unreacted acetic acid. An increase in feed molar ratio (*n*-hexanol : acetic acid) decreases unreacted acetic acid at the outlet of the chromatographic reactor. An increase in temperature increased the desorption rate of *n*-hexyl acetate from the catalyst so that it moves quickly towards the reactor outlet. An increase in feed flow rate decreases the residence time of acetic acid to convert to *n*-hexyl acetate. Complete conversion (100%) of acetic acid was achieved at reaction temperature of 353 K, feed molar ratio (*n*-hexanol : acetic acid) of 3:1, feed flow rate of 0.2 mL/min, and reaction and regeneration steps time of 75 min each, respectively. The outlet from the chromatographic reactor can be collected as products from both the reaction and the regeneration steps for the above-mentioned optimised parameters. Variable flow rate of *n*-hexanol in regeneration step was found to be the best way to minimise the solvent used in a chromatographic reactor. No by-product such as 1-hexene was detected as reported by Schmitt and Hasse (2006). Based on the batch chromatographic reactor experiments, a continuous chromatographic reactor was designed and constructed. Since the column used for the batch chromatographic reactor was fully packed with ion exchange resin, the bed volume is actually the

volume of the column used. Therefore, the bed volume was used as a scale up for the design of the continuous chromatographic reactor. An experiment with the optimised parameters with three columns for the reaction step and one column for the regeneration step was used for synthesis of *n*-hexyl acetate in a continuous chromatographic reactor. The results from the counter-current continuous chromatographic reactor correlate very well with the batch chromatographic reactor experiments for the same parameters. The small error in the values of the composition of all the species was attributed due to the increased dead volume for the longer pipework involved for the continuous chromatographic reactor compared to the batch chromatographic reactor.

Conclusions from this research work and recommendations for future work are summarised in the next chapter.

CHAPTER 7

CONCLUSIONS AND FUTURE WORK

7. CONCLUSIONS AND FUTURE WORK

7.1. INTRODUCTION

Chromatographic reactor (CR) and reactive distillation column (RDC) could potentially be used to increase conversion, yield, selectivity and purity of the product as compared to the conventional reactors. Conclusions and future work from the research work are explained in the following sections.

7.2. CONCLUSIONS

Literature review presented a wide range of applications carried out in batch and multi-functional reactors such as chromatographic reactors (CR) and reactive distillation columns (RDC). Literature review also gave information about the various catalysts that are used in important industrial applications. No kinetic data for the catalysed esterification reaction of acetic acid with *n*-hexanol was reported in the literature.

The objective of this research work on the basis of literature review was therefore to study the kinetics of *n*-hexyl acetate synthesis over a wide range of operating conditions and correlate the findings with different kinetic models, to carry out residue curve map (RCM) determination experiments to elucidate its operation in a reactive distillation columns (RDC), to study *n*-hexyl acetate synthesis over a wide range of operating parameters in a batch chromatographic reactor and to design, construct and commissioning of continuous chromatographic reactor. The following conclusions can be drawn from the current research work.

Catalyst characterisation of several ion exchange catalysts such as scanning electron micrograph (SEM), surface area measurement, pore size distribution, true density and particle size distribution was carried out successfully to elucidate the relationship between the catalytic performance and the structure of the ion exchange resins.

Batch kinetic studies were carried out for *n*-hexyl acetate synthesis in presence of various ion exchange resin catalysts over a wide range of operating conditions such as catalyst loading, feed mole ratio (FMR) of *n*-hexanol to acetic acid, acetic acid concentration and reusability of catalysts to optimise the reaction conditions. Speed of agitation and catalyst particle size had no significant effect on acetic acid conversion. Conversion of acetic acid was found to increase with an increase in temperature and catalyst loading. No evidence of formation of by-product such as 1-hexene or dihexyl ether was found during the batch kinetic experiments. Purolite® CT-124 was found to be the best catalyst for *n*-hexyl acetate synthesis as compared to Purolite® CT-151, Purolite® CT-175 and Purolite® CT-275 catalysts.

Residue curve map (RCM) determination experiments were carried out using the best catalyst that was found out from the batch kinetic studies i.e. Purolite® CT-124 catalyst. The RCM experiments confirmed that the non-reactive azeotropes could be eliminated with the addition of catalyst into the reacting system so that the desired product for the reacting system (i.e. *n*-hexyl acetate) could be obtained successfully over time. A four component minimum boiling reactive azeotrope was obtained from the RCM determination experiments at 375.3 K. The measured molar composition of the reactive azeotrope was 10.23% acetic acid, 0.59% *n*-hexanol, 0.4% *n*-hexyl acetate and 88.78% water. The residue curve map (RCM) suggested a low feed molar ratio (*n*-hexanol to acetic acid) of 1.2 to 2 in the reactive distillation column (RDC) so that *n*-hexyl acetate would only be present in the top product stream.

Heterogeneous and homogeneous kinetic models were used to correlate the experimentally obtained kinetic data. The activity of the components was taken into account instead of the concentration of the components, to account for the non-ideal mixing behaviour of the bulk liquid phase. The heterogeneous kinetic models were unable to predict the experimental

data very well since as all of them gave negative values of adsorption coefficients. Pseudo-homogeneous (PH) model gave a better representation of the kinetic behaviour for this heterogeneous catalytic esterification reaction.

A batch chromatographic reactor was used for the synthesis of *n*-hexyl acetate using Purolite® CT-124 catalyst over range of operating parameters. Complete conversion (100%) of acetic acid was found when experiment was carried out at 353 K, feed molar ratio (*n*-hexanol : acetic acid) of 3:1 and reaction and regeneration steps of 75 min each, respectively. Variable flow rate of *n*-hexanol was found out to be the optimum way to reduce the amount of *n*-hexanol used in the regeneration steps. Increase in temperature increases the desorption rate of *n*-hexyl acetate

Continuous chromatographic reactor was designed constructed and commissioned as part of this project. The results from the counter-current continuous chromatographic reactor correlate very well with the batch chromatographic reactor experiments for the optimised parameters.

The work carried out in this research work has shown promising results towards recovery of acetic acid and synthesis of *n*-hexyl acetate in multi-functional reactors. This research work could therefore be a good platform for recommendation of future work to be carried out and is outlined in the following section.

7.3. FUTURE WORK

Future work may be undertaken as an extension to the work reported in this thesis.

❖ **Batch kinetic modelling**
> ➢ Batch kinetic modelling could be carried out extensively for batch kinetic studies over a large number of parameters such

as feed mole ratio (FMR) of *n*-hexanol to acetic acid, concentration of acetic acid, catalyst loading etc.

❖ **Chromatographic Reactor (CR)**

➢ A number of parameters can be used to further optimise the *n*-hexyl acetate synthesis in a batch chromatographic reactor over wide range of operating conditions such as length of the column, limiting reacting (acetic acid) concentration etc.

➢ In this research work, excess reactant (*n*-hexanol) was chosen as the solvent for regeneration of the column However, another suitable solvent such as acetic anhydride (Gelosa *et al.* 2006) may be used for regeneration of the column which may give yield better results.

➢ Purolite® CT-124 was used as both catalyst and an adsorbent for experiments carried out in a chromatographic reactor. However, mixed proportion of adsorbent and catalyst together may improve the process in a chromatographic reactor.

❖ **Reactive distillation column (RDC)**

➢ Multi-functional reactor such as reactive distillation column (RDC) could be employed to study *n*-hexyl acetate synthesis. The RDC will also be useful to validate the results obtained from residue curve map (RCM) determination experiments.

❖ **Comparison of various processes for *n*-hexyl acetate synthesis**

➢ Comparison of multi-functional reactor (CR and RDC) operation with classical batch reactor could be done.

> ➢ Comparison of chromatographic reactor (CR) and reactive distillation column (RDC) operation for *n*-hexyl acetate synthesis may be carried out.

❖ **Modelling and simulation of multi-functional reactors**

> ➢ Modelling and simulation of chromatographic reactor (CR) and reactive distillation column (RDC) can be carried out. The model could be used to validate the findings from the multi-functional reactor experiments.

CHAPTER 8
REFERENCES

8. REFERENCES

Agar, D. W., Ruppel, W. Extended Reactor Concept for Dynamic Denox Design. *Chemical Engineering Science*, **1988**, 43 (8), 2073 – 2078.

Alcantara, R., Alcantara, E., Canoira, L., Franco, M. J., Herrera, M., Navarro, A. Trimerization of *iso*-Butene over Amberlyst-15 Catalyst. *Reactive and Functional Polymers*, **2000**, 45 (1), 19 – 27.

Alexandratos, S. D. Ion Exchange Resins: A Retrospective from Industrial and Engineering Chemistry Research. *Industrial and Engineering Chemistry Research*, **2009**, 48 (1), 388 – 398.

Ali, S. H. Kinetics of Catalytic Esterification of Propionic Acid with Different Alcohols over Amberlyst-15. *International Journal of Chemical Kinetics*, **2009**, 41 (6), 432 – 448.

Ali, S. H., Merchant, S. Q. Kinetic Study of Dowex 50 Wx8-Catalyzed Esterification and Hydrolysis of Benzyl Acetate. *Industrial and Engineering Chemistry Research*, **2009**, 48 (5), 2519 – 2532.

Ali, S. H., Merchant, S. Q. Kinetics of the Esterification of Acetic Acid with 2-Propanol: Impact of Different Acidic Cation Exchange Resins on Reaction Mechanism. *International Journal of Chemical Kinetics*, **2006**, 38 (10), 593 – 612.

Ali, S. H., Tarakmah, A., Merchant, S. Q., Al-Sahhaf, T. Synthesis of Esters: Development of the Rate Expression for the Dowex 50 Wx8-400 Catalyzed Esterification of Propionic Acid with 1-Propanol. *Chemical Engineering Science*, **2007**, 62 (12), 3197 – 3217.

Altiokka, M. R., Citak, A. Kinetic Study of Esterification of Acetic Acid with *iso*-Butanol in the Presence of Amberlite Catalyst. *Applied Catalysis A: General*, **2003**, 239, 141 – 148.

Armor, J. N. New Catalytic Technology Commercialized in the USA During the 1980's. *Applied Catalysis*, **1991**, 78, 141 – 173.

Barbosa, D., Doherty, M. F. The Simple Distillation of Homogeneous Reactive Mixtures. *Chemical Engineering Science*, **1988**, 43 (3), 541 – 550.

Berman, S., Isbenjian, H., Sedoff, A., Othmer, D. F. Continuous Production of Dibutyl Phthalate in a Distillation Column. *Industrial and Engineering Chemistry*, **1948**, 40 (11), 2139 – 2148.

Bianchi, C. L., Ragaini, V., Pirola, C., Carvoli, G. A New Method to Clean Industrial Water from Acetic Acid via Esterification. *Applied Catalysis B-Environmental*, **2003**, 40 (2), 93 – 99.

Bond, G. C. Heterogeneous Catalysis: Principle and Applications. **1987**, Second Edition, Claredon Press, Oxford.

Boonthamtirawuti, O., Kiatkittipong, W., Arpornwichanop, A., Praserthdam, P., Assabumrungrat, S. Kinetics of Liquid Phase Synthesis of *tert*-Amyl Ethyl Ether from *tert*-Amyl Alcohol and Ethanol over Amberlyst 16. *Journal of Industrial and Engineering Chemistry*, **2009**, 15 (4), 451 – 457.

Bozek-Winkler, E., Gmehling, J. Transesterification of Methyl Acetate and *n*-Butanol Catalyzed by Amberlyst 15. *Industrial and Engineering Chemistry Research*, **2006**, 45 (20), 6648 – 6654.

Bravo, J. L., Pyhalahti, A., Jarvelin, H. Investigations in a Catalytic Distillation Pilot-Plant-Vapor-Liquid-Equilibrium, Kinetics, and Mass-Transfer Issues. *Industrial and Engineering Chemistry Research*, **1993**, 32 (10), 2220 – 2225.

Broughton, D. B., Gerhold, C. G. Continuous Sorption Process Employing Fixed-Bed of Sorbent and Moving Inlets and Outlets. US Patent 2985589, **1961**.

Calvar, N., Gonzalez, B., Dominguez, A. Esterification of Acetic Acid with Ethanol: Reaction Kinetics and Operation in a Packed Bed Reactive Distillation Column. *Chemical Engineering and Processing*, **2007**, 46 (12), 1317 – 1323.

Cerveny, L., Marhoul, A., Kozel, J. Addition of Acetic Acid to Styrene Catalyzed by Ion Exchanger. *Reaction Kinetics and Catalysis Letters*, **1988**, 37 (2), 337 – 342.

Chakrabarti, A., Sharma, M. M. Esterification of Acetic Acid with Styrene: Ion Exchange Resins as Catalysts. *Reactive Polymers*, **1991**, 16 (1), 51 – 59.

Chakrabarti, A., Sharma, M. M. Cyclohexanol from Cyclohexene via Cyclohexyl acetate – Catalysis by Ion Exchange Resin and Acid-Treated Clay. *Reactive Polymers*, **1992**, 18 (2), 107 – 115.

Chakrabarti, A., Sharma, M. M. Cationic Ion Exchange Resins as Catalyst. *Reactive Polymers*, **1993**, 20 (1 – 2), 1 – 45.

Chan, K., Tsai, Y., Lin, H., Lee, M. Esterification of Adipic Acid with Methanol over Amberlyst 35. *Journal of the Taiwan Institute of Chemical Engineers*, **2010**, 41 (4), 414 – 420.

Chopade, S. P., Sharma, M. M. Reaction of Ethanol and Formaldehyde: Use of Versatile Cation exchange Resins as Catalyst in Batch Reactors and Reactive Distillation Columns. *Reactive and Functional Polymers*, **1997**, 32 (1), 53 – 65.

Cunill, F., Iborra, M., Fite, C., Tejero, J., Izquierdo, J. – F. Conversion, Selectivity, and Kinetics of the Addition of *iso*-Propanol to *iso*-Butene Catalyzed by a Macroporous Ion Exchange Resin. *Industrial and Engineering Chemistry Research*, **2000**, 39 (5), 1235 – 1241.

Cunill, F., Tejero, J., Fite, C., Iborra, M., Izquierdo, J. – F. Conversion, Selectivity, and Kinetics of the Dehydration of 1-Pentanol to Di-n-Pentyl Ether Catalyzed by a Microporous Ion Exchange Resin. *Industrial and Engineering Chemistry Research*, **2005**, 44 (2), 318 – 324.

Delgado, P., Sanz, M. T., Beltran, S. Kinetic Study for Esterification of Lactic Acid with Ethanol and Hydrolysis of Ethyl Lactate using an Ion Exchange Resin Catalyst. *Chemical Engineering Journal*, **2007**, 126 (2 – 3), 111 – 118.

Den Hollander, J. L., Stribos, B. I., Van Buel, M. J., Luyben, K. Ch. A. M., Van Der Wielen, L. A. M. Centrifugal Partition Chromatographic Reaction for the Production of Chiral Amino Acids. *Journal of Chromatography B*, **1998**, 711 (1 – 2), 223 – 235.

Den Hollander, J. L., Wong, Y. W., Luyben, K. Ch. A. M., Van Der Wielen, L. A. M. Non-separating effects in a Centrifugal Partition Chromatographic Reactor for the Enzymatic Production of L-amino acids. *Chemical Engineering Science*, **1999**, 54 (15 –16), 3207 – 3215.

Deshmukh, K. S., Gyani, V. C., Mahajani, S. M. Esterification of Butyl Cellosolve with Acetic Acid Using Ion Exchange Resin in Fixed Bed Chromatographic Reactors. *International Journal of Chemical Reactor Engineering*, **2009**, 7, Article A2.

Dhuri, S. M., Mahajani, V. V. Studies in Transesterification of Ethylene Carbonate to Dimethyl Carbonate over Amberlyst A-21 Catalyst. *Journal of Chemical Technology and Biotechnology*, **2006**, 81 (1), 62 – 69.

Doherty, M. F., Perkins, J. D. Dynamics of Distillation Processes .1. Simple Distillation of Multi-Component Non-Reacting, Homogeneous Liquid Mixtures. *Chemical Engineering Science*, **1978**, 33 (3), 281 – 301.

Falk, T., Seidal-Morgenstern, A. Comparison between a Fixed-Bed Reactor and a Chromatographic Reactor. *Chemical Engineering Science*, **1999**, 54 (10), 1479 – 1485.

Falk, T., Seidal-Morgenstern, A. Analysis of a Discontinuously Operated Chromatographic Reactor. *Chemical Engineering Science*, **2002**, 57 (9), 1599 – 1606.

Fien, G. J. A. F., Liu, Y. A. Heuristic Synthesis and Shortcut Design of Separation Processes Using Residue Curve Maps – A Review. *Industrial and Engineering Chemistry Research*, **1994**, 33 (11), 2505 – 2522.

Fish, B. B., Carr, R. W. An Experimental Study of the Counter-Current Moving-Bed Chromatographic Reactor. *Chemical Engineering Science*, **1989**, 44 (9), 1773 – 1783.

Fogler, H. S. Elements of Chemical Reaction Engineering. **1999**, Third Edition, Prentice Hall PTR.

Gangadwala, J., Kienle, A., Stein, E., Mahajani, S. Production of Butyl Acetate by Catalytic Distillation: Process Design Studies. *Industrial and Engineering Chemistry Research*, **2004**, 43 (1), 136 – 143.

Gangadwala, J., Mankar, S., Mahajani, S. Esterification of Acetic Acid with Butanol in the Presence of Ion exchange Resins as Catalysts. *Industrial and Engineering Chemistry Research*, **2003**, 42 (10), 2146 – 2155.

Gelbard, G. Organic Synthesis by Catalysis with Ion Exchange Resins. *Industrial and Engineering Chemistry Research*, **2005**, 44 (23), 8468 – 8498.

Gelosa, D., Ramaioli, M., Valente, G. Chromatographic Reactors: Esterification of Glycerol with Acetic Acid Using Acidic Polymeric Resins. *Industrial and Engineering Chemistry Research*, **2003**, 42 (25), 6536 – 6544.

Gelosa, D., Sliepcevich, A., Morbidelli, M. Chromatographic Reactors with Reactive Desorbents. *Industrial and Engineering Chemistry Research*, **2006**, 45 (11), 3922 – 3925.

Gyani, V. C. (Supervisor – Mahajani, S. M.). Reactive Chromatography. **2010**, PhD Thesis, Indian Institute of Technology, Mumbai, India.

Harmer, M. A., Sun, Q. Solid Acid Catalysis Using Ion exchange Resins. *Applied Catalysis A – General*, **2001**, 221(1 – 2), 45 – 62.

Helfferich, F. Ion Exchange. **1962**, McGraw-Hill, New York, NY.

Hoshimoto, K., Adachi, S., Nougima, H., Ueda, Y. A New Process Combining Adsorption and Enzyme Reaction for Producing Higher-Fructose Syrup. *Biotechnology and Bioengineering*, **1983**, 25 (10), 2371 – 2393.

Howard, A. J., Carta, G., Byers, C. H. Separation of Sugars by Continuous Annular Chromatography. *Industrial and Engineering Chemistry Research*, **1988**, 27, 1873 – 1882.

Izci, A., Bodur, F. Liquid-Phase Esterification of Acetic Acid with *iso-B*utanol Catalyzed by Ion Exchange Resins. *Reactive and Functional Polymers*, **2007**, 67 (12), 1458 – 1464.

Izci, A., Hosguen, H. L. Kinetics of Synthesis of *iso*-Butyl Propionate over Amberlyst-15. *Turkish Journal of Chemistry*, **2007**, 31 (5), 493 – 499.

Jacobs, R., Krishna, R. S. R. Multiple Solutions in Reactive Distillation for Methyl *tert*-Butyl Ether Synthesis. *Industrial and Engineering Chemistry Research*, **1993**, 32 (8), 1706 – 1709.

Jeong, Y. O., Luss, D. Pollutant Destruction in a Reverse Flow Chromatographic Reactor. *Chemical Engineering Science*, **2003**, 58 (7), 1095 – 1102.

Jiménez, L., Garvín, A., Costa-López, J. The Production of Butyl Acetate and Methanol via Reactive and Extractive Distillation. I. Chemical Equilibrium, Kinetics, and Mass-Transfer Issues. *Industrial and Engineering Chemistry Research*, **2002**, 41 (26), 6663 – 6669.

Juza, M., Mazzotti, M., Morbidelli, M. Simulated Moving-Bed Chromatography and its Application to Chirotechnology. *Trends in Biotechnology*, **2000**, 18 (3), 108 – 118.

Kawase, M., Suzuki, T. B., Inoue, K., Yoshimoto, K., Hashimoto, K. Increased Esterification Conversion by Application of the Simulated Moving-Bed Reactor. *Chemical Engineering Science*, **1996**, 51 (11), 2971 – 2976.

Kawase, M., Yasunobu, I., Araki, T., Hashimoto, K. The Simulated Moving-Bed Reactor for Production of Bisphenol A. *Catalysis Today*, **1999**, 48 (1 – 4), 199 – 209.

Kawase, M., Pilgrim, A., Araki, T., Hashimoto, K. Lactosucrose Production Using Simulated Moving-Bed Reactor. *Chemical Engineering Science*, **2001**, 56 (2), 453 – 458.

Krishna, R. Reactive Separations: More Ways to Skin a Cat. *Chemical Engineering Science*, **2002**, 57, 1491 – 1504.

Kruglov, A. V., Bjorklund, M. C., Carr, R. W. Optimisation of the Simulated Counter-Current Moving-Bed Chromatographic Reactor for the Oxidative Coupling of Methane. *Chemical Engineering Science*, **1996**, 51 (11), 2945 – 2950.

Lee, M. J., Chiu, J. Y., Lin, H. M. Kinetics of Catalytic Esterification of Propionic Acid and *n*-Butanol over Amberlyst 35. *Industrial and Engineering Chemistry Research,* **2002**, 41 (12), 2882 – 2887.

Lee, M. J., Chou, P. L., Lin, H. M. Kinetics of Synthesis and Hydrolysis of Ethyl Benzoate over Amberlyst 39. *Industrial and Engineering Chemistry Research*, **2005**, 44 (4), 725 – 732.

Lee, M. J., Wu, H. T., Kang, C. H., Lin, H. M. Kinetics of Catalytic Esterification of Acetic Acid with Amyl Alcohol over Amberlyst 15. *Journal of Chemical Engineering of Japan*, **2001**, 34 (7), 960 – 963.

Lee, M. J., Wu, H. T., Lin, H. M. Kinetics of Catalytic Esterification of Acetic Acid and Amyl Alcohol over Dowex. *Industrial and Engineering Chemistry Research*, **2000**, 39 (11), 4094 – 4099.

Liu, Y., Lotero, E., Goodwin, J. G., Jr. A Comparison of the Esterification of Acetic Acid with Methanol using Heterogeneous versus Homogeneous acid Catalysis. *Journal of Catalysis*, **2006**, 242 (2), 278 – 286.

Lode, F., Houmard, C., Migliorini, C., Mazzoti, M., Morbidelli, M. Continuous Reactive Chromatography. *Chemical Engineering Science*, **2001**, 56 (2), 269 – 291.

Lode, F., Francesconi, G., Mazzoti, M., Morbidelli, M. Synthesis of Methyl Acetate in Simulated Moving-Bed Reactor: Experiment and Modelling. *AIChE Journal*, **2003**, 49 (6), 1516 – 1524.

Mai, P. T., Vu, T. D., Mai, K. X., Seidal-Morgenstern, A. Analysis of Heterogeneously Catalyzed Ester Hydrolysis Performed in a Chromatographic Reactor and in a Reaction Calorimeter. *Industrial and Engineering Chemistry Research*, **2004**, 43 (16), 4691 – 4702.

Mazzzoti, M., Kruglov, A., Neri, B., Gelosa, D., Morbidelli, M. A Continuous Chromatographic Reactor: SMBR. *Chemical Engineering Science*, **1996**, 51 (10), 1827 – 1836.

Mazzotti, M., Neri, B., Gelosa, D., Morbidelli, M. Dynamics of a Chromatographic Reactor: Esterification Catalyzed by Acidic Resins. *Industrial and Engineering Chemistry Research*, **1997**, 36 (8), 3163 – 3172.

Meurer, M., Altenhoner, U., Strube, J., Unitied, A., Schmidt-Traub, H. Dynamic Simulation of a Simulated Moving-Bed Chromatographic Reactor for the Inversion of Sucrose. *Starch–Starke*, **1996**, 48 (11 – 12), 452 – 457.

Minceva, M., Gomes, P. S., Meshko, V., Rodrigues, A. E. Simulated Moving-Bed Reactor for Isomerisation and Separation of *p*-Xylene. *Chemical Engineering Journal*, **2008**, 140 (1 – 3), 305 – 323.

Muresan, E. I., Oprea, S., Hulea, V., Malutan, T., Vata, M. Kinetic Studies for the Esterification of Acetic Acid with Epichlorohydrin over an Anion Exchange Resin Catalyst. *Central European Journal of Chemistry*, **2008**, 6 (3), 419 – 428.

Neumann, R., Sasson, Y. Recovery of Dilute Acetic Acid by Esterification in a Packed Chemorectification Column. *Industrial Engineering Chemical Process Design and Development*, **1984**, 23, 654 – 659.

Olivier, J. P. Improving the Models Used for Calculating the Size Distribution of Micropore Volume of Activated Carbons from Adsorption Data. *Carbon*, **1998**, 36 (10), 1469 – 1472.

Patel, D., Saha, B. Heterogeneous Kinetics and Residue Curve Map (RCM) Determination for Synthesis of *n*-Hexyl Acetate Using Ion Exchange Resins as Catalysts. *Industrial and Engineering Chemistry Research*, **2007**, 46 (10), 3157 – 3169.

Patel, D., Saha, B., Wakeman, R. Optimisation of *n*-Hexyl Acetate Synthesis in a Chromatographic Reactor. *Journal of Ion Exchange*, **2010**, 21 (4), 388 – 391.

Patwardhan, A. A., Sharma, M. M. Esterification of Carboxylic Acids with Olefins using Cation Exchange Resins as Catalysts. *Reactive Polymers*, **1990**, 13 (1 – 2), 161 – 176.

Pereira, C. S. M., Sa Gomes, P., Gandi, G. K., Silva, V. M. T. M., Rodrigues, A. E. Multi-Functional Reactor for the Synthesis of Dimethylacetal. *Industrial and Engineering Chemistry Research*, **2008**, 47 (10), 3515 – 3524.

Pera-Titus, M., Bausach, M., Tejero, J., Iborra, M., Fite, C., Cunill, F., Izquierdo, J. F. Liquid-Phase Synthesis of *iso*-Propyl *tert*-Butyl Ether by Addition of 2-Propanol to *iso*-Butene on the Oversulfonated Ion Exchange Resin Amberlyst-35. *Applied Catalysis A – General*, **2007**, 323, 38 – 50.

Peters, T. A., Benes, N. E., Holmen, A., Keurentjes, J. T. F. Comparison of Commercial Solid Acid Catalysts for the Esterification of Acetic Acid with Butanol. *Applied Catalysis A – General*, **2006**, 297 (2), 182 – 188.

Popken, T., Gotze, L., Gmehling, J. Reaction Kinetics and Chemical Equilibrium of Homogeneously and Heterogeneously Catalyzed Acetic Acid Esterification with Methanol and Methyl Acetate Hydrolysis. *Industrial and Engineering Chemistry Research,* **2000**, 39 (7), 2601 – 2611.

Rangsunvigit, P., Kulprathipanja, S. Phenol Hydroxylation with TS-1 in a Chromatographic Reactor. *Separation Science and Technology*, **2004**, 39 (14), 3301 – 3315.

Ray, A. K., Carr, R. W. Experimental Study of a Laboratory-Scale Simulated Counter-Current Moving-Bed Chromatographic Reactor. *Chemical Engineering Science*, **1995**, 50 (14), 2195 – 2202.

Ray, A. K., Carr, R. W., Aris, R. The Simulated Counter-Current Moving-Bed Chromatographic Reactor: A Novel Reactor-Separator. *Chemical Engineering Science*, **1994**, 49 (4), 469 – 480.

Reid, R. C., Prausnitz, J. M., Poling, B. E. The Properties of Gases and Liquids. **1987**, Fourth Edition, McGraw-Hill: New York.

Saha, B. Ion Exchange Resin Catalysed Etherification of Dicyclopentadiene (DCPD) with Methanol. *Reactive and Functional Polymers*, **1999**, 40 (1), 51 – 60.

Saha, B., Chopade, S. P., Mahajani, S. M. Recovery of Dilute Acetic Acid through Esterification in a Reactive Distillation Column. *Catalysis Today*, **2000**, 60 (1 – 2), 147 – 157.

Saha, B., Iglesias, M., Cumming, I. W., Streat, M. Sorption of Trace Heavy Metals by Thiol Containing Chelating Resins. *Solvent Extraction and Ion Exchange*, **2000**, 18 (1), 133 – 167.

Saha, B., Sharma, M. M. Esterification of Formic Acid, Acrylic Acid and Methacrylic Acid with Cyclohexene in Batch and Distillation Column Reactors: Ion exchange Resins as Catalysts. *Reactive and Functional Polymers*, **1996**, 28 (3), 263 – 278.

Saha, B., Alqahtani, A., Teo, H. T. R. Production of *iso*-Amyl Acetate: Heterogeneous Kinetics and Techno-Feasibility Evaluation for Catalytic Distillation, *International Journal of Chemical Reactor Engineering*, **2005a**, 3, Article A30.

Saha, B., Teo, H. T. R., Alqahtani, A. *iso*-Amyl Acetate Synthesis by Catalytic Distillation. *International Journal of Chemical Reactor Engineering*, **2005b**, 3, Article A11.

Sanz, M. T., Murga, R., Beltran, S., Cabezas, J. L., Coca, J. Autocatalyzed and Ion Exchange-Resin-Catalyzed Esterification Kinetics of Lactic Acid with Methanol. *Industrial & Engineering Chemistry Research*, **2002**, 41 (3), 512 – 517.

Sanz, M. T., Murga, R., Beltran, S., Cabezas, J. L., Coca, J. Kinetic Study for the Reactive System of Lactic Acid Esterification with Methanol: Methyl Lactate Hydrolysis Reaction. *Industrial and Engineering Chemistry Research*, **2004**, 43 (9), 2049 – 2053.

Sanz, M. T., Gmehling, J. Esterification of Acetic Acid with *iso*-Propanol Coupled with Pervaporation. Part I: Kinetics and Pervaporation Studies. *Chemical Engineering Journal*, **2006**, 123 (1 – 2), 1 – 8.

Sanz, M. T., Gmehling, J. Esterification of Acetic Acid with *iso*-Propanol Coupled with Pervaporation. Part II. Study of a Pervaporation Reactor. *Chemical Engineering Journal*, **2006**, 123(1 – 2), 9 – 14.

Schmid, B., Doeker, M., Gmehling, J. Esterification of Ethylene Glycol with Acetic Acid Catalyzed by Amberlyst 36. *Industrial and Engineering Chemistry Research*, **2008**, 47 (3), 698 – 703.

Schmitt, M., Hasse, H. Chemical Equilibrium and Reaction Kinetics of Heterogeneously Catalyzed *n*-Hexyl Acetate Esterification. *Industrial and Engineering Chemistry Research*, **2006**, 45 (12), 4123 – 4132.

Schmitt, M., Hasse, H., Althaus, K., Schoenmakers, H., Gotze, L., Moritz, P. Synthesis of *n*-Hexyl Acetate by Reactive Distillation. *Chemical Engineering and Processing*, **2004**, 43 (3), 397 – 409.

Seader, J. D., Henley, E. J. Separation Process Principles. **1998**, John Wiley and Sons, Inc.

Sharma, M. M. Some Novel Aspects of Cationic Ion Exchange Resins as Catalysts. *Reactive and Functional Polymers*, **1995**, 26 (1 – 3), 3 – 23.

Shi, Y. H., Fan, M. H., Li, N., Brown, R. C., Sung, S. W. The Recovery of Acetic Acid with Sulphur Dioxide. *Biochemical Engineering Journal*, **2005**, 22 (3), 207 – 210.

Shieh, M. T., Barker, P. E. Saccharification of Modified Starch to Maltose in a Semi-Continuous Counter-Current Chromatographic Reactor-Separator (SCCR-S). *Journal of Chemical Technology and Biotechnology*, **1995**, 63, 125 – 134.

Silva, V. M. T. M., Rodrigues, A. E. Dynamics of a Fixed Bed Adsorptive Reactor for Synthesis of Diethylacetal. *AIChE Journal*, **2002**, 48 (3), 625 – 634.

Silva, V. M. T. M., Rodrigues, A. E. Novel Process for Diethylacetal Synthesis. *AIChE Journal*, **2005**, 51 (10), 2752 – 2768.

Solomons, T. W. G., Fryhle, C. B. Organic Chemistry, **2000**, Seventh Edition, Wiley, New York, 829.

Song, W., Venimadhavan, G., Manning, J. M., Malone, M. F., Doherty, M. F. Measurement of Residue Curve Maps and Heterogeneous Kinetics in Methyl Acetate Synthesis. *Industrial and Engineering Chemistry Research*, **1998**, 37 (5), 1917 – 1928.

Steinigeweg, S., Gmehling, J. Transesterification Processes by Combination of Reactive Distillation and Pervaporation. *Chemical Engineering and Processing*, **2004**, 43 (3), 447 – 456.

Strohlein, G., Assuncao, Y., Dube, N., Bardow, A., Mazzotti, M., Morbidelli, M. Esterification of Acrylic Acid with Methanol by Reactive Chromatography: Experiments and Simulations. *Chemical Engineering Science*, **2006**, 61 (16), 5296 – 5306.

Sundmacher, K., Kienle, A. Reactive Distillation-Status and Future Trends, **2003**, Wiley-VCH: Weinheim, Germany.

Suwannakarn, K., Lotero, E., Goodwin, J. G., Jr. Solid Bronsted Acid Catalysis in the Gas-Phase Esterification of Acetic Acid. *Industrial and Engineering Chemistry Research*, **2007**, 46 (22), 7050 – 7056.

Tapp, M., Kauchali, S., Hausberger, B., McGregor, C., Hilderbrandt, D., Glasser, D. An Experimental Simulation of Distillation Column Concentration Profiles Using a Batch Apparatus. *Chemical Engineering Science*, **2003**, 58 (2), 479 – 486.

Taylor, R., Krishna, R. Modelling Reactive Distillation. *Chemical Engineering Science*, **2000**, 55, 5183 – 5229.

Teo, H. T. R., (Supervisor – Saha, B.). Recovery of Dilute Acetic Acid Through Esterification in a Reactive Distillation Column. **2005**, PhD Thesis, Department of Chemical Engineering, Loughborough University, UK.

Teo, H. T. R., Saha, B. Heterogeneous Catalysed Esterification of Acetic Acid with *iso*-Amyl Alcohol: Kinetic Studies. *Journal of Catalysis,* **2004**, 228 (1), 174 – 182.

Tonkovich, A. L. Y., Carr, R. W. A Simulated Counter-Current Moving-Bed Chromatographic Reactor for the Oxidative Coupling of Methane – Experimental Results. *Chemical Engineering Science*, **1994**, 49 (24A), 4647 – 4656.

Toukoniitty, B., Mikkola, J. P., Eranen, K., Salmi, T., Murzin, D. Y. Esterification of Propionic Acid Under Microwave Irradiation over an Ion Exchange Resin. *Catalysis Today,* **2005**, 100 (3 – 4), 431 – 435.

Tsai, Y., Lin, H., Lee, M. Kinetics of Heterogeneous Esterification of Glutaric Acid with Methanol over Amberlyst 35. *Journal of the Taiwan Institute of Chemical Engineers*, **2011**, 42 (2), 271 – 277.

Umar, M., Patel, D., Saha, B. Kinetic Studies of Liquid Phase Ethyl *tert*-Butyl Ether (ETBE) Synthesis using Macroporous and Gelular Ion Exchange Resin Catalysts. *Chemical Engineering Science*, **2009**, 64 (21), 4424 – 4432.

Varisli, D., Dogu, T. Simultaneous Production of *tert*-Amyl Ethyl Ether and *tert*-Amyl Alcohol from *iso*-Amylene-Ethanol-Water Mixtures in a Batch-Reactive Distillation Column. *Industrial and Engineering Chemistry Research*, **2005**, 44 (14), 5227 – 5232.

Viecco, G. A., Caram, H. S. Analysis of the Reverse Flow Chromatographic Reactor. *AIChE Journal*, **2004**, 50 (9), 2266 – 2275.

Viecco, G. A., Caram, H. S. Use of a Reverse Flow Chromatographic Reactor to Enhance Productivity in Consecutive Reaction Systems. *Industrial and Engineering Chemistry Research*, **2005**, 44, 3396 – 3401.

Vora, B., Pujado, P., Imai, T., Fritsch, T. Production of Detergent Olefins and Linear Alkylbenzenes. *Chemistry and Industry*, **1990**, 6, 187 – 191.

Vu, T. D., Seidal-Morgenstern, A., Gruner, S., Kienle, A. Analysis of Ester Hydrolysis Reactions in a Chromatographic Reactor Using Equilibrium Theory and a Rate Model. *Industrial and Engineering Chemistry Research*, **2005**, 44 (25), 9565 – 9574.

Vu-Dinh, Tien (Supervisor – Seidal-Morgenstern, A., Kienle, A.). Analysis of Heterogeneously Catalysed Ester Hydrolysis Reactions in a Fixed-Bed Chromotographic Reactor. **2007**, MEng Thesis, Otto-Von-Guericke University of Magdeburg, Hanoi, Vietnam.

Yadav, G. D., Joshi, A. V. Etherification of *tert*-Amyl Alcohol with Methanol over Ion Exchange Resin. *Organic Process Research and Development,* **2001**, 5 (4), 408 – 414.

Yadav, G. D., Kulkarni, H. B. Ion Exchange Resin Catalysis in the Synthesis of *iso*-Propyl Lactate. *Reactive & Functional Polymers*, **2000**, 44 (2), 153 – 165.

Yadav, G. D., Lande, S. V. Ion Exchange Resin Catalysis in Benign Synthesis of Perfumery Grade *p*-Cresylphenyl Acetate from *p*-Cresol and Phenylacetic Acid. *Organic Process Research and Development*, **2005**, 9 (3), 288 – 293.

Yu, W., Hidajat, K., Ray, A. K. Modelling, Simulation, and Experimental Study of a Simulated Moving-Bed Reactor for the Synthesis of Methyl Acetate Ester. *Industrial and Engineering Chemistry Research*, **2003**, 42 (96), 6743 – 6754.

Yu, W., Hidajat, K., Ray, A. K. Determination of Adsorption and Kinetic Parameters for Methyl Acetate Esterification and Hydrolysis Reaction Catalyzed by Amberlyst-15. *Applied Catalysis A: General*, **2004**, 260 (2), 191 – 205.

Zafer, I., Barker, P. E. An Experimental and Computational Study of a Biochemical Polymerisation Reaction in a Chromatographic Reactor Separator. *Chemical Engineering Science*, **1988**, 43 (9), 2369 – 2375.

Zhang, C. M., Adesina, A. A., Wainwright, M. S. *iso*-Butene Hydration over Amberlyst-15 in a Slurry Reactor. *Chemical Engineering and Processing*, **2003**, 42 (12), 985 – 991.

Zhang, Z., Hidajat, K., Ray, A. K. Application of Simulated Counter-Current Moving-Bed Chromatographic Reactor for MTBE Synthesis. *Industrial and Engineering Chemistry Research*, **2001**, 40 (23), 5305 – 5316.

Zundel, G. Hydration and Intramolecular Interaction: Infrared Investigations with Polyelectrolytic Membranes, **1969**, Academic Press, New York.

CHAPTER 9
APPENDIX

9. APPENDIX

9.1. PUBLICATIONS

9.1.1. Refereed Journal Papers

1. Patel, D. and Saha, B., ''Heterogeneous kinetics and residue curve map (RCM) determination for synthesis of *n*-hexyl acetate using ion-exchange resins as catalysts'', *Industrial and Engineering Chemistry Research*, 46, **2007**, 3157-3169.

2. Umar, M., Patel, D. and Saha, B., ''Kinetic studies of liquid phase ethyl *tert*-butyl ether (ETBE) synthesis using macroporous and gelular ion exchange resin catalysts'', *Chemical Engineering Science*, 64, **2009**, 4424-4432.

3. Patel, D., Saha, B. and Wakeman R., ''Optimisation of *n*-hexyl acetate synthesis in a chromatographic reactor'', *Journal of Ion Exchange*, **2010**, 21(4), 388-391.

4. Patel D. and Saha B. ''Esterification of acetic acid and *n*-hexanol in a chromatographic reactor using ion exchange resin catalyst'', *Applied Catalysis A: General*, in preparation.

9.1.2. Refereed Conferences Papers

5. Saha, B. and Patel, D., ''Synthesis of *n*-hexyl acetate with ion-exchange resins as catalysts: kinetics and technofeasibility studies'', *Fifth Tokyo Conference on Advanced Catalytic Science and Technology*, Tokyo, Japan, 2006, 314-315 (P-337).

6. Saha, B. and Patel, D., ''Ion exchange resins catalysed synthesis of *n*-hexyl acetate'', *Ist International Workshop on Frontiers and Interfaces of Ion Exchange*, Antalya, Turkey, 2006, 63, [CD-ROM].

7. Patel, D., Saha, B. and Wakeman R., "Optimisation of *n*-hexyl acetate in a chromatographic reactor", *The Fifth International Conference on Ion Exchange*, Melbourne, Australia, 2010, 132, (2P-23).

RESEARCH PAPERS

ATTACHED IN THE THESIS

9.2. SAFETY DATA SHEET (SDS)

9.2.1. Chemicals

9.2.1.1. Acetic Acid

9.2.1.2. Acetone

9.2.1.3. *n*-Butanol

9.2.1.4. *n*-Hexanol

9.2.1.5. *n*-Hexyl Acetate

9.2.1.6. Methanol

SAFETY DATA SHEET

OF THE CHEMICALS

ATTACHED IN THE THESIS

9.2.2. Catalysts

9.2.2.1. Purolite® CT-124

9.2.2.2. Purolite® CT-151

9.2.2.3. Purolite® CT-175

9.2.2.4. Purolite® CT-275

SAFETY DATAS SHEET

OF THE CATALYSTS

ATTACHED IN THE THESIS

9.3. CONTROL OF SUBSTANCES HAZARDOUS TO HEALTH (COSHH)

9.3.1. COSHH ASSESSMENT RECORD

Department:	Area/Process/Project:							
Chemical Engineering	**S Building:** Batch Reactor Experiments (S262), Residue Curve Map determination Experiments (S262), Batch Chromatographic Reactor Experiments (S274) and Continuous Chromatographic Reactor Experiments (S156A). **Record Ref. Number: DP-COSHH-REV-05**							

DATA (Tick / insert data from data sheet or other source)							RISK RATING	
Please append the supplier's data sheet to this assessment or state your alternative reference source							(see	

CHEMICAL NAME: **Acetic Acid** **W.E.L.:**		Very toxic	Toxic	Corrosive	Irritant	Harmful	Flammable	**Toxicity Rating: Class 2 (HIGH)**	**RISK:** (Circle response**)**
Risk Phrases: 1. **R10** 2. **R35** 3. 4.	Safety Phrases: 1. 2 3 4	Amount used (kg or L/day) **0 – 0.09 L/day**	Physical state **Liquid**	Period of use (hrs/day) **0 – 12 h/day**	Is containment: Closed **X** Semi closed Open		Routes of exposure: Skin **X** Inhaled **X** Ingested **X**	**Exposure Potential** (Circle response) Ⓛ M H	1. EXTREME 2. HIGH 3. MEDIUM 4. LOW

CHEMICAL NAME: **Acetone** **WEL: TWA : 500 ppm** **STEL: 1500 ppm**		Very toxic	Toxic	Corrosive	Irritant	Harmful 	Flammable 	**Toxicity Rating Class 4 (LOW)**	**RISK:** (Circle response**)**
Risk Phrases: 1. **R11** 2. **R36** 3. **R66** 4. **R67**	Safety Phrases: 1. 2 3 4	Amount used (kg or L/day) **0 – 0.03 L/day**	Physical state **Liquid**	Period of use (hrs/day) **0 – 12 h/day**	Is containment: Closed — X Semi closed — Open —		Routes of exposure: Skin — X Inhaled — X Ingested — X	**Exposure Potential** (Circle response) Ⓛ M H	1. EXTREME 2. HIGH 3. MEDIUM (4. LOW)
CHEMICAL NAME: ***n*-Butanol** **W.E.L. _____**		Very toxic	Toxic	Corrosive 	Irritant	Harmful 	Flammable 	**Toxicity Rating Class 3 (MEDIUM)**	**RISK:** (Circle response**)**
Risk Phrases: 1. **R10** 2. **R22** 3. **R41** 4. **R67** 5. **R37/R38**	Safety Phrases 1. 2. 3. 4.	Amount used (kg or L/day) **0 – 0.03 L/day**	Physical state **Liquid**	Period of use (hrs/day) **0 – 12 h/day**	Is containment: Closed — X Semi closed — Open —		Routes of exposure: Skin — X Inhaled — X Ingested — X	**Exposure Potential** (Circle response) Ⓛ M H	1. EXTREME 2. HIGH 3. MEDIUM (4. LOW)

CHEMICAL NAME: *n*-Hexanol W.E.L. _____		Very toxic	Toxic	Corrosive	Irritant	Harmful ⚠	Flammable	**Toxicity Rating: Class 3 MEDIUM**	**RISK:** (Circle response**)**
Risk Phrases: 1. **R22** 2. 3. 4.	Safety Phrases: 1. 2 3 4	Amount used (kg or l / day) **0 – 1.5 L/day**	Physical state **Liquid**	Period of use (hrs/day) **0 – 12 h/day**	Is containment: Closed · **X** Semi closed · Open ·		Routes of exposure: Skin · **X** Inhaled · **X** Ingested · **X**	**Exposure Potential** (Circle response) Ⓛ M H	1. EXTREME 2. HIGH 3. MEDIUM ④**. LOW**
CHEMICAL NAME: *n*-Hexyl Acetate W.E.L. _____		Very toxic	Toxic	Corrosive	Irritant	Harmful	Flammable 🔥	**Toxicity Rating: Class 4 (LOW)**	**RISK:** (Circle response**)**
Risk Phrases: 1. **R10** 2. 3. 4.	Safety Phrases: 1. **S16** 2 3 4	Amount used (kg or L/day) **0 – 0.005 L/day**	Physical state **Liquid**	Period of use (hrs/day) **0 – 12 h/day**	Is containment: Closed · **X** Semi closed · Open ·		Routes of exposure: Skin · **X** Inhaled · **X** Ingested · **X**	**Exposure Potential** (Circle response) Ⓛ **M** H	1. EXTREME 2. HIGH 3. MEDIUM ④**. LOW**

CHEMICAL NAME: Methanol W.E.L. _____		Very toxic	Toxic	Corrosive	Irritant	Harmful	Flammable	Toxicity Rating: Class 1 (EXTREME)	RISK: (Circle response)
Risk Phrases: 1. **R11** 2. **R23/ 24/25** 3. **R39/ 23/24/25**	Safety Phrases: 1. 2 3 4	Amount used (kg or l / day) **0 – 1 /day**	Physical state **Liquid**	Period of use (hrs/day) **0 – 12 h/day**	Is containment: Closed **X** Semi closed Open		Routes of exposure: Skin **X** Inhaled **X** Ingested **X**	**Exposure Potential** (Circle response) Ⓛ M H	**1. EXTREME** 2. HIGH 3. MEDIUM 4. LOW
MATERIAL NAME: **Purolite® CT-124 / CT-151 / CT-175 / CT-275** W.E.L. _____		Very toxic	Toxic	Corrosive	Irritant	Harmful	Flammable	Toxicity Rating: Class 4 (LOW)	RISK: (Circle response) 1. EXTREME
Risk Phrases: 1. **R36** 2. 3. 4.	Safety Phrases: 1. 2 3. 4.	Amount used (kg or L/day) **0 – 0.5 Kg/day**	Physical state **Solid**	Period of use (hrs/day) **0 – 12 h/day**	Is containment: Closed **X** Semi closed Open		Routes of exposure: Skin **X** Inhaled **X** Ingested **X**	**Exposure Potential** (Circle response) Ⓛ M H	2. HIGH 3. MEDIUM **4. LOW**

Comments based on the conditions of use:

Method of use: Acetic acid and *n*-hexanol are mixed at desired temperature in presence of Purolite® catalyst to produce *n*-hexyl acetate and water in a batch reactor, RCM determination and chromatographic reactor (batch and continuous) experiments.

Methanol is **NOT** used in any experiment. It is used for washing the catalyst along with water. So even though the risk assessment is EXTREME, the risk is actually low because of its non-usage in the experiments.

n-Butanol is used as an internal standard for analysis of all the samples collected from various experiments. *n*-Butanol is added to the sample prior to the analysis of the sample.

Acetone is used as a dilution solvent. It is added along with *n*-butanol to the sample collected during the experiments before injecting the sample into the injection port of the GC.

Present containment: All experiments are conducted in the fume cupboard. All chemicals are handled inside the fume cupboard and stored in the designated places.

Current work practices: Use personal protective equipment (PPE) such as eye wear protection, gloves and lab coat at all times while carrying out the experiments.

Result of air monitoring (if relevant): N/A

Other hazards and considerations:

☒	☒	☒	☐	☐	☐
electrical	mechanical	fire	explosion	radiation	Other specify

Assessment Conclusions:

Use existing written protocol or any instruction as specified below (Attach a copy of the protocol to this COSHH assessment.)	☐ N/A	Do not use or substitute for a less hazardous material	☐ N/A
Modification of work practices/substitution etc: N/A			
Special precautions/control measures/PPE: N/A			
Special storage/handling: N/A			
Disposal method: As per chemicals and catalysts safety data sheet (SDS)			
Procedure in the event of a spillage: Absorb it with inert dry material and keep it in a disposal container			
First aid: As per given in safety data sheet (SDS)			
Further air monitoring required: N/A			
Written protocol required: N/A			
Existing protocol to be referred to: N/A			
Health Surveillance (where applicable): 1. Persons identified: N/A 2.Type of surveillance: N/A			
Date: **22/06/2011**	**Assessor's Signature:**	**Student's Signature:**	**Review Date:** N/A

Guidance on making health risk assessments under the Control of Substances Hazardous to Health Regulations 2002.

General points for consideration:

1. An assessment of the risk of exposure, its nature and its degree needs to be made and recorded on the standard COSHH assessment form. NB Departments may elect to record their assessments using other approved formats such as electronic databases. Approval for the use of alternative records must be obtained from the University HS and E office.

2. Dependent on outcome of the assessment the substance may need to be replaced by a less harmful substance or failing this to be used in a closed system. Or where this is not technically possible the exposure must be reduced to as low a level as is possible.

3. Suitable procedures need to be formulated to deal with any situations of abnormal exposure or emergency conditions that are in any way foreseeable.

4. Appropriate monitoring should be instigated as necessary to determine any occupational exposure and this will be co-ordinated by the Health, Safety & Environment Office. Any health surveillance procedures (if there are any available), need to be adopted and initially this should be discussed with the Health, Safety & Environment Office who will co-ordinate and advise as necessary.

5. Adequate information concerning the hazardous nature of the substance and risks to health needs to be obtained and the Health, Safety & Environment Office will provide such information if this is not available from departmental sources as well as training and instruction necessary to individuals if requested by the Department

Steps to risk assessment

Step 1:

Identify all hazardous substances

Step 2:

Obtain sufficient information to enable an assessment to be made – use the supplier's safety data sheet, information in HSE guidance EH40/2005 or other reputable reference source.

Step 3:

Consider the hazards of the substance and assign a hazard classification (low – extreme) based on Table 9.1 (your data sheet will provide toxicity data. Risk phrases and information indicating if the substance is harmful, irritant, corrosive, toxic or very toxic.

Step 4:

Assess the exposure potential for the material based on the amount used, its volatility/physical form and the manner in which it is handled and used – see Table 9.2

Step 5:

Use the two pieces of information derived from Table 9.1 and Table 9.2 to identify the risk classification according to the matrix shown in Table 9.3

Step 6:

Determine appropriate control measures and implement these effectively.

Table 9.1. Toxicity/Hazard rating: Guidelines for determining hazard categories

Classification	Description of this classification
Class 1 **EXTREME**	See list below *
Class 2 **HIGH**	Any substance defined by <u>CHIP</u> as toxic after repeated or prolonged exposure and given the risk phrase R48 or which meets the same toxicity criteria – see HSE publication L131 Any harmful substance given the risk phrase R68 (possible risk of irreversible effects Any corrosive substance given the risk phrase R35
Class 3 **MEDIUM**	Any substance defined by <u>CHIP</u> as Harmful or Irritant (Given the symbol Xn or Xi) R20, R21 R22, R65) Any corrosive substance given the risk phrase R34
Class 4 **LOW**	Low toxicity or not subject to any labelling criteria defined by <u>CHIP</u> but still potentially harmful

* categories of substances with EXTREME classification:

1. A **carcinogen**; that is a substances that is described by the <u>Risk Phrase</u> R45 "may cause cancer" or R49 "may cause cancer by inhalation", or R40 (Limited evidence of a carcinogenic effect) or that is described in other reliable sources as a cancer suspect agent.

2. All **mutagens** i.e. all substances with <u>Risk phrase</u> 46 or 68 or other substances believed to have similar properties.

3. Very toxic (T+) or poison; substances that are described as <u>Very Toxic</u> (by the criteria given in the HSE publication: Approved Classification and Labelling Guide L131) or as poisons (*e.g.* Risk Phrases R23 to R29, R31-R32). This is especially applicable to those agents that are acutely toxic because here a single dose can cause serious damage. **Compounds of unknown toxicity should be included in this group**.

4. **A Sensitiser** i.e. Risk Phrases R42 or R43.

5**. Explosive**; (*e.g.* Risk Phrases R1 to R6, R9, R16, R44) this term would cover any endothermic compounds which can detonate, e.g. many solid or gaseous diazo compounds, some compounds containing nitro, nitroso or other groups which make oxygen available to carbon or hydrogen in the compound, or solutions which contain fuel/oxidant mixtures, e.g silver perchlorate in ethanol (perchlorates have caused many accidents and all work with solid perchlorates, perchlorates in organic media, or with perchloric acid except in <4M aqueous solution, requires elaborate safety precautions).

6. **Normally pyrophoric**; (*e.g.* R17) this would definitely include silane or phosphine or potassium metal. Substances like lithium aluminium hydride which can be pyrophoric but which are frequently handled without catching fire, can be classified as class 2 if workers have sufficient experience/knowledge.

7. **Described by any of these Risk phrases (or combinations):**

R33	Danger of cumulative effects
R39	Danger of very serious irreversible effects
R47	May cause birth defects
R48	Danger of serious damage to health by prolonged exposure
R60	May impair fertility
R61	May cause harm to the unborn child
R62	Possible risk of impaired fertility
R63	Possible risk to the unborn child

Table 9.2. Typical basis for estimating exposure potential

		Score		
		1	**10**	**100**
A	**Quantity of Substance**	Less than 1g	1-100g	100g+
B	**Physical State**	dense solids; non-volatile liquid; no skin absorption	Dusty solids, lyophilised solids, volatile liquids, low skin adsorption	Gases, highly volatile liquids, aerosols, solutions that promote skin absorption
C	**Characteristics of Operation**	Then material is predominantly used in an enclosed system with a low chance of mishap	Partially open system, low chance of mishap	No physical barrier: Any operation where the chance of mishap is medium or high

Exposure potential is estimated by multiplying the individual scores **A x B x C.**

Score A x B x C	Exposure Potential
< 1000	Low
1000 - 10000	Medium
> 10000	High

Note: Time factors, such as frequency and duration of the activity should also be considered. Short duration tasks, involving a few seconds exposure at infrequent intervals, should not affect the initial estimate, whereas continuous operations on a daily basis would probably raise the estimate to the next higher category.

Table 9.3. Classification of risk and identification of containment regime/control measures (NB: Risk = Hazard x Exposure Potential)

Hazard (see Table 9.1)	Exposure Potential (see Table 9.2)		
	Low	Medium	High
Extreme	**Extreme**: address this case individually		
High	**Medium**	**High**	**High**
Medium	**Low**	**Medium**	**Medium**
Low	**Low**	**Low**	**Low**

Containment regimes determined from the above RISK RATING:

Low   Open bench/environment

Medium   General fume cupboard (or other specially vented area)

High   Specified fume cupboard

Extreme   Unique arrangements must be put in place which meet the highest level of containment practicable **and which must not permit exposure over a <u>Workplace Exposure Limit (WEL.)</u>**

<u>http://www.hse.gov.uk/coshh/table1.pdf</u>

Note:It is necessary to specify any additional controls required to use this material safely. The assessor must discuss these controls with the persons exposed to the substance. Monitoring must be carried out to ensure that the controls are effective. If there is reason to doubt the adequacy of the containment to control the risks further advice should be obtained (e.g. from an occupational safety and health specialist). This assessment must be reviewed annually and countersigned by another COSHH assessor.

9.4. RISK ASSESSMENT
9.4.1. Risk Assessment Record: Batch Kinetic Experiments

Department Chemical Engineering	Location: S Building Room No./Area: S262	Assessor Dipesh Patel	Date 22/06/2011	Assessment Number DP-RA-BR-REV-02
Risk Identified *(see Hazard prompt list over page)*	**Persons at Risk** *(Groups or No.)*	**Controls in Place**	**Assessors Risk Rating** *(H.M.L. see over page)*	**Assessors Actions to Further Reduce Risk**
Hazardous Chemicals (Highly Flammable, Flammable, Toxic, Corrosive, Irritant)	Operator(s)	To wear PPE's (lab coat, eye wear, face mask, gloves) at all times.	3 (C) X 1(L) = 3 Risk Rating = Medium	SDS, COSHH form filled.
Electric Shock	Operator(s)	All equipment is PAT tested before carrying out the experiments.	3 (C) X 1(L) = 3 Risk Rating = Medium	Do not use any equipment after expiry date.
Moving object (Stirrer)	Operator(s)	To securely tightened the stirrer to stirrer motor.	3 (C) X 1(L) = 3 Risk Rating = Medium	N/A
Fumes	Operator(s)	To handle all chemicals inside the fume cupboard.	3 (C) X 1(L) = 3 Risk Rating = Medium	Fume cupboard's safety glass is down at all times, except while taking samples.
Contact with hot surfaces (water bath)	Operator(s)	"Do not touch – it's HOT" warning note on water bath (clearly visible).	2 (C) X 1(L) = 2 Risk Rating = Medium	N/A
Storage of chemicals including waste chemicals.	Operators(s)	To use designated storage facilities To follow waste disposal methods.	3 (C) X 1(L) = 3 Risk Rating = Medium	To use minimum chemicals as possible.
Assessors Comment: Even though the consequences (C) of all hazard is major, the likelihood (L) of all possible hazard is reduced to minimum in all possible scenarios.			**Supervisors Comment:**	
Assessors Signature:	**Date: 22/06/2011**	**Supervisors Signature**		**Loughborough University**
Reassessment Date:		**Date:**		

9.4.2. Risk Assessment Record: Residue Curve Map (RCM) Determination Experiments

Department **Chemical Engineering**	Location: **S Building** Room No./Area: **S262**	Assessor **Dipesh Patel**		Date **22/06/2011**	Assessment Number **DP-RA-RCM-REV-02**
Risk Identified *(see Hazard prompt list over page)*	**Persons at Risk** *(Groups or No.)*	**Controls in Place**		**Assessors Risk Rating** *(H.M.L. see over page)*	**Assessors Actions to Further Reduce Risk**
Hazardous Chemicals (Highly Flammable, Flammable, Toxic, Corrosive, Irritant)	Operator(s)	To wear PPE's (lab coat, eye wear, face mask, gloves) at all times.		3 (C) X 1(L) = 3 Risk Rating = Medium	SDS, COSHH form filled.
Electric Shock	Operator(s)	All equipment is PAT tested before carrying out the experiments.		3 (C) X 1(L) = 3 Risk Rating = Medium	Do not use any equipment after expiry date.
Moving object (Stirrer)	Operator(s)	To securely tightened the stirrer to stirrer motor.		3 (C) X 1(L) = 3 Risk Rating = Medium	N/A
Fumes	Operator(s)	To handle all chemicals inside the fume cupboard.		3 (C) X 1(L) = 3 Risk Rating = Medium	Fume cupboard's safety glass is down at all times, except while taking samples.
Contact with hot surfaces (glass flask)	Operator(s)	"Do not touch – it's HOT" warning note on glass flask (clearly visible).		2 (C) X 1(L) = 2 Risk Rating = Medium	N/A
Storage of chemicals including waste chemicals.	Operators(s)	To use designated storage facilities To follow waste disposal methods.		3 (C) X 1(L) = 3 Risk Rating = Medium	To use minimum chemicals as possible.
Assessors Comment: Even though the consequences (C) of all hazard is major, the likelihood (L) of all possible hazard is reduced to minimum in all possible scenarios.			**Supervisors Comment:**		
Assessors Signature:	**Date: 22/06/2011**		**Supervisors Signature**		
Reassessment Date:			**Date:**		Loughborough University

9.4.3. Risk Assessment Record: Batch Chromatographic Reactor Experiments

Department Chemical Engineering	Location: S Building Room No./Area: S262	Assessor Dipesh Patel	Date 22/06/2011	Assessment Number DP-RA-BCR-REV-02
Risk Identified *(see Hazard prompt list over page)*	**Persons at Risk** *(Groups or No.)*	**Controls in Place**	**Assessors Risk Rating** *(H.M.L. see over page)*	**Assessors Actions to Further Reduce Risk**
Hazardous Chemicals (Highly Flammable, Flammable, Toxic, Corrosive, Irritant)	Operator(s)	To wear PPE's (lab coat, eye wear, face mask, gloves) at all times.	3 (C) X 1(L) = 3 Risk Rating = Medium	SDS, COSHH forms filled.
Electric Shock	Operator(s)	All equipment is PAT tested before carrying out the experiments.	3 (C) X 1(L) = 3 Risk Rating = Medium	Do not use any equipment after expiry date.
Reactants (acetic acid and *n*-hexanol) bottles	Operator(s)	To securely tightened the reactants bottles.	3 (C) X 1(L) = 3 Risk Rating = Medium	N/A
Fumes	Operator(s)	To handle all chemicals inside the fume cupboard.	3 (C) X 1(L) = 3 Risk Rating = Medium	Fume cupboard's safety glass is down at all times, except while taking samples.
Contact with hot surfaces (Oven)	Operator(s)	"Do not touch – it's HOT" warning note on water bath (clearly visible).	2 (C) X 1(L) = 2 Risk Rating = Medium	N/A
Storage of chemicals including waste chemicals.	Operators(s)	To use designated storage facilities To follow waste disposal methods.	3 (C) X 1(L) = 3 Risk Rating = Medium	To use minimum chemicals as possible.
Assessors Comment: Even though the consequences (C) of all hazard is major, the likelihood (L) of all possible hazard is reduced to minimum in all possible scenarios.		**Supervisors Comment:**		
Assessors Signature:	**Date: 22/06/2011**	**Supervisors Signature**		■ Loughborough University
Reassessment Date:		**Date:**		

9.4.4. Risk Assessment Record: Continuous Chromatographic Reactor Experiments

Department **Chemical Engineering**	Location: **S Building** Room No./Area: **S262**		Assessor **Dipesh Patel**	Date **22/06/2011**	Assessment Number **DP-RA-CCR-REV-02**
Risk Identified *(see Hazard prompt list over page)*	**Persons at Risk** *(Groups or No.)*	**Controls in Place**		**Assessors Risk Rating** *(H.M.L. see over page)*	**Assessors Actions to Further Reduce Risk**
Hazardous Chemicals (Highly Flammable, Flammable, Toxic, Corrosive, Irritant)	Operator(s)	To wear PPE's (lab coat, eye wear, face mask, gloves) at all times.		3 (C) X 1(L) = 3 Risk Rating = Medium	SDS, COSHH forms filled.
Electric Shock	Operator(s)	All equipment is PAT tested before carrying out the experiments.		3 (C) X 1(L) = 3 Risk Rating = Medium	Do not use any equipment after expiry date.
Moving object (Stirrer)	Operator(s)	To securely tightened the stirrer to stirrer motor.		3 (C) X 1(L) = 3 Risk Rating = Medium	N/A
Fumes	Operator(s)	To handle all chemicals inside the fume cupboard.		3 (C) X 1(L) = 3 Risk Rating = Medium	Fume cupboard's safety glass is down at all times, except while taking samples.
Contact with hot surfaces (water bath)	Operator(s)	"Do not touch – it's HOT" warning note on water bath (clearly visible).		2 (C) X 1(L) = 2 Risk Rating = Medium	N/A
Storage of chemicals including waste chemicals.	Operators(s)	To use designated storage facilities To follow waste disposal methods.		3 (C) X 1(L) = 3 Risk Rating = Medium	To use minimum chemicals as possible.
Assessors Comment: Even though the consequences (C) of all hazard is major, the likelihood (L) of all possible hazard is reduced to minimum in all possible scenarios.			**Supervisors Comment:**		
Assessors Signature:	**Date: 22/06/2011**		**Supervisors Signature**		**Loughborough University**
Reassessment Date:			**Date:**		

Hazard Prompt Lists

Machinery & Work Equipment – Category 1
- Mechanical Hazards
- Electric Shock
- Vehicles/Transport
- Hand Tools

Hazards associated with Place of Work – Category 2
- Slips, trips and falls on a level
- Falls from a height
- Falling objects/materials
- Striking objects
- Contact with hot/cold materials/surfaces
- Storage and stacking
- Space and confined work area

Hazards associated with materials, substances & physical agents – Category 3
- Dust, fume and gases
- Biological hazards/infection
- Noise/Vibration
- Compressed gases

Hazardous chemicals (CHIP P.10)
- Explosive
- Oxidising
- Extremely flammable
- High flammable
- Flammable
- Very toxic
- Toxic
- Harmful
- Corrosive
- Irritant
- Sensitising
- Carcinogenic
- Entry into confined space/lack of oxygen

Hazards associated with activity, methods of work – Category 4
- Manual handling
- Upper Limb Disorders/Repetitive Strain Injury
- Visual fatigue
- Posture

Hazards associated with Work Organisation (Contractors/Service) – Category 5

Hazards associated with Work Environment – Category 6
- Temperature
- Heating
- Ventilation
- Lighting

Other types of hazard – Category 7
- Violence
- Stress
- Drugs
- Substance abuse

Risk Ratings (High, Medium, Low)

CONSEQUENCE:
3 **Major** (e.g. death or major injury as per RIDDOR or irreversible health damage)
2 **Serious** (e.g. injuries causing absence of more than three days or significant health effects – reversible)
1 **Slight** (other injuries requiring first aid and minor ill health effects)

LIKELIHOOD:
3 **High** (where certain or near certain harm will occur)
2 **Medium** (where harm will frequently occur)
1 **Low** (where harm will seldom occur)

RISK RATING = CONSEQUENCE x **LIKELIHOOD**
High 6 – 9
Medium 2 – 4
Low 1

9.5. METHOD OF ANALYSIS

The methods for analysing gas chromatography results are normalisation, normalisation with response factor, external standard and internal standard. Each of the analysis methods are discussed as follows:

9.5.1. Normalisation (Area%)

Calibration calculation: None

Analysis calculation:

$$\%Conc_i = \frac{Area_i}{\sum_{i=1}^{n} Area_i}$$

Advantages:

- ❖ No calibration required

- ❖ Simple calculation

- ❖ Results independent of injection volume.

Disadvantages:

- ❖ All detected components are included in the calculation.

- ❖ There is no allowance made for the response of each component to the detector.

- ❖ The results are expressed as a percentage of all components detected and not as absolute concentration.

9.5.2. Normalisation with response factor (RF)

Calibration Calculation:

$$RF_i \quad = \quad \frac{Conc_i}{Area_i} \quad x \quad \frac{Area_{ref}}{Conc_{ref}}$$

Analysis Calculation:

$$\%Conc_i \quad = \quad \frac{(Area_i \; x \; RF_i)}{\sum\limits_{i=1}^{n}(Area_i \; x \; RF_i)} \quad x \quad 100\%$$

Advantages:

- ❖ Allowance made for the response of each component to the detector.

- ❖ Results independent of injection volume.

Disadvantages:

- ❖ All detected components are included in the calculation. Therefore, the calibration mixture must contain all components.

- ❖ The results are expressed as a percentage of all components detected and not as absolute concentration.

9.5.3. External Standard

Calibration calculation:

$$R_i = \frac{Area_i}{R_i}$$

Analysis calculation:

$$Conc_i = \frac{Area_i}{R_i}$$

Advantages:

❖ Simple calculation.

❖ The results are expressed as absolute concentration i.e. the units are the same as $Conc_i$ for calibration.

❖ The external standard is often used for gas analysis.

Disadvantages:

❖ Injection volume must be constant.

9.5.4. Internal Standard

Calibration calculation:

$$RF_i = \frac{Conc_i}{Area_i} \quad \times \quad \frac{Area_{IS}}{Conc_{IS}}$$

Analysis calculation:

$$Conc_i = \frac{Area_i \times RF_i \times Conc_{IS}}{Area_{IS}}$$

Advantages:

❖ There is allowance made for the response of each component to the detector.

❖ The results are independent of injection volume.

❖ The results are expressed as absolute concentration.

Disadvantages:

❖ The technique is not readily usable with gaseous samples.

❖ This technique requires the selection of a suitable internal standard.